

DMYTRO FISHMAN

Developing a data analysis pipeline for
automated protein profiling in immunology

TARTU 2022

Institute of Computer Science, Faculty of Science and Technology, University of Tartu, Estonia.

Dissertation has been accepted for the commencement of the degree of Doctor of Philosophy (PhD) in informatics on May 20, 2021 by the Council of the Institute of Computer Science, University of Tartu.

Supervisors

Dr. Hedi Peterson
University of Tartu

Prof. Jaak Vilo
University of Tartu

Prof. Pärt Peterson
University of Tartu

Opponents

Dr. Jessica Da Gama Duarte
Olivia Newton-John Cancer Research Institute, Australia

Dr. Fridtjof Lund-Johansen
Oslo University Hospital, Norway

The public defense will take place on 28 June, 2021 at 09:15 in Zoom.

The publication of this dissertation was financed by the Institute of Computer Science, University of Tartu.

Copyright © 2022 by Dmytro Fishman

ISSN 2613-5906

ISBN 978-9949-03-624-0 (print)

ISBN 978-9949-03-625-7 (PDF)

University of Tartu Press

<http://www.tyk.ee/>

*We're all in it together against Lord
Voldemort and the House Slytherin.*

Robert M Sapolsky

ABSTRACT

Accurate information about protein content in the organism is instrumental for a better understanding of human biology and disease mechanisms. While the presence of certain types of proteins can be life-threatening, the abundance of others is an essential condition for an individual's overall well-being. Protein microarray is a technology that enables the quantification of thousands of proteins in hundreds of human samples in a parallel manner. In a series of studies involving protein microarrays, we have explored and implemented various data science methods for all-around analysing of these data. This analysis has enabled the identification and characterisation of proteins targeted by the autoimmune reaction in patients with the APS1 condition. We have also assessed the utility of applying machine learning methods alongside statistical tests in a study based on protein expression data to evaluate potential biomarkers for endometriosis. The keystone of this work is a web-tool PAWER. PAWER implements relevant computational methods, and provides a semi-automatic way to run the analysis of protein microarray data online in a drag-and-drop and click-and-play style. The source code of the tool is publicly available. The work that laid the foundation of this thesis has been instrumental for a number of subsequent studies of human disease and also inspired a contribution to refining standards for validation of machine learning methods in biology.

CONTENTS

List of Figures	9
List of Tables	11
List of original publications	13
1. Introduction	15
1.1. Main contributions of the thesis	16
2. Introduction to proteins	17
2.1. From DNA to proteins and back	17
2.2. The immune system	18
2.2.1. Autoimmune disorders	21
2.3. DNA microarrays	22
2.4. Protein microarrays	22
2.4.1. Functional protein microarrays	23
3. Protein microarray data analysis	26
3.1. Raw data acquisition	27
3.2. Data pre-processing	28
3.2.1. Background correction and signal transformation	28
3.2.2. Outlier detection	30
3.2.3. Signal normalisation	31
3.3. Statistical analysis	37
3.3.1. Differential analysis	38
3.3.2. Enrichment analysis	42
3.3.3. Multiple testing correction	44
3.4. Machine learning modelling	45
4. Protein microarray analysis in the search for high-affinity ameliorating autoantibodies (Publication I)	49
5. Characterising autoimmune targets further (Publication II)	52
6. Automating protein microarray analysis with Protein Array Web ExploreR (Publication III)	55
6.1. PAWER pipeline	55
6.2. Implementation	56
6.3. Comparison to other tools	58
6.4. Summary	59
7. Validating results of statistical tests using machine learning models on protein expression data (Publication IV)	60

8. Conclusions	63
Bibliography	65
Acknowledgements	78
Sisukokkuvõte (Summary in Estonian)	82
Publications	
AIRE-deficient patients harbor unique high-affinity disease-ameliorating autoantibodies	
Autoantibody repertoire in APECED patients targets two distinct subgroups of proteins	
PAWER: Protein Array Web ExploreR	
Multiplex analysis of 40 cytokines do not allow separation between en- dometriosis patients and controls	
Curriculum Vitae	1
Elulookirjeldus (Curriculum Vitae in Estonian)	4

LIST OF FIGURES

1. Immune system can be broadly divided into two subsystems: innate and adaptive immunity. Two systems supporting each other in their own ways to fight intruders. With the latter being slower and more specific, while the former is faster and more general.	19
2. Structure of a typical antibody. Antibodies use their variable regions (coloured in red) as arms to bind to potential intruders. By binding to a molecule, antibodies send a signal to other immune cells to take action against the intruder.	20
3. Schema of the exemplary protein microarray. In functional protein microarrays, proteins and protein fragments are printed inside spots (blue circles) arranged in rows, columns and blocks.	24
4. A rough outline of data analysis methods used for protein microarray experiments. Raw data after the acquisition is assembled into a large matrix. This matrix passes through a number of steps, including background correction, signal transformation, outlier detection, and normalisation before being used as an input for statistical analysis and machine learning. Next, results of statistical analysis and machine learning modelling are interpreted in the context of the existing body of knowledge.	27
5. Foreground signal, background signal and wider neighbourhood of the spot. The fluorescent signal of the protein is determined by subtracting the median of the immediate background of the spot from the median of its foreground signal. Alternatively, background value can be calculated taking a wider neighbourhood of the spot into consideration.	29
6. An example of a heatmap obtained from a protein microarray experiment using ClustVis tool. Each cell of the heatmap is coloured based on the signal level of the corresponding protein (in rows) across all samples (in columns). Additional meta-information available about samples and proteins is visualised using extra colour legends. Hierarchical clustering results are presented in the form of dendrograms at the top and on the left of the heatmap.	32
7. Normalising protein microarray signal using the robust linear model and control proteins. First, intensity values of the control proteins are modelled as a linear combination of the array (α), block (β), type of control protein, and noise using a robust linear model (purple line). The resulting coefficients for arrays and blocks are considered to be associated with unwanted technical biases. Then the normalised signal is obtained by subtracting the corresponding coefficients associated with a specific array and block.	36

8. Decision tree algorithm uses information about individual protein intensities (P_A and P_B) in order to explain the outcome variable. For example, the decision tree algorithm may assign a class "control" to a sample for which protein A (P_A) has an intensity value less than 4.5. 46
9. Random forest algorithm uses predictions produced by individual decision trees in order to predict an outcome variable. Decision trees that are part of a random forest ensemble are built by randomly discarding a pre-defined number of features and observations. For example, decision tree 1 has been built after discarding protein A intensity and the first control sample. 47
10. PAWER pipeline. Raw GPR files are uploaded to PAWER (1), then the system proceeds to identify foreground and background intensities and a panel of control proteins that can be used for normalisation (2). The robust linear model is then used to estimate and remove the technical artifacts associated with each array and array block (3). Normalised data is then combined with sample metadata (4) to produce a list of differentially expressed proteins (5). PAWER is linked with two other tools (g:Profiler and ClustVis) to enable additional analysis, namely: protein enrichment analysis and cluster analysis of normalised expression values. 57

LIST OF TABLES

1. Comparison between currently available protein microarray analysis tools: Prospector, PAA, PMA, PMD, and PAWER. The presence or absence of relevant features (in columns) are shown as pluses highlighted in green (present features) or minuses in red (absent features). We were not able to obtain results using the PMD tool, thus all the relevant entries are based on the claims made in the original publication and highlighted in gray. 59

LIST OF ABBREVIATIONS

AIRE	autoimmune regulator gene
APECED	autoimmune polyendocrinopathy-candidiasis-ectodermal dystrophy
APS1	autoimmune polyendocrine syndrome type 1
CV	cross-validation
DBSCAN	density-based spatial clustering of applications with noise
DNA	deoxyribonucleic acid
ELISA	enzyme-linked immunosorbent assays
ENSG	Ensembl gene ID
FDR	false discovery rate
GAL	GenePix array list
GPR	GenePix result file format
IQR	interquartile range
PAA	protein array analyser
PAWER	protein microarray web-explorer
PMA	protein microarray analyser
PMD	protein microarray database
RLM	robust linear model
RNA	ribonucleic acid
RPPA	reverse-phase protein arrays
SNP	single nucleotide polymorphism
TIFF	tag image file format
T1D	type 1 diabetes

LIST OF ORIGINAL PUBLICATIONS

Publications included in the thesis

- I Steffen Meyer, Martin Woodward, Christina Hertel, Philip Vlaicu, Yasmin Haque, Jaanika Kärner, Annalisa Macagno, Shimobi C. Onuoha, **Dmytro Fishman**, Hedi Peterson, Kaja Metsküla, Raivo Uibo, Kirsi Jäntti, Kati Hokynar, Anette S.B. Wolff, Kai Krohn, Annamari Ranki, Pärt Peterson, Kai Kisand, Adrian Hayday, Antonella Meloni, Nicolas Kluger, Eystein S. Husebye, Katarina Trebusak Podkrajsek, Tadej Battelino, Nina Bratanic, and Aleksandr Peet. AIRE-deficient patients harbor unique high-affinity disease-ameliorating autoantibodies. **Cell**, July 2016.
- II **Dmytro Fishman**^{*}, Kai Kisand^{*}, Christina Hertel, Mike Rothe, Anu Remm, Maire Pihlap, Priit Adler, Jaak Vilo, Aleksandr Peet, Antonella Meloni, Katarina Trebusak Podkrajsek, Tadej Battelino, Øyvind Bruserud, Anette S.B. Wolff, Eystein S. Husebye, Nicolas Kluger, Kai Krohn, Annamari Ranki, Hedi Peterson, Adrian Hayday, and Pärt Peterson. Autoantibody repertoire in APECED patients targets two distinct subgroups of proteins. **Frontiers in Immunology**, August 2017.
- III **Dmytro Fishman**, Ivan Kuzmin, Priit Adler, Jaak Vilo, and Hedi Peterson. PAWER: Protein Array Web ExploreR. **BMC Bioinformatics**, September 2020
- IV Tamara Knific^{*}, **Dmytro Fishman**^{*}, Andrej Vogler, Manuela Gstöttner, Rene Wenzl, Hedi Peterson, and Tea Lanisnik Rizner. Multiplex analysis of 40 cytokines do not allow separation between endometriosis patients and controls. **Scientific Reports**, November 2019.

Publications not included in the thesis

- I Aigar Ottas, **Dmytro Fishman**, Tiia-Linda Okas, Külli Kingo, and Ursel Soomets. The metabolic analysis of psoriasis identifies the associated metabolites while providing computational models for the monitoring of the disease. **Archives of Dermatological Research**, July 2017.
- II Aigar Ottas, **Dmytro Fishman**, Tiia-Linda Okas, Tõnu Püssa, Peeter Toomik, Aare Märtsen, Külli Kingo, and Ursel Soomets. Blood serum metabolome of atopic dermatitis: Altered energy cycle and the markers of systemic inflammation. **PLOS ONE**, November 2017.
- III William Jones^{*}, Kaur Alasoo^{*}, **Dmytro Fishman**^{*}, and Leopold Parts. Computational biology: deep learning. **Emerging Topics in Life Sciences**, November 2017.

- IV Ardi Tampuu, Maksym Semikin, Naveed Muhammad, **Dmytro Fishman**, Tambet Matiisen. A Survey of End-to-End Driving: Architectures and Training Methods. **IEEE Transactions on Neural Networks and Learning Systems**, March 2020.
- V Ian Walsh*, **Dmytro Fishman***, Dario Garcia-Gasulla, Tiina Titma, The ELIXIR Machine Learning focus group, Jennifer Harrow, Fotis E. Psomopoulos and Silvio C.E. Tosatto. DOME: Recommendations for supervised machine learning validation in biology. **Nature Methods**, May 2021.

Preprints

- I **Dmytro Fishman**, Sten-Oliver Salumaa, Daniel Majoral, Samantha Peel, Jan Wildenhain, Alexander Schreiner, Kaupo Palo, Leopold Parts. Segmenting nuclei in brightfield images with neural networks. **bioRxiv**, August 2019.

* – shared first author.

1. INTRODUCTION

Proteins are essential elements of all living organisms. A great number of life-critical functions depend on these complex molecules. The amount of proteins in an organism's cells is strictly regulated, as an excessive amount or sudden shortage can cause unwanted consequences. Abnormal protein levels can be a sign of a serious malfunction. For example, in the presence of certain types of immune proteins, the immunoglobulins may attack the body's own cells and tissues causing various autoimmune conditions, such as diabetes or multiple sclerosis. Therefore, an ability to accurately assess protein concentrations in the body can be the key to the understanding of various important biological processes including disease mechanisms.

Protein microarray is a popular approach for quantifying protein concentrations in a sample. Hundreds or even thousands of protein concentrations can be measured in parallel. Depending on what is captured on the slide, it is possible to measure either the full proteome of the cell or more specifically autoantibodies present in the sample. Hence, term "protein profiling" in the title of the thesis refers to the computational analysis of such protein targets, mostly autoantibodies, derived from protein microarray experiments. Although protein microarrays do not always provide precise information about the number of proteins participating in the process in a particular sample, their readings help to steer the analysis towards the most promising targets.

Despite protein microarrays having a lot in common with DNA microarrays, due to different biological assumptions, not all computational methods developed for the latter translate well to the former. Therefore, methods tailored specifically to protein microarrays are absolutely necessary to efficiently use the full capabilities of the platform.

The classical protein data analysis pipeline is complex and consists of a series of computational methods applied sequentially. Methods for reducing technical noise, detecting and removing outlier observations, and normalising resulting signal values are all necessary to ensure the validity of the analysis. Statistical tests, as well as machine learning methods, are used to identify individual proteins as well as their combinations with sufficiently contrasting concentration levels between experimental conditions. Finally, enrichment analysis tools help to put such proteins into the perspective of the most prevalent biological functions. In this thesis, we explored computational methods and optimised the data analysis pipeline applicable to data acquired from protein microarray experiments. As a result, we developed and released a web-tool that helps to perform the entire analysis in a semi-automatic fashion. Methods described in this work were put into practice and validated in several protein microarray-related publications.

The work towards this thesis started with an analysis of protein microarray data from a study that explored the autoimmune content of the blood from patients with autoimmune polyendocrine syndrome type 1 (APS1) [1]. In order to define

an initial list of proteins targeted by the autoimmune reaction in APS1 patients, we implemented a protein microarray-specific pre-processing pipeline as well as performed differential analysis.

We aimed at a more profound understanding of the mechanisms behind APS1 condition and autoimmunity in general. Therefore, protein targets identified in the previous publication were studied further [2]. We analysed multiple open databases and public protein datasets to determine common biological factors behind selected protein targets. We used a web server for the functional enrichment analysis to validate our results.

A focal point of this PhD work is the protein microarray web-explorer (PAWER) – an R-based web-tool, developed to enable semi-automatic protein microarray analysis [3]. PAWER incorporates all the relevant computational methods implemented in the previous papers. Its intuitive user interface and step-by-step workflow are designed to help perform protein microarray analysis with ease.

Finally, in the fourth publication included in this thesis, we have explored the value of applying machine learning models along with classical statistical methods discussed in the previous publications. Here we analysed a case-control study of endometriosis [4]. Prior statistical analysis had shown that no individual proteins are capable of distinguishing endometriosis patients from controls based on proteins found in the blood. We used several powerful machine learning methods to evaluate the predictive performance of combinations of proteins. In line with statistical test results, neither model achieved performance significantly better than the random chance. Therefore, machine learning results supported the hypothesis that neither measuring individual proteins nor in combination with others can predict endometriosis and thus help to diagnose the disease in the given samples.

1.1. Main contributions of the thesis

1. Enabling a series of biological findings with a help of a custom all-around protein microarray data analysis pipeline, from protein microarray specific pre-processing and signal normalisation to differential and enrichment analysis.
2. Development of the protein array web-explorer – intuitive web-tool that incorporates computational methods relevant to protein microarrays and enables semi-automatic analysis of protein microarray data.
3. Exploring the application of machine learning methods to protein concentration data, adding a new dimension to classical biomarker discovery practice.

2. INTRODUCTION TO PROTEINS

Life is beautiful in its complexity, and proteins are some of the most fundamental biological elements that enable this complexity. Often referred to as “workhorses” of the cell, proteins are responsible for almost every imaginable item on organisms’ to-do list [5]. Proteins carry out tasks ranging from building tissue and replicating deoxyribonucleic acid (DNA) to enabling timely immune response and facilitating oxygen delivery, albeit different types of proteins are at work. The number of proteins present at any given moment is strictly regulated by cells [6], as any significant deviation from the norm may cause malfunction and even disease. Therefore, information about protein abundance can offer valuable insight into the mechanisms of various diseases. In this work, we focused on quantifying protein abundance in a human body via protein microarray technology. The current chapter will present the biological context relevant to this thesis.

2.1. From DNA to proteins and back

One of the key principles behind the scientific approach is being open to new evidence that contradicts established doctrines. However, there is one scientific dogma that remained present in the discourse over the years – the central dogma of molecular biology. Coined by Francis Crick in 1957 and published in 1958 [7], it states that DNA in the cell nucleus gets transcribed into ribonucleic acid (RNA), which in its turn is used to produce proteins. Although being proven wrong on a number of occasions, e.g., transcription factor proteins that regulate RNA production, the central dogma remains a useful approximation for the most important biological interactions in a cell.

DNA is a long double-stranded molecule that consists of four nucleotides: adenine (A), thymine (T), guanine (G), and cytosine (C). Nucleotides form pair-wise bonds (A with T and C with G), helping to hold two strands of DNA together. Human DNA is made up of approximately 3.6 billion nucleotide pairs forming our complete genetic blueprint. Albeit an impressive number, only a fraction of DNA has been associated with relevant biological functions in the organism. These functional regions are called genes. The role of the majority of DNA remains largely unestablished. Because DNA is a static molecule that never leaves the cell nucleus, to execute biological functions, genes need to send instructions to the rest of the organism. They do it via the process of transcription, which transfers information stored in genes into a molecule called RNA. RNA travels to structures called ribosomes, where both take part in synthesising proteins.

Proteins are complex molecules made up of 20 amino acids, each with its unique chemical properties [8]. Proteins vastly vary in length from about 200 to almost 27,000 amino acids [9]. Such variability naturally implies rich structural and functional diversity of resulting molecules. The total number of proteins in humans remains a subject of scientific debate, with estimates ranging from

modest 20,000 proteins, if assumed that one gene is responsible for one protein (i.e., canonical proteins) to hundreds of thousands if the combinatorial nature of gene expression and alternative splicing is taken into account [10]. While some proteins leave the native cell to operate elsewhere (e.g., pancreas produces insulin to help regulate blood sugar level), others remain to help facilitate domestic processes, including regulating the gene expression. Transcription factor proteins bind to DNA and either suppress or enhance RNA production of nearby genes, directly violating the basic premise of the central dogma of molecular biology. This creates a cycle of regulation, where genes create RNA that initiates the production of proteins, which in their turn regulates the gene expression.

Proteins do most of the work in cells and tissues and are required for many critical processes in the body [8]. For example, the immune system employs special types of proteins – antibodies to recognise foreign substances and fight infections. Most of the work presented in this thesis is focused on antibodies and their role in immune response, therefore the following section will dive into immunity.

2.2. The immune system

Despite continuous advances in the understanding of the immune system, the subject of the matter remains so vast and complex that we consider an in-depth discussion of immunity to be well beyond the scope of this thesis. The section below is meant to introduce readers to the most central concepts that are essential for the autoimmunity discussion that will follow.

The term *immunity* comes from Latin *immūnitās*, which referred to legal protection offered to Roman senators during their time in the office [11]. In biology, immunity is defined as the defense system of an organism from infections and other intruders. The immune system is a large network of cells, tissues, and organs that tirelessly work together to protect the organism from anything that is recognised as an ‘invader’ or ‘foreign’, for example, bacteria, virus, parasite, cancer cell, or toxin [12]. While not all invaders are necessarily harmful, those foreign substances that have disease-causing potential are called *pathogens*.

The immune system can be broadly divided into two main subsystems: *innate* and *adaptive* immunity [12] (Figure 1). Innate immunity is the first line of any organism’s defence, it employs a wide set of strategies that are not directed against anyone pathogen in particular, but rather designed to protect against all possible threats. Skin is a prominent example and a key component of the innate immune system. Skin acts as a primary physical barrier between pathogens and the organism. The adaptive or acquired immunity supports innate immunity in defending against intruders. The adaptive immune system interacts with molecules (most often proteins), known as *antigens*. Antigens are present on the surface of the pathogens and can guide the immune response [13]. Unlike innate immunity, which has evolved to be antigen-independent, adaptive immunity is highly

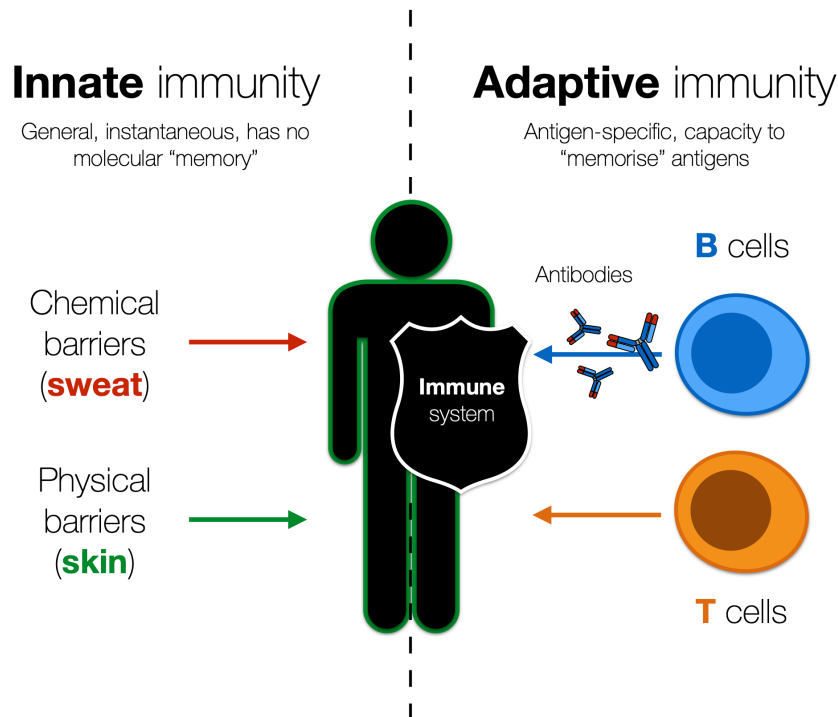


Figure 1. Immune system can be broadly divided into two subsystems: innate and adaptive immunity. Two systems supporting each other in their own ways to fight intruders. With the latter being slower and more specific, while the former is faster and more general.

specific to *antigens* in its response.

The two main types of cells involved in the adaptive immune system are B and T cells. While the T cells target intracellular pathogens by directly triggering cell death mechanisms in the pathogen-infected cells, the B cells are mainly involved in targeting extracellular pathogens. After recognising foreign antigens on the surface of the pathogen, B cells differentiate into *plasma B cells* that produce *antibodies*. An antibody is a large Y-shaped protein that binds to a specific antigen. The structure of a typical antibody is presented in Figure 2. Produced antibodies bind to the cognate antigen which results in neutralization of this particular pathogen. Remaining antibodies are then circulating in the bloodstream where they can initiate the immune response.

Normally, the adaptive immune system produces T cells, B cells, and antibodies that are capable of living harmoniously together with the body's own cells, which are usually referred to as *self* [14]. Albeit, sometimes, due to various environmental and genetic factors, the immune system produces cells and proteins that can harm its own host, in a process called an *autoimmune reaction* or *autoimmunity*. Such cells are then called *self-reactive* or *auto-reactive*, as they attack domestic cells. These attacks may have a negligible effect if they occur rarely

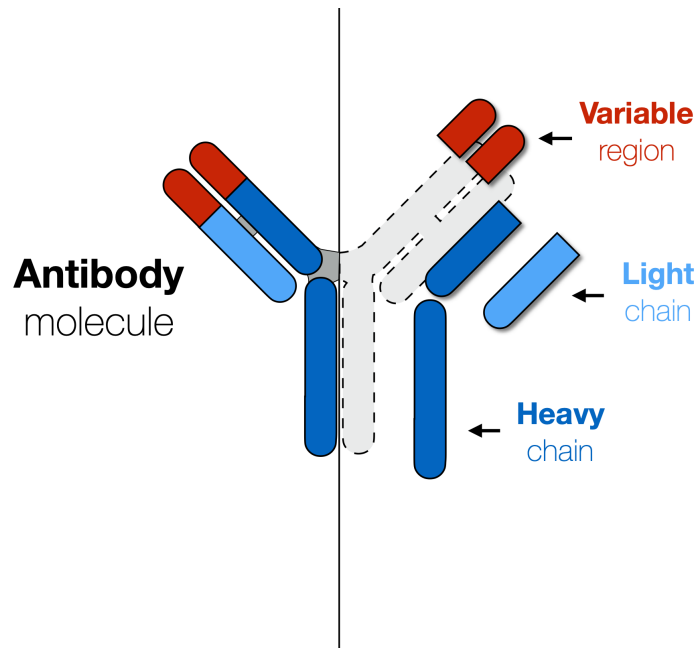


Figure 2. Structure of a typical antibody. Antibodies use their variable regions (coloured in red) as arms to bind to potential intruders. By binding to a molecule, antibodies send a signal to other immune cells to take action against the intruder.

or are mild [15]. However, more systematic failures accumulate and may lead to serious damage, causing various pathologies or even, in some circumstances – premature death, and more so among women [16].

Typically, self-reactive B cells and T cells are safely removed or silenced by the immune system prior to any serious harm [17]. Two mechanisms are mainly responsible for eliminating malfunctioned immune cells: *central* and *peripheral* tolerance [15]. Central tolerance normally occurs inside primary lymphoid organs: thymus and bone marrow and it targets self-reactive T cells and B cells in their infancy. Peripheral tolerance acts as a backup filter as it selects out self-reactive immune cells which central tolerance has failed to identify and neutralize.

As part of the central tolerance, T cells undergo a two-stage selection procedure in the thymus [15]. In the first stage (positive selection), immature T cells are tested for their ability to interact with special antigen-presenting cells in the thymus. T cells-to-be that show a lack of interest in such targets at this stage is eliminated. Later, in the second stage (negative selection), T cells are tested for the binding capacity to self. For this, a set of *self-antigens* (i.e. antigens that belong to the body's own cells) is assembled with help of the autoimmune regulator gene (AIRE) and displayed to prospective T cells that successfully passed the first stage [18]. Only cells that ignore self-antigens are subject to further development [19]. B cells are also subjects to central tolerance, although the exact details remain poorly understood [1]. Nevertheless, the tolerance in B cells is

partly T cell-dependent, with defective T cells contributing to the production of autoreactive B cells [20, 21]. In healthy situations, B cells produce antibodies for our protection against pathogens but in case of bypassing defensive mechanisms of the immune system, self-reactive B cells produce antibodies that tag the organism's own cells and may trigger autoimmunity. Such self-reactive antibodies are called *autoantibodies*. Thus, failure to recognise and mitigate self-reactive T and B cells may potentially lead to the accumulation of autoantibodies and result in autoimmune disorders [22].

2.2.1. Autoimmune disorders

Autoimmune diseases affect about 5% to 7% of the world population, with the majority of patients being women [23]. The most famous examples of autoimmune diseases are type 1 diabetes (T1D), celiac disease and multiple sclerosis [24]. For instance, the onset of type 1 diabetes is caused by an autoimmune reaction against insulin-producing β cells in the pancreas [25], exogenous gluten proteins are linked to the autoimmune reaction in celiac disease [26, 27] while patients with multiple sclerosis harbor autoantibodies against myelin i.e. fatty tissue in the brain and spinal cord that facilitates neurotransmission [28].

One of the autoimmune disorders – autoimmune polyendocrinopathy-candidiasis-ectodermal dystrophy (APECED) or autoimmune polyendocrine syndrome type 1, is of particular importance for the researchers and doctors who study autoimmunity. APECED is a rare disorder caused by a small modification in genetic code. Mutations in the AIRE gene alter negative selection mechanisms that normally prevent the body from producing harmful autoantibodies. As a result, a wide range of autoantibodies is released into the bloodstream, causing various types of damage to the organism's own cells and tissues. Many of these autoantibodies that are produced in APECED are shared with other diseases such as autoantibodies against β cells in T1D [2]. Precisely due to such high diversity of self-reactive antibodies, APECED is considered an important disease model that helps to understand the processes that drive autoimmunity in general [29]. The study of APECED is central for two publications included in this thesis, which we will examine in later chapters.

Autoantibodies have been shown to play an important role in many other diseases: various cancers, neurodegenerative diseases, cardiovascular and infectious disorders. However, the direction of the association between autoantibodies and disease onset is not always clear – do autoantibodies cause disease or whether autoimmunity is merely a side effect [30]? Nevertheless, it has been demonstrated that the presence of autoantibodies in blood, may suggest the development of a disease and provide information about its nature and intensity [31]. Studies show that the information about the quantity of disease-specific autoantibodies may provide decisive diagnostic information [24, 25, 32–35]. Therefore, detecting and characterising autoantibodies present in the organism may shed light on the

disease development.

One of the earliest attempts to experimentally detect the presence of an antibody engaged in a reaction against a patient's own tissue was successfully carried out in 1955 by Dr. Henry Kunkel [36]. Dr. Kunkel used antibodies tagged with a fluorescent marker (also known as secondary antibodies) to detect autoantibodies in lupus erythematosus cells extracted from the serum of patients with systemic lupus erythematosus disease [37]. Later, a number of simpler and more accurate methods have been developed: radiobinding assay, western blot, and enzyme-linked immunosorbent assays (ELISA). These methods allowed for the detection of antibodies associated with a pre-defined antigen [38]. A need for an *a priori* hypothesis about the antigen was a significant limiting factor, preventing the discovery of autoantibodies against new previously deemed unrelated antigens. Therefore, in order to discover novel autoantibodies, researchers needed a way to screen a much wider range of potential candidate molecules in a high-throughput manner [24].

2.3. DNA microarrays

DNA microarray technology was developed in the 1990s by the American researcher Patric O. Brown and has revolutionised the analysis of biological systems [38, 39]. DNA microarray is a collection of microscopic DNA fragments, short sections of genes printed on a solid surface [38]. A biological sample containing fluorescently labeled complementary DNA or RNA molecules can be then applied to each array enabling researchers to quantify the expression of each gene i.e. gene productivity. DNA microarrays were the first high-throughput technology enabling quantification of gene expression in a parallel fashion using minimal sample input requirements [38]. Soon after the first DNA microarrays appeared it was demonstrated that similar technology involving protein binding molecules can be used to estimate the number of proteins, including autoantibodies from patients' blood [38]. Therefore DNA microarrays have played a pivotal role in the emergence and the development of protein microarrays.

2.4. Protein microarrays

Similar to DNA microarrays, protein microarrays (or protein chips) contain a large collection of individually isolated (purified) molecules, densely printed on the solid glass-based surface [34]. Based on the type of molecule incubated on the slide, protein microarrays can be categorised into three broad groups: *functional*, *analytical*, and *reverse-phase* [40, 41]. Functional protein microarrays are produced by printing full-length proteins on the glass surface. Printing the entire protein helps to preserve its original structure and as a result, also function. Functional protein microarrays detect autoantibodies that bind to the proteins on the slide. This type of arrays gained a lot of popularity in the last decade, with the

number of clinical applications steadily growing [42]. In contrast to functional microarrays, analytical or capture arrays utilize panels of antibodies attached to the slide to detect and measure proteins from the sample [41]. Instead of printing an arbitrary set of antibodies or proteins on the slide, in reverse-phase protein microarrays (RPPA or also known as lysate arrays), all proteins from a specific cell interior (lysate) are printed and the antibody binding from the sample is detected [41, 43]. In this thesis, we are going to focus solely on functional protein microarrays that are used to detect and measure the abundance of autoantibodies in the blood [38].

2.4.1. Functional protein microarrays

In order to use functional protein microarrays to accurately quantify the amounts of autoantibodies, at first, a sample in the form of plasma, serum or other solution from a human subject is applied to protein microarray slides. Autoantibodies from human sample bind to proteins immobilized on microarray surface in spots or tiny cavities in the glass. Array slides are then washed and dried to get rid of all molecules that failed to bind and remained on the surface. Later, autoantibodies that have genuinely bound to spotted proteins are detected by applying fluorescently labeled secondary antibodies. Microarrays are then again washed and dried. Fluorescent signals coming from each well are acquired with a microarray scanner and later analysed using computer software [34]. The amount of light coming from each well is associated with the levels of autoantibody binding to the specific protein (from this well). Schema of a typical protein microarray is presented in Figure 3.

Fabrication and further handling of functional protein microarrays is a complex process. It involves multiple consecutive steps including printing and immobilization of proteins on the slide surface, incubation with a sample, repeated washing, and drying and scanning of arrays. Hence, a substantial number of technical factors influence the quality of the resulting autoantibody binding signal [44]. Uncalibrated printing machinery may result in uneven distribution of proteins in spots or in proteins being carried over to neighbouring sites by the printing pin. Irregular washing and drying of the slides can also cause the variation of the actual protein content [45]. Several studies have reported a cross-talk between neighbouring spots that resulted in unlikely highly correlated signals between neighbouring spots [2, 46]. Technical variability introduced by mechanical liabilities can mask the true underlying biological signal [47]. Therefore, sufficient care must be taken in design, fabrication, and subsequent analysis to account for possible technical biases.

ProtoArray human protein microarray. One of the most popular examples of wide coverage commercial protein microarrays is ProtoArray[®]. Originally designed and manufactured by Invitrogen company, ProtoArray[®] became a part of the Life Technologies brand in 2008 that was later acquired by Thermo Fisher

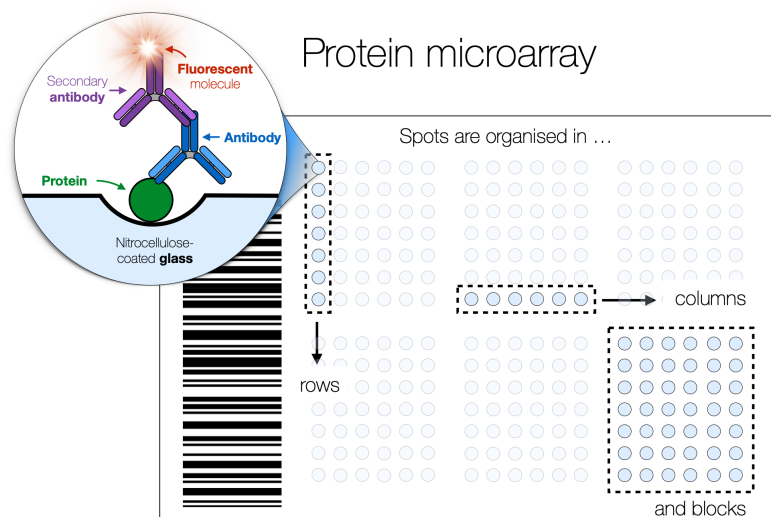


Figure 3. Schema of the exemplary protein microarray. In functional protein microarrays, proteins and protein fragments are printed inside spots (blue circles) arranged in rows, columns and blocks.

Scientific in 2014. ProtoArray[®] includes more than 9,000 full-length human proteins as well as several thousand control proteins. All proteins are spotted twice on the array to enable quality control. More than 6,100 proteins that are included on the chip are potential drug targets and thus, relevant to disease processes. Data from ProtoArray[®] experiments can be analysed by a number of publicly available tools including the manufacturer's own – ProtoArray Prospector. ProtoArray[®] has a broad spectrum of potential applications, including discovering novel disease biomarkers via analysing autoimmune reactions, discovery, validation, and development of novel drug targets [44]. Nevertheless, the majority of studies that used the technology have focused on discovering and characterizing autoimmune targets from the blood in a specific disease [1, 2, 24, 33, 34, 48].

Experimental data produced via ProtoArray[®] platform has been shown to suffer from a multitude of technical errors [44]. Printing and contamination artifacts, non-specific protein binding, and high background signal all were shown to contribute to the distortion of biological findings, and reduced reproducibility of the experiments [44]. In later chapters, we discuss some methodological ways to tackle these challenges. Perhaps in part due to the aforementioned technical biases in 2018, Thermo Fisher Scientific has discontinued all the services related to ProtoArray[®]. Despite this, a large number of experiments involving ProtoArray[®] had been performed, and much of this data was made available through data repositories like Gene Expression Omnibus [49] and ArrayExpress [50]. This publicly

available data remains valuable for many researchers who plan to either reproduce old results or make their own analysis of protein microarray data.

HuProt human protein microarray. HuProt is an actively maintained alternative platform to ProtoArray[®]. Initially developed by CDI laboratory at John Hopkins University in 2012 [44, 51], HuProt contained 16,368 full-length functional proteins, representing 12,586 protein-coding genes [44, 52]. At the time of writing, the most recent Human Protein Microarray v4.0 in total contains more than 21,000 unique human proteins and protein variants, covering more than 81% of the canonical human proteome. Similar to ProtoArray[®], HuProt has mostly been used for detecting and evaluating autoimmune reaction in patients across various disorders, including: primary biliary cirrhosis [51], ovarian [53] and gastric cancers [54], neuropsychiatric lupus [55] and Behcet's syndrome [56]. As a data generation platform, HuProt was shown to be susceptible to similar biases as ProtoArray[®], including non-specific binding and printing contamination [44].

Custom protein microarrays. Both equipment and constituents necessary for creating custom protein microarrays are commercially available from private and public vendors. Also, fully assembled protein microarrays are available on the market. Coverage of commercial microarray products ranges from arrays with few dozens of carefully selected proteins to vast collections that include almost the entire known proteome [38].

In preparation for this thesis, mostly data from ProtoArray[®] and HuProt protein microarrays were used.

3. PROTEIN MICROARRAY DATA ANALYSIS

Protein microarray chips are high-throughput platforms capable of measuring thousands of protein interactions in parallel across multiple samples [57]. Computational analysis of a typical protein microarray study starts with acquiring high-resolution images of stained protein arrays, using the special microarray scanner (e.g. GenePix Microarray scanner). Signal information about each spot on the array is then extracted into a file by segmentation and registration software (e.g. GenePix Pro 7). Each array usually results in one file. Data from such files is then used to assemble a data matrix, which serves as an input to the analysis pipeline. Each column in such a matrix represents an individual sample while a row is associated with a protein. This initial matrix is called raw data, as it has not been “purified” by pre-processing methods. Techniques such as background correction, signal transformation, outlier detection, and normalisation are essential for further statistical analysis as they help to remove or at least minimise the effects of technical noise and thus, enable a fair comparison between samples. Normalised and pre-processed data can be visualised and explored further. If a study follows a case-control design [58] (including Publications I, II, and IV in this thesis), it is possible to compare protein signals in patients with those in healthy individuals. This enables researchers to pinpoint proteins in which concentration levels can reliably differentiate patients from controls. Such differential proteins can both be used as clinical biomarkers as well as reveal important insights about the mechanisms of the disease.

Protein microarray analysis has notably benefited from the set of analytical methods developed for DNA microarrays, as both technologies enable measurement of numerous molecules immobilised on the slide surface, e.g. the array scanning approach [47]. But as it soon turned out, not all statistical methods designed for the DNA microarrays may directly be applied to the protein microarrays, as the latter is grounded on different biological assumptions. Namely, DNA microarrays assume comparable levels of gene expression across individuals regardless of their clinical condition. While this may be true for genes, the number of autoantibodies present in the blood of a healthy person and a patient is vastly different [44, 47, 57]. Such discrepancy between assumptions has motivated the use of a different normalisation strategy from the one used in DNA microarrays, which will be discussed in the sections below.

In this thesis, we describe a set of computational methods used to analyse functional protein microarray experiments. These techniques are bundled together into a general data analysis pipeline (Figure 4), which treats raw GPR files as an input while providing normalised data, a list of differential proteins, and the results of the enrichment analysis as an output. The pipeline was first designed as means to analyse data in Publication I, it was later expanded for Publication II, and finally packaged and released to the public as a web-tool (PAWER) in Publication III. Finally, in Publication IV we have explored the utility of using

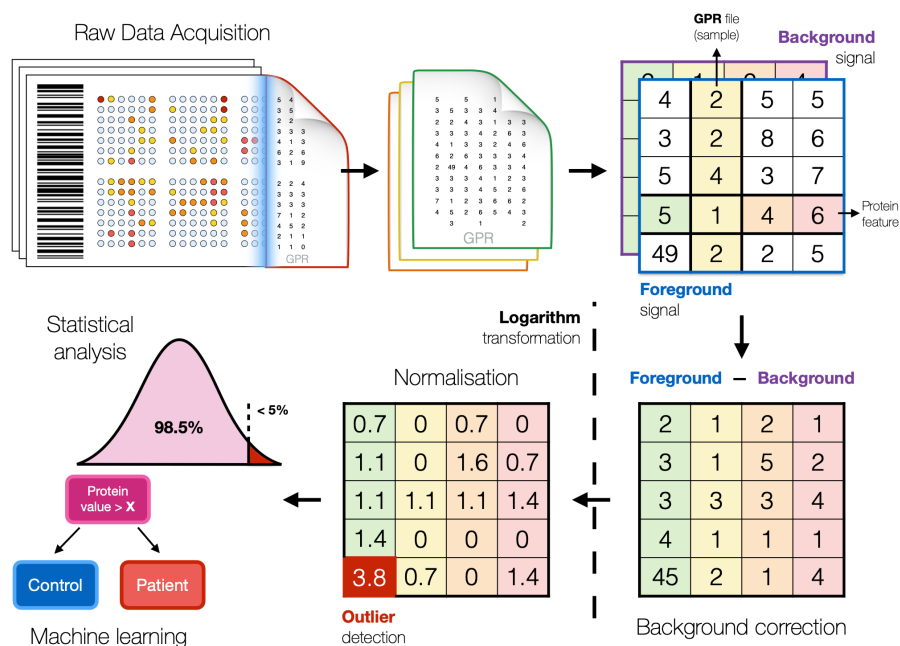


Figure 4. A rough outline of data analysis methods used for protein microarray experiments. Raw data after the acquisition is assembled into a large matrix. This matrix passes through a number of steps, including background correction, signal transformation, outlier detection, and normalisation before being used as an input for statistical analysis and machine learning. Next, results of statistical analysis and machine learning modelling are interpreted in the context of the existing body of knowledge.

machine learning methods alongside classical statistical algorithms described in previous publications with a goal to increase the choice of methods available for analysis. Below, we describe each essential part of our pipeline in detail.

3.1. Raw data acquisition

The process of data acquisition starts with scanning incubated arrays with a special microarray scanner that produces high-resolution 16-bit images. These images are saved in Tag Image File Format (TIFF) data format and later processed by the image segmentation and registration software (e.g. GenePix Pro 7). This software accurately detects each spot and quantifies its signal intensity with respect to the local background. Then the software uses information about each spot's location and contents to link estimated intensity values with corresponding proteins that were printed on the microarray. Data about array design and spatial location of each protein is stored in an auxiliary GenePix Array List (GAL) file and can be added separately to the analysis. Finally, estimated intensities from an

individual array are saved into GenePix Result (GPR) file – a *de facto* standard format for storing protein microarray data [24]. Each collected sample normally corresponds to one GPR file. Typical protein microarray studies collect dozens or even hundreds of samples, resulting in a corresponding number of GPR files.

GPR files are text files in disguise, hence, they are tab-delimited text files that can be read by most popular spreadsheet programs such as Microsoft Excel. GPR files contain a header with relevant meta-information about the experiment and the data matrix, which contains raw fluorescent intensity values of each spot on the chip. If several fluorescent molecules with different wavelengths were used in the experiment, foreground and background signals are measured and reported for each. Different types of arrays may have vastly different contents of both meta-information and intensity matrix. In this thesis, mostly GPR files from ProtoArray and HuProt platforms were analysed, thus we will focus on them.

3.2. Data pre-processing

At the beginning of the protein microarray analysis, researchers extract individual raw signal values from GPR files and combine them into a large matrix of raw data. Multiple studies have shown that raw protein microarray data should not be used directly in the computational analysis [24, 44, 47]. Various technical issues discussed previously can introduce a significant amount of noise into the output signal [24, 44, 47]. This noise can hinder the analysis by masking the true signal, rendering the final results indecisive. Therefore, raw data must be carefully pre-processed prior to any further analysis. Pre-processing helps to identify and get rid of technical noise at the same time preserving valuable biological signal. Below we discuss a set of common pre-processing strategies, which can be applied in various orders depending on the experimental setup.

3.2.1. Background correction and signal transformation

In functional protein microarrays, proteins of interest are immobilized in rows and columns on the glass surface forming a grid of spots [59]. After a slide is incubated with a sample solution (usually blood), autoantibodies bind to immobilized proteins. One of the technical challenges related to correctly quantifying the fluorescent signal emitted by the labeling antibody is to discriminate signal produced by the genuine biological reaction and local residuary background light [44, 59]. The true signal is usually derived by subtracting the median background intensity of the spot, i.e. *background signal*, from the amount of fluorescent signal registered within the spot, i.e. *foreground signal* (Figure 5) [24]. However, several other more elaborate background corrections methods have been proposed in the past [45, 60, 61]. For example, it has been suggested that instead of using an immediate local background intensity it is beneficial to consider a wider neighbourhood of the spot when calculating the median background signal [45].

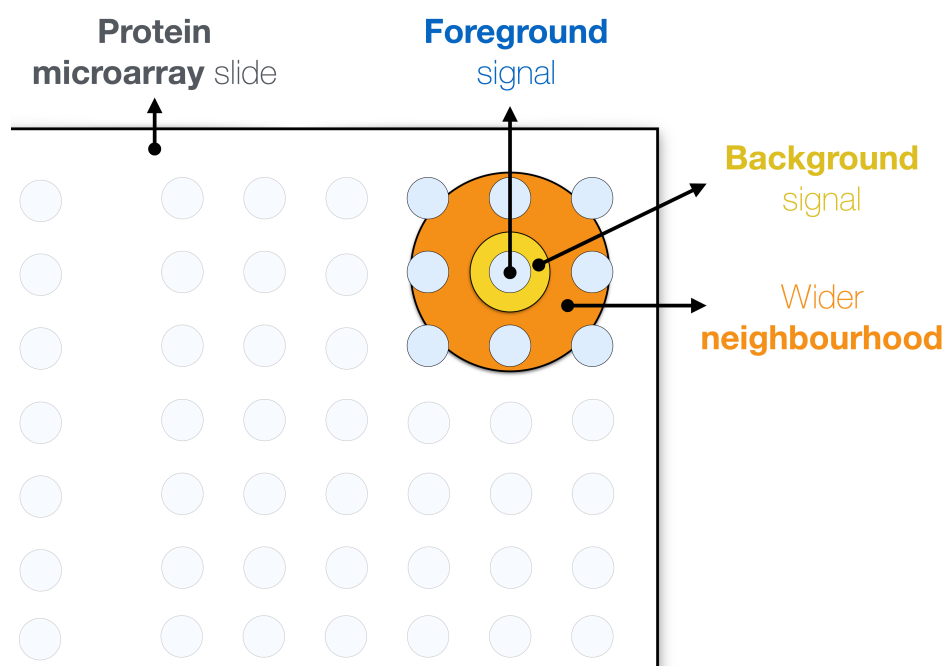


Figure 5. Foreground signal, background signal and wider neighbourhood of the spot. The fluorescent signal of the protein is determined by subtracting the median of the immediate background of the spot from the median of its foreground signal. Alternatively, background value can be calculated taking a wider neighbourhood of the spot into consideration.

Another commonplace practice in biomedical research is to apply one of the data transform techniques. For example, log-transformation is known to make fold changes symmetric around zero, reduce the skew in the data, and provide a good approximation for the normal distribution – desirable property for many methods [24,62], including protein microarray specific normalisation strategy that we are going to discuss in a later section. In spite of some researchers revealing negative effects of logarithm-based data transformation [62], it remains popular and was used in a number of recently published works related to protein microarray analysis [46,48], including Publications I and II included into this thesis [1,2].

3.2.2. Outlier detection

In order to satisfy assumptions imposed by most of the statistical methods, protein expression levels registered by a panel of protein microarrays should follow a normal distribution: most of the values being close to the average signal with few very low and high values in the tails. However, in practice, due to a multitude of technical factors e.g. inattentive handling of microarray slides, sample quality, or manufacturing errors, proteins can exhibit expression levels vastly inconsistent with the rest of the data. Such proteins are known as *outliers* or “anomalous data points”. In protein microarray experiments, both individual proteins and entire microarray slides may exhibit abnormal expression levels and thus considered anomalous. The presence of outliers can be unfavourable for the downstream analysis and resulting conclusions [63]. Hence, once detected, such values usually are either removed completely or substituted with a reasonable approximation e.g. average or median of the corresponding protein.

Several methods exist to automatically detect outliers. One of the most popular and suitable for data that follows normal distribution is to label as outliers all data points that fall outside three standard deviations from the corresponding mean (*i.e. three-sigma rule* or *empirical rule*). The common assumption is that such extreme values are unlikely to be generated by the same biological process as the rest of the data. This reasoning is based on the definition of the normal distribution, for which 95.45% of its data lie within two standard deviations from its mean, while 99.73% within three standard deviations. If the value is either larger or smaller than the aforementioned threshold of three standard deviations, it has only 0.27% of the chance to come from the same distribution as other values. This line of thought is valid only in case data follows the normal distribution. In other circumstances, the above calculations may not apply. In practice, it has been shown that protein expression profiles vary a lot between individuals rarely resulting in signal values that follow the normal distribution [1,2,64,65]. Therefore data from protein microarray experiments must be transformed (e.g. using log-transform) if the three-sigma rule is to be applied.

Another popular approach for identifying outliers is using boxplots [66]. Boxplots are graphical structures, that show how the data points are spread out. Box-

plots have at least two relevant merits. Firstly, they offer a natural way to visualise the data, and secondly, they can be used to detect outliers in a way that is indifferent to the underlying data distribution. Boxplot summarises data using five quantitative measures: minimum, three quartiles, and maximum. While the second quartile (Q_2) corresponds to a median (middle value), the first (Q_1), and the third (Q_3) quartiles enclose the first 25% and 75% of data distribution respectively. The distance between the first and third quartiles is called the interquartile range (IQR) and given by $Q_3 - Q_1$. Genuine data points must be larger than $Q_1 - 1,5 * IQR$ and smaller than $Q_3 + 1,5 * IQR$. Data points outside this range are considered to be outliers. Boxplots are usually rendered as rectangles (hence the name “boxplot”) with a fixed width, and length equal to IQR , with outliers, visualised as circles outside of the box either at the top or bottom of the figure. Although boxplots can be plotted side by side to compare distributions of multiple features, they are not suitable for identifying outliers from multivariate data (i.e. data points characterized by more than one feature).

Clustering techniques in combination with various visualisation strategies can be used to recognise outliers in multivariate data, such as protein microarray readouts. Hierarchical clustering is an algorithm that recursively groups data into clusters based on a predefined distance metric e.g. Euclidean distance [67]. The result of hierarchical clustering is a dendrogram. Dendrogram visually shows the arrangement of clusters produced by the algorithm. Anomalous samples or proteins will stand out far from the rest of the clusters on the dendrogram, making them easy to spot and remove. Dendrograms are often coupled with another visualisation approach named heatmaps (Figure 6). Heatmaps use colour to represent the magnitude of individual signals. Heatmaps supplement dendrograms with an additional context about single expression values. Despite enabling rich visualisations, hierarchical clustering does not label samples as outliers automatically. One of several metrics can be used on top of hierarchical clustering results to detect clusters and therefore identify outliers (e.g. elbow method and silhouette score). Density-based spatial clustering of applications with noise (DBSCAN) is another clustering method that uses the spatial density of points as a factor for creating clusters [68]. Data points from the low-density regions, far from established clusters are considered to be outliers or noise. Therefore, unlike hierarchical clustering, DBSCAN can detect outliers without human intervention. However, DBSCAN requires several key parameters to be fixed to work. Although DBSCAN is the only technique mentioned in this section that was not explicitly applied in publications included in this thesis, we consider it to be an important addition, potentially valuable for the readers that may decide to use it in their work.

3.2.3. Signal normalisation

One of the primary goals of protein microarrays is to compare the amount of binding between individual samples or groups of samples (e.g. healthy and controls).

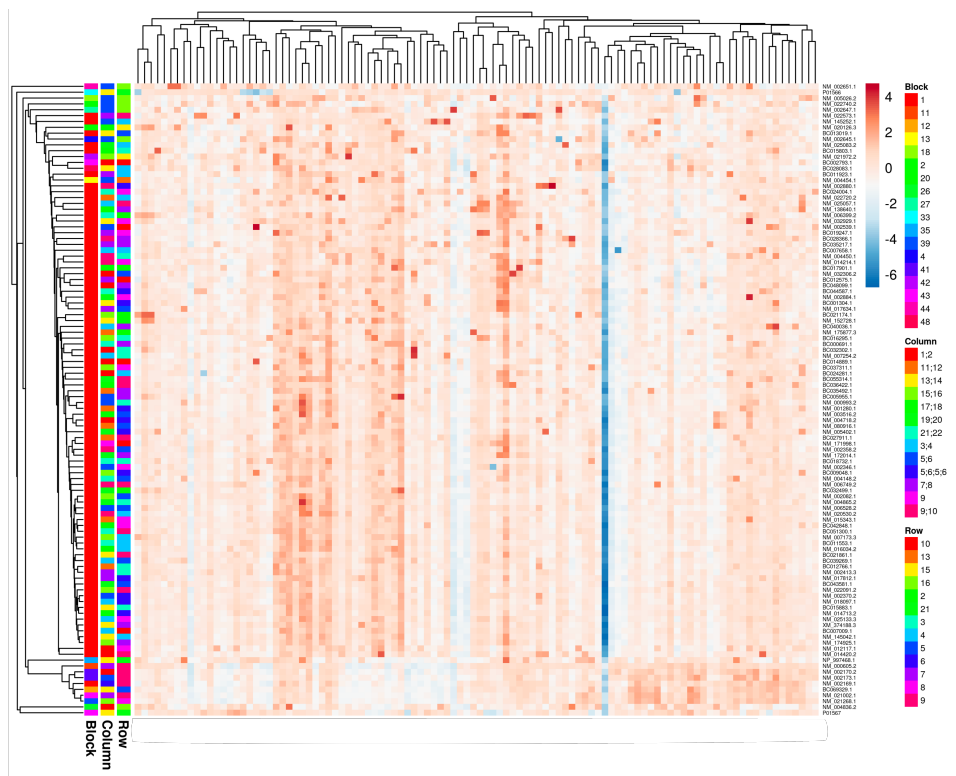


Figure 6. An example of a heatmap obtained from a protein microarray experiment using ClustVis tool. Each cell of the heatmap is coloured based on the signal level of the corresponding protein (in rows) across all samples (in columns). Additional meta-information available about samples and proteins is visualised using extra colour legends. Hierarchical clustering results are presented in the form of dendrograms at the top and on the left of the heatmap.

For this process to yield realistic results, the protein binding signal measured from multiple arrays must be comparable. This can be problematic due to the potential difference in the number of proteins printed on the slides and other technical factors that can introduce systematic biases [45]. Such biases may significantly distort or shift signal distribution for some or all proteins on one or several protein microarrays. Therefore, unlike the above-mentioned data pre-processing approaches, signal normalisation acts globally combining information about signal variation from all arrays and proteins to successfully eliminate non-biological differences. The most commonly used approaches for protein signal normalisation were adopted from the DNA microarray context. These techniques, make strong assumptions about underlying signal distribution, which are not always in line with biological mechanisms at work in protein microarrays [24, 47, 60]. Protein microarray-specific normalisation strategy based on robust linear model [47] makes use of control proteins printed on each array and block. Control proteins can be positive or negative, but in either case, they are assumed to exhibit constant signal levels across all samples. Any differences in signal values of these proteins are considered to be technogenic and thus, corrected for. Below we present some of the most popular approaches for signal normalisation implemented in the computational tools used for protein microarray analysis [3, 44, 69].

Global scaling. One of the standard methods for most DNA microarrays (e.g. Affymetrix platform) that was also applied in protein microarrays is the global scaling approach [47, 70, 71]. In short, the signal levels of each array are divided by the median signal of the corresponding array. Namely, for each array S , normalised signal S_n would be calculated as

$$S_n = S / \text{median}(S)$$

[47, 71]. This ensures that the median signal is the same across all arrays. The global scaling method assumes that the total amount of signal is the same in all arrays. Although this assumption may hold for DNA microarrays, where approximately the same number of genes is expressed regardless of the phenotype, it may not be true for protein microarrays [44]. For example blood from patients with an autoimmune disease is expected to contain more autoantibodies and therefore produce a higher total signal comparing to serum from healthy individuals.

Quantile normalisation. Quantile normalisation substitutes the largest value in each array with a median (or mean) of the largest values across arrays, all second largest values with a median of the second-largest values, etc. [47, 70]. This algorithm assumes that signal distribution for all arrays is nearly the same while major differences between samples are mainly of technical, not the biological origin, which can be the case for DNA microarrays [44]. However, as discussed previously, the autoimmune profile has been shown to be very heterogeneous [1, 2, 64, 65] with a subset of protein features demonstrating a signal very different from the rest of the platform. Therefore, samples can produce distinct distributions due to genuine biological differences. Quantile normalisation thus

eliminates such biologically legible differences, by equalising the underlying distributions.

Cyclic loess. Cyclic loess normalization is performed for a pair of microarrays, and its main intuition is usually described using the so-called M versus A plot (MA plot) [72]. Here M is the difference of \log_2 expression values, and A is the average of \log_2 values. More formally, for a pair of arrays i and j and protein p ,

$$M_p = \log_2(x_{pi}) - \log_2(x_{pj}) = \log_2(x_{pi}/x_{pj})$$

and

$$A_p = \frac{1}{2}(\log_2(x_{pi}) + \log_2(x_{pj})) = \frac{1}{2}\log_2(x_{pi} * x_{pj})$$

[70]. Thus, the MA plot for any pair of microarrays can be illustrated as a scatter plot with M_p on the y-axis and A_p on the x-axis. Similar to quantile, cyclic loess normalization assumes that the expression of the vast majority of genes (in the case of DNA microarrays) does not change between the conditions, therefore two perfectly normalized arrays would result in a MA plot in which points are scattered around $M = 0$ line [72]. Locally estimated scatterplot smoothing curve, which is also referred to as *loess* is computed for the given MA plot to estimate the deviation from the ideal $M = 0$ line [73]. A correction factor is then applied to individual signals of both arrays to achieve convergence of the loess curve and the ideal line. If there are multiple arrays in the experiment, the above procedure is applied until all possible pairs have been compared and normalised. Typically, several cycles of the algorithm are required for the final convergence [72]. However, if the number of arrays is large, a substantial amount of time is needed to make sure all arrays are normalised.

Robust linear model. Robust linear model (RLM) [47] makes use of special sets of proteins – controls that are often built into protein microarrays to enable normalisation of the signal. Controls can be either positive, that are guaranteed to have a high signal regardless of the blood content, or negative that should not react with serum under any circumstances, for example on microarray slides it is common to use empty spots as negative controls. Controls are present on every array as well as in every block of proteins on each array. Any significant deviation in the control signal may indicate the presence of unwanted noise or bias. Hence, RLM is employing controls to quantify and control for potential biases associated with arrays and blocks.

To estimate such biases, observed signal s_{ijk_r} from the array i , block j , control protein k and probe r is modelled as a linear combination of the following coefficients: α_i from an array, β_j from a block, τ_k from a protein feature and random noise ε_r using the following formula [47]:

$$s_{ijk_r} = \alpha_i + \beta_j + \tau_k + \varepsilon_r \quad (3.1)$$

The linear model presented by 3.1 is built iteratively via a re-weighted least-squares algorithm that assigns weights to individual observations depending on

their distance to the fitted curve. In order to make the algorithm more robust to outliers, the median is used instead of the more conventional sum of least squares to drive the optimization process [47]. Once the model is trained, the coefficients associated with each array and block are calculated (α and β in 3.1). The values of these coefficients describe how much signal of control proteins on a particular array or block deviates from the average. These deviations are considered to be of technogenic origin and thus, the normalised signal is calculated by subtracting corresponding coefficients from the signal of each spot as follows:

$$s'_{ijk} = s_{ijk} - (\alpha_i + \beta_j)$$

for all possible i and j values. Figure 7 describes the normalisation process using RLM. In publications presented in this thesis, RLM normalisation was implemented in R, using functions from MASS [74] and limma [75] packages.

There is another, likely more familiar way to represent the linear model presented equation by 3.1 using matrix and vector notation:

$$\mathbf{y} = \mathbf{X}\mathbf{w} + \varepsilon \quad (3.2)$$

Here, we will discuss how the latter equation (3.2) can be translated into the former (3.1) using an artificial example. Variable \mathbf{w} from the latter equation is a vector of all coefficients of the linear model, namely: $\{w_0, w_1, \dots, w_n\}$, where n is the total number of coefficients included into the linear model. These coefficients reflect contributions from arrays, blocks and protein features. If we decide to call coefficients that represent contributions from arrays α , from blocks β and from protein types τ , vector \mathbf{w} will transform into $\{\alpha_0, \alpha_1, \dots, \alpha_{n_a}, \beta_0, \beta_1, \dots, \beta_{n_b}, \tau_0, \tau_1, \dots, \tau_{n_t}\}$, where n_a , n_b and n_t represent the total number of arrays, blocks and types of control proteins respectively, such that $n_a + n_b + n_t = n$. Matrix \mathbf{X} in equation 3.2 is of size $S \times n$, where S is the total number of control signals in the experiment, including all possible copies. For example, the total number of control signals (S) in the experiment with two arrays, two blocks on each array, and three types of controls is 12 ($2 \times 2 \times 3$), provided that each control protein is present in each block and each array. At the same time, the number of coefficients n in \mathbf{w} for the same example is 7 (2 arrays + 2 blocks + 3 control types). Each row in \mathbf{X} encodes the location of one control signal. In the same imaginary protein microarray experiment with two arrays, two blocks and three control proteins, the first row of matrix \mathbf{X} might look as follows: $\{1, 0, 0, 1, 0, 1, 0\}$. This control protein therefore comes from the first array (first 1), second block (second 1 at fourth position) and happens to be the second type of control proteins (third 1 at sixth position). The dot product between the first row of matrix \mathbf{X} and vector \mathbf{w} will produce the following result: $\alpha_0 * 1 + \alpha_1 * 0 + \beta_0 * 0 + \beta_1 * 1 + \tau_0 * 0 + \tau_1 * 1 + \tau_2 * 0$. After a straightforward simplification, we get $\alpha_0 + \beta_1 + \tau_1$. Therefore, $\mathbf{X}_0\mathbf{w} = \alpha_0 + \beta_1 + \tau_1$. If we insert this result into the linear model equation above, we get $y_0 = \alpha_0 + \beta_1 + \tau_1 + \varepsilon$,

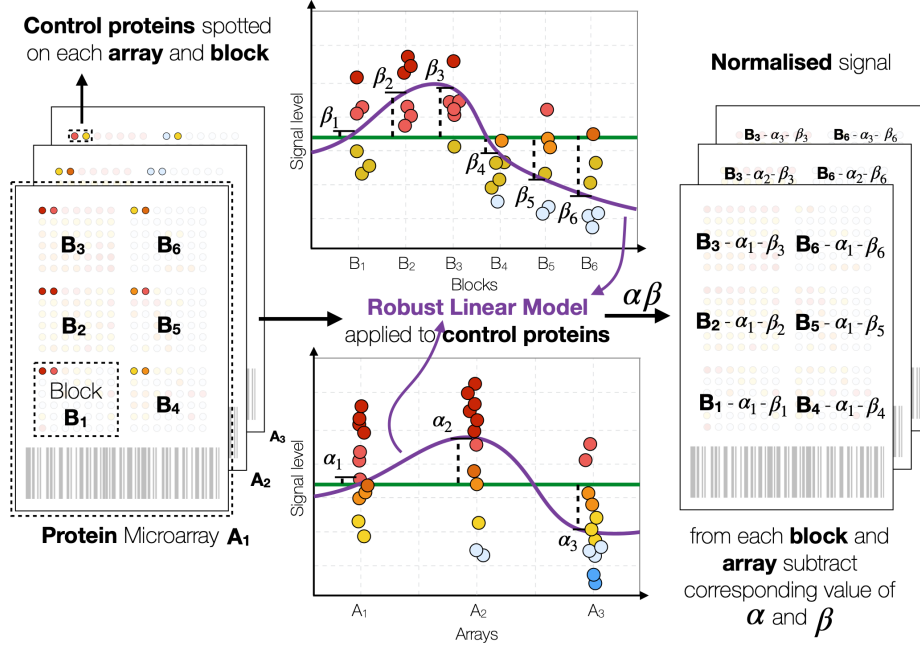


Figure 7. Normalising protein microarray signal using the robust linear model and control proteins. First, intensity values of the control proteins are modelled as a linear combination of the array (α), block (β), type of control protein, and noise using a robust linear model (purple line). The resulting coefficients for arrays and blocks are considered to be associated with unwanted technical biases. Then the normalised signal is obtained by subtracting the corresponding coefficients associated with a specific array and block.

where y_0 is modelled signal of the corresponding control protein. Random noise ε is sampled from the normal distribution for each control protein independently. All in all, in a generic case we get $y_{ijk} = \alpha_i + \beta_j + \tau_k + \varepsilon_r$, where i, j, k and r are indexes of corresponding array, block, protein type and protein signal. This final equation is equivalent to 3.1.

RLM is considered a preferred normalization strategy for protein microarrays as it exploits protein microarray specific control proteins and does not assume the near equal signal distribution across arrays [47]. On the other hand, RLM assumes a normal distribution of the underlying signal to work well. Logarithm transformation that was discussed earlier, can be applied to the raw protein microarray data to approximate the normal distribution.

Unfortunately, a source code of the RLM method was not available at a time when work that laid the foundation of this thesis was performed. RLM was implemented as part of Prospector software – a standard analysis tool provided by the manufacturer of ProtoArray. At the same time, Prospector had a prohibitive limit on the number of input samples, rendering it futile for larger studies as ours [76].

Later, RLM was introduced in a protein array analyser (PAA) – an R package developed by Michael Turewicz [69]. However, for a significant stretch of time RLM was nowhere to be found and thus, we had to create our own implementation of the RLM normalisation module for publications I, II, and later released it to the research community as part of the web-tool (publication III of this thesis). The absence of a source code, as well as a pseudo-code of the RLM method in the original publication [47], made re-implementation of the RLM one of the most challenging part of the protein microarray analysis pipeline built in this thesis.

3.3. Statistical analysis

After protein data was properly pre-processed, relevant statistical methods can be applied. Statistical analysis is a vast field with a large number of techniques available at researchers' disposal. Characteristics of data and the research question determine the choice of the statistical method. For example, often researchers are looking for proteins that are capable of reliably distinguishing between two (or more) groups of samples, e.g. disease versus controls. Such protein features, in which intensity levels are sufficiently different between studied conditions are considered significantly differential and can be used as important biological markers suggesting the presence or absence of the condition in question often called *outcome variable*. To assess the relationship between the intensity of a single protein and the outcome variable, univariate analysis tools are used. If simple univariate analysis yields no results or there is a good reason to believe that multiple proteins in combination can be predictive of the sample's outcome, multivariate analysis can be performed. Finally, once influential proteins are identified with either multivariate or univariate techniques, the enrichment analysis can be used to discover their common properties. The following sections focus on statistical methods used in this thesis, while adjacent methods are described only briefly.

Although statistical tests that we are going to talk about further, work slightly differently, some basic notions remain universal. The common starting point in hypothesis testing is defining a baseline or a *null hypothesis* (H_0) – a general statement about the absence of the assumed phenomenon. For example, H_0 may be formulated as observing no difference between means of protein intensity signals of two groups of samples. Namely $H_0 : \mu_1 = \mu_2$, where μ_1 and μ_2 are means of the group 1 and group 2 respectively. An opposite to H_0 , *alternative hypothesis* (H_1) thus can be formulated as $H_1 : \mu_1 \neq \mu_2$. The statistical test usually results in either rejecting the H_0 and thus favouring the alternative hypothesis or failing to reject the null hypothesis. In either case, employing statistical tests inevitably entails a number of background *assumptions*, which are made either about the data or about the ways how the data has been gathered. An example of a data-based assumption could be that protein intensity signals follow a normal distribution. Invalid assumptions may lead to invalid test results, therefore it is of utmost importance to establish correct assumptions and choose an appropriate test.

Statistical tests use a numeric quantity derived from data to perform the hypothesis test. This quantity is commonly referred to as *test statistic*. The observed value of the test statistic can be calculated from the data at hand and compared with a known theoretical distribution of the test statistic under the null hypothesis (null distribution). If the observed value of the test statistic is at the far ends of the distribution i.e. either much larger or smaller than most of the values in the distribution, it is considered to be sufficient evidence for rejecting the null hypothesis. However, instead of relying on vague notions such as “far ends” or “much larger”, researchers compute a probability of the observed value of the test statistic to be sampled from the null distribution - a *p-value*. If the *p-value* is less than some pre-defined threshold value, the corresponding H_0 should be rejected. Common threshold values are 5% and 1%, more about this in the following sections.

Finally, most of the statistical tests can generally be divided into two large categories: one-sample and two-sample tests. A one-sample test explores the possibility of the mean of the sample being statistically different from the known population mean. Two-sample tests are used to assess the significance of the difference between means of two groups (e.g. patients and controls). Two-sample tests can be paired or unpaired (or independent). The unpaired two-sample test assumes no overlap between tested groups (e.g. two independent groups of mice). As it follows from the name, a two-sample test can compare only two groups. If there is a need to estimate the significance of the difference between three or more groups, an analysis of variance can be performed (also known as ANOVA). The sizes of groups to be compared and corresponding variances also influence the choice of the test. In this thesis, we make use of both one-sample and independent two-sample tests, which are discussed further in more detail.

3.3.1. Differential analysis

Many studies involving protein microarrays follow case-control study design (including Publications I and II in this thesis), where protein concentrations in patients can be compared to those in healthy individuals [58]. Proteins that can reliably differentiate between patients and controls are referred to as differential and process of identifying such proteins – differential analysis [24,57]. More formally differential proteins are the proteins for which the probability to observe the corresponding value of the test statistic to be sampled from the null distribution is below the acceptable significance threshold leading to rejection of the null hypothesis.

Differential proteins can be used to explore the mechanisms of the disease (such as in Publications I and II) or as a screening tool – measuring autoantibody reaction to these proteins in the general population can ideally reveal individuals at risk (Publication IV). These individuals could be treated early and less aggressively, increasing their chances for long-term well-being. Below we discuss different statistical methods used in this thesis to detect differential proteins.

Z-score analysis. A substantial number of protein microarray-based studies (including Publications I and II in this thesis) have used an approach referred to as *Z-score analysis* or *Z-test* to define differential proteins [1, 2, 46, 57, 59].

Classical Z-test is used to either evaluate the difference between two groups of samples or a group and a known population. The null hypothesis for the latter case can be formulated as $H_0 : \mu = \mu_0$ in two-sided version or as either $H_0 : \mu \geq \mu_0$ and $H_0 : \mu \leq \mu_0$ for one-sided version, where μ , μ_0 are group and population mean respectively. Z-test uses *Z-scores* (or standard scores) as a test statistic, which can be defined as

$$z = \frac{\mu - \mu_0}{\sigma} \quad (3.3)$$

where z is the Z-score for a given group of samples with a mean μ , while μ_0 and σ are population mean and standard deviation respectively. The distribution of Z-scores under the null hypothesis is well-known and can be approximated by a corresponding normal distribution. The group with unusually high or low Z-score value is considered to have a mean value different from the one of null-distribution. The relevant p-value can be estimated as the percentage of the null distribution falling above or below the observed Z-score.

However, unlike the classical Z-test described above, in protein microarray analysis it is common to use individual spot's concentration values x in a place of group mean μ in 3.3 [57], leading to:

$$z = \frac{x - \mu_0}{\sigma} \quad (3.4)$$

This approach is similar to the *three-sigma rule* described in the outlier detection section, as protein concentrations with a Z-score of more than 3 or less than -3 in one or more samples are considered to be significantly differential [1, 2, 57]. However, due to the potentially high number of tests, such a strategy may lead to a substantial number of proteins deemed differential by mistake (see a section on multiple testing correction). Such risk can still be justified in the case the goal is not to identify proteins that are consistently differential across all patients, but proteins that have abnormally higher concentration values only in a handful of patients. This is the case for APECED patients, who develop heterogeneous sets of autoantibodies that may differ from patient to patient and thus target vastly different sets of proteins spotted on protein microarray slides.

Two main assumptions should be met in order for Z-test to be applicable: Z-scores should follow a normal distribution and population parameters i.e. mean and standard deviation should be known in advance, which is not always possible. Often population mean and standard deviation can be estimated using the sample mean and standard deviation, which transforms Z-test into a t-test.

Student's t-test. The Student's t-test (or a t-test) is one of the most popular statistical approaches for hypothesis testing. The test was named after William Sealy Gosset who published the method under the alias "Student".

In this thesis we have employed a two-sample version of the t-test, which explores the difference between two groups of protein microarray slides (patients and controls), H_0 for such test has the following familiar formulation $H_0 : \mu_1 = \mu_2$, where μ_1 and μ_2 are means of the group 1 and group 2 respectively. An alternative hypothesis (H_1) is therefore $H_1 : \mu_1 \neq \mu_2$. Similar to Z-score analysis which is relying on Z-scores, the t-test computes t-values (denoted as t), which are used to decide the outcome of the test. T-value is a test statistic for the t-test and calculated using the following formula:

$$t = \frac{\mu_1 - \mu_2}{s_p \sqrt{\frac{1}{n_1} + \frac{1}{n_2}}} \quad (3.5)$$

where

$$s_p = \sqrt{\frac{s_1^2}{2} + \frac{s_2^2}{2}} \quad (3.6)$$

Above, s_p is a pooled standard deviation (3.6), n_1 and n_2 represent the number of samples in group 1 and group 2 respectively, while s_1 and s_2 are the standard deviations of these two groups. The formula for t (3.5) is valid as long as there is a good reason to believe that groups have similar sizes and are sampled from the populations with equal variances. In other circumstances, slightly different formulas for t and s_p must be applied. From the definition, it follows that t is the distance between group means in units of pooled standard deviation. If the null hypothesis is true the value of t should be close to 0, suggesting no difference between the two means. However, the larger the value of t , the less likely is H_0 . Thus, using computed t -value it is possible to quantify the p-value by comparing t to a null-distribution. If the p-value is less than a predefined threshold, the null hypothesis is considered to be false and can be rejected. It is common to use 0.05 as a threshold imposed on p-values. Rejection of H_0 under 0.05 threshold can be interpreted as that there is less than 5% chance that the observed difference between groups is due to random chance.

Multiple assumptions should be satisfied for the above equations and reasoning to work. The above-mentioned equality of group sizes and variances is one of such assumptions. The other assumptions are described below. T-test should be applied only to continuous data. Also, sample means from populations being compared should follow the normal distribution, which makes the t-test a member of *parametric tests* family, i.e. tests that rely on a specific probability distribution. Compared groups should be independent of each other (no overlap, unless paired t-test is used). Lastly, samples i.e. patients and controls should be independent of each other. The aforementioned assumptions are by default assumed to be satisfied, therefore it is the responsibility of the researcher to make sure that data is suitable, otherwise, results produced by the t-test may not be sensible. The normality assumption is especially hard to satisfy for the researchers working with highly heterogeneous protein microarray data. In such cases, more

powerful alternatives to classical t-test can be used, such as moderated t-test [77] or Mann–Whitney U test [78] discussed in the next section.

The t-test can be expressed in terms of linear models discussed in the previous sections and can be formulated as $\mathbf{y} = \mathbf{X}\mathbf{w} + \varepsilon$ (3.2). Here we will pay no attention to ε term as it is independent for each sample and cannot be accounted for. In our case, \mathbf{X} is an indicator of whether a sample was drawn from the first or second group and thus can be written simply as x_i . The above equation (3.2) can be reformulated as follows: $y_i = x_i\mathbf{w}$, where y_i is predicted signal value of i -th sample. This equation can be further simplified $y_i = w_0 + w_1 * x_i$. If an i -th sample is drawn from the first group, x_i becomes 0 and the whole equation transforms into $y_i = w_0 + w_1 * 0$ or simply $y_i = w_0$. Hence, w_0 is a predicted signal for the samples in the first group. Since the best way to summarise a set of points is via their mean, w_0 represents a mean signal of the first group. When sample is from the second group, the x_i equals to 1 and thus the core equation changes to $y_i = w_0 + w_1$. With this, we model the second group by adding w_1 to the mean of the first group w_0 , and therefore w_1 is the difference between the means of the two groups. The null hypothesis can be formulated accordingly as $H_0 : w_1 = 0$. Not only the linear model formulation of the t-test can help to understand the procedure better, but it also facilitates the implementation using programming languages. Various statistical software packages e.g. *limma* in R, uses linear model formulation as a basis for t-test implementation. T-test-based expression analysis performed and presented in Publication II of this thesis was implemented in *limma* and formulated in terms of the linear model.

Mann–Whitney U test. Mann–Whitney U test (also known as the Wilcoxon rank-sum test) is an alternative to the two-sample equal variance t-test discussed before [78]. Contrary to the t-test, the Mann–Whitney U test belongs to the family of *non-parametric tests* that do not rely on any particular parameterized distribution for hypothesis testing. Therefore, it is applicable to data that does not necessarily follow the normal distribution as is often the case in biology. Under null hypothesis H_0 the two compared distributions should be considered equal. More formally, the probability of an observation from the first group to be larger (or smaller) than an observation from the second group is not consistently different from the probability of the opposite, namely, that observation from the second group being larger (or smaller) than an observation from the first group. Thus, the Mann–Whitney U test assumes that observations are comparable, i.e. it is possible to say if one is bigger than the other. In linear model formulation, Mann–Whitney U test is very similar to the standard t-test, except the model is built on ranks of x and y instead of actual values: $rank(y_i) = w_0 + w_1 * rank(x_i)$. In this thesis, the Mann–Whitney U test has been used in an attempt to identify differential cytokines (Publication IV).

Permutation test. Another way to compare two independent groups of samples without assuming a particular distribution is called a permutation test (or randomization test) [79]. It starts with calculating a predefined test statistic on the original

data. In the case of two independent groups, we may decide to calculate the difference between two means μ_1 and μ_2 of two groups with n_1 and n_2 samples respectively. Hence, $df_o = \mu_1 - \mu_2$ is considered an observed value of the test statistic for the original data. In order to obtain a distribution of the test statistic under a null hypothesis $H_0 : \mu_1 = \mu_2$, the permutation test performs the following steps. First, it randomly shuffles all the data and assigns n_1 first observations to the new first group. The remaining n_2 samples are assigned to the second group. Next, the difference between means of randomly created groups df_r is calculated. If obtained value df_r is larger than df_o , the pre-initialized counter i is increased by 1. Later, the data is reshuffled again and all the same, steps are repeated a large number of times (e.g. 10,000), each time a new df_r is computed. To estimate the corresponding p-value, the observed value of test statistic df_o should be compared to the distribution of test statistic under the null hypothesis, thus the distribution of df_r . This can be done by dividing the resulting value of the counter i by the number of repetitions that were performed. For example, if after 10,000 repetitions only on seven occasions df_r was larger than df_o , the probability to observe df_r as extreme as df_o under the null hypothesis is 0.0007, which is less than a classical significance threshold of 0.05, and therefore small enough to reject the null hypothesis.

There is no need to calculate all possible permutations of the original data, as this number can be extremely large (e.g. two groups with 30 observations in each will result in 1.18×10^{17} possible permutations) [80]. Instead, a large enough random sample of all possible combinations would be sufficient. The larger the sample, the more precise estimate it will generate. Such a sampling procedure is usually referred to as the Monte Carlo approach. Modern software tools, as well as processing hardware, enable researchers to shuffle their data enough times to obtain sufficiently precise estimates in almost no time, making randomization tests a practical solution to hypothesis testing.

In the research presented in this thesis (in Publication II) we used a permutation test to test a hypothesis that proteins targeted by the autoantibodies in the blood of APECED-positive patients originate from genetically more conservative (i.e. those that accumulate fewer mutations over time) regions of the DNA.

3.3.2. Enrichment analysis

The identified set of significantly differential proteins (i.e. proteins with signal levels significantly different between conditions) can be interpreted with respect to the existing body of knowledge. Such interpretation can be the key to the understanding of biological processes, e.g. mechanisms of the disease. Autoimmune disorders such as APS1, discussed in earlier chapters, are caused by the genetic mutations that undermine the immune system's native ability to prevent self-targeting antibodies from entering the bloodstream. Hence, APS1 patients' blood is filled with a large number of aggressive autoantibodies. Researchers an-

alyze a pool of proteins that are targeted by released autoantibodies, trying to identify properties and functions that are common among the targets. Pinpointing these properties and functions might shed some light on autoantibodies and the autoimmune process, for example, it may provide clues as to autoantibodies' origin. In general, the process of determining properties that are over-represented in a group of proteins or genes is usually referred to as *enrichment analysis*. Enrichment analysis is often performed by quantifying the size of the overlap between a group of proteins with a known biological property, e.g. proteins expressed in lymphoid cells, and a group in question. A statistical test is then used, e.g. hypergeometric test, to estimate the probability that this overlap or larger was observed by random chance. If such probability is deemed sufficiently low ($< 5\%$), the overlap between groups is considered significant and therefore, genuine. In this case, the group in question is said to share the same biological property as a group with which it was compared. A large number of public databases, such as Gene Ontology [49], KEGG [81], Reactome [82], Human Phenotype Ontology [83] and Human Protein Atlas [84] are available with protein and gene groups characterized with various biological properties and functions. Hence, in practice, enrichment analysis means comparing the obtained group of target proteins to hundreds or even thousands of groups stored in public databases. A number of potential databases and datasets that can be searched to find relevant terms has long become prohibitively large for humans to manually work through. Thus many software tools, e.g. g:Profiler [85] were developed to automate the enrichment analysis, saving dozens of researchers' work hours. In this thesis, specifically in publication II, we have used g:Profiler as well as a hypergeometric test to identify enriched terms in the group of targeted proteins.

Hypergeometric test. We can explain the idea of the hypergeometric test with the following example: we are drawing balls from the urn which contains balls of two colours: white and black. We took a fixed number of balls from this urn. Some of the balls turned out to be black and some white. The hypergeometric test attempts to answer the following question – what is the probability of observing as many white balls as we have or more if the balls were drawn from this urn at random. In the context of this thesis, it is possible to reformulate this example as follows: the urn is a protein microarray platform (e.g. ProtoArray), the balls drawn from the urn represent the list of differential proteins we extracted, white balls are the proteins that represent a specific biological function and black balls are all the remaining proteins. The null hypothesis here is that the overlap between the list of extracted proteins and proteins associated with some biological process is of the same size as it would be expected if we drew the proteins from the platform at random. Therefore, we ought to find a probability to observe as many proteins that belong to a biological process as we do in our list if we drew these proteins from the protein microarray platform at random. More formally, the probability to draw k proteins that are associated with a biological process of interest in our list by chance $p(k)$ can be calculated as follows:

$$p(k) = \frac{\binom{K}{k} \binom{N-K}{n-k}}{\binom{N}{n}} \quad (3.7)$$

where K is the number of such proteins in total on the platform. The number of proteins in our list is n and N is the number of proteins overall on the platform. By inserting all possible values of k (from 0 to n) into 3.7 it is possible to obtain corresponding hypergeometric distribution. By accumulating parts of the distribution that correspond to actual k_{actual} observed from the data, it is possible to estimate the probability to observe k as extreme as k_{actual} or larger by chance. If this probability is low enough (less than 0.05) we reject the null hypothesis and assume that there are more proteins associated with a biological property among extracted proteins than what we can expect at random. Although we have used g:Profiler to determine biological processes common among targeted proteins, we still applied the hypergeometric test in Publication II to be able to perform enrichment analysis on datasets that were not part of the g:Profiler tool and also to cross-check our findings.

3.3.3. Multiple testing correction

Let us recall that the p-value implies the probability to observe the current outcome of the experiment or even more extreme under the null hypothesis. If this probability is less than 5% it is commonly accepted that the null hypothesis is unlikely to be true and therefore can be safely rejected. Here, “unlikely” does not mean “impossible”, thus it is still imaginable to obtain a p-value less than 5% under the null hypothesis by chance and the probability of this event is the same 5%. Although 5% does not seem to be a very high value, consider an example, which involves 20 simultaneous tests with the same p-value threshold of 5% [86]. Let us calculate the probability of having at least one test out of 20 to generate a p-value of 5% or less by pure luck. This is equivalent to asking for the probability to obtain at least one head by tossing a biased coin (which has a 95% chance of coming tails) 20 times. This probability can be calculated as follows:

$$\begin{aligned} p(\text{at least 1 significant test}) &= 1 - p(\text{no significant tests})^{20} \\ &= 1 - (1 - 0.05)^{20} \\ &= 1 - 0.36 \\ &= 0.64. \end{aligned} \quad (3.8)$$

There is a 64% chance to obtain at least one falsely significant result out of 20 independent tests. Differential analysis for a protein microarray implies running statistical tests described in the previous section for each of thousands of proteins seeded on the platform. For example, analysing a typical HuProt protein microarray experiment would mean performing about 20,000 tests simultaneously. For

each test, a p-value will be produced, and the null hypothesis is rejected if the corresponding p-value is less than 0.05. If we assume the absence of true differential proteins on the platform, 5%, namely 1000 ($0.05 \times 20,000$) proteins will be considered significant simply by chance (because the number of tests is so large). For example, for the ProtoArray study discussed in Publication II, this would mean that half of the proteins in the positive group are false. Therefore, the number of tests needs to be taken into account when performing statistical analysis. A number of methods have been proposed to adjust the classical statistical significance threshold of 5%.

Bonferroni correction. The simplest multiple testing correction approach is called the Bonferroni correction [87]. This method adjusts the p-value threshold by dividing it by the number of experiments. In the above example of HuProt array with ~ 20000 proteins and threshold of 0.05, the new significance threshold becomes $0.05/20000 = 2.5 \times 10^{-6}$. Applied to n tests with a p-value threshold of α Bonferroni correction ensures that the probability of observing at least one false significant result is α [88], while it is usually sufficient to optimize for some acceptable proportion of false predictions. Thus this procedure was commonly regarded as overly strict for most of the practical applications [86, 88].

Benjamini and Hochberg correction. The method by Benjamini and Hochberg (also known as FDR correction) attempts to keep the number of falsely significant results at a certain predefined level (e.g. 5%) [89]. The proportion of falsely admitted associations (false positives) among all significant results is called a false discovery rate. The method starts with ordering all m unadjusted p-values in a descending order [86]. Then for the i -th p-value p_i , the algorithm checks if this value is less or equal to $(i/m) \times \alpha$, where α is acceptable level of FDR. As soon as such p_i was found consider it to be a significant threshold. We used the method by Benjamini and Hochberg to correct unadjusted p-values for multiple testing in publications II and IV.

3.4. Machine learning modelling

While classical statistical methods help to analyse the significance of each protein feature separately [90], more sophisticated methods, such as machine learning algorithms, are needed to assess the predictive performance of multiple proteins combined. Machine learning (sometimes also can be referred to as artificial intelligence) is a field of computer science that develops algorithms capable of learning valuable relationships from data without being explicitly programmed. Such relationships can then be used further by the same machine learning models to accurately predict the value of the outcome variable in new unseen data. Machine learning models are frequently used in biology in an attempt to build diagnostic tools for certain diseases (e.g. publication IV of this thesis). Depending on outcome variable type (discrete or continuous) machine learning models can be broadly divided into classification and regression algorithms. Myriads of machine

Decision Tree Algorithm

By asking a simple **question** about value of P_A and P_B decision tree tries to predict a **class** (Control, Patient)

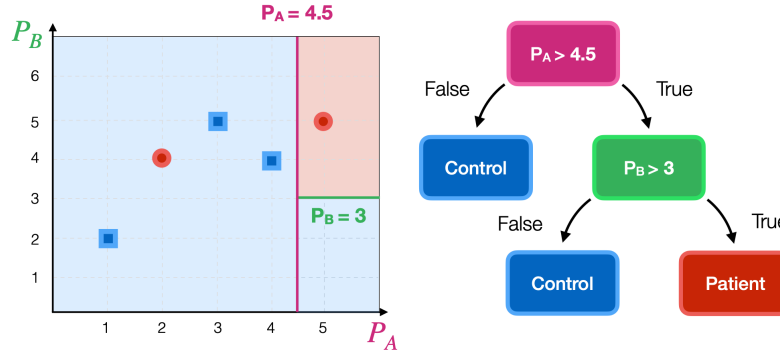


Figure 8. Decision tree algorithm uses information about individual protein intensities (P_A and P_B) in order to explain the outcome variable. For example, the decision tree algorithm may assign a class "control" to a sample for which protein A (P_A) has an intensity value less than 4.5.

learning algorithms have been developed for each of these categories [91]. Some of the most popular machine learning methods capable of working with both continuous and discrete outcome variables are decision trees [92], and random forest [93].

The decision tree algorithm. Decision tree algorithm [94] uses values of input features (e.g. protein intensities) to infer the value of the outcome variable. A decision tree has a recursive structure with a root at its origin and leaves at the bottom. Each node can potentially have two children nodes. All nodes except leaves encode conditions in a form of questions. For example one of the nodes may inquire if the normalised intensity of protein A has a value of more than 4.5 in order to decide on a value of the outcome variable (Figure 8). The tree starts with checking if the input data satisfies the initial condition at the root and descends down the tree depending on the outcome. Leaf nodes of the tree determine the outcome of the algorithm: class in the case of classification or continuous value for regression. To build the tree the decision tree algorithm uses values of all available features.

The random forest algorithm. The random forest algorithm [93] can be considered an extension of the decision tree algorithm discussed above. Instead of building one tree and inferring the predictions from that tree, the random forest algorithm creates several trees, which are used to predict the value of the out-

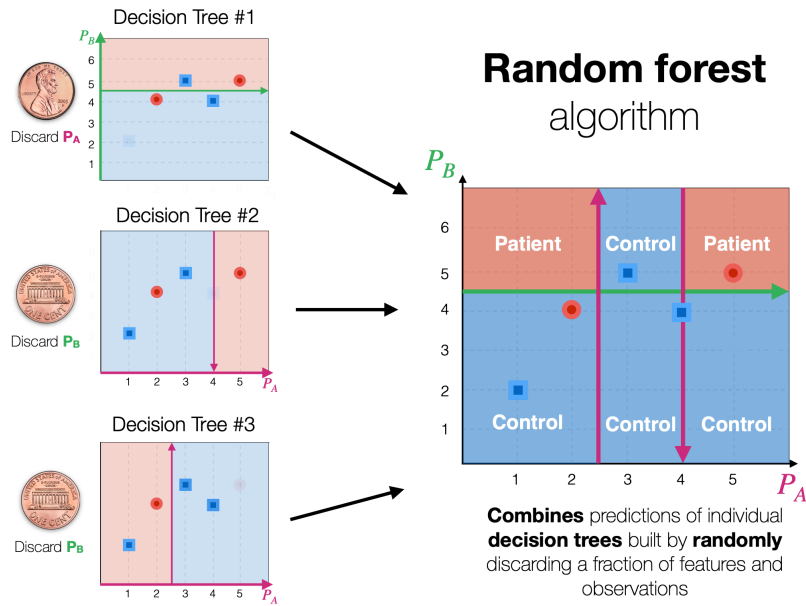


Figure 9. Random forest algorithm uses predictions produced by individual decision trees in order to predict an outcome variable. Decision trees that are part of a random forest ensemble are built by randomly discarding a pre-defined number of features and observations. For example, decision tree 1 has been built after discarding protein A intensity and the first control sample.

come variable in parallel. Predictions from the individual trees are then combined together to obtain the final joint prediction. Such approach is often called *ensemble learning* or *ensembling*. The random forest algorithm has another important difference from the decision tree algorithm. The individual trees are constructed using a random subset of input features and input data points (e.g. proteins). For example, it is common to use random 80% of samples for each tree in the forest and when building a tree, nodes are optimized using only random 80% of the features (Figure 9). This has been shown to make random forest models extremely robust to noise and highly generalizable to unseen data.

Evaluating machine learning models. Creating a fully functional machine learning model (e.g. for diagnosis), starts with exposing it to data that closely resembles the data on which it is expected to perform well in the future. This initial dataset is called *training data*. Most machine learning algorithms (including random forest algorithm) have various parameters that can be tweaked in the hope to obtain a better working model. By tweaking such parameters, machine learning models can be made powerful enough to completely memorize all possible aspects of the training data. Counterintuitively, this can be harmful to the model's performance on new data, if its distribution exhibits even the slightest deviation from the distribution of the training set. Therefore, correctly estimating the perfor-

mance when training machine learning algorithms and tweaking their parameters is a very important step in creating a viable data analysis pipeline. The performance of a model is usually evaluated using independent parts of data (referred to as validation or test set). This approach implies detaching a substantial part of data from the training set, which may not be used for model training. However, if the number of samples is limited, which is usually the case in biological research, creating a separate validation set can be prohibitively data-expensive. Another way to evaluate the performance of the model is called the cross-validation (CV) algorithm. It starts by randomly splitting the initial data set into a finite number of chunks (folds). The total number of folds depends on the size of the data set, often ranging between 3 and 6. At every iteration of the CV algorithm, the machine learning model is trained on all folds except one, the remaining fold is used as a validation set, allowing to take a snapshot of the model's performance. Part of the data that serves as a validation set is changed at every iteration, allowing to obtain several performance estimates using one data set. The cross-validation algorithm provides a safe way to estimate the unbiased performance of the model under different sets of parameters without letting the model memorize training data. Once the perfect combination of parameters was found and its performance estimated, the model can be trained on the entire dataset. The cross-validation approach was used in the publication IV of this thesis as well as in our previous work [95] to efficiently evaluate machine learning models.

At present, it is impossible to imagine a section on machine learning that would ignore a connection between machine learning and deep learning techniques. Deep learning algorithms are machine learning methods that use a popular type of machine learning models – neural networks to tackle the most challenging problems, often previously unsolvable by humans. Since the success of the AlexNet neural network in 2010 [96] these methods have been considered to be the most advanced form of machine learning. Although deep learning approaches are considered to be state-of-the-art in many areas, including biology [97,98], due to several substantial limitations of neural networks (e.g. low transparency and data-intensive nature of training), here we have focused on less complex, yet still powerful machine learning methods that have been used in publication IV of this thesis.

4. PROTEIN MICROARRAY ANALYSIS IN THE SEARCH FOR HIGH-AFFINITY AMELIORATING AUTOANTIBODIES (PUBLICATION I)

The AIRE gene has an important role in central tolerance as it is responsible for assembling self-antigens used in T cell maturation [18, 99, 100]. These antigens are presented to T cells during the so-called *negative selection phase*. Binding between prospective T cells and self-antigens indicates the potentially self-reactive tendency of T cells. As a result, such T cells are deemed dangerous for the organism and normally are removed from the pool of potential immune cells.

Occasional genetic mutations can alter or even cease the function of AIRE, jeopardising central T cell tolerance [100] and thus resulting in the accumulation of self-reactive immune cells in the bloodstream. T cells have been linked with activation of B cells [101] that produce autoantibodies. The theory emerged that genetically deficient AIRE gene may distort not only the selection of T cells but also may indirectly create autoimmune B cells and as a result – disease-causing autoantibodies. Despite such an important role, precise molecular mechanisms of AIRE have remained poorly understood [29]. Genetic alternations of AIRE cause the APECED/APS1 autoimmune condition mentioned previously. This disease is characterised by large numbers of autoantibodies against self-antigens expressed in the peripheral organs present in the patients' blood [102]. Although this condition is rather rare in the general population (depending on the country it can range from 1 in 25,000 to 1 in 1,000,000), it is often considered as a model disease for human autoimmunity. We, therefore, reasoned that studying autoantibodies from a sufficiently large set of APS1/APECED patients may help to gain a better understanding of the interplay between AIRE and autoimmunity, for example, collect evidence for the hypothesis that specific protein features may be an indirect cause of B cell autoimmunity [1, 2, 29].

Overall, eighty-one APS1/APECED patients of five distinct geographical origins were recruited into the study that was published in 2016 [1]. Some of the patients were sampled several times over the course of the study, resulting in a total of ninety-seven patient samples. Control samples were extracted from nine first-degree relatives and twelve healthy volunteers. In total, data from a hundred eighteen samples were analysed. Protein microarray chips from Fisher Scientific (ProtoArray) were used to quantitatively measure the presence of autoantibodies in these samples.

According to a standard data acquisition pipeline, ProtoArray chips were scanned with a GenePix scanner, resulting in hundred eighteen GPR files. Signal was acquired from each GPR file using *readMAimages* function from *limma* package in R. Data was pre-processed and normalised using robust linear model [47]. Later, in order to identify proteins that showed higher levels of autoimmune reaction, the signal from each spot was transformed into Z-score by subtracting the mean

and dividing by the standard deviation of the combined healthy and first-degree relatives group. We considered a protein to be a positive hit if the corresponding Z-score had a value of 3 or larger in at least one sample. This resulted in a high number of positive targets (3,731) jointly recognised by the group of patients and 406 proteins recognized by controls. This observation was in concordance with a widely held view that APS1/APECED patients are very heterogeneous in the nature of their autoimmune response with only a handful of proteins (such as type I interferon family) being recognised by the majority of patients [64, 65], while other constituting a private set.

To conclude, this paper had at least two major findings. Firstly, our statistical analysis showed that APS1/APECED patients as a group develop a unique set of autoantibodies that recognise approximately a hundred body's own proteins. Almost all samples contained high concentrations of autoantibodies against a small set of proteins (about 10), such as type I interferon or interleukin-22 (IL22). The remaining proteins were collectively recognised by autoantibodies present only in a handful of individuals. Thus, it was observed that blood from all 81 patients collectively contained autoantibodies against more than 3,700 human proteins (which is about 14% of the canonical proteome). Secondly and perhaps even more importantly, the presence of autoantibodies against type I interferons had a surprising negative correlation with type I diabetes. In this publication, our main contribution is of two folds: implementation of a protein microarray specific data pre-processing pipeline, including re-implementation of the robust linear model for normalisation and identification of positive hits using Z-scores. A more comprehensive analysis of autoimmune targets was performed in Publication II, which will be discussed in the following chapter.

An important comment was brought to our attention several years after the publication. A group of independent researchers pointed out that the mean and standard deviation of combined control and healthy relatives group that we have used to calculate Z-scores is inherently small. Thus, such a procedure is bound to produce higher numbers of proteins with Z-scores above the aforementioned threshold of 3 in patients [103]. Hence, they concluded that it is likely that a large part of reported in the paper 3,731 positive proteins are false positives – a side effect of employing an imperfect statistical method. The authors of the comment suggested that using classical statistical methods for comparing two distributions would alleviate the problem and produce more trustworthy results. In our response, published along with the original criticism [104], we emphasized the goal of the study – broadly characterize the nature of auto-reactivity in APS1/APECED patients. We showed that this goal implied maintaining a false-negative rate as low as possible. Moreover, we stressed an important clinical aspect of APS1/APECED, namely that each patient is highly individual in the range of symptoms, which manifests in diverse sets of autoantibodies present in the blood of patients [104]. In this vein, classical statistical tests such as Fisher's exact test [105] or moderated t-test [75] may not have been applicable as they would

filter out proteins recognised only by few individuals, as insignificant. While we have not denied the fact this approach could have led to the higher number of false positives, we nevertheless used it in our analysis, as true targets were to be verified by independent lab experiments and follow-up studies [1, 2, 106–108]. This argument is relevant to the analysis performed for the second publication.

The comment published in eLife [103] and our subsequent response [104] enabled us to appreciate the complexity involved in devising a precise rule for identifying true-positive autoantibody targets in protein microarray experiments. Where the classical statistical methods are deemed unsuitable for the task due to the stochastic nature of the autoimmunogenesis, the ad hoc solutions may lack the desirable precision. Arguably the most common way to respond to such a challenge is to employ several orthogonal assays to confirm the findings. Hence, there seems to be a need for the non-parametric technique that would enable robust yet non-restrictive analysis of inherently variable signal intensities often exhibited by the protein microarrays.

5. CHARACTERISING AUTOIMMUNE TARGETS FURTHER (PUBLICATION II)

Autoantibodies have been shown to play an important role in the onset and progression of various autoimmune diseases [109,110]. Yet, while recently a lot more has been discovered about cellular and genetic factors that contribute to the emergence of autoimmunity, our understanding of properties of involved autoantibodies remains limited [2]. We made an initial attempt to characterise autoantibodies and their targets in Publication I [1], where we showed that patients' blood contains high concentrations of autoantibodies against a set of well-known proteins. Some of these proteins such as type I interferons (especially IFN- α), became diagnostic markers for APECED [18]. Autoantibodies against other proteins, like IL17A, IL17F and IL22 were shown to contribute to the onset of chronic mucocutaneous candidiasis – another distinctive feature of APECED [2,111]. Previous studies suggested that there are autoantibodies that are shared between APECED and other complex autoimmune diseases, such as Addison's disease [109] and T1D [110]. But the number of such commonly targeted and widely known proteins, is small, comparing to the total number of proteins collectively targeted by autoantibodies in all patients (3,731 in total). Hence, in Publication II we focused on an in-depth analysis of autoimmune targets identified in Publication I.

Protein data from the same samples as in Publication I was pre-processed using an earlier developed pipeline with few minor modifications. As before, the background-subtracted signal (we used basic median local background subtraction) was log-transformed before being normalised using RLM. The resulting values were standardized using the mean and standard deviation of control samples. After several studies that have employed ProtoArrays highlighted a danger of cross-contamination between neighbouring protein spots [46] we decided to add another quality control step into our pipeline. Thus, unlike the workflow of the first publication, here, we removed 31 proteins with unexpectedly highly correlated signals (with Pearson's coefficient of 0.6 or higher) with the expression of nearby proteins or well-known protein targets (e.g. IFN- α). The remaining proteins with a standardized score of 3 or higher in three or more patients were considered to be true positive targets [2]. Additional filtering criteria of three patients were introduced in this work to reduce the number of possible false positives that could distort the analysis. This requirement narrowed down the list of positive proteins from an initial 3,731 to 963, which we later referred to simply as the "positive group". Although the positive group was significantly decreased in size, it remained big enough to include proteins recognised "privately" i.e. by fewer patients, and therefore capable of providing details on the mechanisms of the autoimmunity.

Most of the further analysis was centered around characterisation of the positive group, by matching our protein list with various public databases and analysing

available meta-information about samples. In the course of this research, we looked for biological processes that are over-represented in the positive group. We quantified the number of single nucleotide polymorphisms (SNPs) and APECED related mutations as well as the level of evolutionary conservation of relevant gene regions. We also performed differential and clustering analysis with respect to associated clinical conditions, which however revealed few notable results. Finally, we ran a longitudinal analysis of protein expression patterns in the positive group. Performing all these experiments involved a number of technical challenges, solutions to which, are our main contributions to this publication.

First and foremost, in order to be able to use public databases in our analysis we needed a way to unambiguously compare entities stored in these databases (usually proteins or genes) with our positive group. Most of the tools and datasets, employed in this work, operated with Ensembl gene IDs (ENSG). While for a few others, symbolic gene names must have been used. Analysing overlaps with these databases meant converting all native Protoarray names used by the manufacturer (approximately nine thousand Reference Sequence IDs), into ENSGs and gene names. We used g:Covert web-tool [85] available at <https://biit.cs.ut.ee/gprofiler/convert> to obtain initial results. But a substantial number of missing and duplicated gene ids in the results presented themselves as a serious problem for further analysis. On one hand, due to factors such as alternative splicing, when a gene can be associated with multiple proteins, some number of duplicated IDs was expected. However, a lot of protein IDs were not converted by g:Convert into ENSGs at all. To impute as many missing gene IDs as possible, we parsed the official ProtoArray content file, applied g:Convert tool, and manually searched NCBI [112] and Ensembl databases [113]. Eventually, the number of proteins that could not have been translated was reduced to 324, which is below 4% of all proteins on the platform.

Next, data from all relevant databases must have been acquired and unified prior to further analysis. Often datasets that we required for the analysis were redistributed over multiple files and stored in different formats, using conflicting or inconsistent notations. Sometimes, we had to prepare a custom dataset based on public records. For example, to compare the mutation rate of the positive group with the overall platform, we extracted information about all mutations in the human genome and then programmatically searched for SNPs associated with relevant genes and gene regions (introns, exons, etc.).

Finally, we proceeded to analyse the autoimmune targets by comparing them to data from public databases [81–84]. Some databases contained only gene lists associated with a certain biological class (e.g. genes expressed only in some tissue), while others supplemented genes with quantitative measures (e.g. level of evolutionary conservation). Therefore, the third major technical challenge we faced in this work can be broadly described as building a multi-headed statistical pipeline to characterise various biological properties of our positive group. We used a number of statistical tests to accomplish this, each in a specific con-

text. The hypergeometric test was used to assess the significance of the overlap between the positive group and various biological processes, permutation test to compare quantitative characteristics, various univariate tests to check for statistical differences between distributions. The resulting p-values were adjusted using the Benjamini-Hochberg method [89] to account for a large number of tests executed in parallel. Finally, we applied a classical significance threshold of 0.05 to adjusted p-values to find statistically relevant properties of the positive group. To cross-check the results of our statistical pipeline, we submitted the list of positive targets to g:Profiler web-tool [85]. We used an unordered query with all ProtoArray proteins as a statistical background [2].

Described contributions helped us to discover a number of features shared by the autoimmune targets. For example, we have shown that our positive group was on average significantly more evolutionary conservative (i.e. had fewer mutations) comparing to other proteins from the platform (with an adjusted p-value of 0.0162). A significant proportion of the proteins from the positive group are found in the cell nucleus or cytosol. We also reported a significant association between the number of recognised proteins in each sample and the three most common APS1 mutations. Lastly, based on our results we hypothesised that APECED “autoimmunome” is comprised of two distinct groups of autoantibodies, one of which is likely to be traced back to the AIRE gene discussed in the previous chapter, while the other originates from lymphoid tissue [2]. These observations expanded our understanding of the biological properties of autoimmune targets in APECED. Protein microarray data used as a basis for Publications I and II can be found online via the accession number “E-MTAB-5369” on ArrayExpress website.

To summarise, in this publication, we performed an analysis of autoimmune protein targets in APECED [2]. The main engineering and data analysis challenges include lossless conversion of ProtoArray protein IDs into ENSGs and gene names, the transformation of the data from more than fifteen public databases into a format usable for further analysis with a multitude of statistical approaches. The substantial complexity of the performed analysis presented a need for a user-friendly tool that would automate the most laborious parts of the protein microarray analysis. We went on to build such a tool that will be presented separately in the next chapter.

6. AUTOMATING PROTEIN MICROARRAY ANALYSIS WITH PROTEIN ARRAY WEB EXPLORER (PUBLICATION III)

Building a complete protein microarray analysis pipeline presented in the previous two sections proved to be time-consuming as well as required skills in statistics and programming. People with such background are not always available in biological labs – primary sources of protein microarray data. At the same time, the existing analysis tools are either outdated (e.g. manufacturer’s own tool – Prospector) or require familiarity with programming to work with [69] or hard to use. As the resulting protein microarray analysis became a real challenge for the practitioners. Therefore, we decided to develop a user-friendly web-tool – Protein Array Web ExploreR that enables biologists, who produce data, to carry out protein microarray analysis independently using publicly available web service. PAWER is based on *pawer* – the R package that was first developed as part of this work.

6.1. PAWER pipeline

To start the analysis, PAWER expects fluorescent signal array readings – GenePix Results files as an input. Files are read in and assembled into a single data matrix using *limma* package in R [75]. Then the protein signal is estimated by subtracting the background signals from foreground intensities. Depending on the platform background subtraction is done using either default values (for ProtoArray or HuProt) or user-defined feature names. The resulting values are first log-transformed and then normalised via the robust linear model algorithm [47]. RLM models signal of control proteins that by default should exhibit no variation between conditions, using protein location (array and block) and the protein type. Later non-zero coefficients related to individual arrays and blocks are subtracted from the corresponding signal intensities to correct for existing biases. Control proteins that are used as a basis for the linear model can also be chosen manually by the user, through a convenient search interface. Otherwise, several reasonable default options are provided. The obtained normalised data matrix can be downloaded as a separate file. This file can then be used as an input to other tools to obtain additional insights. To enable principal component and clustering analysis of the normalised protein microarray data, PAWER is explicitly linked to ClustVis tool [114]. The user only needs to click a button and upload the file with normalised data to run the additional analysis.

Next, the user can provide meta-information about samples in order to identify proteins in which intensity levels significantly differ between conditions. Metadata can be either uploaded as a separate file or entered manually by clicking on a corresponding radio button for each GPR file in the input. Once the metadata has

been successfully uploaded, PAWER performs differential protein analysis. In this work, we used a moderated t-test, implemented in *limma* package [75]. In order to perform a moderated t-test, the number of samples must be larger than the number of conditions (at least by one). Therefore, since currently, PAWER supports only binary conditions, it requires at least three samples (in total) to perform the differential analysis. As in publication II, the Benjamini-Hochberg method [89] has been used to adjust computed p-values for multiple tests and thus, greatly reduce the number of false-positive proteins. Proteins with adjusted p-values of less than 0.05 are displayed in the results table along with boxplots that illustrate the distribution of the signal of each protein in the table. The content of the table can be changed by selecting only a subset of proteins. Both the table and boxplot visualization can be downloaded separately.

Proteins that exhibit differential levels of the signal across studied conditions are then characterised using *gprofiler2* R package, which is an interface to g:Profiler web service [85]. g:Profiler runs the enrichment analysis using differential proteins as a query. The top six most significant enrichment terms are visualised in a form of a bar plot that can also be downloaded. More visualisations and the remaining list of relevant enrichment terms can be accessed directly via g:Profiler by pressing “Open in g:Profiler” button in PAWER. The overall pipeline is presented in Figure 10.

One of our focuses for PAWER was designing a user-friendly interface, which would enable people with no special computer science background to carry out independent protein microarray analysis. To fulfill this vision, we added a comprehensive help page that helps new users to get started with PAWER. We recognised that preparing the data in the right format can be a problem for adapting bioinformatics tools as PAWER. Therefore, a sample data set with a corresponding metadata file is available for download from the main page as an example of the file format that PAWER expects. Also, demo results are linked from the home page. Initially, we developed PAWER for GPR files generated from ProtoArray and HuProt [115] platforms. Later, through additional customisation, PAWER has been made in principle compatible with any protein microarray system as long as it produces text files with consistent headers and a few key parameters (e.g. names of foreground and background intensity features) are specified.

6.2. Implementation

PAWER consists of two major parts: R package *paweR* at its computational core and the web interface. The heart of PAWER – *paweR* was written in R version 3.4.2 and uses functions from the following packages: *limma* [75], *reshape2* [116], *MASS* [74] and *gprofiler2* [85]. The web interface was implemented as a single-page application using React.js and Redux architecture on the client-side and node.js on the server-side. The figures are created and rendered with a help of D3.js [117] and DataTables libraries. Both the R package and the web-

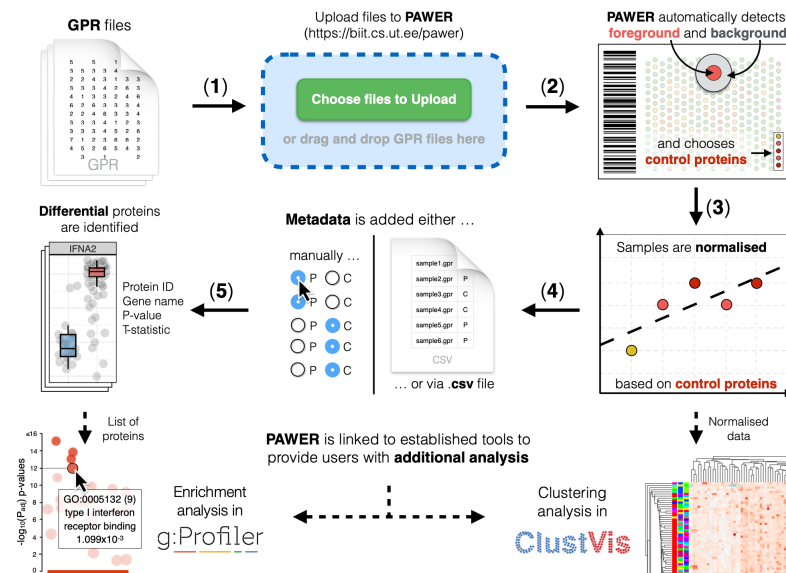


Figure 10. PAWER pipeline. Raw GPR files are uploaded to PAWER (1), then the system proceeds to identify foreground and background intensities and a panel of control proteins that can be used for normalisation (2). The robust linear model is then used to estimate and remove the technical artifacts associated with each array and array block (3). Normalised data is then combined with sample metadata (4) to produce a list of differentially expressed proteins (5). PAWER is linked with two other tools (g:Profiler and ClustVis) to enable additional analysis, namely: protein enrichment analysis and cluster analysis of normalised expression values.

server code are freely available under the GNU GPL v2. license.

6.3. Comparison to other tools

To the best of our knowledge there are four major tools available for protein microarray analysis (besides PAWER): Prospector, ProtoArray Analyser (PAA) [69], protein microarray analyser (PMA) [60] and an online tool available as part of the protein microarray database (PMD) [118]. When we started working on the first publication, the only option to analyse ProtoArray data was through Prospector software. Prospector was software developed and distributed by the manufacturer of the ProtoArray platform – Invitrogen, which later has been acquired by Thermo Fisher Scientific. The initial version of the Prospector did not allow us to analyse more than 65 samples at the same time [76], rendering it impractical for larger studies (e.g. publications I and II of this thesis). Although in later versions this limitation has been removed, the software still remained closed sourced and compatible only with outdated operating systems – Windows XP and Windows 7. Later, ProtoArray analyser – open-source R package was introduced [69]. PAA has become a standard tool for a lot of bioinformaticians that worked with protein microarray data. Most of the data analysis pipeline described in the previous sections (except enrichment analysis) has been implemented and thus accessible via PAA. Although, being very powerful, PAA still required substantial programming skills in order to be used efficiently. Another tool for analyzing protein microarray data – PMA, was developed and publicly published in 2018 [60]. PMA is a multiplatform Java application, that can be used by anyone through the point and click interface. Notably, PMA has implemented a lot of state-of-the-art computational methods for protein microarray analysis [60]. However, the lack of supporting documentation and maintenance, a large number of confusing parameters, and unclear input format, make this application hard to use. Also, PMA is not a stand-alone tool, after the signal normalisation is performed with PMA it requires other resources to be employed for the downstream analysis. Lastly, a tool that resides on the PMD website is the only web-based solution developed prior to current work [118]. According to the original publication, PMD offers an all-encompassing analysis of protein microarrays, including enrichment and differential analysis. However, when thoroughly tested using existing GPR files, the tool failed to produce results. Error messages displayed to the user, come straight from R and generally are not easy to understand to non-specialists. Moreover, no documentation file linked from the PMD tool page was accessible at the time of writing. Details of the implemented algorithms could be found in neither the original publication nor on the website. In response to the above-mentioned challenges, we developed PAWER – a freely available web-tool as a user-friendly way to analyse protein microarray data. PAWER attempts to combine the key features of the above-listed tools: it has an online interface like PMD, there is a rigid R core and separate R package (similar to PAA), it provides all-around analysis us-

ing state-of-the-art computational methods like PMA. The comparison between PAWER and other tools is presented in Table 1.

Table 1. Comparison between currently available protein microarray analysis tools: Prospector, PAA, PMA, PMD, and PAWER. The presence or absence of relevant features (in columns) are shown as pluses highlighted in green (present features) or minuses in red (absent features). We were not able to obtain results using the PMD tool, thus all the relevant entries are based on the claims made in the original publication and highlighted in gray.

Tool name	License	Last updated	Platform	GUI	Normalisation	Biomarker identification	Functional annotation	Downloadable visuals
Prospector	No license specified	2015	Windows 7 desktop application	+	+	+	-	-
PAA	BSD 3	2019	R package	-	+	+	-	+
PMA	No license specified	2018	Java desktop application	+	+	-	-	-
PMD	No license specified	2020	Web server R code	+	+	+	+	+
PAWER	GNU GPL V2.	2020	Web server, R package	+	+	+	+	+

6.4. Summary

PAWER is the only web-based solution solely focusing on providing state-of-the-art analysis methods for protein microarray experiments data. All the data and visualisations are freely downloadable from the website. User-friendly interface, comprehensive help page, pre-loaded results page, and sample data set – all make PAWER very easy to get started with and execute one's own analysis. Code for both: R package and web interface is publicly available.

7. VALIDATING RESULTS OF STATISTICAL TESTS USING MACHINE LEARNING MODELS ON PROTEIN EXPRESSION DATA (PUBLICATION IV)

In this final publication, a research group from the Faculty of Medicine at the University of Ljubljana (Slovenia) in collaboration with Medical University Vienna (Austria) measured the protein expression from patients' blood in an attempt to identify early signs of the common gynecological condition – endometriosis. Endometriosis is a benign gynecological disease that results in endometriotic lesions found outside the uterine cavity [4]. Endometriosis is an inflammatory disease, which often manifests itself in pelvic pain and results in infertility. As many inflammatory processes are regulated by a set of secreted proteins called cytokines [119], researchers hypothesised that levels of cytokines in patient blood can be predictive of disease status and can potentially be used as biomarkers in clinic.

The aforementioned problem definition presented itself as a suitable scenario for the case-control study. Such a study would normally employ univariate statistical tests to identify a handful of cytokines with concentration levels sufficiently different between endometriosis positive (cases) and negative (controls) subjects. While we would expect complex interactions between molecules to be the most decisive in biology, univariate tests will only spot protein features that can sufficiently explain the output variable in isolation from other inputs [120]. Hence, in order to discover more relevant biomarkers, more sophisticated analysis, capable of exploring multivariate associations between protein features must be performed. Additionally, case-control studies have been shown to be prone to various biases [121, 122]. It has been suggested that any evidence obtained from case-control studies must be carefully scrutinised and reviewed from multiple angles [122]. In this publication, we employed machine learning methods as a means to explore multivariate relationships between protein features and confirm observations made by the univariate tests with respect to single variables. We have already applied such a strategy in our own work on modelling severity score of Psoriasis [95].

In this publication, unlike previous papers, presented in this thesis, quantification of protein expression was performed using the xMAP Luminex platform, not protein microarrays. xMAP Luminex technology is a flow cytometric method based on colour-coded microspheres (also known as beads) [123]. Microspheres coupled with target-specific antibodies are used to capture target molecules from the sample. Colour coding enables the system to unambiguously identify each type of beads, hence, accurately recognise the presence of target molecules. [124]. According to the manufacturer's website, up to 500 different microspheres can be designed targeting as many molecules. Unlike protein microarrays, where thousands of proteins are incubated on the glass surface, and one sample essentially

corresponds to one array, the xMAP platform allows to measure one sample per well, making this approach much more affordable if the narrower set of proteins of interest is known in advance. In this work, xMAP Luminex platform was used to measure the concentration levels of 40 cytokines, mostly chemokines that have not been previously studied in the context of diagnosing endometriosis [4].

After samples were collected (210 samples in total), the expression of target proteins was measured using xMAP Luminex technology in accordance with relevant guidelines and protocols. Initial pre-processing of the raw data was done by the proprietary software tool – Bio-Plex™ Manager Software. Clinical and demographic data about subjects were included in the analysis.

We have first analysed individual protein features using a two-sided Wilcoxon rank-sum test (Mann-Whitney U test). The resulting p-values were corrected using the Bonferroni method to account for multiple tests (as many as there are protein features) being performed at the same time. The protein feature was considered to have significantly different expression levels between conditions if the corresponding corrected p-value was less than 0.05. In this work, none of the analysed cytokines and cytokine ratios showed statistically significant differences. Hence, univariate statistics suggested an absence of a meaningful association between cytokine levels in the blood and endometriosis. Next, we hypothesized that a more complex multivariate relationship can be present. To validate this hypothesis, we employed machine learning.

In terms of machine learning, we were dealing with a supervised learning problem as the outcome variable (diagnosis) was collected and available in advance. The binary nature of the outcome variable (endometriosis positive or negative) suggested a need to employ classification algorithms. A lot of classification models have been created and made readily available for researchers as part of software libraries (e.g. *caret* in R or *scikit-learn* in Python). These models differ in many aspects. As the goal of our research was to build a diagnostic model that could be used in clinical practice, the model's explainability was an important factor. Hence, we decided to use the decision tree algorithm (implemented in *rpart* package [125]). To validate the results of the decision tree algorithm, we also trained three other classification algorithms: random forest [93], generalised linear model [126] and weighted k-nearest neighbour algorithm [127]. Selected models (all but decision tree and random forest) represented intrinsically different families of machine learning methods, at the same being powerful enough to capture complex non-linear relationships between input features and the outcome [4]. Therefore, all four models were further trained on cytokines' concentrations in an attempt to predict the diagnosis.

Powerful machine learning models (such as the ones we have selected), trained on a fairly small set of observations, are fully capable of memorizing the signal distribution [128]. Evaluated on familiar examples, such models eagerly report highly optimistic performance that does not necessarily reflect a true differentiating power. This problem is known in the machine learning community as *overfit-*

ting. In order to obtain realistic results, it is a common practice to divide the data into a few independent non-overlapping parts. These usually referred to as training, validation, and test (or hold out) sets. Models are then trained on the training set, higher-order parameters are optimised using validation data and the final performance is assessed using the test set. For small datasets this approach can result in poorly performing models, as a sizeable part of data is not used for training. To utilise data more effectively, we applied repeated 4-fold cross-validation (CV) algorithm. This algorithm shuffles and then divides data into four equal parts, three-quarters of which are used for training while the last set is treated as a nominal validation set. This was done to generate unbiased performance estimates for each selected model without the need for a separate test set. The median of obtained estimates was thus considered an approximation of the final performance. In this work, none of the models showed performance sufficiently different from what can be expected at random, thus, confirming results obtained by univariate tests.

To summarise, in this collaborative work, we looked for an association between cytokines expression in blood with the presence or absence of endometriosis. Neither univariate tests nor machine learning algorithms found protein features that could alone or in combination accurately explain the value of the outcome variable. Our main contribution in this publication is two-fold: firstly, we used four different machine learning algorithms to support and validate the results of the univariate statistics, and secondly, we employed repeated 4-fold cross-validation instead of explicit validation and test sets to estimate the performance of selected machine learning models. The first contribution improved the trustworthiness of reported results, while the second enabled us to train models efficiently without fear of overfitting to available data. Although this work is based on data generated by other than the protein microarray platform, we feel that it fits nicely into the overall narrative of analysing protein expression data using means of modern data science.

This work has become pivotal for the contribution that the authors of this thesis have made to the DOME recommendations for supervised machine learning validation in biology which was accepted for publication in Nature Methods [128]. DOME presents a set of community-wide recommendations aiming at establishing standards for describing key aspects of machine learning pipelines: data, optimization strategies, models, and evaluation. These recommendations should improve the quality as well as increase the reproducibility of biological papers that employ machine learning models.

8. CONCLUSIONS

Accurate information about protein levels in the organism has shown to be a valuable asset in the understanding of human biology. The presence of certain types of proteins is associated with a threat to health and well-being, while the abundance of others can be life-saving. One of the ways to estimate protein quantities is through protein microarrays. Although, in many ways similar to DNA microarrays, protein microarrays are subject to distinct biological assumptions, rendering computational methods designed for DNA microarrays inadequate. An overarching theme of this thesis is exploring computational methods needed for all-around analysis of protein microarrays. To fulfill this vision, we have employed various approaches from statistics, data science, and machine learning.

In Publication I, we performed extensive data pre-processing including data normalisation and filtering in order to explore the protein profile of the autoimmune disorder APS1. We expanded this analysis further in Publication II as we discovered a group of proteins that were more likely to exhibit high-intensity levels in patients comparing to controls. We thoroughly characterised this group of positive proteins, using a vast number of publicly available datasets and tools for the enrichment analysis. Having recognised the amount of work and complexity such thorough analysis demands, we decided to develop an intuitive web-based tool for protein microarray analysis. Protein microarray web explorer has been developed and presented in Publication III. PAWER was built for researchers without a programming background. In publication IV we have explored the usefulness of machine learning methods for the analysis of protein concentrations. In collaboration with clinical partners from Slovenia and Austria, we have employed statistical tests as well as more sophisticated machine learning methods to differentiate between endometrium cases and controls, based on protein data. Here, we used a more data-efficient cross-validation approach to estimate the performance of the machine learning models. Both machine learning and classical statistical analysis have failed to tell the difference between samples, suggesting an absence of reliable biomarkers among cytokines measured in the study. Although data for this publication, unlike other papers was obtained using xMAP Luminex technology, we believe that similar methods can be applied to protein microarray experiments.

The capstone and the most important contribution of this thesis is the web-tool PAWER. PAWER encompasses all the important parts of the protein microarray analysis implemented in other publications, namely: the entire pre-processing pipeline including the normalisation strategy using robust linear model, differential, and enrichment analysis. The source code of the tool is available online.

To conclude, the work included in this thesis has explored a set of computational methods available for the protein microarray analysis as well as included practical recommendations both of which could be useful for those who plan to carry out their own analysis of protein expression data. The most essential meth-

ods presented here were included in the web-tool PAWER, allowing researchers to perform semi-automated analysis online in a drag-and-drop and point-and-click manner. A number of research projects have also benefited from work presented in the thesis, including BioEndoCar (<https://bioendocar.eu/>) – an international consortium with an aim to combine protein microarray data with information about blood metabolites to identify diagnostic and prognostic markers for endometrial cancer. The first-hand experience of applying machine learning methods in a biological context has inspired a contribution to the first set of recommendations for validating machine learning methods in biological studies [128]. These guidelines if adopted widely by the community may increase trust in machine learning research as well as improve the reproducibility of published findings, accelerating the progress in the field.

BIBLIOGRAPHY

- [1] Steffen Meyer, Martin Woodward, Christina Hertel, Philip Vlaicu, Yasmin Haque, Jaanika Kärner, Annalisa Macagno, Shimobi C. Onuoha, Dmytro Fishman, Hedi Peterson, Kaja Metsküla, Raivo Uiho, Kirsi Jääntti, Kati Hokynar, Anette S.B. Wolff, Kai Krohn, Annamari Ranki, Pärt Peterson, Kai Kisand, Adrian Hayday, Antonella Meloni, Nicolas Kluger, Eystein S. Husebye, Katarina Trebusak Podkrajsek, Tadej Battelino, Nina Bratanic, and Aleksandr Peet. AIRE-deficient patients harbor unique high-affinity disease-ameliorating autoantibodies. *Cell*, 166(3):582–595, July 2016.
- [2] Dmytro Fishman, Kai Kisand, Christina Hertel, Mike Rothe, Anu Remm, Maire Pihlap, Priit Adler, Jaak Vilo, Aleksandr Peet, Antonella Meloni, Katarina Trebusak Podkrajsek, Tadej Battelino, Øyvind Bruserud, Anette S. B. Wolff, Eystein S. Husebye, Nicolas Kluger, Kai Krohn, Annamari Ranki, Hedi Peterson, Adrian Hayday, and Pärt Peterson. Autoantibody repertoire in APECED patients targets two distinct subgroups of proteins. *Frontiers in Immunology*, 8, August 2017.
- [3] Dmytro Fishman, Ivan Kuzmin, Jaak Vilo, and Hedi Peterson. PAWER: Protein array web ExploreR. *BMC Bioinformatics*, July 2019.
- [4] Tamara Knific, Dmytro Fishman, Andrej Vogler, Manuela Gstöttner, René Wenzl, Hedi Peterson, and Tea Lanišnik Rižner. Multiplex analysis of 40 cytokines do not allow separation between endometriosis patients and controls. *Scientific Reports*, 9(1), November 2019.
- [5] Robert M. Sapolsky. *Behave: The Biology of Humans at Our Best and Worst*. Penguin Press, 2017.
- [6] Christine Vogel and Edward M. Marcotte. Insights into the regulation of protein abundance from proteomic and transcriptomic analyses. *Nature Reviews Genetics*, 13(4):227–232, March 2012.
- [7] Francis Harry Compton Crick. On protein synthesis. *Symp Soc Exp Biol*, 12:138–163, 1958.
- [8] Bruce Alberts, Alexander Johnson, Julian Lewis, Martin Raff, Keith Roberts, and Peter Walter. *Molecular Biology of the Cell*. Garland Science, 2002.
- [9] Alice B. Fulton and William B. Isaacs. Titin, a huge, elastic sarcomeric protein with a probable role in morphogenesis. *BioEssays*, 13(4):157–161, April 1991.
- [10] Elena A. Ponomarenko, Ekaterina V. Poverennaya, Ekaterina V. Ilgisonis, Mikhail A. Pyatnitskiy, Arthur T. Kopylov, Victor G. Zgoda, Andrey V. Lisitsa, and Alexander I. Archakov. The size of the human proteome: The width and depth. *International Journal of Analytical Chemistry*, 2016:1–6, 2016.

- [11] Abul K. Abbas, Andrew H. H. Lichtman, and Shiv Pillai. *Cellular and Molecular Immunology: with STUDENT CONSULT Online Access (Abbas, Cellular and Molecular Immunology)*. Saunders, 2011.
- [12] Jean S. Marshall, Richard Warrington, Wade Watson, and Harold L. Kim. An introduction to immunology and immunopathology. *Allergy, Asthma & Clinical Immunology*, 14(S2), September 2018.
- [13] David D. Chaplin. Overview of the immune response. *Journal of Allergy and Clinical Immunology*, 125(2):S3–S23, February 2010.
- [14] Ludger Klein, Bruno Kyewski, Paul M. Allen, and Kristin A. Hogquist. Positive and negative selection of the t cell repertoire: what thymocytes see (and don't see). *Nature Reviews Immunology*, 14(6):377–391, May 2014.
- [15] Sergio Romagnani. Immunological tolerance and autoimmunity. *Internal and Emergency Medicine*, 1(3):187–196, September 2006.
- [16] S J Walsh and L M Rau. Autoimmune diseases: a leading cause of death among young and middle-aged women in the united states. *American Journal of Public Health*, 90(9):1463–1466, September 2000.
- [17] Keith Elkon and Paolo Casali. Nature and functions of autoantibodies. *Nature Clinical Practice Rheumatology*, 4(9):491–498, September 2008.
- [18] Kai Kisand and Pärt Peterson. Autoimmune polyendocrinopathy candidiasis ectodermal dystrophy: known and novel aspects of the syndrome. *Annals of the New York Academy of Sciences*, 1246(1):77–91, December 2011.
- [19] Estelle Bettelli, Yijun Carrier, Wenda Gao, Thomas Korn, Terry B. Strom, Mohamed Oukka, Howard L. Weiner, and Vijay K. Kuchroo. Reciprocal developmental pathways for the generation of pathogenic effector TH17 and regulatory t cells. *Nature*, 441(7090):235–238, April 2006.
- [20] Tuure Kinnunen, Nicolas Chamberlain, Henner Morbach, Jinyoung Choi, Sangtaek Kim, Joseph Craft, Lloyd Mayer, Caterina Cancrini, Laura Passerini, Rosa Bacchetta, Hans D. Ochs, Troy R. Torgerson, and Eric Meffre. Accumulation of peripheral autoreactive b cells in the absence of functional human regulatory t cells. *Blood*, 121(9):1595–1603, February 2013.
- [21] Eric Meffre and Hedda Wardemann. B-cell tolerance checkpoints in health and autoimmunity. *Current Opinion in Immunology*, 20(6):632–638, December 2008.
- [22] Takeshi Tsubata. B-cell tolerance and autoimmunity. *F1000Research*, 6:391, March 2017.
- [23] Dennis Flaherty. *Immunology for Pharmacy - Elsevier eBook on Vital-Source (Retail Access Card)*. Mosby, 2011.
- [24] Laura Abel, Simone Kutschki, Michael Turewicz, Martin Eisenacher, Jale Stoutjesdijk, Helmut E. Meyer, Dirk Woitalla, and Caroline May. Autoim-

- immune profiling with protein microarrays in clinical applications. *Biochimica et Biophysica Acta (BBA) - Proteins and Proteomics*, 1844(5):977–987, May 2014.
- [25] C. Pihoker, L. K. Gilliam, C. S. Hampe, and A. Lernmark. Autoantibodies in diabetes. *Diabetes*, 54(Supplement 2):S52–S61, November 2005.
 - [26] Ludvig M. Sollid and Bana Jabri. Triggers and drivers of autoimmunity: lessons from coeliac disease. *Nature Reviews Immunology*, 13(4):294–302, March 2013.
 - [27] Eugenia Lauret and Luis Rodrigo. Celiac disease and autoimmune-associated conditions. *BioMed Research International*, 2013:1–17, 2013.
 - [28] Judith Fraussen, Nele Claes, Laura de Bock, and Veerle Somers. Targets of the humoral autoimmune response in multiple sclerosis. *Autoimmunity Reviews*, 13(11):1126–1137, November 2014.
 - [29] P. Peterson, J. Pitkanen, N. Sillanpaa, and K. Krohn. Autoimmune polyendocrinopathy candidiasis ectodermal dystrophy (APECED): a model disease to study molecular aspects of endocrine autoimmunity. *Clinical and Experimental Immunology*, 135(3):348–357, March 2004.
 - [30] Farhanah Aziz, Muneera Smith, and Jonathan M Blackburn. Autoantibody-based diagnostic biomarkers: Technological approaches to discovery and validation. In *Autoantibodies and Cytokines*. IntechOpen, April 2019.
 - [31] David Leslie, Peter Lipsky, and Abner Louis Notkins. Autoantibodies as predictors of disease. *Journal of Clinical Investigation*, 108(10):1417–1422, November 2001.
 - [32] Peter Delves. *Encyclopedia of immunology*. Academic Press, San Diego, 1998.
 - [33] Eric Nagele, Min Han, Cassandra DeMarshall, Benjamin Belinka, and Robert Nagele. Diagnosis of alzheimer’s disease based on disease-specific autoantibody profiles in human sera. *PLoS ONE*, 6(8):e23112, August 2011.
 - [34] Yi Huang and Heng Zhu. Protein array-based approaches for biomarker discovery in cancer. *Genomics, Proteomics & Bioinformatics*, 15(2):73–81, April 2017.
 - [35] Shabarni Gupta, K. P. Manubhai, Shuvolina Mukherjee, and Sanjeeva Srivastava. Serum profiling for identification of autoantibody signatures in diseases using protein microarrays. In *Methods in Molecular Biology*, pages 303–315. Springer New York, 2017.
 - [36] H Holman. The discovery of autoantibody to deoxyribonucleic acid. *Lupus*, 20(5):441–442, February 2011.
 - [37] A. L. Hepburn. The LE cell. *Rheumatology*, 40(7):826–827, July 2001.

- [38] Jacob M. Rosenberg and Paul J. Utz. Protein microarrays: A new tool for the study of autoantibodies in immunodeficiency. *Frontiers in Immunology*, 6, April 2015.
- [39] Jens Sobek, Kerstin Bartscherer, Anette Jacob, Jvrg Hoheisel, and Philipp Angenendt. Microarray technology as a universal tool for high-throughput analysis of biological systems. *Combinatorial Chemistry & High Throughput Screening*, 9(5):365–380, June 2006.
- [40] David A. Hall, Jason Ptacek, and Michael Snyder. Protein microarray technology. *Mechanisms of Ageing and Development*, 128(1):161–167, January 2007.
- [41] Cedric D Moore, Olutobi Z Ajala, and Heng Zhu. Applications in high-content functional protein microarrays. *Current Opinion in Chemical Biology*, 30:21–27, February 2016.
- [42] Heng Zhu and Jiang Qian. Applications of functional protein microarrays in basic and clinical research. In *Advances in Genetics Volume 79*, pages 123–155. Elsevier, 2012.
- [43] Monica Neagu, Marinela Bostan, and Carolina Constantin. Protein microarray technology: Assisting personalized medicine in oncology (review). *World Academy of Sciences Journal*, June 2019.
- [44] Jessica G. Duarte and Jonathan M. Blackburn. Advances in the development of human protein microarrays. *Expert Review of Proteomics*, 14(7):627–641, July 2017.
- [45] Xiaowei Zhu, Mark Gerstein, and Michael Snyder. Procat: a data analysis approach for protein microarrays. *Genome Biology*, 7(11):R110, 2006.
- [46] Nils Landegren, Donald Sharon, Eva Freyhult, Åsa Hallgren, Daniel Eriksson, Per-Henrik Edqvist, Sophie Bensing, Jeanette Wahlberg, Lawrence M. Nelson, Jan Gustafsson, Eystein S. Husebye, Mark S. Anderson, Michael Snyder, and Olle Kämpe. Proteome-wide survey of the autoimmune target repertoire in autoimmune polyendocrine syndrome type 1. *Scientific Reports*, 6(1), February 2016.
- [47] A. Sboner, A. Karpikov, G. Chen, M. Smith, D. Mattoon, M. Dawn, L. Freeman-Cook, B. Schweitzer, and M. B. Gerstein. Robust-linear-model normalization to reduce technical variability in functional protein microarrays. *J. Proteome Res.*, 8(12):5451–5464, Dec 2009. [PubMed:19817483] [doi:].
- [48] Jintao Long, Genhua Pan, Emmanuel Ifeakor, Robert Belshaw, and Xinzhong Li. Discovery of novel biomarkers for alzheimer’s disease from blood. *Disease Markers*, 2016:1–9, 2016.
- [49] T. Barrett, S. E. Wilhite, P. Ledoux, C. Evangelista, I. F. Kim, M. Tomashevsky, K. A. Marshall, K. H. Phillippy, P. M. Sherman, M. Holko, A. Yefanov, H. Lee, N. Zhang, C. L. Robertson, N. Serova, S. Davis,

- and A. Soboleva. NCBI GEO: archive for functional genomics data sets–update. *Nucleic Acids Res.*, 41(Database issue):D991–995, Jan 2013. [PubMed:23193258] [doi:10.1093/nar/gks1193] [PubMedCentral:PMC3531084].
- [50] Awais Athar, Anja Füllgrabe, Nancy George, Haider Iqbal, Laura Huerta, Ahmed Ali, Catherine Snow, Nuno A Fonseca, Robert Petryszak, Irene Papatheodorou, Ugis Sarkans, and Alvis Brazma. ArrayExpress update – from bulk to single-cell expression data. *Nucleic Acids Research*, 47(D1):D711–D715, 10 2018.
 - [51] Chao-Jun Hu, Guang Song, Wei Huang, Guo-Zhen Liu, Chui-Wen Deng, Hai-Pan Zeng, Li Wang, Feng-Chun Zhang, Xuan Zhang, Jun Seop Jeong, Seth Blackshaw, Li-Zhi Jiang, Heng Zhu, Lin Wu, and Yong-Zhe Li. Identification of new autoantigens for primary biliary cirrhosis using human proteome microarrays. *Molecular & Cellular Proteomics*, 11(9):669–680, May 2012.
 - [52] Jun Seop Jeong, Lizhi Jiang, Edisa Albino, Josean Marrero, Hee Sool Rho, Jianfei Hu, Shaohui Hu, Carlos Vera, Diane Bayron-Poueymiroy, Zulily Ann Rivera-Pacheco, Leonardo Ramos, Cecil Torres-Castro, Jiang Qian, Joseph Bonaventura, Jef D. Boeke, Wendy Y. Yap, Ignacio Pino, Daniel J. Eichinger, Heng Zhu, and Seth Blackshaw. Rapid identification of monospecific monoclonal antibodies using a human proteome microarray. *Molecular & Cellular Proteomics*, 11(6):O111.016253, February 2012.
 - [53] Jin-Gyoung Jung, Alexander Stoeck, Bin Guan, Ren-Chin Wu, Heng Zhu, Seth Blackshaw, Ie-Ming Shih, and Tian-Li Wang. Notch3 interactome analysis identified WWP2 as a negative regulator of notch3 signaling in ovarian cancer. *PLoS Genetics*, 10(10):e1004751, October 2014.
 - [54] Lina Yang, Jingfang Wang, Jianfang Li, Hainan Zhang, Shujuan Guo, Min Yan, Zhenggang Zhu, Bin Lan, Youcheng Ding, Ming Xu, Wei Li, Xiaonian Gu, Chong Qi, Heng Zhu, Zhifeng Shao, Bingya Liu, and Sheng-Ce Tao. Identification of serum biomarkers for gastric cancer diagnosis using a human proteome microarray. *Molecular & Cellular Proteomics*, 15(2):614–623, November 2015.
 - [55] Chaojun Hu, Wei Huang, Hua Chen, Guang Song, Ping Li, Qiang Shan, Xuan Zhang, Fengchun Zhang, Heng Zhu, Lin Wu, and Yongzhe Li. Autoantibody profiling on human proteome microarray for biomarker discovery in cerebrospinal fluid and sera of neuropsychiatric lupus. *PLOS ONE*, 10(5):e0126643, May 2015.
 - [56] Chao-Jun Hu, Jian-Bo Pan, Guang Song, Xiao-Ting Wen, Zi-Yan Wu, Si Chen, Wen-Xiu Mo, Feng-Chun Zhang, Jiang Qian, Heng Zhu, and Yong-Zhe Li. Identification of novel biomarkers for behcet disease diagnosis using human proteome microarray approach. *Molecular & Cellular Proteomics*, 16(2):147–156, October 2016.

- [57] David S. DeLuca, Ovidiu Marina, Surajit Ray, Guang Lan Zhang, Catherine J. Wu, and Vladimir Brusic. Data processing and analysis for protein microarrays. In *Protein Microarray for Disease Analysis*, pages 337–347. Humana Press, 2011.
- [58] Yingye Zheng. Study design considerations for cancer biomarker discoveries. *The Journal of Applied Laboratory Medicine*, 3(2):282–289, May 2018.
- [59] Paula Díez, Noelia Dasilva, María González-González, Sergio Matarraz, Juan Casado-Vela, Alberto Orfao, and Manuel Fuentes. Data analysis strategies for protein microarrays. *Microarrays*, 1(2):64–83, August 2012.
- [60] Jessica Da Gama Duarte, Ryan W. Goosen, Peter J. Lawry, and Jonathan M. Blackburn. PMA: Protein microarray analyser, a user-friendly tool for data processing and normalization. *BMC Research Notes*, 11(1), February 2018.
- [61] M. E. Ritchie, J. Silver, A. Oshlack, M. Holmes, D. Diyagama, A. Holloway, and G. K. Smyth. A comparison of background correction methods for two-colour microarrays. *Bioinformatics*, 23(20):2700–2707, August 2007.
- [62] Changyong Feng, Hongyue Wang, Naiji Lu, Tian Chen, Hua He, Ying Lu, and Xin M. Tu. Log-transformation and its implications for data analysis. *Shanghai Archives of Psychiatry*, 26(2):105–109, April 2014.
- [63] Ronald K. Pearson, Gregory E. Gonye, and James S. Schwaber. Outliers in microarray data analysis. In *Methods of Microarray Data Analysis III*, pages 41–55. Kluwer Academic Publishers, 2003.
- [64] Kai Kisand, Anette S. Bøe Wolff, Katarina Trebušak Podkrajšek, Liina Tserel, Maire Link, Kalle V. Kisand, Elisabeth Ersvaer, Jaakko Perheentupa, Martina Moter Erichsen, Nina Bratanic, Antonella Meloni, Filomena Cetani, Roberto Perniola, Berrin Ergun-Longmire, Noel Maclaren, Kai J. E. Krohn, Mikuláš Pura, Berthold Schalke, Philipp Ströbel, Maria Isabel Leite, Tadej Battelino, Eystein S. Husebye, Pärt Peterson, Nick Willcox, and Anthony Meager. Chronic mucocutaneous candidiasis in APECED or thymoma patients correlates with autoimmunity to th17-associated cytokines. *The Journal of Experimental Medicine*, 207(2):299–308, February 2010.
- [65] Anne Puel, Rainer Döffinger, Angels Natividad, Maya Chrabieh, Gabriela Barcenás-Morales, Capucine Picard, Aurélie Cobat, Marie Ouachée-Chardin, Antoine Toulon, Jacinta Bustamante, Saleh Al-Muhsen, Mohammed Al-Owain, Peter D. Arkwright, Colm Costigan, Vivienne McConnell, Andrew J. Cant, Mario Abinun, Michel Polak, Pierre-François Bougnères, Dinakantha Kumaratne, László Marodi, Amit Nahum, Chaim Roifman, Stéphane Blanche, Alain Fischer, Christine Bodemer, Laurent Abel, Desa Lilic, and Jean-Laurent Casanova. Autoantibodies against IL-17a, IL-17f, and IL-22 in patients with chronic mucocutaneous candidiasis

- and autoimmune polyendocrine syndrome type i. *The Journal of Experimental Medicine*, 207(2):291–297, February 2010.
- [66] Robert McGill, John W Tukey, and Wayne A Larsen. Variations of box plots. *The American Statistician*, 32(1):12–16, 1978.
 - [67] Marie Lisandra Zepeda-Mendoza and Osbaldo Resendis-Antonio. Hierarchical agglomerative clustering. In *Encyclopedia of Systems Biology*, pages 886–887. Springer New York, 2013.
 - [68] Martin Ester, Hans-Peter Kriegel, Jörg Sander, and Xiaowei Xu. A density-based algorithm for discovering clusters in large spatial databases with noise. In *Proceedings of the Second International Conference on Knowledge Discovery and Data Mining*, KDD’96, page 226–231. AAAI Press, 1996.
 - [69] Michael Turewicz, Maike Ahrens, Caroline May, Katrin Marcus, and Martin Eisenacher. PAA: an r/bioconductor package for biomarker discovery with protein microarrays. *Bioinformatics*, 32(10):1577–1579, January 2016.
 - [70] B.M. Bolstad, R.A Irizarry, M. Astrand, and T.P. Speed. A comparison of normalization methods for high density oligonucleotide array data based on variance and bias. *Bioinformatics*, 19(2):185–193, January 2003.
 - [71] Wei Wu, Nilesh Dave, GeorgeC Tseng, Thomas Richards, EricP Xing, and Naftali Kaminski. Comparison of normalization methods for codelink bioarray data. *BMC Bioinformatics*, 6(1):309, 2005.
 - [72] K. V. Ballman, D. E. Grill, A. L. Oberg, and T. M. Therneau. Faster cyclic loess: normalizing RNA arrays via linear models. *Bioinformatics*, 20(16):2778–2786, May 2004.
 - [73] William S. Cleveland. Robust locally weighted regression and smoothing scatterplots. *Journal of the American Statistical Association*, 74(368):829–836, December 1979.
 - [74] William N Venables and Brian D Ripley. *Modern applied statistics with S-PLUS*. Springer Science & Business Media, 2013.
 - [75] G. K. Smyth. Linear models and empirical bayes methods for assessing differential expression in microarray experiments. *Stat Appl Genet Mol Biol*, 3:Article3, 2004. [PubMed:16646809] [doi:].
 - [76] Michael Turewicz, Caroline May, Maike Ahrens, Dirk Voitalla, Ralf Gold, Swaantje Casjens, Beate Pesch, Thomas Brüning, Helmut E. Meyer, Eckhard Nordhoff, Miriam Böckmann, Christian Stephan, and Martin Eisenacher. Improving the default data analysis workflow for large autoimmune biomarker discovery studies with ProtoArrays. *PROTEOMICS*, 13(14):2083–2087, June 2013.

- [77] Gordon K Smyth. Linear models and empirical bayes methods for assessing differential expression in microarray experiments. *Statistical Applications in Genetics and Molecular Biology*, 3(1):1–25, January 2004.
- [78] H. B. Mann and D. R. Whitney. On a test of whether one of two random variables is stochastically larger than the other. *The Annals of Mathematical Statistics*, 18(1):50–60, March 1947.
- [79] Eugene S. Edgington. Randomization tests. In *International Encyclopedia of Statistical Science*, pages 1182–1183. Springer Berlin Heidelberg, 2011.
- [80] David Howell. *Statistical methods for psychology*. Thomson Wadsworth, Australia Belmont, CA, 2010.
- [81] Minoru Kanehisa, Miho Furumichi, Mao Tanabe, Yoko Sato, and Kanae Morishima. KEGG: new perspectives on genomes, pathways, diseases and drugs. *Nucleic Acids Research*, 45(D1):D353–D361, November 2016.
- [82] Antonio Fabregat, Steven Jupe, Lisa Matthews, Konstantinos Sidiropoulos, Marc Gillespie, Phani Garapati, Robin Haw, Bijay Jassal, Florian Korninger, Bruce May, Marija Milacic, Corina Duenas Roca, Karen Rothfels, Cristoffer Sevilla, Veronica Shamovsky, Solomon Shorser, Thawfeek Varusai, Guilherme Viteri, Joel Weiser, Guanming Wu, Lincoln Stein, Henning Hermjakob, and Peter D’Eustachio. The reactome pathway knowledge-base. *Nucleic Acids Research*, 46(D1):D649–D655, November 2017.
- [83] Sebastian Köhler, Leigh Carmody, Nicole Vasilevsky, Julius O B Jacobsen, Daniel Danis, Jean-Philippe Gourdine, Michael Gargano, Nomi L Harris, Nicolas Matentzoglou, Julie A McMurphy, David Osumi-Sutherland, Valentina Cipriani, James P Balhoff, Tom Conlin, Hannah Blau, Gareth Baynam, Richard Palmer, Dylan Gratian, Hugh Dawkins, Michael Segal, Anna C Jansen, Ahmed Muaz, Willie H Chang, Jenna Bergerson, Stanley J F Lalederkind, Zafer Yüksel, Sergi Beltran, Alexandra F Freeman, Panagiotis I Sergouniotis, Daniel Durkin, Andrea L Storm, Marc Hanauer, Michael Brudno, Susan M Bello, Murat Sincan, Kayli Rageth, Matthew T Wheeler, Renske Oegema, Halima Loughi, Maria G Della Rocca, Rachel Thompson, Francisco Castellanos, James Priest, Charlotte Cunningham-Rundles, Ayushi Hegde, Ruth C Lovering, Catherine Hajek, Annie Olry, Luigi Notarangelo, Morgan Similuk, Xingmin A Zhang, David Gómez-Andrés, Hanns Lochmüller, Hélène Dollfus, Sergio Rosenzweig, Shruti Marwaha, Ana Rath, Kathleen Sullivan, Cynthia Smith, Joshua D Milner, Dorothée Leroux, Cornelius F Boerkoel, Amy Klion, Melody C Carter, Tudor Groza, Damian Smedley, Melissa A Haendel, Chris Mungall, and Peter N Robinson. Expansion of the human phenotype ontology (HPO) knowledge base and resources. *Nucleic Acids Research*, 47(D1):D1018–D1027, November 2018.
- [84] Mathias Uhlén, Linn Fagerberg, Björn M Hallström, Cecilia Lindskog, Per Oksvold, Adil Mardinoglu, Åsa Sivertsson, Caroline Kampf,

- Evelina Sjöstedt, Anna Asplund, et al. Tissue-based map of the human proteome. *Science*, 347(6220):1260419, 2015. [PubMed:25613900] [doi:10.1126/science.1260419].
- [85] Uku Raudvere, Liis Kolberg, Ivan Kuzmin, Tambet Arak, Priit Adler, Hedi Peterson, and Jaak Vilo. g:profiler: a web server for functional enrichment analysis and conversions of gene lists (2019 update). *Nucleic Acids Research*, 47(W1):W191–W198, May 2019.
 - [86] Megan Goldman. Lecture notes in stat c141/bioeng c141 - statistics for bioinformatics, 2008.
 - [87] Carlo Bonferroni. Teoria statistica delle classi e calcolo delle probabilit . *Pubblicazioni del R Istituto Superiore di Scienze Economiche e Commerciali di Firenze*, 8:3–62, 1936.
 - [88] William S Noble. How does multiple testing correction work? *Nature Biotechnology*, 27(12):1135–1137, December 2009.
 - [89] Yoav Benjamini and Yosef Hochberg. Controlling the false discovery rate - a practical and powerful approach to multiple testing. *J. Royal Statist. Soc., Series B*, 57:289 – 300, 11 1995.
 - [90] Bruno D. Zumbo. Univariate tests. In *Encyclopedia of Quality of Life and Well-Being Research*, pages 6819–6820. Springer Netherlands, 2014.
 - [91] Adi L Tarca, Vincent J Carey, Xue wen Chen, Roberto Romero, and Sorin Dr aghici. Machine learning and its applications to biology. *PLoS Computational Biology*, 3(6):e116, June 2007.
 - [92] J. R. Quinlan. Induction of decision trees. *Machine Learning*, 1(1):81–106, March 1986.
 - [93] Leo Breiman. Random forests. *Machine Learning*, 45(1):5–32, 2001.
 - [94] Leo Breiman, Jerome H. Friedman, Richard A. Olshen, and Charles J. Stone. *Classification And Regression Trees*. Routledge, October 2017.
 - [95] Aigar Ottas, Dmytro Fishman, Tiia-Linda Okas, K lli Kingo, and Ursel Soomets. The metabolic analysis of psoriasis identifies the associated metabolites while providing computational models for the monitoring of the disease. *Archives of Dermatological Research*, 309(7):519–528, July 2017.
 - [96] Alex Krizhevsky, Ilya Sutskever, and Geoffrey E Hinton. Imagenet classification with deep convolutional neural networks. In F. Pereira, C. J. C. Burges, L. Bottou, and K. Q. Weinberger, editors, *Advances in Neural Information Processing Systems 25*, pages 1097–1105. Curran Associates, Inc., 2012.
 - [97] Christof Angermueller, Tanel P rnamaa, Leopold Parts, and Oliver Stegle. Deep learning for computational biology. *Molecular Systems Biology*, 12(7):878, July 2016.

- [98] William Jones, Kaur Alasoo, Dmytro Fishman, and Leopold Parts. Computational biology: deep learning. *Emerging Topics in Life Sciences*, 1(3):257–274, November 2017.
- [99] Vivian Kont, Martti Laan, Kai Kisand, Andres Merits, Hamish S. Scott, and Pärt Peterson. Modulation of aire regulates the expression of tissue-restricted antigens. *Molecular Immunology*, 45(1):25–33, January 2008.
- [100] Kentaro Nagamine, Pärt Peterson, Hamish S. Scott, Jun Kudoh, Shinsei Minoshima, Maarit Heino, Kai J. E. Krohn, Maria D. Lalioti, Primus E. Mullis, Stylianos E. Antonarakis, Kazuhiko Kawasaki, Shuichi Asakawa, Fumiaki Ito, and Nobuyoshi Shimizu. Positional cloning of the APECED gene. *Nature Genetics*, 17(4):393–398, December 1997.
- [101] A. Coutinho, G. Pobor, S. Pettersson, T. Leandersson, S. Forsgren, P. Pereira, A. Bandeira, and C. Martinez-A. T cell-dependent b cell activation. *Immunological Reviews*, 78(1):211–224, April 1984.
- [102] Nicolas Kluger, Annamari Ranki, and Kai Krohn. APECED: is this a model for failure of t cell and b cell tolerance? *Frontiers in Immunology*, 3, 2012.
- [103] Nils Landegren, Lindsey B Rosen, Eva Freyhult, Daniel Eriksson, Tove Fall, Gustav Smith, Elise M N Ferre, Petter Brodin, Donald Sharon, Michael Snyder, Michail Lionakis, Mark Anderson, and Olle Kämpe. Comment on 'AIRE-deficient patients harbor unique high-affinity disease-ameliorating autoantibodies'. *eLife*, 8, June 2019.
- [104] Christina Hertel, Dmytro Fishman, Anna Lorenc, Annamari Ranki, Kai Krohn, Pärt Peterson, Kai Kisand, and Andrian Hayday. Response to comment on 'aire-deficient patients harbor unique high-affinity disease-ameliorating autoantibodies', 2019.
- [105] R. A. Fisher. On the interpretation of χ^2 from contingency tables, and the calculation of p. *Journal of the Royal Statistical Society*, 85(1):87, January 1922.
- [106] Mathieu P. Rodero, Jérémie Decalf, Vincent Bondet, David Hunt, Gillian I. Rice, Scott Werneke, Sarah L. McGlasson, Marie-Alexandra Alyanakian, Brigitte Bader-Meunier, Christine Barnerias, Nathalia Bellon, Alexandre Belot, Christine Bodemer, Tracy A. Briggs, Isabelle Desguerre, Marie-Louise Frémond, Marie Hully, Arn M.J.M. van den Maagdenberg, Isabelle Melki, Isabelle Meyts, Lucile Musset, Nadine Pelzer, Pierre Quartier, Gisela M. Terwindt, Joanna Wardlaw, Stewart Wiseman, Frédéric Rieux-Laucat, Yoann Rose, Bénédicte Neven, Christina Hertel, Adrian Hayday, Matthew L. Albert, Flore Rozenberg, Yanick J. Crow, and Darragh Duffy. Detection of interferon alpha protein reveals differential levels and cellular sources in disease. *The Journal of Experimental Medicine*, 214(5):1547–1555, April 2017.
- [107] Marie-Louise Frémond, Carolina Ugenti, Lien Van Eyck, Isabelle Melki, Vincent Bondet, Naoki Kitabayashi, Christina Hertel, Adrian Hayday,

- B  n  dicte Neven, Yoann Rose, Darragh Duffy, Yanick J. Crow, and Mathieu P. Rodero. Brief report: Blockade of TANK-binding kinase 1/IKK  inhibits mutant stimulator of interferon genes (STING)-mediated inflammatory responses in human peripheral blood mononuclear cells. *Arthritis & Rheumatology*, 69(7):1495–1501, June 2017.
- [108] Joel Sng, Burcu Ayoglu, Jeff W. Chen, Jean-Nicolas Schickel, Elise M. N. Ferre, Salom   Glauzy, Neil Romberg, Manfred Hoenig, Charlotte Cunningham-Rundles, Paul J. Utz, Michail S. Lionakis, and Eric Meffre. AIRE expression controls the peripheral selection of autoreactive b cells. *Science Immunology*, 4(34):eaav6778, April 2019.
- [109] Eirik Bratland and Eystein S. Husebye. Cellular immunity and immunopathology in autoimmune addison’s disease. *Molecular and Cellular Endocrinology*, 336(1-2):180–190, April 2011.
- [110] Kevan C. Herold, Dario A. A. Vignali, Anne Cooke, and Jeffrey A. Bluestone. Type 1 diabetes: translating mechanistic observations into effective clinical outcomes. *Nature Reviews Immunology*, 13(4):243–256, March 2013.
- [111] Satoshi Okada, Anne Puel, Jean-Laurent Casanova, and Masao Kobayashi. Chronic mucocutaneous candidiasis disease associated with inborn errors of IL-17 immunity. *Clinical & Translational Immunology*, 5(12):e114, December 2016.
- [112] NCBI Resource Coordinators. Database resources of the National Center for Biotechnology Information. *Nucleic Acids Research*, 46(D1):D8–D13, 11 2017.
- [113] Andrew D Yates, Premanand Achuthan, Wasiu Akanni, James Allen, Jamie Allen, Jorge Alvarez-Jarreta, M Ridwan Amode, Irina M Armean, Andrey G Azov, Ruth Bennett, Jyothish Bhai, Konstantinos Billis, Sanjay Boddu, Jos   Carlos Marug  n, Carla Cummins, Claire Davidson, Kamalkumar Dodiya, Reham Fatima, Astrid Gall, Carlos Garcia Giron, Laurent Gil, Tiago Grego, Leanne Haggerty, Erin Haskell, Thibaut Hourlier, Osagie G Izuogu, Sophie H Janacek, Thomas Juettemann, Mike Kay, Ilias Lavidas, Tuan Le, Diana Lemos, Jose Gonzalez Martinez, Thomas Maurel, Mark McDowall, Aoife McMahon, Shamika Mohanan, Benjamin Moore, Michael Nuhn, Denye N Oheh, Anne Parker, Andrew Parton, Mateus Patricio, Manoj Pandian Sakthivel, Ahamed Imran Abdul Salam, Bianca M Schmitt, Helen Schuilenburg, Dan Sheppard, Mira Sycheva, Marek Szuba, Kieron Taylor, Anja Thormann, Glen Threadgold, Alessandro Vullo, Brandon Walts, Andrea Winterbottom, Amonida Zadissa, Marc Chakiachvili, Bethany Flint, Adam Frankish, Sarah E Hunt, Garth Iisley, Myrto Kostadima, Nick Langridge, Jane E Loveland, Fergal J Martin, Joannella Morales, Jonathan M Mudge, Matthieu Muffato, Emily Perry, Magali Ruffier, Stephen J Trevanion, Fiona Cunningham, Kevin L Howe, Daniel R

- Zerbino, and Paul Flicek. Ensembl 2020. *Nucleic Acids Research*, November 2019.
- [114] Tauno Metsalu and Jaak Vilo. ClustVis: a web tool for visualizing clustering of multivariate data using principal component analysis and heatmap. *Nucleic Acids Research*, 43(W1):W566–W570, May 2015. [PubMed:25969447] [PubMedCentral: PMC4489295].
 - [115] J. S. Jeong, L. Jiang, E. Albino, J. Marrero, H. S. Rho, J. Hu, S. Hu, C. Vera, D. Bayron-Poueymiroy, Z. A. Rivera-Pacheco, L. Ramos, C. Torres-Castro, J. Qian, J. Bonaventura, J. D. Boeke, W. Y. Yap, I. Pino, D. J. Eichinger, H. Zhu, and S. Blackshaw. Rapid identification of monospecific monoclonal antibodies using a human proteome microarray. *Mol. Cell Proteomics*, 11(6):O111.016253, Jun 2012. [PubMed:22307071] [doi:10.1074/mcp.O111.016253] [PubMedCentral: PMC3433917].
 - [116] Hadley Wickham et al. Reshaping data with the reshape package. *Journal of Statistical Software*, 21(12):1–20, 2007. [doi:].
 - [117] M. Bostock, V. Ogievetsky, and J. Heer. D³: Data-Driven Documents. *IEEE Trans Vis Comput Graph*, 17(12):2301–2309, Dec 2011. [PubMed:22034350].
 - [118] Zhaowei Xu, Likun Huang, Hainan Zhang, Yang Li, Shujuan Guo, Nan Wang, Shi hua Wang, Ziqing Chen, Jingfang Wang, and Sheng ce Tao. PMD: A resource for archiving and analyzing protein microarray data. *Scientific Reports*, 6(1), January 2016.
 - [119] Jun-Ming Zhang and Jianxiong An. Cytokines, inflammation, and pain. *International Anesthesiology Clinics*, 45(2):27–37, 2007.
 - [120] Vân Anh Huynh-Thu, Yvan Saeys, Louis Wehenkel, and Pierre Geurts. Statistical interpretation of machine learning-based feature importance scores for biomarker discovery. *Bioinformatics*, 28(13):1766–1774, April 2012.
 - [121] C J Mann. Observational research methods. research design II: cohort, cross sectional, and case-control studies. *Emergency Medicine Journal*, 20(1):54–60, January 2003.
 - [122] Alexander Melamed and Julian N Robinson. Case-control studies can be useful but have many limitations. *BJOG: An International Journal of Obstetrics & Gynaecology*, 126(1):23–23, June 2018.
 - [123] Ju-Hee Kang, Hugo Vanderstichele, John Q. Trojanowski, and Leslie M. Shaw. Simultaneous analysis of cerebrospinal fluid biomarkers using microsphere-based xMAP multiplex technology for early detection of alzheimer’s disease. *Methods*, 56(4):484–493, April 2012.
 - [124] K Kellar. Multiplexed microsphere-based flow cytometric assays. *Experimental Hematology*, 30(11):1227–1237, November 2002.

- [125] Carolin Strobl, James Malley, and Gerhard Tutz. An introduction to recursive partitioning: Rationale, application, and characteristics of classification and regression trees, bagging, and random forests. *Psychological Methods*, 14(4):323–348, December 2009.
- [126] J. A. Nelder and R. W. M. Wedderburn. Generalized linear models. *Journal of the Royal Statistical Society. Series A (General)*, 135(3):370, 1972.
- [127] Jianping Gou, Lan Du, Yuhong Zhang, and Taisong Xiong. A new distance-weighted k -nearest neighbor classifier. *J. Inf. Comput. Sci.*, 9, 11 2011.
- [128] Ian Walsh, Dmytro Fishman, Dario Garcia-Gasulla, Tiina Titma, The ELIXIR Machine Learning focus group, Jen Harrow, Fotis E. Psomopoulos, and Silvio C. E. Tosatto. Dome: Recommendations for machine learning validation in biology. *Nature Methods*, 2020.

ACKNOWLEDGEMENTS

Although it is hard to make a truly exhaustive list of all the people I met and who influenced me, below is my diligent attempt to give credit to as many of them as possible.

I met *Jaak Vilo* on my first semester as a Master's student at the University of Tartu. He has been teaching one of the core courses in our curriculum - advanced algorithms. In the beginning, our expectations were not very high - in my previous university, no one would anticipate great teaching skills from the institute's head. Yet, we were wrong. Jaak's lectures were and are interactive, not only he asked questions from the audience, but he was also genuinely interested in hearing the answers. I admired his ability to admit that he does not know everything and allowing students to correct him. His respectful and supportive attitude towards students inspired me. Later, I learned that Jaak is also the head of the bioinformatics research team - a group of people with a primarily technical background who use computer science to help improve our understanding of the human condition. Jaak also has been the one to invite me to apply for PhD in his group. I am incredibly grateful to Jaak for guiding me towards bioinformatics and teaching. I have never regretted my choice.

When *Hedi Peterson* returned to Tartu from her post-doc in Switzerland, I was already in the middle of the first year of my PhD. Yet, very soon, she has become a go-to person and a support for all young PhD students in our group, including myself. She has successfully combined a scientific advisor, psychologist, and friend's roles, helping us stay motivated, productive, and happy. Needless to say that we needed the last two roles as often as the first.

Work on this thesis was not always easy and did not come without moments of despair. On multiple such occasions, I approached Hedi asking if this would make sense to change the topic and maybe try something else. Yet every time, she would remain adamant and convinced me to keep trying. It is largely owing to her support at these darkest hours this thesis finally came to be. Moreover, all four publications included in this thesis have been carried out under her close supervision.

Hedi's contribution to the text of this thesis deserves a paragraph on its own. Although this work formally has only one author, if this would be a popular science book, Hedi Peterson would undoubtedly be its well-deserved co-author. Her clever and always-to-the-point edits have helped me to improve this text significantly. She has been through the entire writing process from the very early and barely readable drafts to the very end, fixing minor typos. Her almost superhuman capacity to find flaws both big and small and attention to details is as impressive as it is terrifying, making people who do not know her suspect that some extraterrestrial forces are at work.

I am fortunate that one day Hedi decided not to make an app but to make the difference.

When I started the work on Publication I, I had a very rudimentary understanding of basic biology and a completely non-existent comprehension of immunology. Although I certainly did not become an expert in immunology, yet everything I do know about the field, I owe to *Pärt Peterson* and *Kai Kisand*. Their seemingly endless patience when answering my borderline stupid questions on the one hand and a capacity to take very seriously my comments related to computer science and statistics on the other created a safe environment for interdisciplinary research so much needed for an early-stage PhD student. This tandem will remain in my memory as an example of perfect clinical collaborators, a source of wisdom and guidance. Pärt has also provided so much appreciated feedback on this thesis and defense presentation. He has edited a chapter related to immunity.

After I first met Jaak and realised that by joining the bioinformatics group, one could learn to employ computer science methods for the good of all humanity, most of the hard work on turning me into someone at least partially resembling a bioinformatician took over *Konstantin Tretjakov*. Kostja has supervised my Master's thesis, dedicating a lot of time to developing my writing and reasoning skills. Kostja has also significantly influenced me as a lecturer. I hope one day to solve at least one percent of all riddles that Kostja gave me.

Learning from the best never stopped as later I met a bright-eyed group leader from Sanger Institute - *Leopold Parts*. I am fortunate to have Leo as a senior member and a co-lead of the medical imaging research group in collaboration with PerkinElmer. Not only Leo served as a role model of a successful scientist and kept inspiring me throughout the years, but he has also actively helped and supported me as a mentor and unofficial fourth supervisor of this thesis.

I want to pay a special tribute to all three of my reviewers: *Raivo Kolde*, *Jessica Da Gama Duarte* and *Fridtjof Lund-Johansen*. Their comments have significantly improved both the content and the presentation of this thesis.

Members of the bioinformatics and information technology (BIIT) research group will always have a special place in my mind and heart. *Priit (Lemps) Adler* - a mentor and a friend, I learn a lot from you. Big thank you to *Liis Kolberg* and *Uku Raudvere* for all the invaluable help with this thesis. I cannot thank enough to *Kaido Lepik* for his cool-headed support in times of need as well as for the joint sports activities. *Ivan Kuzmin* who has been my dear teacher of web development as well as an active maintainer of the PAWER tool we have developed for Publication III. He has also set in motion my interest in philosophy and showed a lot of new ways to look at the world. I want to thank *Kaur Alasoo* for his comments

on the PAWER paper - I am looking forward to our future joint paper. Thanks to *Ahto Salumeets* for his valuable comments on the immunity chapter as well as great scientific discussions. I owe a lot in various ways to *Elena Sügis, Nurlan Kerimov, Mari-Liis Allikivi, Erik Jaaniso, Joonas Puura, Sulev Reisberg, Sven Laur, Anna Leontjeva, Ilya Kuzovkin, Meelis Kull, Ulvi Talas, Kateryna Peikova, Balaji R, Oliver Nisumaa, Siyuan Gao, Tambet Arak, Tauno Metsalu, Vijayachitra Modhukur* and *Tõnis Tasa*.

I would like to express my deepest gratitude to PerkinElmer project family: *Kaupo Palo, Leopold Parts, Olavi Ollikainen, Hartwig Preckel, Sten-Oliver Salumaa, Mikhail Papkov, Mohammed Ali, Tõnis Laasfeld, Dmytro Urukov, Kaspar Hollo, Iaroslav Plutenko, Tetiana Rabiichuk, Tarun Khajuria, Oleh Misko, Oles Pryhoda, Bohdan Petryshak, Roman Ring, Oliver Meikar* and *Daniel Majoral*.

Warmest thanks to BioEndoCar project partners: *Tea Lanišnik Rižner, Andrea Romano, Tamara Knific, Eva Hafner, Jerzy Adamski, Janina Tokarz, Christoph Schröder, Camille Lowy* and *Andrzej Semczuk*. This is one of the most medically relevant projects I have been part of.

Many thanks to Autonomous Driving Lab researchers and students including but not limited to *Tambet Matiisen, Anne Jääger, Meelis Kull, Ardi Tampuu, Naveed Muhammad, Alexander Nolte, Karl Kruusamäe, Raimundas Matulevicius, Arun Singh, Amnir Hadachi, Edgar Sepp, Navid Roshan, Dmytro Zabolotnii, Jan Aare van Gent, Kertu Toompea, Maxandre Ogeret, Thomas Churchman* and *Tanya Shtym*. I am proud to be part of this immensely cool and important project.

Special thanks to the admin team of the institute of computer science who have created an outstanding work environment: *Jaak Vilo, Mark Fishel, Piret Orav, Jaanika Seli, Heili Kase, Natali Belinska, Ülle Holm, Liivi Luik, Anne Jääger, Anastasiia Shevchenko, Annet Muru, Anni Suvi, Henry Narits, Martin Kaljula, Reili Liiver, Anneli Väinumäe, Kätoliin Jääger, Sairi Petti* and *Daisy Alatare*.

Also, my profound appreciation to three brave human beings that together with me are trying to make the difference for all: *Priit Salumaa, Bohdan Petryshak* and *Martin Reim*.

I am grateful to all students that I have ever had the pleasure to teach or supervise. Please, know that I have learned from you as much and even more than you have learned from me.

Thanks to my family and friends for their unconditional love and limitless support that kept me going.

Finally, last but definitely not least, thank you to my beloved wife - Lena. A political scientist by education and an artist at heart, she has willingly succumbed herself to the fields of machine learning, artificial intelligence, statistics, bioinformatics, and programming by agreeing to be the subject of my lecture and workshop rehearsals. She possesses a unique ability to add color, joy, and purpose to my life. It is my true pleasure to share a planet and an epoch with this caring and gentle being.

SISUKOKKUVÕTE

Andmeanalüüsi töövooloomine valkude automaatseks kirjeldamiseks immunoloogias

Valgud on kõigi elusorganismide olulised koostisosad. Nendest keerukatest molekulidest sõltub suur hulk eluliselt olulisi funktsioone. Valkude kogus organismi rakkudes on rangelt reguleeritud, kuna liigne kogus või äge puudus võib põhjustada soovimatuid tagajärgi. Ebanormaalne valkude tase võib olla tõsise talitlushäire märk. Seetõttu võib võime täpselt hinnata valkude kontsentratsiooni kehas olla haiguse mehhanismide mõistmise võti.

Valgu mikrokiibid on populaarne viis valkude kontsentratsiooni mõõtmiseks vereproovist. Sel moel saab paralleelselt mõõta sadade või isegi tuhandete valkude kontsentratsioone. Ehkki valgukiipidel on palju ühist DNA-mikrokiipidega, ei sobi kõik DNA-mikrokiipide jaoks välja töötatud arvutusmeetodid erinevate bioloogiliste eelduste tõttu valgukiipidele. Seetõttu on valgukiipide kui andmete tootmise platvormi kõigi võimaluste tõhusaks kasutamiseks hädavajalikud spetsiaalselt neile kohandatud meetodid.

Klassikaline valguandmete analüüs on keeruline ja koosneb järjestikku rakendatud arvutusmeetodite seeriast. Analüüsi paikapidavuse tagamiseks on vajalikud meetodid tehnilise müra vähendamiseks, väärtuste tuvastamiseks ja eemaldamiseks ning saadud signaali väärtuste normaliseerimiseks. Statistilisi teste ja masinõppe meetodeid kasutatakse nii individuaalsete valkude kui ka nende kombinatsioonide tuvastamiseks võttes arvesse valke, mille tasemed on katsetingimuste vahel piisavalt erinevad. Lõpuks aitavad funktsionaalse rikastamise analüüsi tööriistad viia sellised valgud kõige levinumate bioloogiliste funktsioonide konteksti. Käesolevas töös uurisime valgu mikrokiibi katsetest saadud andmete analüüsiks kasutatavaid arvutuslikke meetodeid ja optimeerisime nende andmete analüüsi töövoogu. Selle tulemusena töötasime välja veebitööriista, mis aitab kogu seda analüüsi poolautomaatselt läbi viia. Doktoritöös kirjeldatud meetodeid rakendasime praktikas mitmes valgu mikrokiipidega seotud teadustöös.

Käesolevas dissertatsioonis kirjeldame esmalt uuringut, kus valgu mikrokiipidega mõõdeti 1. Tüüpi autoimmuunse polüendokrinopaatia sündroomiga (APS1) patsientide vere autoantikehade sisaldust. APS1 patsientidel autoimmuunse reaktsiooni sihtmärgiks olevate valkude esialgse loendi määratlemiseks viisime läbi valgu mikrokiibi-spetsiifilise eeltöötluse analüüsi töövoogu ja diferentsiaalanalüüsi.

Meie eesmärk oli APS1 seisundi ja autoimmuunsuse taga olevate mehhanismide sügavam mõistmine. Seetõttu uurisime esimeses artiklis tuvastatud valgu sihtmärke edasi. Töö käigus analüüsisime mitmeid avalikke andmebaase ja valkude funktsionaalse rikastamise andmekogusid, et teha kindlaks valgu sihtmärkide taga olevad ühised bioloogilised tegurid. Tulemuste kinnitamiseks viisime läbi funktsionaalse rikastamise analüüsi kasutades g:Profileri veebitööriista.

Saadud valgu mikrokiipide analüüsi kogemuse põhjal sidusime loodud and-

meanalüüsi vahendid R-programmeerimiskeele põhiseks veebitööriistaks PAWER. PAWER, mis on loodud valgu mikrokiibi andmete analüüsi poolautomaatseks läbiviimiseks, on käesoleva doktoritöö põhitulemuseks. Selle intuitiivne kasutajaliides ja järkjärguline töövoog on loodud valgu mikrokiibi analüüsi hõlpsaks teostamiseks nii bioloogide kui bioinformaatikute poolt.

Käesoleva doktoritöö neljandas artiklis uurisime masinõppe mudelite ja varasemates artiklites käsitletud klassikaliste statistiliste meetodite koos rakendamise väärtust. Selles töös analüüsisime endometrioosi juhtkontrolluuringut. Eelnev statistiline analüüs näitas, et verest mõõdetud valgutasemete põhjal pole ükski üksik valk võimeline eristama endometrioosi põdevaid patsiente tervetest. Valkude kombinatsioonide ennustusvõime hindamiseks kasutasime erinevaid masinõppe meetodeid. Sarnaselt statistiliste testide tulemustega ei saavutanud masinõppe mudelid juhuslikkusest oluliselt erinevat tulemust. Seetõttu kinnitasid masinõppe tulemused hüpoteesi, et ei üksikute valkude mõõtmine ega ka valkude kombinatsioonid ei võimalda ennustada endometrioosi ja aidata haigust diagnoosida antud valimi baasil.

PUBLICATIONS

S. Meyer, M. Woodward, C. Hertel, P. Vlaicu, Y. Haque, J. Kärner, A. Macagno, S. Onuoha, **D. Fishman**, H. Peterson, K. Metsküla, R. Uibo, K. Jäntti, K. Hoky-nar, A. Wolff, K. Krohn, A. Ranki, P. Peterson, K. Kisand, A. Hayday, A. Meloni, N. Kluger, E. Husebye, K. Trebusak Podkrajsek, T. Battelino, N. Bratanic, and A. Peet.

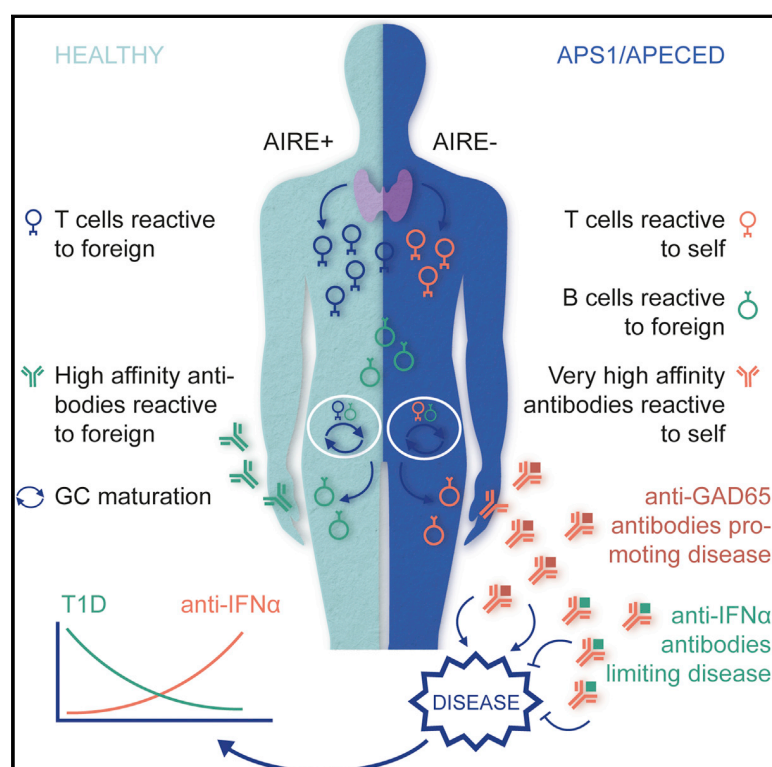
AIRE-deficient patients harbor unique high-affinity disease-ameliorating autoantibodies

Cell, 166(3):582–595, July 2016

The article is reprinted with permission of the copyright owner.

AIRE-Deficient Patients Harbor Unique High-Affinity Disease-Ameliorating Autoantibodies

Graphical Abstract



Authors

Steffen Meyer, Martin Woodward, Christina Hertel, ..., Pärt Peterson, Kai Kisand, Adrian Hayday

Correspondence

kai.kisand@ut.ee (K.K.),
adrian.hayday@kcl.ac.uk (A.H.)

In Brief

Self-reactive antibodies specific for type I interferons are associated with protection against type I diabetes in patients with an autoimmune syndrome caused by mutations in AIRE.

Highlights

- Each AIRE-deficient patient has a private repertoire of autoantibody reactivities
- Loss of B cell tolerance occurs during T cell-dependent somatic hypermutation
- Patient autoantibodies have unprecedented affinities for conformational epitopes
- Patient autoantibodies can display disease-ameliorating properties in vivo



Meyer et al., 2016, Cell 166, 582–595
July 28, 2016 © 2016 The Authors. Published by Elsevier Inc.
<http://dx.doi.org/10.1016/j.cell.2016.06.024>

AIRE-Deficient Patients Harbor Unique High-Affinity Disease-Ameliorating Autoantibodies

Steffen Meyer,^{1,11} Martin Woodward,^{2,11} Christina Hertel,^{1,11} Philip Vlaicu,^{1,11} Yasmin Haque,^{2,11} Jaanika Kärner,^{3,11} Annalisa Macagno,⁴ Shimobi C. Onuoha,⁴ Dmytro Fishman,^{5,6} Hedi Peterson,^{5,6} Kaja Metsküla,⁷ Raivo Uibo,⁷ Kirsi Jääntti,⁸ Kati Hokynar,⁸ Anette S.B. Wolff,⁹ APECED patient collaborative, Kai Krohn,⁸ Annamari Ranki,¹⁰ Pärt Peterson,³ Kai Kisand,^{3,*} and Adrian Hayday^{2,*}

¹ImmunoQure AG, Königsallee 90, 2012 Düsseldorf, Germany

²Peter Gorer Department of Immunobiology, King's College, London SE19RT, UK

³Molecular Pathology, Institute of Biomedicine and Translational Medicine, University of Tartu, Ravila 19, Tartu 50411, Estonia

⁴ImmunoQure Research AG, Wagistrasse 14, 8952 Schlieren, Switzerland

⁵Institute of Computer Science, University of Tartu, Liivi 2, Tartu 50409, Estonia

⁶Quretec Ltd., Ülikooli 6A, Tartu 51003, Estonia

⁷Department of Immunology, Institute of Biomedicine and Translational Medicine, University of Tartu, Ravila 19, Tartu 50411, Estonia

⁸Clinical Research Institute HUCH Ltd., Haartmaninkatu 8, 00290 Helsinki, Finland

⁹Department of Clinical Science, University of Bergen, Laboratory Building, 8th floor, 5021 Bergen, Norway

¹⁰Department of Dermatology, Allergology and Venereology, Institute of Clinical Medicine, University of Helsinki, Skin and Allergy Hospital, Helsinki University Central Hospital, Meilahdentie 2, 00250 Helsinki, Finland

¹¹Co-first author

*Correspondence: kai.kisand@ut.ee (K.K.), adrian.hayday@kcl.ac.uk (A.H.)

<http://dx.doi.org/10.1016/j.cell.2016.06.024>

SUMMARY

APS1/APECED patients are defined by defects in the autoimmune regulator (AIRE) that mediates central T cell tolerance to many self-antigens. AIRE deficiency also affects B cell tolerance, but this is incompletely understood. Here we show that most APS1/APECED patients displayed B cell autoreactivity toward unique sets of approximately 100 self-proteins. Thereby, autoantibodies from 81 patients collectively detected many thousands of human proteins. The loss of B cell tolerance seemingly occurred during antibody affinity maturation, an obligatorily T cell-dependent step. Consistent with this, many APS1/APECED patients harbored extremely high-affinity, neutralizing autoantibodies, particularly against specific cytokines. Such antibodies were biologically active in vitro and in vivo, and those neutralizing type I interferons (IFNs) showed a striking inverse correlation with type I diabetes, not shown by other anti-cytokine antibodies. Thus, naturally occurring human autoantibodies may actively limit disease and be of therapeutic utility.

INTRODUCTION

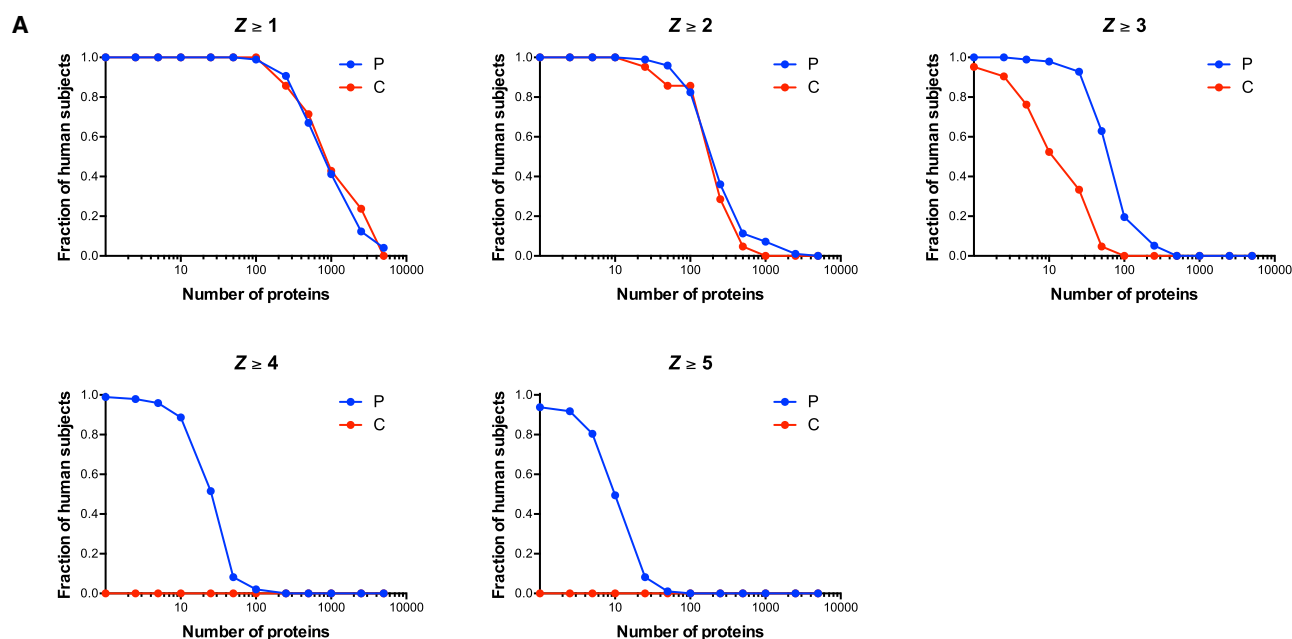
T lymphocyte tolerance is essential for limiting autoimmune disease. Tolerance occurs “centrally” when developing thymocytes with strongly self-reactive T cell receptors (TCRs) are deleted following engagement of self-antigen-derived peptides presented by major histocompatibility complex (MHC) antigens. The expression of thousands of tissue-specific self-antigens

(TSAs) by medullary thymic epithelial cells (mTEC) is directly promoted by AIRE, a poorly understood transcriptional regulator (Mathis and Benoist, 2009; Klein et al., 2014). Reflecting its importance, AIRE deficiency is defined by the APS1/APECED syndrome for which autoimmune polyendocrinopathy and chronic mucocutaneous candidiasis are pathognomonic (Nagamine et al., 1997).

There are also several mechanisms of peripheral T cell tolerance, including requirements for co-stimulatory signals for the activation of naive T cells; the expression of molecular “brakes” (e.g., CTLA-4, PD-1) by activated T cells; and the suppression of effector T cells in *trans* by FOXP3-expressing T-regulatory (T-reg) cells. Reflecting its importance, FOXP3 deficiency is defined by early-onset, life-threatening autoimmunity (Bennett et al., 2001; Wildin et al., 2001).

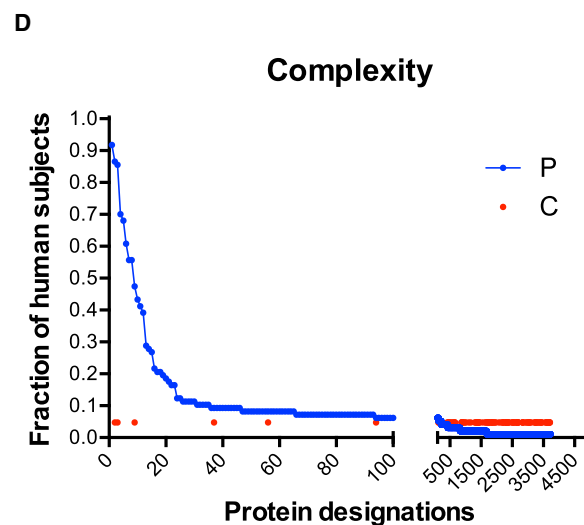
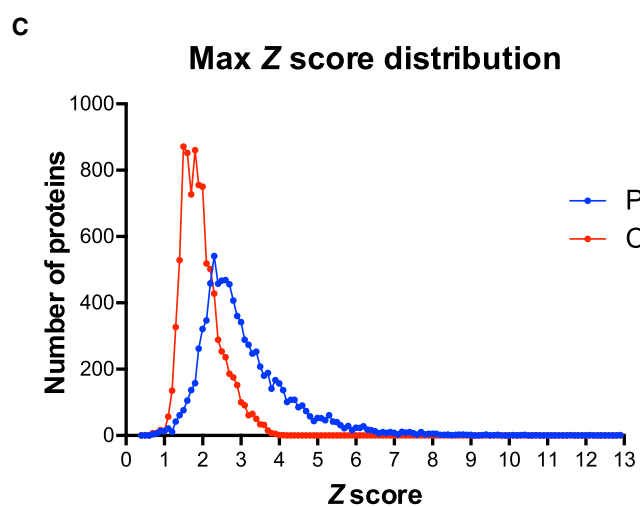
Central and peripheral tolerance mechanisms have likewise been hypothesized to shape the B cell compartment. Thus, self-reactive B cells developing in the bone marrow may be censored by clonal deletion, clonal anergy, or B cell receptor (BCR) editing in which secondary gene rearrangements replace the initial BCR with a new specificity (Goodnow et al., 2010; Pillai et al., 2011; Übelhart and Jumaa, 2015). Peripheral B cell tolerance is less well characterized, although some checkpoints have been inferred. For example, immature transitional B cells recently emigrated from the bone marrow contain many autoreactive and polyreactive cells, whereas there are relatively few among mature naive B cells, strongly suggesting that tolerance is imposed as transitional B cells differentiate into naive B cells (Wardemann et al., 2003).

Interestingly, this B cell checkpoint is T cell dependent, as reflected by its impairment in patients with T-reg deficiencies (Kinnunen et al., 2013). Likewise, CD40L and MHC class II deficiencies that each impair T-B interactions also display more autoreactive B cells (Meffre and Wardemann, 2008). These



B

	Average # hits		# distinct proteins			Complexity factor	
	P	C	P	C	shared	P	C
Z ≥ 3	82.45	19.33	3731	406	126	0.47	1.00
Z ≥ 4	29.44	0.10	1536	2	0	0.54	0.95
Z ≥ 5	12.26	0.00	636	-	-	0.53	-



(legend on next page)

considerations raise the possibility that B cell tolerance is largely governed by the state of T cell tolerance.

Certainly, any autoreactive B cell that might progress through to the naive B cell compartment of a healthy individual should lack cognate autoreactive T cells to help it mature. Likewise, T cell help is required in the germinal center (GC) reaction in which B cells undergo somatic hyper-mutation (SHM) of the immunoglobulin (Ig) variable (V) region genes, thereby driving T cell-dependent selective expansion of clones with increased antigen affinity (Brink, 2014). The question that then arises is whether major defects in central T cell tolerance provoke wide-ranging losses of B cell tolerance at either or both of these stages.

An approach to assessing this is to examine B cell reactivities in AIRE-deficient APS1/APECED patients whose under-expression of TSAs in the thymus is predicted to lead to increased numbers of peripheral autoreactive T cells. Thus, there are reports of APS1/APECED patients carrying autoantibodies against twenty-five TSAs, with prevalence ranging from 6% to 69% (Kisand and Peterson, 2015). Their specificities include steroidogenic enzymes, consistent with the patients' polyendocrinopathies (Krohn et al., 1992; Uibo et al., 1994; Winqvist et al., 1993). In addition, most patients display autoreactivities toward type I IFNs and T helper (Th)-17-related cytokines, antibodies to which limit resistance to *Candida* infection (Kisand et al., 2010; Meager et al., 2006; Puel et al., 2010).

These findings notwithstanding, there has been no large-scale analysis of the scope and nature of autoantibodies in APS1/APECED patients, thereby resolving how T cell tolerance impacts upon B cell tolerance in humans. By analyzing 81 APS1/APECED patients, we found that each was much more likely than a healthy relative or an unrelated control to harbor strong serum reactivities toward ~100 human proteins. About 10 of those, including type I IFNs and interleukin-22 (IL22), were recognized by almost all patients, whereas others were mostly "private specificities." Hence, 81 patients collectively harbored antibodies toward >3,700 human proteins.

Focusing on antibodies to type I IFNs, IL22, and IL17, we found unexpectedly that most were reactive to conformational determinants and included highly mutated antibodies of sub-picomolar affinity. Because their gemline counterparts were not self-reactive, B cell autoreactivity was most probably driven by self-reactive T cells in the GC reaction. The autoantibodies commonly neutralized their targets in vivo, and APS1/APECED patients with signature type 1 diabetes (T1D)-associated antibodies (e.g., anti-GAD65) commonly failed to develop T1D so long as they harbored powerfully neutralizing IFN α -specific antibodies. Thus, autoantibodies naturally arising in subjects with defective central T cell tolerance may be disease ameliorating.

RESULTS

High-Titer Autoreactivities in APS1/APECED

Sera from 81 APS1/APECED patients from discrete Finnish, Norwegian, Slovenian, and Sardinian cohorts were directed against a ProtoArray displaying ~9000 immobilized recombinant human proteins or protein fragments. Because some patients were sampled longitudinally, 97 sera were assayed in total. Control sera were from healthy first-degree relatives ($n = 9$) and healthy unrelated volunteers ($n = 12$) across the same age range. Data readouts for the binding of individual sera were normalized by applying robust linear modeling (Sboner et al., 2009), whereafter each signal was assigned a Z score denoting the number of standard deviations (SD) above or below the mean of the combined healthy relatives and controls.

Most patients and the combined controls displayed Z scores of 1–2 for ~200 proteins (Figure 1A). However, when the convention was employed of defining $Z \geq 3$ as bona fide positives, the patients segregated from the two control cohorts, considered either jointly or separately. Thus, each control serum displayed reactivities of $Z \geq 3$ toward an average of ≤ 20 proteins, with most recognizing < 10 (Figures 1A, 1B, and S1A). Given that there was inter-individual variation, the 21 control sera collectively displayed $Z \geq 3$ reactivities toward 406 distinct proteins, i.e., ~5% of those displayed on the array (Figure 1B). For only 2 proteins was $Z \geq 4$, and for none was $Z \geq 5$ (Figures 1A and 1B). Hence, as expected, the control cohorts largely lacked high-titer serum autoreactivities.

Conversely, most patients at any one time displayed $Z \geq 3$ autoreactivities toward ≥ 80 proteins (Figures 1A, 1B, and S1A). These data were re-analyzed with stringent procedures to minimize false-positives, including exclusion of any signals that might have arisen from cross-sample print contamination. With this achieved, the patients' "private" autoantibody repertoires collectively detected 3,731 distinct targets (Figure 1B). Furthermore, almost all patients displayed $Z \geq 4$ scores for at least 10 proteins (mean of ~30), collectively recognizing > 1,500 proteins, and > 50% of patients displayed $Z \geq 5$ scores for ≥ 10 proteins (mean of > 12), collectively recognizing 636 proteins (Figures 1A and 1B). Hence, high-level reactivity toward multiple self-proteins was a disease-defining property. This was further illustrated by the qualitative difference in Z score distribution curves for patients versus controls, which cannot simply be explained by there being 5-fold more patient sera (Figure 1C). Thus, whereas sampling greater numbers would likely have increased the protein species detected by control cohorts at $Z \geq 4$, it would not bridge the 1,000-fold gap between two proteins detected by 21 control sera versus > 1,500 proteins detected by 97 patient sera (Figure 1B).

Figure 1. Immune Response Profiling of APS1/APECED

(A) Distributions of hits between patients and controls at different Z scores.

(B) Z scores for all samples against all protein features and mean hits for each group calculated for $Z \geq 3$, $Z \geq 4$, and $Z \geq 5$. The number of distinct proteins targeted in each group (P, $n = 97$; C, $n = 21$) at Z scores denoted. The complexity factor was calculated by dividing the number of distinct proteins by average number of hits per patient.

(C) The max Z score distribution of all proteins in patient and control groups.

(D) Fraction of patients recognizing each of 3,731 proteins at $Z \geq 3$. Red dots depict 126 proteins shared between patients and controls.

In sum, 81 different patients collectively displayed strong reactivities to >40% of human proteins arrayed. For most proteins (blue dots 13–3731, [Figure 1D](#)), reactivities were spread across the cohort, reflecting high inter-patient variation, whereas ~12 proteins (blue dots 1–12, [Figure 1D](#)), including several type I IFNs, were recognized by > 60% of patients, as reported ([Meager et al., 2006](#)). However, the “public specificities” were not enriched among the 126 reactivities shared between patients and controls at $z > 3$ (red dots, [Figure 1D](#)), emphasizing that their common autoantigenicity is unique to the patients. Patient autoreactivity frequencies were largely comparable across geographical locations, albeit somewhat less in Norway and Slovenia, and age ranges ([Figures S1B and S1C](#)). Indeed, most anti-IFN autoantibodies of APECED patients were reported to increase early in life and remain stable thereafter ([Meager et al., 2006](#); [Wolff et al., 2013](#)).

The collective targets of patient antibodies included intracellular, trans-membrane, and secreted proteins. Because many proteins displayed on the ProtoArray may be denatured, there may be false-negatives that underestimate patient reactivities to conformational determinants. Although a detailed analysis of the types of proteins targeted will be presented, it is evident that the proteins most commonly detected by patient sera included numerous cytokines, particularly type I IFNs, for which reason this study focuses on the nature of those autoreactivities.

Strong, Selective Anti-Cytokine Reactivities

Human type I IFN genes include 13 IFN α genes, 1 IFN β gene, and 1 IFN ω gene. There is also a type II IFN γ gene and three type III IFN λ genes. IFN γ is largely limited to lymphocytes, whereas type I and type III IFNs are broadly expressed, with their functional uniqueness and/or redundancy unresolved ([Ivashkin and Donlin, 2014](#)). As assessed by ProtoArray, patient sera showed significantly stronger reactivities than controls toward all IFN α subtypes, albeit the reactivities to some (e.g., $\alpha 1/13$, $\alpha 5$, and $\alpha 14$) were higher than those to others (e.g., $\alpha 2$, $\alpha 16$, and $\alpha 21$) ([Figure 2A](#)). The differential between patients versus controls was emphasized by luciferase-based immunoprecipitation (LIPS) in which many target proteins were recognized in their native conformations ([Figure 2B](#)). Many patients showed strong reactivities to IFN ω but rarely toward IFN β ([Figure 2B](#)) and never toward IFN κ and IFN ϵ , two phylogenetically distant type I IFNs (data not shown). By contrast, patient sera harbored reactivities significantly above controls toward IL1 α , IL5, IL6, IL17A, IL17F, IL20, IL22, IL28A (IFN $\lambda 2$), IL28B (IFN $\lambda 3$), and IL29 (IFN $\lambda 1$) ([Figure 2C](#)). Whereas reactivities toward some targets (e.g., IL17F, IL22) were common to most patients, reactivities toward others (e.g., IL20, IL28, IL6) were not ([Table S1](#)), and with the exception of IL5, patient sera mostly did not detect either Th2 cytokines (e.g., IL4 and IL13) or IL21, a Tfh (T follicular helper) cell cytokine that drives high-affinity antibody maturation. There were also no reactivities toward G-CSF and GM-CSF ([Table S1](#)), which drive the development of myeloid cells associated with the patients' inflammatory endocrinopathies.

Cytokine reactivities were largely validated by ELISA, which confirmed that IFN γ was only rarely and weakly recognized by patient sera ([Figure 2D](#); [Table S1](#)) and that there was no reactivity toward TNF α (data not shown). By contrast, ELISA revealed au-

toantibodies toward IL32 α and IL32 γ , two poorly characterized proinflammatory cytokines ([Figure 2D](#); [Table S1](#)). In sum, 81 APS1/APECED patient sera collectively displayed strong reactivities to a very selective subset of human cytokines.

Very High-Affinity Human Antibodies

To understand the nature of patient serum reactivities, nine IFN α -specific monoclonal antibodies (mAbs) were derived by limit-dilution cloning from memory B cells of four patients. Two were characterized in detail (26B9 and 19D11), whereas a more limited analysis of the others strongly argued that the properties of 26B9 and 19D11 were generally representative of patients' cytokine-specific antibodies. First, their V_H and V_K sequences were highly mutated relative to their germline counterparts, with non-conservative replacements enriched in complementarity-determining regions (CDRs), as expected (white; [Figure 3A](#)). The antibodies bore no obvious resemblance to each other in V-gene segment or CDR3 usage. Conversely, a third anti-IFN α antibody, 50E11, shared with 19D11 the same V_H (IGHV1-69) and junctional (IGHJ4) segments and a very similar light chain (IGKV3-11 versus V3-20) ([Figure S2A](#)). However, there were very different template-independent nucleotide insertions in the V_H CDR3s of 19D11 and 50E11, and the somatic mutation patterns were different: whereas 19D11 and 26B9 showed high mutation frequencies in V_H CDR2 and V_K CDR1, 50E11 did not ([Figures 3A and S2A](#)).

The recombinant antibodies 26B9 and 19D11 harvested from transfected CHO cells were immobilized on surface plasmon resonance (SPR) chips over which were run recombinant human IFN $\alpha 2b$, IFN $\alpha 4$, IFN $\alpha 14$, and IFN ω , the latter being recognized by 26B9 but not by 19D11 ([Figure 3B](#)). These experiments revealed very slow off-rates reflecting extremely high affinities of the antibodies for their targets, ranging from $K_D = 3.28 \times 10^{-14}$ M for 26B9 toward IFN $\alpha 14$ to $K_D = 2.09 \times 10^{-11}$ M for 26B9 toward IFN $\alpha 2b$ ([Figures 3B and 3C](#)). Sub-picomolar/near-femtomolar dissociation constants were likewise shown by 19D11 ([Figures 3B and 3C](#)). Thus, APS1/APECED patients harbor some of the strongest affinity antibodies described.

18-mer peptides spanning IFN $\alpha 2b$ and IFN ω were used to map linear epitopes recognized by 26B9 and 19D11. However, no specific reactivities were detected (data not shown), consistent with the antibodies binding conformational determinants shared by several type I IFNs. Also, the antibodies reacted poorly or not at all to mouse IFNs ([Table S2](#)).

To investigate the origins of the high-affinity, conformation-specific antibodies, germline counterparts for 19D11, 26B9, and 50E11, albeit with the same CDR3-VDJ sequences, were expressed and tested by LIPS against recombinant human IFN $\alpha 2b$, IFN $\alpha 8$, and IFN $\alpha 14$. There was no measurable interaction with any target ([Figure 3D](#)), although the antibodies' quality was evident from their comparable detection by anti-human IgG ([Figure S2B](#)). These data argue that the strong autoreactivity toward IFNs developed de novo during affinity maturation, rather than being an intrinsic property of the germline repertoire that is enhanced by affinity maturation.

The high affinities of 26B9 and 19D11 were not unique. Thus, a patient-derived IgG κ mAb (20A10) specific for IL20 (which is not a target detected by most patients; [Figure 2C](#); [Table S1](#))

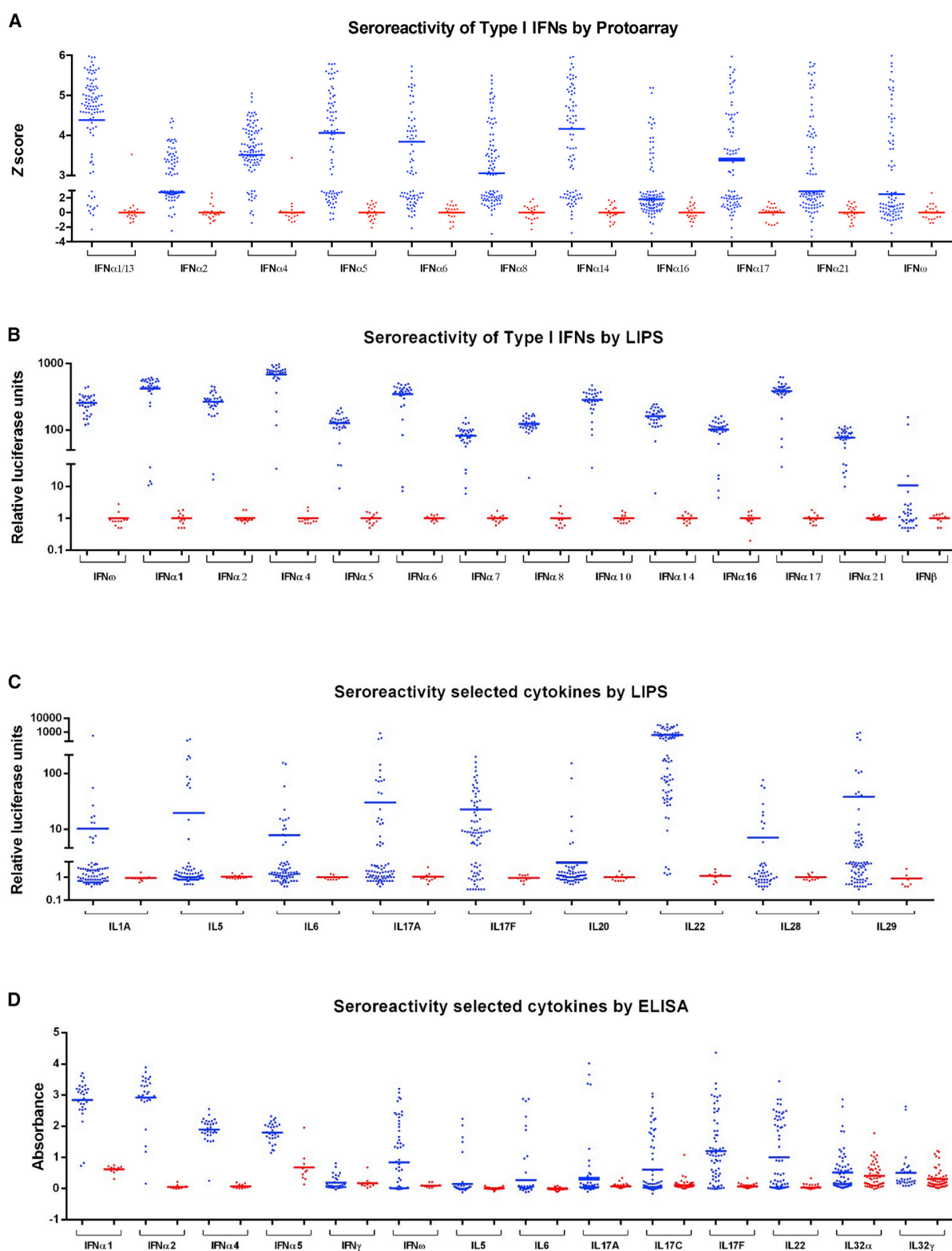
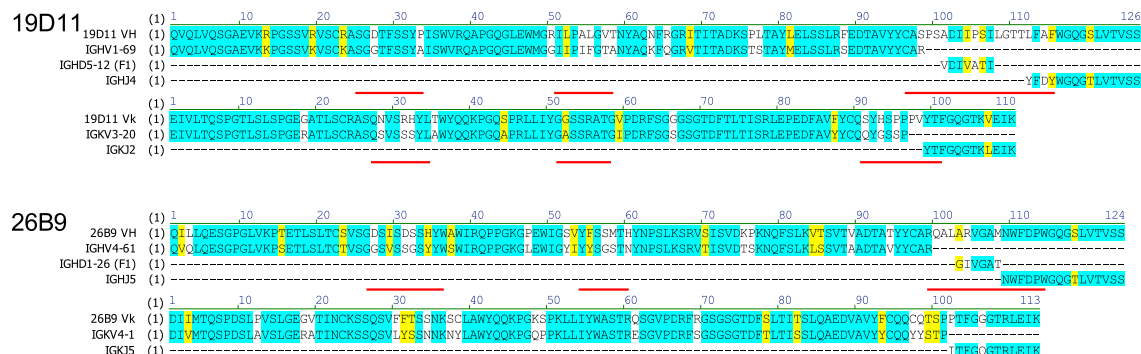


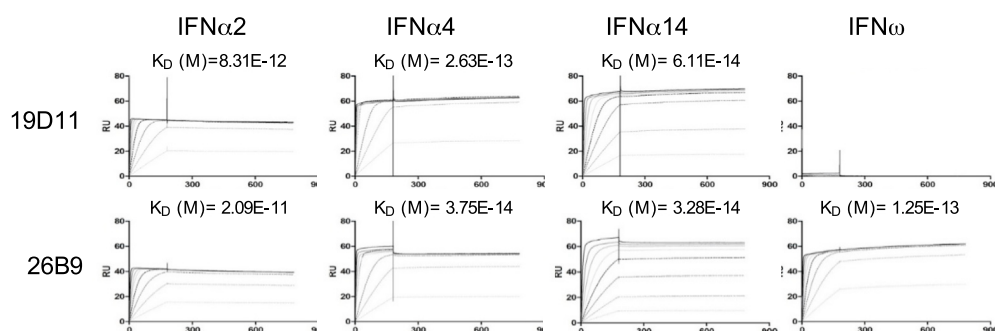
Figure 2. Serology of APS1/APECED to IFNs and Other Cytokines

Seroreactivity of APS1/APECED patients (blue) and controls (red) toward selected interferons and cytokines as measured in ProtoArray (A), LIPS (B and C), and ELISA (D).

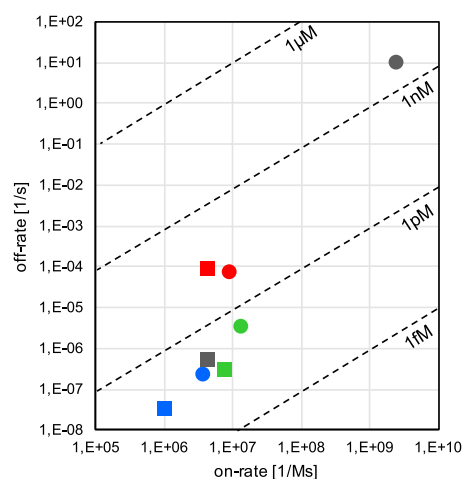
A



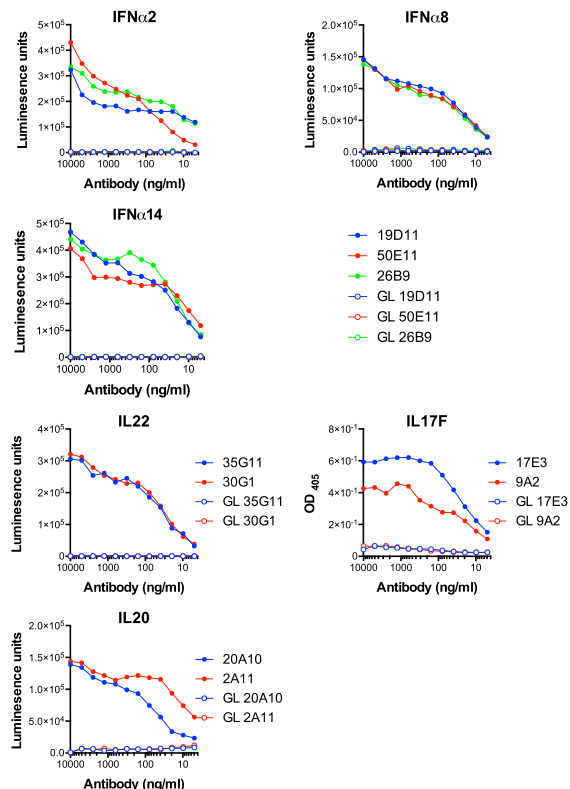
B



C



D



(legend on next page)

displayed a K_D of 9.1×10^{-14} M, (Table S3). Likewise one IgG κ mAb (17E3) and one IgG λ mAb (24D3), each specific for IL17F, displayed dissociation constants of <10 pM, and one IgG κ antibody (30G1) and one IgG λ antibody (35G11) specific for IL22 displayed dissociation constants of 37 pM and 39 pM, respectively. As a comparison, a CHO cell-expressed form of fezakinumab, a humanized anti-IL22 mAb tested in the clinic, displayed a K_D of 54 pM (Table S3). The only exception to this pattern was 2C2, an IgG λ mAb specific for IL32 γ (for which no human antibody has been reported), which displayed nanomolar dissociation (Table S3).

Similar to IFN α antibodies, most cytokine-specific antibodies did not detect linear peptides from relevant target proteins, strongly suggestive of complex conformational determinants (data not shown). The one exception was 20A10, which bound to an IL20 peptide and within which key amino acids were identified by mutagenesis (Figures S2C and S2D).

The antibody sequences of IL17F-reactive 17E3 and 9A2 and of IL22-reactive 30G1 and 35G11 displayed myriad non-conservative mutations enriched in the CDRs. Again their germline counterparts did not detect the respective targets (Figures 3D, S2E, and S2F). Moreover, neither patient-derived antibodies nor their germline counterparts showed any general autoreactivity (judged by immunofluorescent staining of tissue sections or HEP-2 cells) or reactivity to *Candida albicans*, thus arguing against candida infection being the trigger for autoantibody generation (data not shown).

The highly mutated CDRs of all studied antibodies suggested that they derived from GC reactions that partially rely on Tfh cells. Aberrant generation and/or activation of Tfh cells has been described in several autoimmune diseases (Ueno et al., 2015), but when four pediatric and four adult APS1/APECED were compared to controls, we found no differences in the percentages of circulating CXCR5⁺ Tfh cells, or their activation state, as judged by ICOS (inducible costimulator) and CCR7 levels (Figure S3).

Biologically Active Human Antibodies

To test the biological activities of 19D11 and 26B9, HEK293 cells transfected with type I IFN-stimulated response elements (ISRE) fused to firefly luciferase were treated with recombinant forms of each of 12 IFN α subtypes and IFN ω in the presence or absence of increasing concentrations of 19D11 or 26B9. Following treatment, firefly luciferase values were normalized to those of co-transfected *Renilla* luciferase, so as to control for variations in transfection efficiency. Both antibodies strongly inhibited the IFN-dependent response, with median IC₅₀ values of 2.83 ng/ml for 26B9 and 0.9 ng/ml for 19D11 (Figure 4A; Table S4). By comparison, median IC₅₀ values of 76.24 ng/ml and

10.86 ng/ml, respectively, were displayed by in-house-generated recombinant sifalimumab and rontalizumab, two anti-IFN mAbs used in clinical trials for systemic lupus erythematosus patients (Table S4).

Predictably, the antibodies varied in their inhibition of IFN-stimulated responses. Thus, 26B9 neutralized IFN ω , but not IFN α 16, and only poorly inhibited IFN α 8 (Figure 4A; Table S4). Likewise, in the same assay, rontalizumab failed to efficiently neutralize IFN α 6, IFN α 7 and IFN α 10, whereas sifalimumab neutralized several IFN α subtypes only weakly. By contrast, 19D11 neutralized all 12 IFN α subtypes tested (Table S4).

Patient-derived IFN-specific mAbs were also assessed for their capacity to inhibit STAT1 phosphorylation in cells treated with each of 12 IFN α subtypes, IFN ω , IFN β , or IFN γ (Figures 4B, 4C, and 4D). As predicted from the luciferase assay, 19D11 inhibited STAT1 phosphorylation levels (normalized to total STAT1 or tubulin) driven by all IFN α subtypes but did not affect responses to IFN ω , IFN β , or IFN γ . By contrast, 25C3, an additional patient-derived mAb (Table S2), was highly selective for discrete IFN α subtypes, whereas other antibodies tested, including 26B9, showed neutralization profiles between those of 19D11 and 25C3 (Figures 4B–4D). Only 26B9 and 31B4 neutralized IFN ω , and none neutralized IFN β or IFN γ . By comparison, sifalimumab, rontalizumab, and AGS-009 (another IFN α -targeting mAb in clinical development) showed variable and less uniform inhibition of STAT1 phosphorylation induced by different IFN α subtypes (Figure S4A).

The striking biological activities of patient mAbs were not limited to those specific for IFNs in that potent functional target neutralization was shown by mAbs targeting IL17F, IL22, IL32 γ , and IL20, respectively (Figure S4B).

Biologically Active Human Antibodies In Vivo

We next asked whether patient autoantibodies could functionally neutralize targets in vivo. To test this, mice were treated intraperitoneally (i.p.) with a single aliquot of antibodies 26B9, 19D11, or sifalimumab, and their ears inoculated intradermally (i.d.) on days 1, 3, 6, and 8 with recombinant human IFN α 5 or IFN α 14 (Figure 5A) and IFN ω (data not shown). Relative to repeated inoculation with vehicle/PBS, the cytokines induced ear swelling, reflecting an inflammatory response that includes rapid TNF α and IFN γ induction (Figures S5A and S5B). This ear swelling was significantly inhibited by single injections of antibodies (Figure 5B). Again, neutralization varied toward the effector IFN α subtype: 26B9 and 19D11, but not sifalimumab, largely ablated the IFN α 5 response, whereas all three partially yet significantly limited swelling induced by IFN α 14 (Figure 5B).

Specific, antibody-mediated neutralization in vivo was likewise seen when the same assay was applied to human IL17F

Figure 3. Affinity of Patient-Derived mAbs

(A) Amino acid sequences of 26B9 and 19D11 anti-IFN antibodies aligned with closest corresponding germline IgV_H, D_H, J_H, V_L, and J_L sequences. Identities highlighted in blue; conservative mutations in yellow; non-conservative in white; CDRs underlined in red.

(B) Plasmon resonance data: antibodies 19D11 and 26B9 were immobilized on Biacore chips; different concentrations of recombinant human IFN α 2b, IFN α 4, IFN α 14, and IFN ω were passed over; response units were recorded; and dissociation constants (K_D) calculated.

(C) Scatter chart of K_D values derived from (B).

(D) Binding determined by LIPS of APS1/APECED-derived mAbs and of germline counterparts to IFN α 2, IFN α 8, IFN α 14 (19D11, 50E11, and 26B9), IL22 (35G11 and 30G1), and IL20 (20A10 and 2A11). Binding to immobilized IL17F (17E3 and 9A2) was determined by ELISA.

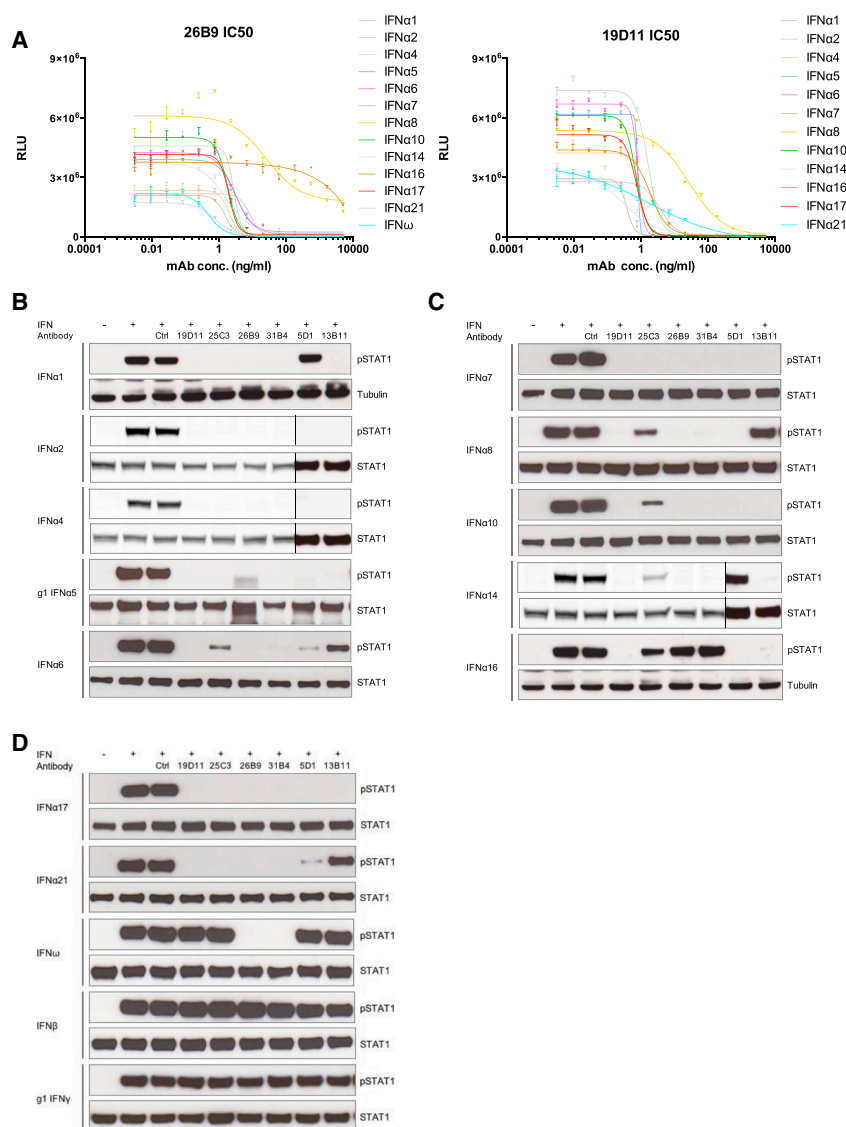


Figure 4. In Vitro Neutralization

(A) IC₅₀ analysis of APS1/APECED-derived anti-IFN mAbs 19D11 and 26B9 in HEK293T MSR cells transfected with ISRE dual-luciferase reporter constructs and treated with IFN α subtypes shown. Error bars correspond to SEM of multiple measurements.

(B–D) IFN-induced STAT1 tyrosine phosphorylation detected by western blot and normalized to total STAT1 or to tubulin levels as loading controls. Vertical lines in (B) and (C) denote cropped lanes.

Clinical Correlates of Neutralizing Antibodies

Given the results from animal models, it was appropriate to consider the potential impact of APS1/APECED antibodies in the patients themselves. Because circulating IFN α levels are extremely low in human peripheral blood, even following vaccination (Sobolev et al., 2016), circulating IFN levels do not offer robust biomarkers of anti-IFN α antibodies. Neither does measurement of interferon-stimulated genes (ISGs) because many, e.g., CXCL10, can be upregulated by type II IFNs (Welcher et al., 2015). By contrast, antibody activities may be reliably reflected in discrete pathologies, as in the correlation of anti-IL22 with candidiasis.

In this regard, many datasets, particularly in mouse models, suggest that type I IFN contributes to type 1 diabetes (T1D) (Carrero et al., 2013; Downes et al., 2010; Foulis et al., 1987; Huang et al., 1995; Li et al., 2008). Although APECED/APS1 patients by definition suffer from polyendocrinopathy, T1D affects only ~10%–20% of patients and manifests primarily in adulthood (Husebye et al., 2009;

or IL32 γ (Figures 6A and 6B). For IL17 neutralization, the data are clearly consistent with the known capacity of APS1/APECED patients' antibodies to neutralize Th17-family cytokines (Kisand et al., 2010; Puel et al., 2010), thereby predisposing to *Candida* infection.

Additionally, the detection of mouse IL22 by antibody 30G1 offered an opportunity to measure its bio-activity toward endogenous IL22, a primary effector of imiquimod (IMQ)-induced dermatitis used to model psoriasis (van der Fits et al., 2009). IMQ-induced pathology measured by modified PASI scoring was significantly ameliorated by 30G1 relative to IgG control, particularly following an initial inflammatory response (Figures 6C and S6). Again, 30G1 was at least as effective as an in-house-expressed anti-IL22 antibody, fezakinumab (see above) (Figure 6C). Collectively these data establish the capacity of patient anti-cytokine antibodies to limit pathologies induced by their targets in vivo.

Kisand and Peterson, 2015). This is despite the fact that radioimmunoassays have revealed that many APS1/APECED patients carry GAD65-reactive autoantibodies, a clinically applied biomarker for likely onset of T1D (Ziegler et al., 2013). Consistent with this, ProtoArray and LIPS data showed that many patients carried GAD65- and/or GAD67-reactive antibodies, but among them relatively few presented with T1D (red dots, Figures 7A and 7B). Collectively, these many observations suggest that patients at risk of T1D, as judged by anti-GAD65/GAD67, might fail to develop T1D if they harbored powerfully neutralizing anti-IFN α antibodies. Indeed, we reported a seemingly exceptional APS1/APECED patient, completely lacking IFN α -neutralizing antibodies and presenting with T1D (Kisand et al., 2008).

To investigate this, the 8 patients presenting with T1D (red dots, Figure 7B; mean age \pm SD, 48 \pm 11 years) were compared with an available cohort of 13 patients without

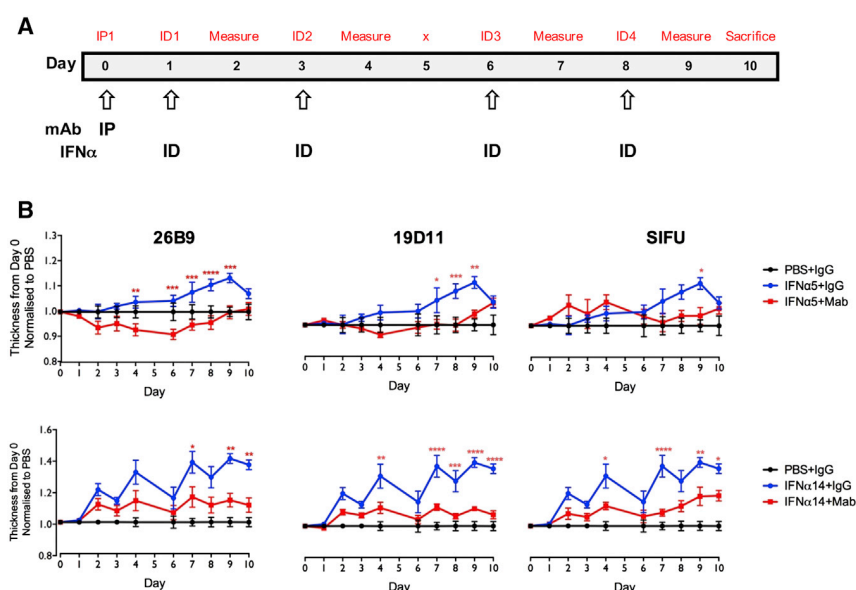


Figure 5. Biological Activity of IFN mAbs

(A) Experimental timeline: mAb administered i.p. at day 0; human IFN α administered i.d. on days 1, 3, 6, and 8. Ear thickness measured on all days (prior to cytokine injection) except for day 5.

(B) I.p.-administered IFN mAbs reduced IFN α -induced ear inflammation.

Significance calculated by two-way ANOVA, with * $p \leq 0.05$, ** $p \leq 0.01$, *** $p \leq 0.001$, and **** $p \leq 0.0001$. Error bars denote SEM.

DISCUSSION

This analysis of the impact of AIRE deficiency on human B cells has revealed a signature pattern of humoral autoreactivity with general implications for our understanding of autoimmunity. First, the autoantibodies studied were mostly extremely high affinity and specific for native conformational epitopes. These properties were shared by antibodies

specific for cytokines targeted by most patients (e.g., IFN α , IL17, IL22) and by antibodies specific for IL20 to which few patients displayed reactivity. Because such properties are very rare among antibodies raised by immunization, when B cells are primed de novo to antigen for short periods of time, it seems inappropriate to continue to model one type of mAb on the other.

Second, essentially all 81 APS1/APECED patients studied showed strong reactivities toward a common set of 10–15 proteins, coupled with patient-specific reactivity profiles toward 80–90 additional proteins. This limited frequency (< 1% of proteins displayed on the array) is consistent with a recent report that B cell tolerance was not globally disrupted in 51 APS1/APECED patients sampled (Landegren et al., 2016). Nonetheless, the patient-to-patient variation in reactivity profiles meant that the 97 sera analyzed in our study collectively harbored antibodies toward over 3,500 proteins.

The patient-to-patient variation argues that B cell autoimmunity resulting from AIRE deficiency is not simply an amplification of sporadic, low-level autoreactivities seen in healthy controls but has distinct origins. By this perspective, defects in central T cell tolerance may underpin other autoimmune and autoinflammatory pathologies attributed to high-affinity autoantibodies. Whereas this contrasts with the widely held view that autoimmune diseases mostly reflect peripheral tolerance defects, it aligns with data that central tolerance defects contribute to the NOD mouse model of T1D (Geng et al., 1998; Zucchelli et al., 2005). Moreover, wherever autoantibodies reflect central T cell tolerance defects, donor-to-donor variation is to be expected, as individuals will generate distinct TCR repertoires via quasi-random gene rearrangements, will be exposed to different physiologic and environmental triggers that promote the selective outgrowth of autoreactive T cell clones, and will differ in immune response modifier genes (e.g., HLA) that regulate the magnitude of antigen-specific responses.

T1D but with strong GAD65 reactivity (relative luciferase units > 5) (blue dots, Figure 7B; mean age \pm SD, 31 \pm 12 years). Consistent with T1D developing in adult APS1/APECED patients, GAD65 reactivities mostly arose post-adolescence, and hence the patient cohorts comprised 20 adults and one 8 year old.

As expected, all 21 patients harbored antibodies to IFN α and IFN ω (see Figure 2B), but when tested for IFN α and IFN ω neutralization, the antibodies showed a striking segregation with clinical status (Figures 7C, 7D, and S7A): patients without T1D collectively neutralized all IFN α subtypes, whereas those with T1D showed only low or negligible neutralization. Particularly strong differences were seen vis-a-vis IFN α 1, IFN α 2, IFN α 5, IFN α 8, IFN α 14, and IFN α 17 neutralization (Figure 7C). The two subgroups of the 21 patients also showed statistically significant differences in neutralizing IFN ω , but the difference was weaker than for IFN α (Figure S7A). Interestingly, the two GAD65-reactive non-diabetics who displayed relatively low IFN α neutralization were young adults who may be en route to developing T1D.

In a small subcohort of GAD65/67-reactive patients for whom longitudinal samples were available, the three T1D patients (red bars) again showed lower IFN α neutralization relative to the two patients without T1D. Moreover, one patient was able to neutralize IFN α 4 in 1978 but by 2012 could no longer do so and presented with T1D (Figure S7B).

Such striking correlations with T1D (Figure 7D) were not evident for any other naturally arising anti-cytokine antibodies, supporting the view that IFN α may contribute critically to the natural progression of T1D. Moreover, although the data do not prove that active anti-IFN antibodies underpin selective protection from T1D, they provide a firm foundation for exploring the potentials of APS1/APECED-derived autoantibodies to ameliorate other major diseases that are rarely if ever present in APS1/APECED patients.

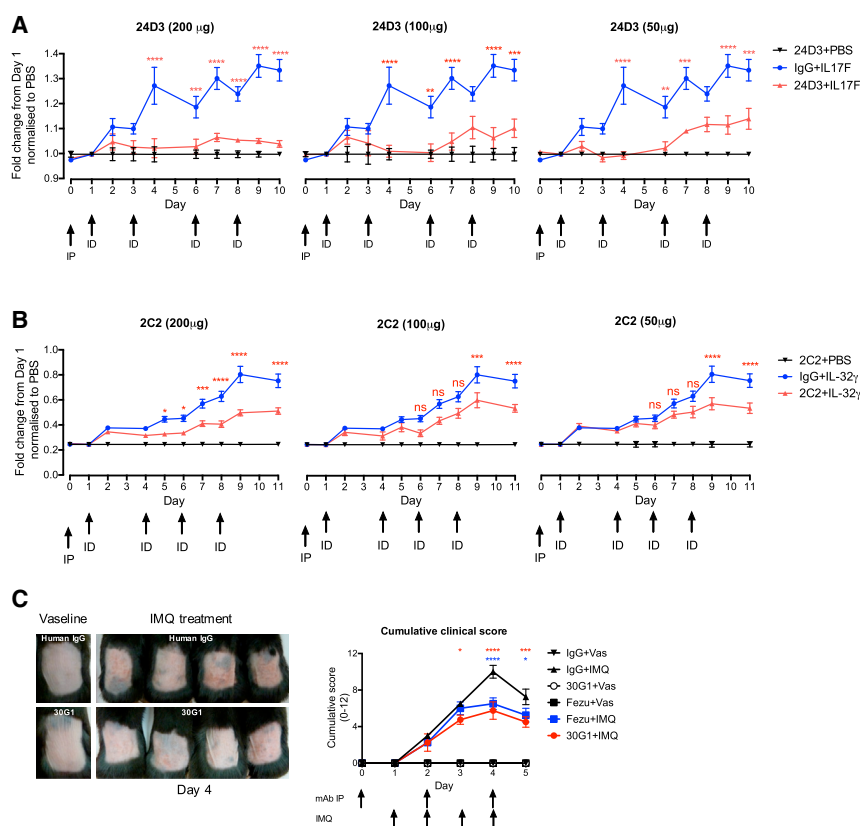


Figure 6. In Vivo Activity of Cytokine-Reactive mAbs

(A) mAb administered i.p. at day 0, and human IL17F administered i.d. on days 1, 3, 6, and 8. Ear thickness measured on all days (prior to cytokine injection) except day 5.

(B) As in (A), but with human IL32 γ administered i.d.

(C) anti-IL22-specific mAb injected i.p. into 9-week mice prior to and during IMQ treatment. Efficacy measured by Psoriasis Area and Severity Index (PASI).

Significance calculated by two-way ANOVA, with * $p \leq 0.05$, ** $p \leq 0.01$, *** $p \leq 0.001$, and **** $p \leq 0.0001$. Error bars denote SEM.

ably reflect dysregulated GC reactions, wherein autoreactive T cells, e.g., Tfh cells, that were not tolerized in the thymus promote the competitive outgrowth and affinity maturation of B cells that were initially primed to exogenous antigen(s) but whose mutated IgGs bind to self-proteins. Consistent with this, autoantibodies targeting thyroid-stimulating hormone receptor in Graves' disease cross-react to *Yersinia enterocolitica* antigens (Brink, 2014; Hargreaves et al., 2013), and activated peripheral blood Tfh cells correlate positively with serum autoantibodies and disease activity/severity in multiple autoimmune diseases (Ueno et al., 2015). Although our analysis of four adult and four pediatric APS1/APECED patients revealed no alterations in Tfh cell numbers relative to age-matched healthy controls, this did not exclude Tfh cells being enriched in autoreactive specificities. Moreover, no patients displayed neutralizing autoantibodies to IL21, a major mediator of Tfh cells in the GC.

This etiology of APS1/APECED B cell autoimmunity is strikingly similar to proposed origins of highly mutated anti-desmoglein-3 antibodies in autoimmune pemphigus (Di Zenzo et al., 2012) and of anti-GM-CSF antibodies pathognomonic in pulmonary alveolar proteinosis (Piccoli et al., 2015). In those studies, as in this, the closest germline counterparts ("unmutated common ancestors" [UCAs]) showed no reactivity toward the targets of the affinity-matured autoantibodies. By contrast, germline versions of antiviral antibodies showed only slightly reduced binding to target viral antigens (Corti et al., 2011, 2013). Moreover, it is not the case that UCAs intrinsically lack autoreactivity, as germline counterparts of some autoantibodies with few replacement mutations showed autoantigen reactivity in pemphigus patients (Cho et al., 2014). The underlying defect(s) in T cell tolerance that dysregulate affinity maturation in pemphigus, pulmonary alveolar proteinosis, and other organ-specific autoimmune diseases may be limited to few antigens, by contrast to broad-spectrum defects in APS1/APECED.

Autoantibodies to some non-tissue-restricted antigens, including multiple type I IFN α subtypes, are displayed by almost all patients, sometimes early post-partum (Wolff et al., 2013). Most likely, the immunogenicity of these proteins arises by mechanisms distinct from those shaping patient-specific autoantibody repertoires. Possibly the public autoantibodies arise from a direct impact of AIRE deficiency on B cell tolerance, for example, via the dysregulation of AIRE-expressing thymic B cells that resemble GC B cells by several criteria (Yamano et al., 2015). Arguing against this, however, autoantibodies to type I IFNs, Th17 cytokines, and additional self-proteins are found in thymoma patients with AIRE-sufficient B cells (Kisand et al., 2011; Meager et al., 1997; Wolff et al., 2014). This likewise argues against autoantibodies to type I IFNs and Th17 cytokines originating from defects in lymph node AIRE⁺ cells termed eTACs (Gardner et al., 2008). Although studies in mice have suggested tolerizing roles of eTACs, the functions of their rare human counterparts are unknown (Poliani et al., 2010).

AIRE deficiency may, however, act indirectly on thymic B cells, for example by hyperactivity of functionally competent thymic $\gamma\delta$ cells (Ribot et al., 2009) that may likewise be dysregulated in thymoma. Such cells may create an intra-thymic milieu favoring priming rather than tolerance of thymic B cells toward proteins highly expressed in the thymus (Dudakov et al., 2012; Meager et al., 2006).

Notwithstanding this possibility, our findings suggest that high-affinity autoantibodies in APS1/APECED patients prob-

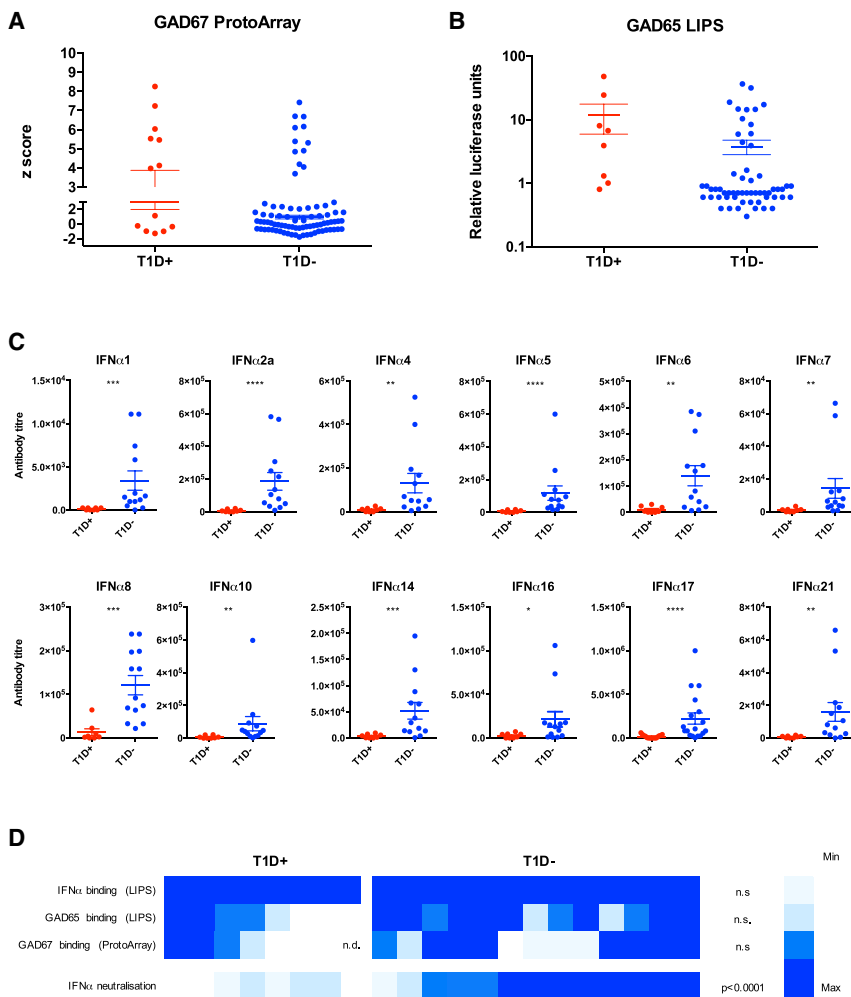


Figure 7. Clinical Correlation of T1D and IFN Neutralization

(A and B) Seroreactivity to GAD67 and GAD65 measured by ProtoArray and LIPS in APS1/APECED patients with (red) or without (blue) T1D. (C) IFN α -neutralizing titers in patients with T1D ($n = 8$) and anti-GAD65 seropositive patients without T1D ($n = 13$). y axis shows inhibitory concentration IC_{50} reflecting serum dilutions at which IFN activity was reduced 50%. (D) Heatmap of seroreactivity toward GAD67, GAD65, and IFN α analyzed by ProtoArray and LIPS combined with neutralization capacity in patients with and without T1D. Significance calculated by Mann Whitney using GraphPad Prism v.6, with $*p < 0.05$, $**p < 0.01$, $***p < 0.001$, $****p < 0.0001$. Error bars denote SEM. Significance values in (D) compare T1D $^{+}$ and T1D $^{-}$ groups for each parameter.

use of therapeutic mAbs. In this regard, it is striking that despite their severe flaws in central T cell tolerance, APS1/APECED patients do not present with systemic sclerosis, Sjögren's syndrome, MS, or SLE. These pathologies are considered to involve interplays of IL17/Th17 and type I IFNs—two main targets of APS1/APECED autoantibodies (Ambrosi et al., 2012). Likewise, Th17-driven psoriasis was diagnosed in only two of our patients, each of whom lacked autoantibodies to IL17A, IL17F, and IL22 (our unpublished data). Furthermore, atopy/allergy is seemingly rare among APS1/APECED patients, although whether anti-IL5 antibodies underpin this requires more study.

That almost all APS1/APECED-derived mAbs were biologically active in vivo against a range of cytokine targets has profound implications for patients. Clearly, immune-effector responses may be reduced, as in the association of anti-IL22 with susceptibility to *Candidiasis* (Kisand et al., 2010). Likewise, gut barrier integrity may be compromised, leading to increased levels of anti-commensal antibodies (Hetemäki et al., 2016). Conversely, despite the common neutralization of IFN α and IFN ω , APS1/APECED patients do not show severe viral infections, as were recently reported for a child genetically impaired in type I IFN (Ciancanelli et al., 2015). Possibly preserved IFN β function mediates anti-viral protection in APS1/APECED patients.

On the other hand, some autoantibodies may target key mediators of immunopathologies, thereby ameliorating disease. Thus, a unique correlation was observed between antibody-mediated neutralization of IFN α and failure to develop T1D, providing a novel strand of support for animal studies arguing that targeting type I IFNs could be effective in T1D. The concept that naturally arising autoantibodies may be beneficial is not widely considered, despite its underpinning the widespread

For now, the data presented by this study strongly suggest that antibodies recovered from APS1/APECED patients include ones with profound therapeutic and diagnostic potential.

EXPERIMENTAL PROCEDURES

More details are available in the [Supplemental Experimental Procedures](#).

Human Samples

Eighty-one APS1/APECED patients were diagnosed by mutational analysis of *AIRE* and by autoantibodies to type I IFNs. All provided informed consent, and many were analyzed previously (Kisand et al., 2011; Kluger et al., 2015; Meloni et al., 2012; Wolff et al., 2007). Approvals by local ethics committees are described in the [Supplemental Experimental Procedures](#). Ages at serum sampling were 4–73 years; mean = 31.9. For protoarray there were 12 age-matched controls and 9 healthy first-degree relatives, and there were additional healthy controls for LIPS and ELISA.

Immune Response Profiling by ProtoArray

Sera of patients, healthy relatives, and controls were tested against > 9,000 human proteins displayed on the Human Protein Microarray v5.1 (ThermoFisher Scientific). Preprocessing methods were applied to account for technical variability. First, corresponding local background intensity was subtracted,

whereafter values were log-transformed and subjected to robust linear normalization (Sboner et al., 2009). Z scores were calculated as the number of standard deviations of the signal from the mean of the corresponding controls and healthy relatives; $Z \geq 3$ was considered positive. After scoring, stringent quality assessment was undertaken, including high correlation coefficients of duplicate spots of printed proteins (average $r = 0.92$), reactivity toward known autoantibody targets, and perfect correlation of signals for proteins spotted in different locations. Printing contaminants were identified as proteins showing high correlation coefficients with known APECED antibody targets and were further verified by cross-reference to another protoarray (5.0) used for 23 patients and 7 controls. Thus, 31 suspect false-positives were identified and excluded from further consideration.

Antibody Isolation and Cloning

Cloning, production, and purification of human mAbs were performed as described (patent application WO2013/098419). In brief, memory B cells ($CD22^+$, IgD^- , IgM^- , $CD3^-$, $CD8^-$, and $CD54^-$) were flow-sorted (MoFlo) from patient PBMC, incubated transiently with EBV-containing B95-8 supernatant (SN) for 3.5 hr at 37°C , and then incubated in Transferrin- and CpG-supplemented IMDM at 37°C , 5% CO_2 , at 10 cells/well in 96-well plates coated with irradiated PBMC feeders. Short-term, oligoclonal B cell culture SN were analyzed for IgG and antigen-specific antibodies detected by ELISA and/or LIPS. Positive wells were harvested, cells single-cell-sorted into reverse transcriptase (RT) buffer (Life Technologies), and RT-PCR performed using Superscript III (Life Technologies) and random hexamers. IgG V_H , V_L , and V_K regions were amplified from cDNA by two-step nested PCR reaction using Advantage 2 cDNA polymerase (Clontech) and primer mixes specific for germline families (VBASE database). Nested primers attached restriction sites for V-region cloning into expression vectors providing $IgG1$, $Ig\kappa$, or $Ig\lambda$ constant regions. Recombinant antibodies were produced in HEK293T cells and antigen specificity analyzed by ELISA. Corresponding closest germline region sequences were identified using the VBASE2 database (Retter et al., 2005). CDRs were identified by IMGT definitions (Lefranc, 2003).

Complete Ig - V_H and V_L regions described in US7741449 (Sifalimumab), US7087726 B2 (Rontalizumab), US8361463 (ACO-1), and US20070258982 A1 (Fezakinumab) were ordered as CHO-codon-optimized synthetic constructs (GenScript) and expressed as above.

mAb Characterization In Vitro

EC_{50} binding of mAbs was determined by ELISA. Neutralizing capacities of type I IFN-specific mAbs were studied using phospho-STAT1 quantification in immunoblot and ISRE-luciferase reporter assay. IL17F, IL22, IL20, and IL32 neutralization assays were performed on respective responsive cell lines. mAb affinities were measured with a Biacore T200 (GE Healthcare). Epitope mapping used overlapping 18-mer peptides.

mAb Characterization In Vivo

C57BL/6J (WT; from Charles River) mice were administered i.p. with mAbs (day 0) and inoculated i.d. on days 1, 3, 6, and 8 with cognate human cytokines, IFN α 2a, IFN α 2b, IFN α 4, IFN α 14, IL17F, and IL32 γ , and their ear thicknesses measured with a micrometer. For IL22 mAbs cross-reactive to mouse, bioactivity was assessed in imiquimod-treated mice.

SUPPLEMENTAL INFORMATION

Supplemental Information includes Supplemental Experimental Procedures, seven figures, and four tables and can be found with this article online at <http://dx.doi.org/10.1016/j.cell.2016.06.024>.

CONSORTIA

The members of the APECED patient collaborative are Antonella Meloni, Nicolas Kluger, Eystein S. Husebye, Katarina Trebusak Podkrajsek, Tadej Battelino, Nina Bratanic, and Aleksandr Peet.

AUTHOR CONTRIBUTIONS

S.M., A.M., and S.C.O. cloned monoclonal antibodies from patient samples, and K.J. and K.H. assisted. S.M., P.V., and A.M. characterized antibodies in vitro; M.W. and Y.H. did so in vivo. C.H. analyzed ProtoArray data and wrote and edited the paper. J.K. assayed neutralization by sera and Tfh subsets and performed LIPS. D.F. and H.P. analyzed ProtoArray data. K.M. and R.U. screened sera for T1D autoantibodies and tested germline antibody specificities. K. Krohn and A.R. developed the clinical database, sampled Finnish patients, and employed ELISA. A.S.B.W. sampled Norwegian patients, contributed to the clinical database, and assayed antibodies. APECED patient collaborative contributed to the clinical database and sampled respective patients. P.P., K. Kisand, and A.H. supervised research, reviewed data, and wrote and edited the paper.

ACKNOWLEDGMENTS

We are indebted to patients; to the Finnish APECED and Addison patients' association; and to attending physicians and carers. We thank M. Rothe, P. Adler, A. Remm, M. Pihlap, M. Karlsberg, A. Tallqvist, M. Tuukkanen, L. Prassmayer, M. Wördehoff, A. Peters, R. Repke, B. Mathis, and particularly E. Stuart and K. Henco for critical insight and support. We thank staff of the Biological Services Unit at King's College London. Funding was by the following: ImmunoQure AG, the Wellcome Trust, and CRUK (to A.H.) and Estonian Research Council grant IUT2-2 and European Union Project 2014-2020.4.01.15-0012 (to J.K., P.P., and K. Kisand). P.P., K. Krohn, K. Kisand, A.R., and A.H. are cofounders and shareholders of ImmunoQure AG, and A.M., C.H., P.V., S.C.O., and S.M. were/are employees of ImmunoQure AG.

Received: January 27, 2016

Revised: April 24, 2016

Accepted: June 10, 2016

Published: July 14 2016

REFERENCES

- Ambrosi, A., Espinosa, A., and Wahren-Herlenius, M. (2012). IL-17: a new actor in IFN-driven systemic autoimmune diseases. *Eur. J. Immunol.* 42, 2274–2284.
- Bennett, C.L., Christie, J., Ramsdell, F., Brunkow, M.E., Ferguson, P.J., Whitesell, L., Kelly, T.E., Saulsbury, F.T., Chance, P.F., and Ochs, H.D. (2001). The immune dysregulation, polyendocrinopathy, enteropathy, X-linked syndrome (IPEX) is caused by mutations of FOXP3. *Nat. Genet.* 27, 20–21.
- Brink, R. (2014). The imperfect control of self-reactive germinal center B cells. *Curr. Opin. Immunol.* 28, 97–101.
- Carrero, J.A., Calderon, B., Towfic, F., Artyomov, M.N., and Unanue, E.R. (2013). Defining the transcriptional and cellular landscape of type 1 diabetes in the NOD mouse. *PLoS ONE* 8, e59701.
- Cho, M.J., Lo, A.S., Mao, X., Nagler, A.R., Ellebrecht, C.T., Mukherjee, E.M., Hammers, C.M., Choi, E.J., Sharma, P.M., Uduman, M., et al. (2014). Shared VH1-46 gene usage by pemphigus vulgaris autoantibodies indicates common humoral immune responses among patients. *Nat. Commun.* 5, 4167.
- Ciancanelli, M.J., Huang, S.X., Luthra, P., Garner, H., Itan, Y., Volpi, S., Lafaille, F.G., Trouillet, C., Schmolke, M., Albrecht, R.A., et al. (2015). Infectious disease. Life-threatening influenza and impaired interferon amplification in human IRF7 deficiency. *Science* 348, 448–453.
- Corti, D., Voss, J., Gamblin, S.J., Codoni, G., Macagno, A., Jarrossay, D., Vachieri, S.G., Pinna, D., Minola, A., Vanzetta, F., et al. (2011). A neutralizing antibody selected from plasma cells that binds to group 1 and group 2 influenza A hemagglutinins. *Science* 333, 850–856.
- Corti, D., Bianchi, S., Vanzetta, F., Minola, A., Perez, L., Agatic, G., Guarino, B., Silacci, C., Marcandalli, J., Marsland, B.J., et al. (2013). Cross-neutralization of four paramyxoviruses by a human monoclonal antibody. *Nature* 501, 439–443.
- Di Zenzo, G., Di Lullo, G., Corti, D., Calabresi, V., Sinistro, A., Vanzetta, F., Didona, B., Cianchini, G., Hertl, M., Eming, R., et al. (2012). Pemphigus

- autoantibodies generated through somatic mutations target the desmoglein-3 cis-interface. *J. Clin. Invest.* 122, 3781–3790.
- Downes, K., Pekalski, M., Angus, K.L., Hardy, M., Nutland, S., Smyth, D.J., Walker, N.M., Wallace, C., and Todd, J.A. (2010). Reduced expression of IFIH1 is protective for type 1 diabetes. *PLoS ONE* 5, e12646.
- Dudakov, J.A., Hanash, A.M., Jenq, R.R., Young, L.F., Ghosh, A., Singer, N.V., West, M.L., Smith, O.M., Holland, A.M., Tsai, J.J., et al. (2012). Interleukin-22 drives endogenous thymic regeneration in mice. *Science* 336, 91–95.
- Foulis, A.K., Farquharson, M.A., and Meager, A. (1987). Immunoreactive alpha-interferon in insulin-secreting beta cells in type 1 diabetes mellitus. *Lancet* 2, 1423–1427.
- Gardner, J.M., Devoss, J.J., Friedman, R.S., Wong, D.J., Tan, Y.X., Zhou, X., Johannes, K.P., Su, M.A., Chang, H.Y., Krummel, M.F., and Anderson, M.S. (2008). Deletional tolerance mediated by extrathymic Aire-expressing cells. *Science* 321, 843–847.
- Geng, L., Solimena, M., Flavell, R.A., Sherwin, R.S., and Hayday, A.C. (1998). Widespread expression of an autoantigen-GAD65 transgene does not tolerate non-obese diabetic mice and can exacerbate disease. *Proc. Natl. Acad. Sci. USA* 95, 10055–10060.
- Goodnow, C.C., Vinuesa, C.G., Randall, K.L., Mackay, F., and Brink, R. (2010). Control systems and decision making for antibody production. *Nat. Immunol.* 11, 681–688.
- Hargreaves, C.E., Grasso, M., Hampe, C.S., Stenkova, A., Atkinson, S., Joshua, G.W., Wren, B.W., Buckle, A.M., Dunn-Walters, D., and Banga, J.P. (2013). *Yersinia enterocolitica* provides the link between thyroid-stimulating antibodies and their germline counterparts in Graves' disease. *J. Immunol.* 190, 5373–5381.
- Hetmäki, I., Jarva, H., Kluger, N., Baldauf, H.M., Laakso, S., Bratland, E., Husebye, E.S., Kisand, K., Ranki, A., Peterson, P., and Arstila, T.P. (2016). Anticommensal responses are associated with regulatory T cell defect in autoimmune polyendocrinopathy-candidiasis-ectodermal dystrophy patients. *J. Immunol.* 196, 2955–2964.
- Huang, X., Yang, J., Goddard, A., Foulis, A., James, R.F., Lernmark, A., Pujol-Borrell, R., Rabinovitch, A., Somoza, N., and Stewart, T.A. (1995). Interferon expression in the pancreases of patients with type I diabetes. *Diabetes* 44, 658–664.
- Husebye, E.S., Perheentupa, J., Rautemaa, R., and Kämpe, O. (2009). Clinical manifestations and management of patients with autoimmune polyendocrine syndrome type I. *J. Intern. Med.* 265, 514–529.
- Ivashkiv, L.B., and Donlin, L.T. (2014). Regulation of type I interferon responses. *Nat. Rev. Immunol.* 14, 36–49.
- Kinnunen, T., Chamberlain, N., Morbach, H., Choi, J., Kim, S., Craft, J., Mayer, L., Cancrini, C., Passerini, L., Bacchetta, R., et al. (2013). Accumulation of peripheral autoreactive B cells in the absence of functional human regulatory T cells. *Blood* 121, 1595–1603.
- Kisand, K., and Peterson, P. (2015). Autoimmune polyendocrinopathy candidiasis ectodermal dystrophy. *J. Clin. Immunol.* 35, 463–478.
- Kisand, K., Link, M., Wolff, A.S., Meager, A., Tserel, L., Org, T., Murumägi, A., Uibo, R., Willcox, N., Trebusak Podkrajsek, K., et al. (2008). Interferon autoantibodies associated with AIRE deficiency decrease the expression of IFN-stimulated genes. *Blood* 112, 2657–2666.
- Kisand, K., Bøe Wolff, A.S., Podkrajsek, K.T., Tserel, L., Link, M., Kisand, K.V., Ersvaer, E., Perheentupa, J., Erichsen, M.M., Bratanic, N., et al. (2010). Chronic mucocutaneous candidiasis in APECED or thymoma patients correlates with autoimmunity to Th17-associated cytokines. *J. Exp. Med.* 207, 299–308.
- Kisand, K., Lilic, D., Casanova, J.L., Peterson, P., Meager, A., and Willcox, N. (2011). Mucocutaneous candidiasis and autoimmunity against cytokines in APECED and thymoma patients: clinical and pathogenetic implications. *Eur. J. Immunol.* 41, 1517–1527.
- Klein, L., Kyewski, B., Allen, P.M., and Hogquist, K.A. (2014). Positive and negative selection of the T cell repertoire: what thymocytes see (and don't see). *Nat. Rev. Immunol.* 14, 377–391.
- Kluger, N., Jokinen, M., Lintulahti, A., Krohn, K., and Ranki, A. (2015). Gastrointestinal immunity against tryptophan hydroxylase-1, aromatic L-amino-acid decarboxylase, AIE-75, villin and Paneth cells in APECED. *Clin. Immunol.* 158, 212–220.
- Krohn, K., Uibo, R., Aavik, E., Peterson, P., and Savilahti, K. (1992). Identification by molecular cloning of an autoantigen associated with Addison's disease as steroid 17 alpha-hydroxylase. *Lancet* 339, 770–773.
- Landegren, N., Sharon, D., Freyhult, E., Hallgren, Å., Eriksson, D., Edqvist, P.-H., Bensing, S., Wahlberg, J., Nelson, L.M., Gustafsson, J., et al. (2016). Proteome-wide survey of the autoimmune target repertoire in autoimmune polyendocrine syndrome type 1. *Sci. Rep.* 6, 20104.
- Lefranc, M.P. (2003). IMGT, the international ImMunoGeneTics database. *Nucleic Acids Res.* 31, 307–310.
- Li, Q., Xu, B., Michie, S.A., Rubins, K.H., Schreiber, R.D., and McDevitt, H.O. (2008). Interferon-alpha initiates type 1 diabetes in nonobese diabetic mice. *Proc. Natl. Acad. Sci. USA* 105, 12439–12444.
- Mathis, D., and Benoist, C. (2009). Aire. *Annu. Rev. Immunol.* 27, 287–312.
- Meager, A., Vincent, A., Newsom-Davis, J., and Willcox, N. (1997). Spontaneous neutralising antibodies to interferon—alpha and interleukin-12 in thymoma-associated autoimmune disease. *Lancet* 350, 1596–1597.
- Meager, A., Visvalingam, K., Peterson, P., Möll, K., Murumägi, A., Krohn, K., Eskelin, P., Perheentupa, J., Husebye, E., Kadota, Y., and Willcox, N. (2006). Anti-interferon autoantibodies in autoimmune polyendocrinopathy syndrome type 1. *PLoS Med.* 3, e289.
- Meffre, E., and Wardemann, H. (2008). B-cell tolerance checkpoints in health and autoimmunity. *Curr. Opin. Immunol.* 20, 632–638.
- Meloni, A., Willcox, N., Meager, A., Atzeni, M., Wolff, A.S., Husebye, E.S., Fucas, M., Rosatelli, M.C., Cao, A., and Congia, M. (2012). Autoimmune polyendocrine syndrome type 1: an extensive longitudinal study in Sardinian patients. *J. Clin. Endocrinol. Metab.* 97, 1114–1124.
- Nagamine, K., Peterson, P., Scott, H.S., Kudoh, J., Minoshima, S., Heino, M., Krohn, K.J., Lalioti, M.D., Mullis, P.E., Antonarakis, S.E., et al. (1997). Positional cloning of the APECED gene. *Nat. Genet.* 17, 393–398.
- Piccoli, L., Campo, I., Fregni, C.S., Rodriguez, B.M., Minola, A., Sallusto, F., Luisetti, M., Corti, D., and Lanzavecchia, A. (2015). Neutralization and clearance of GM-CSF by autoantibodies in pulmonary alveolar proteinosis. *Nat. Commun.* 6, 7375.
- Pillai, S., Mattoo, H., and Cariappa, A. (2011). B cells and autoimmunity. *Curr. Opin. Immunol.* 23, 721–731.
- Poliani, P.L., Kisand, K., Marrella, V., Ravanini, M., Notarangelo, L.D., Villa, A., Peterson, P., and Facchetti, F. (2010). Human peripheral lymphoid tissues contain autoimmune regulator-expressing dendritic cells. *Am. J. Pathol.* 176, 1104–1112.
- Puel, A., Döffinger, R., Natividad, A., Chrabieh, M., Barcenas-Morales, G., Picard, C., Cobat, A., Ouachée-Chardin, M., Toulon, A., Bustamante, J., et al. (2010). Autoantibodies against IL-17A, IL-17F, and IL-22 in patients with chronic mucocutaneous candidiasis and autoimmune polyendocrine syndrome type I. *J. Exp. Med.* 207, 291–297.
- Retter, I., Althaus, H.H., Münch, R., and Müller, W. (2005). VBASE2, an integrative V gene database. *Nucleic Acids Res.* 33, D671–D674.
- Ribot, J.C., deBarros, A., Pang, D.J., Neves, J.F., Peperzak, V., Roberts, S.J., Girardi, M., Borst, J., Hayday, A.C., Pennington, D.J., and Silva-Santos, B. (2009). CD27 is a thymic determinant of the balance between interferon-gamma- and interleukin 17-producing gammadelta T cell subsets. *Nat. Immunol.* 10, 427–436.
- Sboner, A., Karpikov, A., Chen, G., Smith, M., Mattoon, D., Freeman-Cook, L., Schweitzer, B., and Gerstein, M.B. (2009). Robust-linear-model normalization to reduce technical variability in functional protein microarrays. *J. Proteome Res.* 8, 5451–5464.
- Sobolev, O., Binda, E., O'Farrell, S., Lorenc, A., Pradines, J., Huang, Y., Duffner, J., Schulz, R., Cason, J., Zambon, M., et al. (2016). Adjuvanted influenza-H1N1 vaccination reveals lymphoid signatures of age-dependent early responses and of clinical adverse events. *Nat. Immunol.* 17, 204–213.

- Übelhart, R., and Jumaa, H. (2015). Autoreactivity and the positive selection of B cells. *Eur. J. Immunol.* *45*, 2971–2977.
- Ueno, H., Banchereau, J., and Vinuesa, C.G. (2015). Pathophysiology of T follicular helper cells in humans and mice. *Nat. Immunol.* *16*, 142–152.
- Uibo, R., Aavik, E., Peterson, P., Perheentupa, J., Aranko, S., Pelkonen, R., and Krohn, K.J. (1994). Autoantibodies to cytochrome P450 enzymes P450sc α , P450c17, and P450c21 in autoimmune polyglandular disease types I and II and in isolated Addison's disease. *J. Clin. Endocrinol. Metab.* *78*, 323–328.
- van der Fits, L., Mourits, S., Voerman, J.S., Kant, M., Boon, L., Laman, J.D., Cornelissen, F., Mus, A.M., Floencia, E., Prens, E.P., and Lubberts, E. (2009). Imiquimod-induced psoriasis-like skin inflammation in mice is mediated via the IL-23/IL-17 axis. *J. Immunol.* *182*, 5836–5845.
- Wardemann, H., Yurasov, S., Schaefer, A., Young, J.W., Meffre, E., and Nussenzweig, M.C. (2003). Predominant autoantibody production by early human B cell precursors. *Science* *301*, 1374–1377.
- Welcher, A.A., Boedigheimer, M., Kivitz, A.J., Amoura, Z., Buyon, J., Rudinskaya, A., Latinis, K., Chiu, K., Oliner, K.S., Damore, M.A., et al. (2015). Blockade of interferon-gamma normalizes interferon-regulated gene expression and serum CXCL10 levels in patients with systemic lupus erythematosus. *Arthritis Rheumatol.* *67*, 2713–2722.
- Wildin, R.S., Ramsdell, F., Peake, J., Faravelli, F., Casanova, J.L., Buist, N., Levy-Lahad, E., Mazzella, M., Goulet, O., Perroni, L., et al. (2001). X-linked neonatal diabetes mellitus, enteropathy and endocrinopathy syndrome is the human equivalent of mouse scurfy. *Nat. Genet.* *27*, 18–20.
- Winqvist, O., Gustafsson, J., Rorsman, F., Karlsson, F.A., and Kämpe, O. (1993). Two different cytochrome P450 enzymes are the adrenal antigens in autoimmune polyendocrine syndrome type I and Addison's disease. *J. Clin. Invest.* *92*, 2377–2385.
- Wolff, A.S., Erichsen, M.M., Meager, A., Magitta, N.F., Myhre, A.G., Bollerslev, J., Fougner, K.J., Lima, K., Knappskog, P.M., and Husebye, E.S. (2007). Autoimmune polyendocrine syndrome type 1 in Norway: phenotypic variation, autoantibodies, and novel mutations in the autoimmune regulator gene. *J. Clin. Endocrinol. Metab.* *92*, 595–603.
- Wolff, A.S., Sarkadi, A.K., Maródi, L., Kärner, J., Orlova, E., Oftedal, B.E., Kisand, K., Oláh, E., Meloni, A., Myhre, A.G., et al. (2013). Anti-cytokine autoantibodies preceding onset of autoimmune polyendocrine syndrome type I features in early childhood. *J. Clin. Immunol.* *33*, 1341–1348.
- Wolff, A.S., Kärner, J., Owe, J.F., Oftedal, B.E., Gilhus, N.E., Erichsen, M.M., Kämpe, O., Meager, A., Peterson, P., Kisand, K., et al. (2014). Clinical and serologic parallels to APS-I in patients with thymomas and autoantigen transcripts in their tumors. *J. Immunol.* *193*, 3880–3890.
- Yamano, T., Nedjic, J., Hinterberger, M., Steinert, M., Koser, S., Pinto, S., Gerdes, N., Lutgens, E., Ishimaru, N., Busslinger, M., et al. (2015). Thymic B cells are licensed to present self antigens for central T cell tolerance induction. *Immunity* *42*, 1048–1061.
- Ziegler, A.G., Rewers, M., Simell, O., Simell, T., Lempainen, J., Steck, A., Winkler, C., Ilonen, J., Veijola, R., Knip, M., et al. (2013). Seroconversion to multiple islet autoantibodies and risk of progression to diabetes in children. *JAMA* *309*, 2473–2479.
- Zucchelli, S., Holler, P., Yamagata, T., Roy, M., Benoist, C., and Mathis, D. (2005). Defective central tolerance induction in NOD mice: genomics and genetics. *Immunity* *22*, 385–396.

D. Fishman, K. Kisand, C. Hertel, M. Rothe, A. Remm, M. Pihlap, P. Adler, J. Vilo, A. Peet, A. Meloni, K. Trebusak Podkrajsek, T. Battelino, Ø. Bruserud, A. Wolff, E. Husebye, N. Kluger, K. Krohn, A. Ranki, H. Peterson, A. Hayday, and P. Peterson

Autoantibody repertoire in APECED patients targets two distinct subgroups of proteins

Frontiers in Immunology, 8, August 2017

The article is reprinted with permission of the copyright owner.



Autoantibody Repertoire in APECED Patients Targets Two Distinct Subgroups of Proteins

Dmytro Fishman^{1,2†}, Kai Kisand^{3†}, Christina Hertel⁴, Mike Rothe^{4†}, Anu Remm³, Maire Pihlap³, Priit Adler^{1,2}, Jaak Vilo^{1,2}, Aleksandr Peet⁵, Antonella Meloni^{6,7}, Katarina Trebusak Podkrajsek⁸, Tadej Battelino⁸, Øyvind Bruserud⁹, Anette S. B. Wolff⁹, Eystein S. Husebye⁹, Nicolas Kluger¹⁰, Kai Krohn¹⁰, Annamari Ranki¹⁰, Hedi Peterson^{1,2}, Adrian Hayday¹¹ and Pärt Peterson^{3*}

OPEN ACCESS

Edited by:

Ludger Klein,
Ludwig-Maximilians-Universität
München, Germany

Reviewed by:

Mitsuru Matsumoto,
Tokushima University, Japan
Graham Anderson,
University of Birmingham,
United Kingdom

*Correspondence:

Pärt Peterson
part.peterson@ut.ee

†Present address:

Mike Rothe,
IBA Lifesciences, Goettingen,
Germany

*These authors have contributed
equally to this work.

Specialty section:

This article was submitted
to Immunological Tolerance
and Regulation,
a section of the journal
Frontiers in Immunology

Received: 21 June 2017

Accepted: 31 July 2017

Published: 16 August 2017

Citation:

Fishman D, Kisand K, Hertel C,
Rothe M, Remm A, Pihlap M, Adler P,
Vilo J, Peet A, Meloni A,
Podkrajsek KT, Battelino T,
Bruserud Ø, Wolff ASB, Husebye ES,
Kluger N, Krohn K, Ranki A,
Peterson H, Hayday A and
Peterson P (2017) Autoantibody
Repertoire in APECED
Patients Targets Two Distinct
Subgroups of Proteins.
Front. Immunol. 8:976.
doi: 10.3389/fimmu.2017.00976

¹Institute of Computer Science, University of Tartu, Tartu, Estonia, ²Quretec Ltd., Tartu, Estonia, ³Institute of Biomedical and Translational Medicine, University of Tartu, Tartu, Estonia, ⁴ImmunoQure AG, Düsseldorf, Germany, ⁵Children's Clinic of Tartu University Hospital, Tartu, Estonia, ⁶Pediatric Clinic II, Ospedale Microcitico, Cagliari, Italy, ⁷Department of Biomedical and Biotechnological Science, University of Cagliari, Cagliari, Italy, ⁸Department of Pediatric Endocrinology, Diabetes and Metabolism, University Children's Hospital, University Medical Centre Ljubljana, Ljubljana, Slovenia, ⁹Department of Clinical Science, University of Bergen, Bergen, Norway, ¹⁰Department of Dermatology, Allergology and Venereology, Institute of Clinical Medicine, University of Helsinki, Skin and Allergy Hospital, Helsinki University Central Hospital, Helsinki, Finland, ¹¹Peter Gorer Department of Immunobiology, King's College, Guy's Hospital, London, United Kingdom

High titer autoantibodies produced by B lymphocytes are clinically important features of many common autoimmune diseases. APECED patients with deficient autoimmune regulator (AIRE) gene collectively display a broad repertoire of high titer autoantibodies, including some which are pathognomonic for major autoimmune diseases. AIRE deficiency severely reduces thymic expression of gene-products ordinarily restricted to discrete peripheral tissues, and developing T cells reactive to those gene-products are not inactivated during their development. However, the extent of the autoantibody repertoire in APECED and its relation to thymic expression of self-antigens are unclear. We here undertook a broad protein array approach to assess autoantibody repertoire in APECED patients. Our results show that in addition to shared autoantigen reactivities, APECED patients display high inter-individual variation in their autoantigen profiles, which collectively are enriched in evolutionarily conserved, cytosolic and nuclear phosphoproteins. The APECED autoantigens have two major origins; proteins expressed in thymic medullary epithelial cells and proteins expressed in lymphoid cells. These findings support the hypothesis that specific protein properties strongly contribute to the etiology of B cell autoimmunity.

Keywords: autoimmune regulator, autoantibodies, immune tolerance, thymus, autoantigen

INTRODUCTION

Many severe multifactorial autoimmune diseases are in part defined by pathognomonic antibodies that provide important clinical tests of disease predisposition or status. However, whereas our knowledge of the genetic and cellular factors contributing to multifactorial autoimmune diseases is increasing, we remain largely ignorant of properties of autoantigens and why only selected proteins are targeted in autoimmunity (1). To investigate B cell autoantibody repertoire, we have examined APECED (autoimmune polyendocrinopathy with candidiasis and ectodermal dysplasia) patients (2), defined by rare monogenic defects in the autoimmune regulator (AIRE) gene that drives the expression of tissue-restricted self-antigens in medullary thymic epithelial cells (mTEC) (3–5). T cell

progenitors with strong reactivity toward such self-antigens are eliminated or functionally inactivated. Lacking AIRE function, APECED patients predictably accumulate many autoreactive T cells, but in addition they collectively display high titer autoantibodies to multiple self-proteins (2).

The antibodies with the highest reported titers target type I interferons (IFNs) and have become diagnostic or even prognostic markers for APECED (6). Neutralizing type I IFN antibodies mostly appear early in life (7), inhibit IFN-stimulated gene expression (8), and were recently shown to correlate inversely with the onset of type 1 diabetes (T1D) in APECED (9). A second group of APECED-associated autoantibodies targets Th17-associated cytokines, IL17A, IL17F, and IL22, emerges early in the disease course (7), and is associated with chronic mucocutaneous candidiasis (10, 11), another defining feature of APECED. Interestingly, our in-depth studies of anti-cytokine antibodies harbored by APECED patients showed that the functionally rearranged immunoglobulin gene sequences were heavily mutated, encoding antibodies of extremely high affinity that we hypothesized to result from B cell dysregulation in germinal center reactions (9). Such etiology can be contrasted with the amplification and maturation of natural, polyreactive autoantibodies that are normally of relatively low affinity, which has been proposed to underpin sporadic autoreactivity in otherwise healthy individuals (12).

There is a prominent set of APECED-associated autoantibodies that are shared with multifactorial autoimmune diseases, such as those directed against glutamic acid decarboxylase (GAD)1 and GAD2 in T1D (13), or against CYP21A2 in Addison's disease (14). Therefore, the comprehensive analysis of autoantibodies in APECED may offer improved insight into the etiology of such diseases. These autoantibodies have often been identified by candidate or cDNA expression library screenings. However, proteome arrays provide unprecedentedly broad coverage to identify novel target proteins, such as melanoma MAGEB antigens and testis-specific PDILT, which were recently identified as autoantigens in APECED (15).

To gain further insight, we searched common features of autoantigenic proteins by a systematic analysis of a protein microarray platform, which allows large-scale, unbiased screening of autoantibody reactivities. Herein, we report a broad spectrum of autoantigens that is collectively targeted by 82 APECED patients. This APECED "autoimmunome" is not a random collection of proteins but comprises two sub-groups, those whose expression is most likely AIRE-regulated in the thymus and those enriched in lymphoid tissue. Moreover, these autoantigens are enriched in evolutionarily conserved cytosolic and nuclear proteins with high propensity for post-translational modifications. Reactivity to an increased number of such autoantigens was a stronger correlate of clinical symptoms than was either patient age or time since disease onset.

MATERIALS AND METHODS

Patient Samples

Altogether 100 sera samples from 82 individual patients were profiled in Protoarray, as described (9). For longitudinal analysis, we collected 2 samples from 11 patients; 3 samples from 2 patients; and 4 samples from 1 APECED patient. Only one serum sample

(with maximal number of positive hits) per patient was used in all analyses, except in longitudinal analysis where multiple samples taken at different time points were available from 14 patients. The patients were from Finland, Italy, Norway, Slovenia, and Estonia and diagnosed according to mutational analysis of the AIRE gene and by the presence of autoantibodies to type I IFNs. The mean age of the patients was 31 years. The main characteristics of the patients are given in Table S1 in Supplementary Material. The control group consisted of 20 individuals (12 healthy volunteers and 8 healthy first-degree relatives of the Italian APECED patient cohort). The study was carried out in accordance with the recommendations of local ethics committees (Finland: HUS Medical ERB, 8/13/03/01/2009; Slovenia: National Medical Ethics Committee number 22/09/09 and 28/02/13; Italy: Ethics Committee Prot. PG/2015/20440; Norway: Research Ethics Committee of Western Norway, health registry number 047.96, bio-bank number 2013-1504, project number 2012/1850; Estonia: Research Ethics Committee of the University of Tartu, 235/M-23) with written informed consent from all subjects, as described earlier (9). All subjects gave written informed consent in accordance with the Declaration of Helsinki.

Protein Array Screening

The autoantibody screening was performed by ISO9001 certified Custom ProtoArray Service Lab at Invitrogen (Thermo Fisher Scientific). Briefly, the protein arrays (ProtoArray v5.1) were probed as described in Invitrogen's protocol for Immune Response BioMarker Profiling using detection reagent (Alexa Fluor 647 Goat Anti-Human IgG A21445, Invitrogen) and blocking buffer (Blocking Buffer Kit PA055, Invitrogen). Arrays were scanned using a GenePix 4000B fluorescent scanner, and the data were acquired with GenePix® Pro software. The arrays were probed with sera at a dilution of 1:500.

Data Cleaning, Normalization, and Print Contamination

Previous studies involving protein microarrays (16) have shown that raw intensity values should not be compared directly because of technical, physical, chemical, and individual variability, occurring mostly at the production stage. In order to preserve true biological signal and concurrently eliminate potential technical noise, we applied a robust linear model (RLM) approach (17), using *rlm* function in R. RLM is considered to be the state of the art normalization technique for protein microarray data (18) and is applied on control probes that are assumed to have constant positive signal across all arrays. We used human-IgG and V5 control series for normalization as reported (17). Background subtracted signal was log-transformed prior to applying RLM to approximate for normal distribution (Figure S1 in Supplementary Material). To address printing contamination, we excluded all autoantibody targets that showed high correlation (>0.6) with previously reported autoantigens. In addition, we identified and eliminated highly correlated proteins located in the neighboring wells on the array. In total, we identified and removed 31 false positives, some of which were prevalently positive across many samples (Figure S2 in Supplementary Material). The normalized signal was standardized using mean and SD of healthy samples

(including healthy heterozygous relatives). Proteins, with standardized signal (z -score) above 3 in three or more patients were regarded as autoantigens. The full list of the positive proteins is provided in Table S2 in Supplementary Material.

Differential Data Analysis and Clustering of Autoantibody Reactions

In order to identify the proteins correlating with various clinical manifestations, we used moderated t -statistics implemented in *ebayes* function from *limma* R package (19) on normalized intensities from all 9,000 proteins. Obtained p -values were corrected using false discovery rate correction method and top significant proteins (corrected p -value < 0.05) were extracted for each manifestation resulting in six significant associations. Unsupervised hierarchical clustering using *pheatmap* package in R, which internally uses *hclust* function for clustering rows and columns of matrix. Linear regression analysis of dependency between number of positive hits and number of manifestation was analyzed with *lm* method in R.

Variability of APECED Autoantigen Profile over Time

We extracted data for 14 patients with multiple samples and formed all possible pairs of samples that belong to the same patients and divided these pairs into two broad categories: pairs of samples that were obtained > 10 years apart (eight samples, on average 24.4 years apart) and samples that were obtained < 10 years apart (13 samples, on average 1.5 years apart). Reactive proteins were compared between samples of the same patient and the percentage of the proteins that were specific to early, late, or shared between samples for both of the categories was computed. As expected, samples taken close in time had more reactive proteins in common, then samples obtained more than 10 years apart. Samples taken more than 10 years apart show higher percentage of late sample specific proteins, which might mean that with time repertoire of reactive proteins gets larger.

Correlation with APECED Mutations

We divided the patients into three groups based on their mutations: (1) homozygous for p.R139X, (2) homozygous for p.R257X, and (3) homozygous p.L323fsX373 or compound heterozygotes of either p.L323fsX373 or missense mutations. We used pairwise comparisons of Tukey and Kramer (Nemenyi) test with Tukey-Dist approximation for independent samples.

The Enrichment Analyses for Protein Characteristics

To assess intrinsic features of positive reactivities, we used data from the following public databases: Human Protein Atlas (20), Compartments DB (21), dbPTM (22), UniProt Knowledgebase (23), Ensembl (24), OrthoDB8 (25), and SUPERFAMILY (26). We used *gconvert* function from *gProfileR* package in R (27) to convert names of genes and proteins into Ensembl gene identifiers (ENSG). Size of the overlap between our group of positive proteins and every set extracted from each database was estimated. Using hypergeometric test for each overlap,

we computed probability values to estimate how likely it was to observe this overlap or larger by random chance. We used false discovery rate procedure to adjust obtained p -values and significance threshold of 0.05 to reject a null-hypothesis. To double check our findings, we used g:Profiler web-tool (27) by submitting our list of positive proteins and running unordered query with ProtoArray content as a background to account for any design bias.

Single Nucleotide Polymorphism (SNP) and Evolutionary Conservation Analysis

For SNP analysis, we retrieved all SNPs associated with each gene on our platform that was found in Ensembl database (7,284 genes). To retrieve this information, we used R command *useMart* and the following parameters: *useMart*("ENSEMBL_MART_ENSEMBL", dataset = "hsapiens_gene_ensembl", host = "www.ensembl.org"). We then calculated the number of SNPs within boundaries of the gene and SNPs that are located at the exon regions of the gene. We normalized these values by associated gene length (distance between two furthest associated SNPs), by gene length, and by accumulative length exon regions of each gene, respectively. To compare positive proteins with the rest of platform in terms SNP counts, we first sampled 10,000 random groups of genes of the same size as our group of reactive proteins. For each group, we computed mean counts of two categories. For evolutionary conservation analysis, the data were obtained from <ftp://cegg.unige.ch/OrthoDB8/Eukaryotes/>. We downloaded four pairs of genes and annotations for all_species, mammalia, metazoa, and vertebrata. In all four gene files, we filtered out genes not related to *Homo sapiens* and converted Ensembl protein IDs into gene IDs using *biodbnet* (<http://biodbnet.abcc.ncicrf.gov/db/db2db.php>) software. We calculated an average evolution rate for our group of reactive proteins (for all genes that had evolutionary rate recorded in DB). Then we sampled 10,000 random groups of the same size as our reactive group and calculated an average evolutionary rate.

Luciferase Immunoprecipitation (LIPS) Analysis

Luciferase immunoprecipitation assay was performed as reported (28, 29). Autoantigen cDNAs were cloned into modified pNanoluc vector (Promega, Madison, WI, USA) downstream of naturally secreted NanoLuc luciferase (Nluc). HEK293 cells were transfected with the plasmid constructs and cell culture medium containing Nluc-fusion proteins was collected after 48 h. Serum samples were first incubated with the fusion protein solutions overnight, then Protein G agarose beads were added and incubated at room temperature for 1 h in 96-well microfilter plates (Merck Millipore, Billerica, MA, USA) to capture antibodies and immune complexes to the beads. After the washing to remove unbound fusion proteins, a luciferase substrate (furimazine) was added to reaction, and luminescence intensity (LU) was measured in Victor X Multilabel Plate Reader (PerkinElmer Life Sciences, Waltham, MA, USA). Results were expressed as relative units LU sample/average LU of healthy control samples. The positive/

negative discrimination level was set to the mean plus three SDs of the healthy control samples.

RESULTS

Protoarray Screening of APECED Sera

The basis for our unbiased study of APECED autoreactivities was a protein microarray (Protoarray) of approximately 9,000 proteins printed to a single glass slide. Against this array, we screened 100 sera from 82 patients of Finnish, Norwegian, Slovenian, Sardinian, and Estonian origins, together with control sera obtained from healthy heterozygous relatives ($n = 8$) and unrelated healthy controls ($n = 12$) across the same age range.

The arrays were normalized by RLM (17) based on control protein intensities with further standardization and limitation of false-positives (described in Materials and Methods). The positive proteins were defined as signals with a z -score (the number of standard deviations SDs from the mean of combined controls) of greater than 3 (which is more stringent than the common practice of calling hits at $z > 2$). Although APECED patients altogether displayed significantly different set of autoreactivities in comparison to controls, the reactivity profiles contained multiple patient-specific reactivities in addition to shared autoantibodies (9). Therefore, to intensify the likely biological and clinical significance of hits, we considered a protein to be an autoantigen only when it was recognized by ≥ 3 individual patient samples (see Materials and Methods). When this additional stringency was applied, proteins encoded by 963 unique Refseq genes qualified as autoantigens.

Autoantigen Repertoire Contains Shared and Individual Reactivities

As expected, multiple sera displayed strong reactivities toward approximately 20 proteins that were previously reported as APECED autoantigens, including type I IFNs (**Figure 1A**), Th17 cytokines, GAD1, GAD2, DDC, TGM4, GIF, HSD3B2, BPIFB1, TSGA10, CYP1A2, KCNRG, and AQP2 (**Figure 1B**). Moreover, most such reactivities were also detected by LIPS assay (Figure S1 in Supplementary Material). It should be noted that apart of HSD3B2, the set of proteins on Protoarray did not include the steroidogenic enzymes CYP21A2, CYP17A1, and CYP11A1, which have been demonstrated as autoantigens in APECED.

Among shared reactivities, the highest titers were shown by interferon- α (IFNA)-specific antibodies, for which we identified some strong correlations (coefficients from 0.41 to 0.98), the highest being between IFNA2 and IFNA4 (correlation ~ 0.98), and IFNA6 and IFNA17 (correlation ~ 0.93) (**Figure 1C**). These correlations could not be explained by the levels of primary sequence similarity or by close phylogenetic relationships (Figure S2 in Supplementary Material), and are instead likely to reflect shared conformational epitopes in IFNA proteins. Likewise, there was commonly a strong correlation (coefficient from 0.41 to 0.62) of IFNA reactivity with reactivity toward IFN- ω (IFNW) (**Figure 1C**).

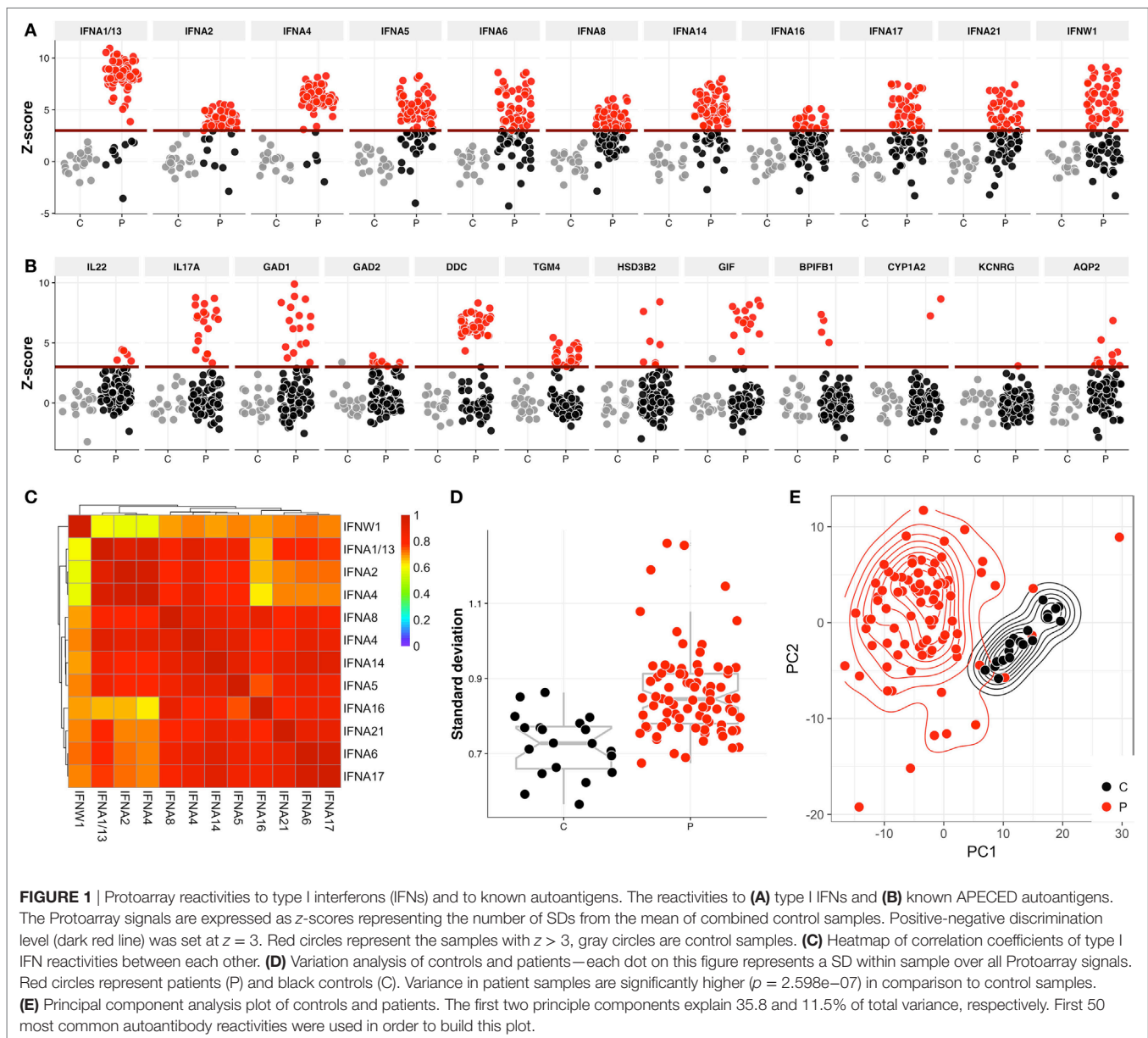
In addition to shared reactivities, we found high inter-individual variation in the number and identity of autoantigens

(**Figure 1D**). To analyze a covariance of sample groups, we performed a principal component analysis, which showed that the relatively homogenous group of combined healthy relatives and control samples readily segregated from the patient samples that displayed a large intra-group variability (**Figure 1E**).

Multiple Specificities Include Cancer-Testis and Testis-Specific Autoantigens

Among the strong, “rare” specificities, there was a number of potential autoantigens depicted in **Figure 2A**. Of these, LCN1 was reported as an autoantigen in Sjögren syndrome patients (30), and HMGB1 was reported to be associated with the production of anti-DNA autoantibodies in systemic lupus erythematosus (31). To extend the Protoarray results, we used LIPS to assay reactivity toward eight of these proteins (LCN1, MKNK2, POMZP3, BAALC, FGF12, HMGB1, RPL12, and S100A7A) of sera from a subgroup of 30 Finnish APECED patients (**Figure 2B**). The first three showed particularly strong positive correlations between Protoarray and LIPS results (**Figure 2C**), but given that the reactivities were often rare and that the patient groups tested in the two assays did not completely overlap, it was not surprising that correlations were not always statistically significant. Of note, however, this did not reflect a general tendency of the Protoarray to reveal false positives, since some sera showed much stronger LIPS reactivity to defined targets (e.g., RPL12, FGF12, HMGB1; **Figure 2C**). Indeed, this may reflect the potential of the Protoarray to underestimate reactivities of conformation-specific autoantibodies, because of the denatured states of many of the arrayed proteins and protein fragments.

Interestingly, we noted reactivities toward ~ 20 so-called “cancer-testis autoantigens” (CT-As) (**Figure 2D**). CT-As can be expressed in a wide variety of malignant tumors, where they are known to be immunogenic, but their expression in normal tissue is mostly restricted to germ cells in testis, fetal ovary, and placenta (32). The extent of reactivity revealed by our screen far exceeded the previous report of shared APECED reactivity to CT-As PDILT and MAGEB2 (**Figure 2D**) in a large-scale screening of another APECED cohort (15). Rather, we found reactivities toward several proteins from the MAGE-A—MAGE-B family that are expressed in melanoma and other tumor types but which in normal tissues are expressed only in the testis; reactivities toward GAGE1 and GAGE7B, which are members of another X-chromosome linked, CT-A family; and reactivities toward SPAG8 and SPAG16 (**Figure 2D**). The latter two in particular highlight the cross-over of APECED serum autoreactivities with other pathophysiologicals, in that SPAG8 was initially identified as a sperm-associated antigen target of serum of an infertile woman (33), while SPAG16 is expressed in sperm and in reactive astrocytes of lesions in multiple sclerosis patients in whom it has been identified as an autoantibody target (34). Of note, both males and females showed autoreactivities toward several sperm-specific proteins (**Figure 2E**). Protoarray reactivities toward 11 testis specific and CT-antigens tested showed good overall correlation with LIPS (**Figures 2E,F**).

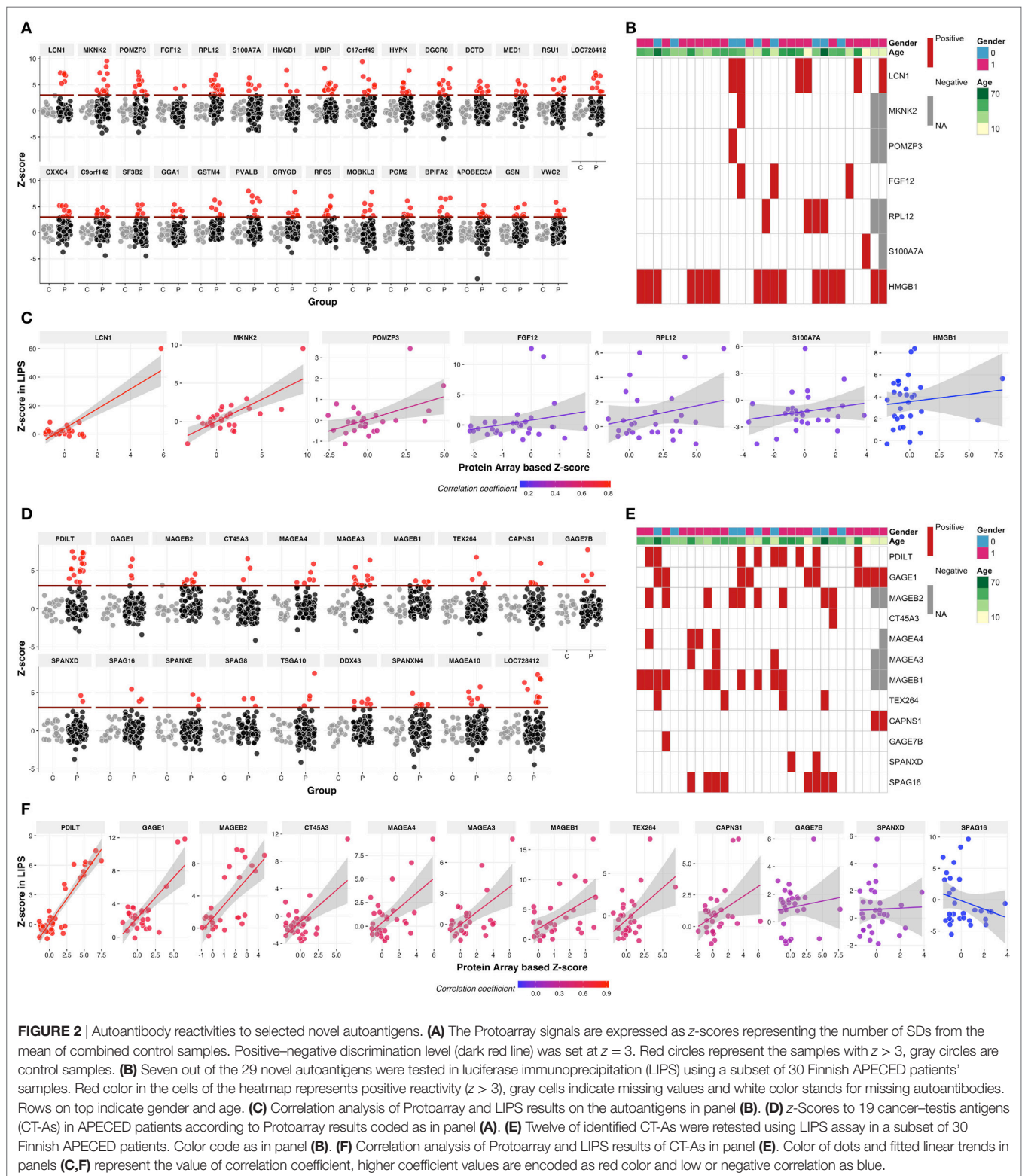


Autoantibody Correlations with Clinical Manifestations

We next analyzed whether immunoreactivities to certain autoantigens correlated with disease components of individual APECED patients (**Figure 3**). Pernicious anemia correlated with seven reactivities, including gastrointestinal factor GIF that is an established autoantigen in pernicious anemia patients (35); five specificities, including GAD1 and GAD2, correlated with vitiligo; and autoantibodies to GABPB2 correlated with autoimmune hepatitis in APECED patients. By contrast, several associations described previously among small-scale studies, e.g., DDC with AIH and vitiligo (36, 37), were not revealed. In addition, we confirmed that reactivity toward prostate specific antigen, TGM4, was almost restricted to post-pubertal males (Figure S3 in Supplementary Material) (38).

To test whether the autoantibody reactivities might segregate APECED patients into subgroups, we performed unsupervised hierarchical clustering of patients and the 50 most-reactive autoantigens, from which we excluded type I IFNs. This analysis clearly revealed two patient sub-groups with overall low and high reactivity repertoires, respectively (**Figure 4A**). An overlay of this heatmap with clinical data showed that the number of autoantigens targeted was positively correlated with the number of clinical manifestations, as confirmed by linear regression (**Figures 4B,C**).

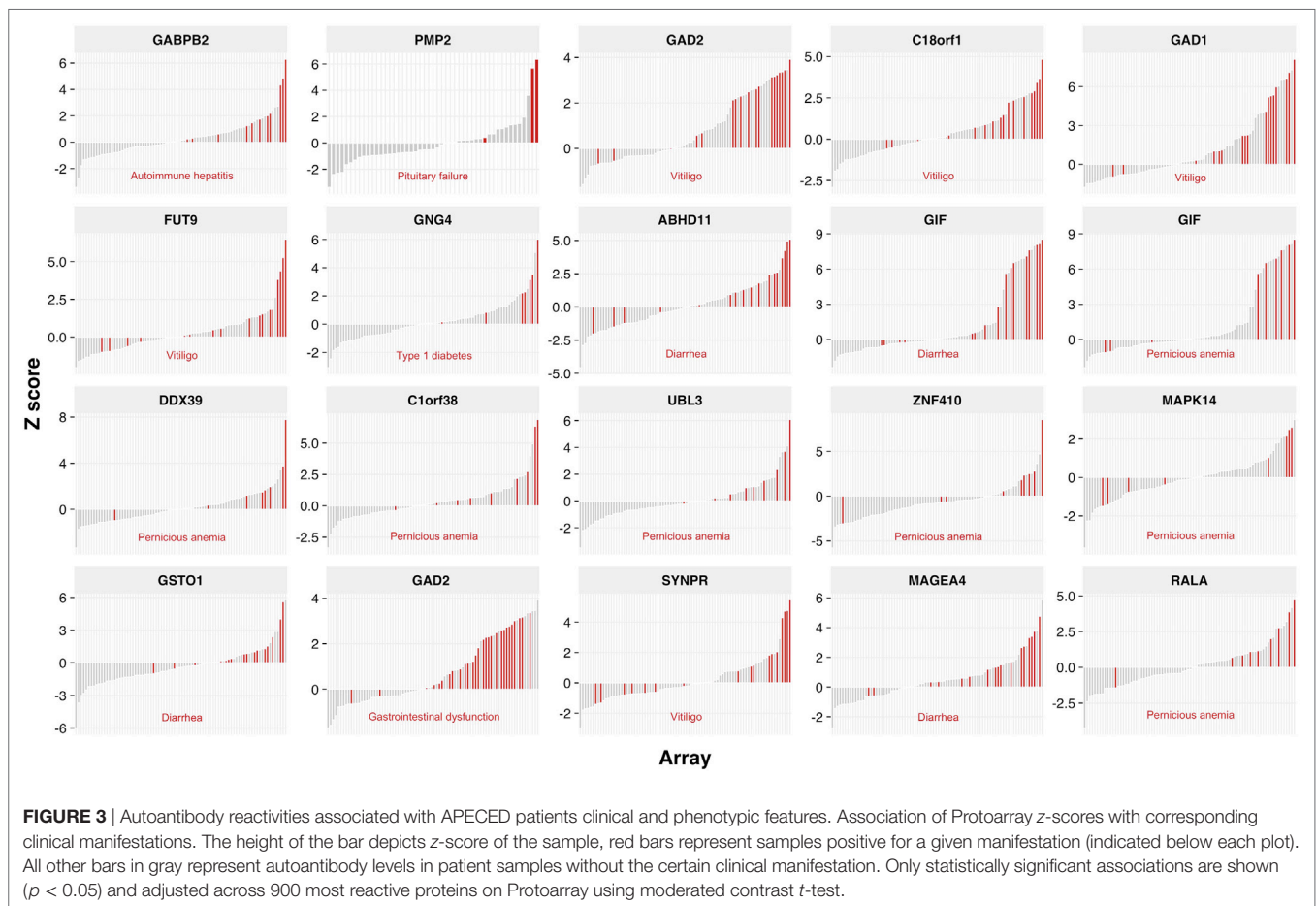
As the number of disease components in APECED patients is known to increase over time, we tested whether the number of autoantibody targets in each patient is likewise related to the age of onset of the first clinical manifestation. However, the trend toward correlation between the number of diseases and either age or time since diagnosis was not significant (Figure S4



in Supplementary Material), arguing that neither can independently explain the accumulation of multiple clinical entities in APECED. Instead, these findings add further weight to the conclusion that the complexity of the autoantibody response is

a major underlying factor for the expansion of clinical profile in APECED.

Previous studies have shown changes in autoantibody profiles over time. To understand the dynamics of autoantibody



repertoire, we studied 14 APECED patients whose sera were collected at least twice in different time points and, thus, analyzed longitudinally by Protoarray. In most patients ($n = 11$), the number of proteins recognized by autoantibodies increased with time (**Figure 4D**), whereas in only three patients the number of reactivities decreased or remained almost unchanged. We next studied whether the target antigen profile in APECED patients broadens over time. For this, we compared the samples taken less than 10 years apart with the samples spanning more than 10 years in three separate categories: (i) target specific to early sample, (ii) target shared in early and late sample, and (iii) target specific to late sample. Expectedly, the proportion of targets specific to late sample was larger indicating that the samples taken closer in time shared more reactivity to autoantigens than samples obtained more than 10 years apart (**Figure 4E**).

Nature of APECED Autoantigens

Of the many AIRE truncating mutations identified in APECED patients, the most prevalent are p.R257X creating a premature stop codon in exon 6, and a 13bp deletion, p.L323fsX373, changing the reading frame and causing a premature stop codon in exon 8. Although both mutations are present in APECED patients with various ethnic backgrounds, the R257X is commonly found among Finnish (83% of APECED alleles), Norwegian and Slovenian patients. By contrast, the earliest

AIRE truncation occurs in Sardinian patients who share a p.R139X mutation that introduces a premature stop codon prior to the SAND domain (Sp100, AIRE-1, NucP41/75, DEAF-1), an ~80 residue region common to many chromatin-regulating factors. When we divided the patients into three groups based on these genetic etiologies [(1) homozygous for p.R139, (2) homozygous for p.R257X, and (3) homozygous p.L323fsX373, or compound heterozygotes of either p.L323fsX373 or missense mutations], we found patients in Groups 1 and 2 to react to a wider spectrum of autoantigens (**Figure 5A**), thereby correlating autoantibody reactivities with the p.R139X and p.R257X truncation mutations.

Intrinsic features of proteins that might promote their autoantigenicity are not known. Indeed, the available information on the repertoire of autoantibody target proteins is fragmented, and based on this, few if any overt similarities have emerged among proteins identified as autoantigens. Given the scale of the analysis described here, we systematically analyzed our list of autoantibody target proteins for any parameters that might be enriched relative to proteins that were not targets (**Figure 5B**; Table S2 in Supplementary Material).

We first studied the subcellular localizations of APECED autoantigens by employing two different approaches: (i) the Compartments resource that integrates sequence-based and manually curated subcellular localization information from

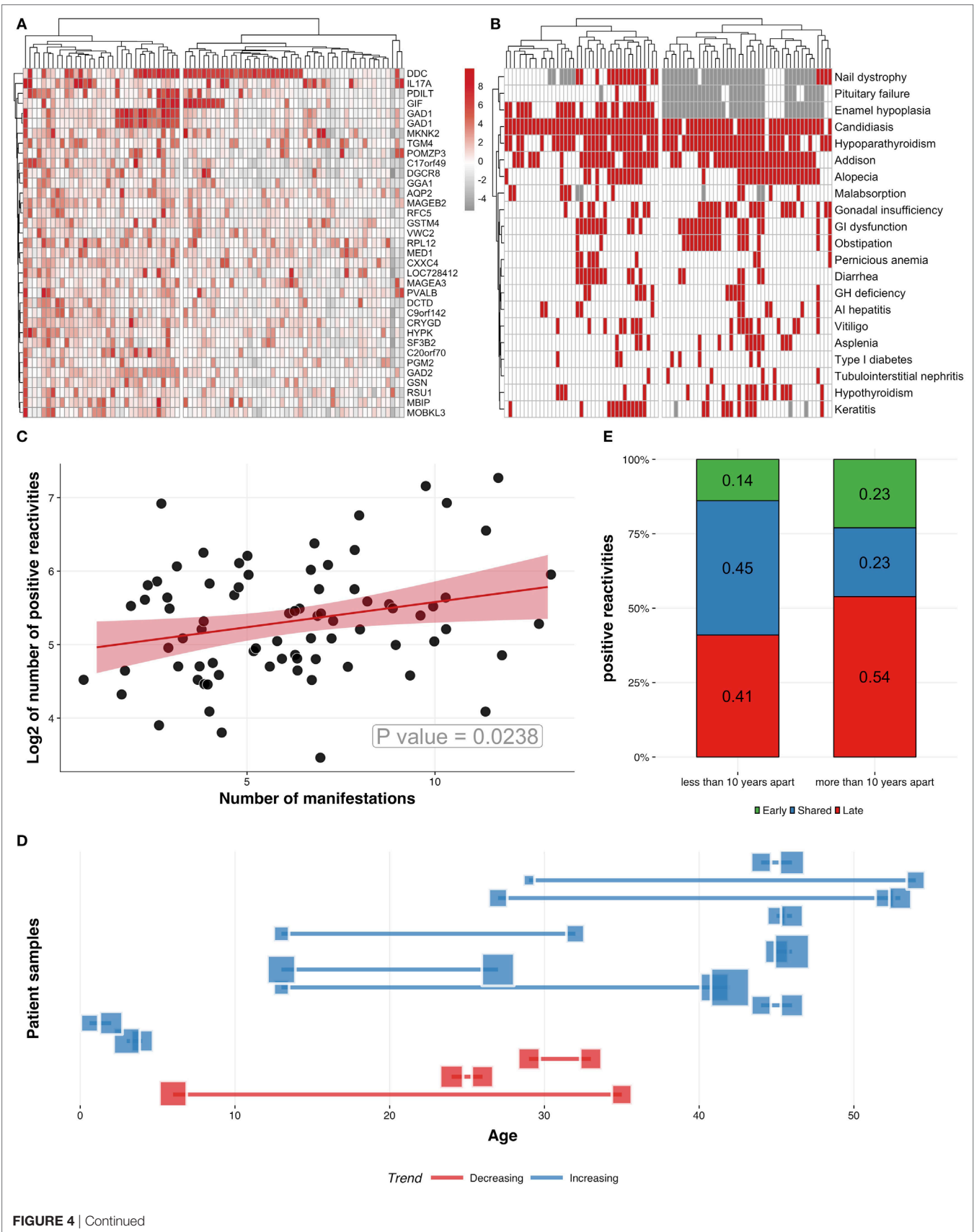
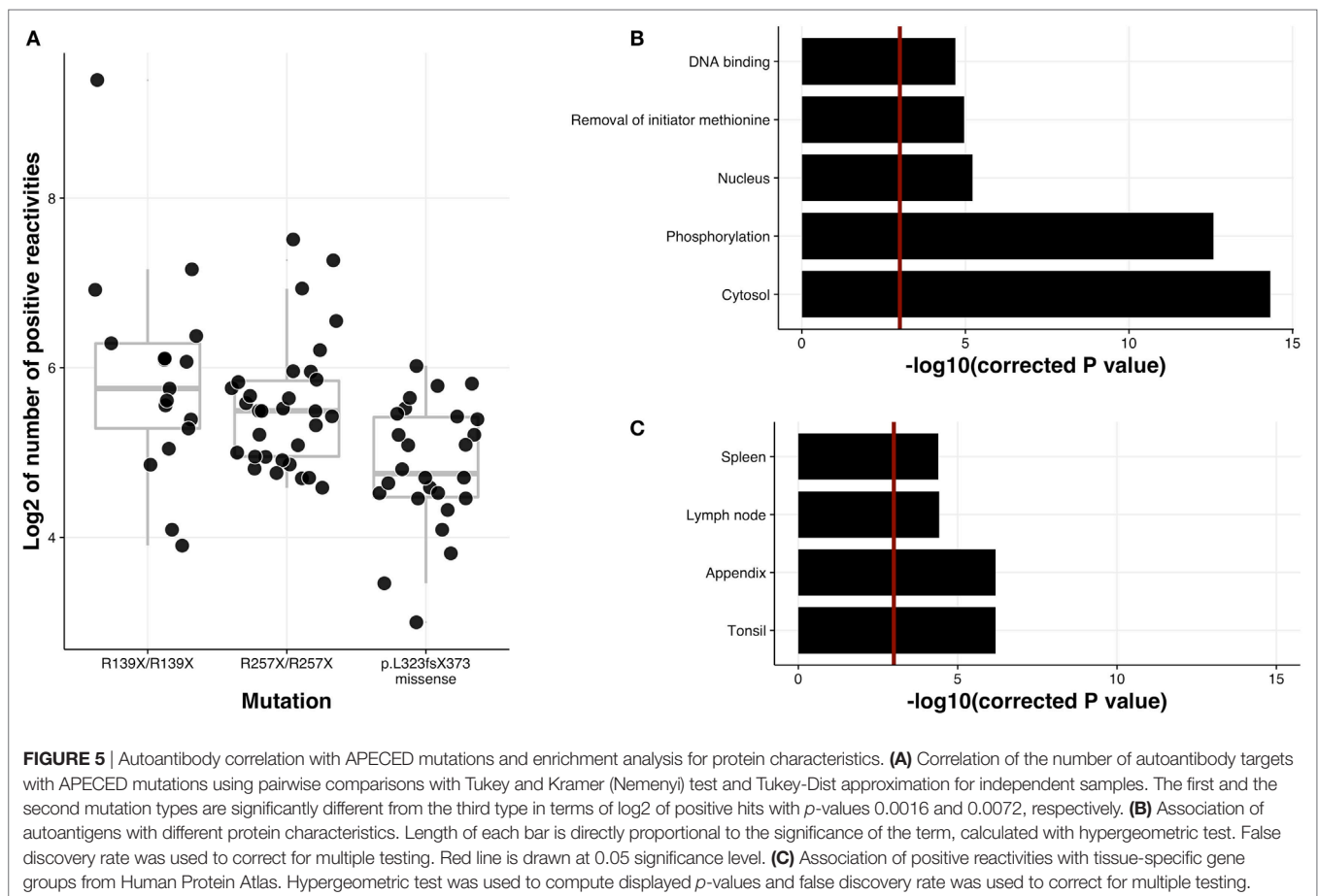


FIGURE 4 | Continued

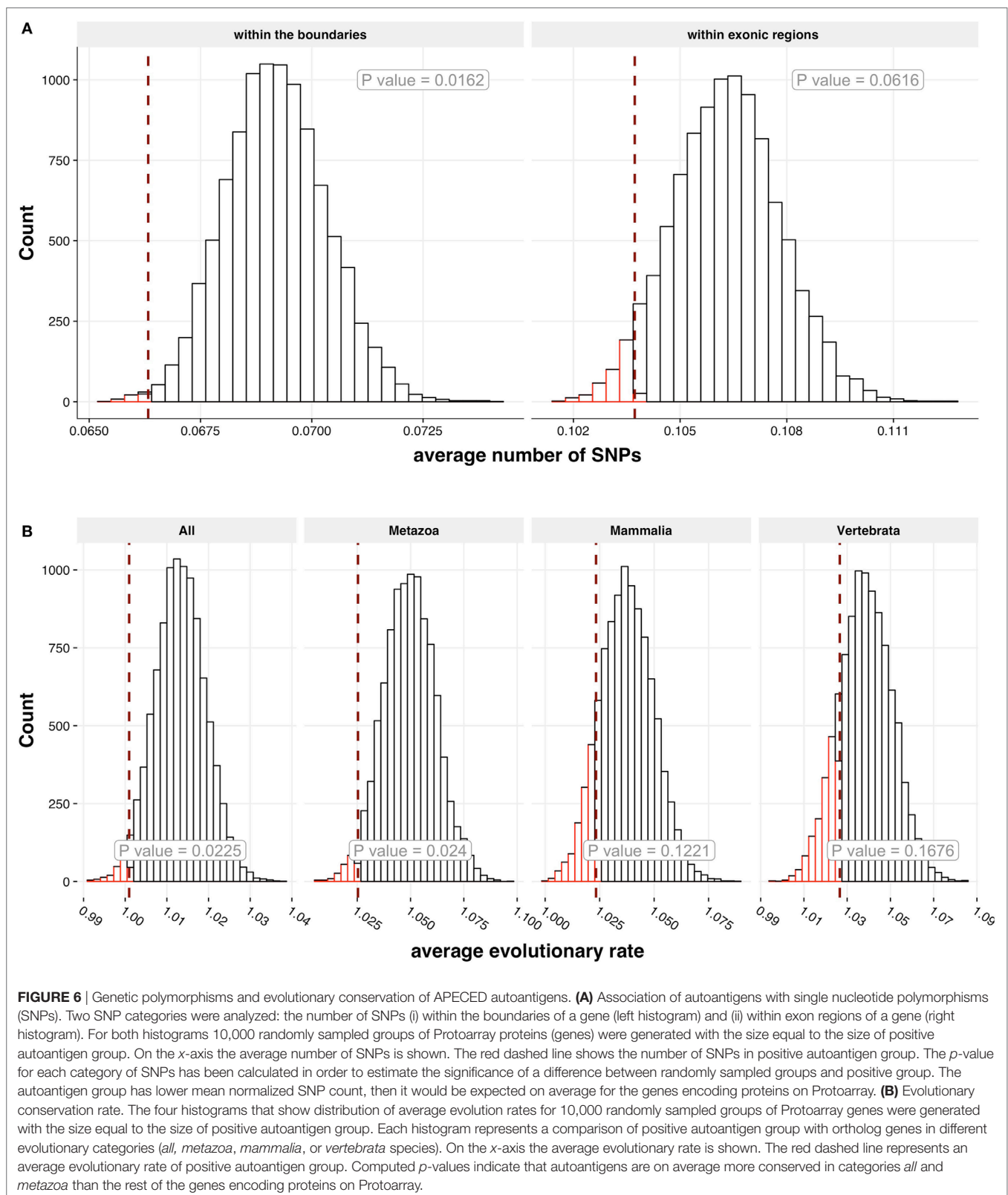
Characteristics of APECED patients and Protoarray reactivities. **(A)** Clustering patients and z-scores for the 50 most commonly recognized autoantigens using hierarchical clustering algorithm. **(B)** Clustering patients (columns) according to their clinical manifestations (rows). Red squares represent the presence of a given manifestation, while white and gray show absence of manifestation and missing information, respectively. **(C)** Positive correlation between the number of manifestations and the number of autoantigens ($z > 3$, logarithmized), correlation coefficient -0.29 . **(D)** Analysis of longitudinal serum samples taken at different time points. Blue squares and connecting lines ($n = 11$) correspond to samples with increased number of autoantigens and red squares and connecting lines ($n = 3$) correspond to samples with decreased or unchanged number of autoantigens. Each line and connected squares correspond to one APECED patient with samples collected at different time points. The locations of the squares on y-scale correspond to the age of the patient when the samples were collected. The sizes of the blue and red squares correspond to the number of positive autoantigens in corresponding samples. **(E)** The change of autoantigen profiles in samples collected longitudinally. The two columns show the autoantibody reactivities in patient samples taken less than 10 or more than 10 years apart. The autoantigens were compared between the samples of the same patient and divided into three categories according to their specificity: (i) specific to early sample, (ii) shared in early and late sample, and (iii) specific to late sample. The numbers in columns indicate the proportions of each category. Samples taken more than 10 years apart show higher percentage of autoantigens in the late samples, indicating that the autoantibody repertoire gets broader with time.



PSORT and YLoc databases and (ii) g:Profiler that searches for a cellular component as one of the Gene Ontology categories (27). The majority of autoantigens were significantly associated with intracellular location (adj. p -values $2.62e-07$ and $7.20e-03$ for Compartments and g:Profiler analysis, respectively), and in particular with either a cytosolic location (adj. p -values $6.04e-07$ and $3.01e-05$ for Compartments and g:Profiler analysis, respectively) or, to a lesser extent, a nuclear location ($p = 0.0054$) (Table S2 in Supplementary Material).

Posttranslational modifications have been proposed to contribute to autoimmune responses (39). Indeed, when we

compared our database with dbPTM datasets (22) comprising an integrated resource for protein posttranslational modifications, we found that the autoantigens were strongly enriched in proteins with histidine/serine/threonine phosphorylation (adj. $p = 3.34e-06$ for HST). The association was significant even when threonine and serine phosphorylation were compared separately (adj. p -value $4.22e-06$ for threonine only and $8.43e-04$ for serine only). However, tyrosine phosphorylation alone was not enriched and adding tyrosine phosphorylation as a category to the accumulated list of phosphorylated proteins decreased the significance level. We searched for the enrichment



of specific protein features in UniProtKB and Superfamily databases comprising a collection of protein function information. This analysis surprisingly revealed that autoantigens were

enriched for proteins from which the initiator methionine is processed by methionine aminopeptidases (adj. *p* = 0.0070) and representation of proteins with DNA binding potential

(adj. $p = 0.0091$) (Supplementary Table S2 in Supplementary Material).

The genes encoding autoantigens have been suggested to be enriched for SNPs (40). However, when we studied SNP data from Ensembl.org, the genes encoding APECED autoantigens displayed fewer SNPs in their gene regions ($p = 0.0126$) as well as in exons ($p = 0.0592$) (Figure 6A). To study how evolutionary conserved the APECED autoantigen gene families (41) are, we used OrthoDB8 database to retrieve the calculated evolutionary rates of the autoantigen genes (as human counterparts) against ortholog genes in four different taxonomic levels (all species, metazoan, vertebrata, and mammalian species). We found that the genes encoding APECED autoantigens showed significant association with the two conserved taxonomic levels (all species, $p = 0.0225$; metazoan species, $p = 0.024$; and a similar trend in mammalian and vertebrata species categories) (Figure 6B) indicating an evolutionary conserved nature of APECED autoantigens. Thus, in comparison to all genes in the genome, APECED autoantigen genes have less genetic polymorphisms and are more conserved in evolution.

Autoantigens Segregate Based on mTEC Expression and AIRE Dependence

The key role of AIRE is considered to be the establishment of tolerance toward proteins restricted to discrete peripheral tissues, the so-called tissue-restricted (TR) antigens. However, unexpectedly, we did not find the APECED autoimmunome to be appreciably enriched in TR antigens. In fact, when each tissue was analyzed separately using the Human Protein Atlas database (20), the APECED autoantigens showed the strongest significant correlation with gene expression in lymphoid tissues, specifically tonsils, spleen, appendix, and lymph nodes (Figure 5C; Table S2 in Supplementary Material).

These findings notwithstanding, given that AIRE is the driving cause of APECED, we hypothesized that the autoantibody repertoire might target two components: TR antigens and non-tissue-restricted (NTR) antigens enriched in AIRE-independent lymphoid tissue proteins. To test this hypothesis, we divided the genes encoding the autoantigens according to their TR or NTR expression pattern (Table S2 in Supplementary Material). We then cross-referenced mouse databases on the expression of genes by mature mTECs and to its subsets, including those where thymic AIRE expression is limited or lacking by knockout approach (42) (note the necessity to use mouse databases reflected by the lack of comprehensive human thymus gene expression data). Having converted human gene accession numbers to mouse counterparts, we found a very strong overlap of genes encoding APECED TR autoantigens with genes more highly expressed in mature mTEC compared to two Aire-negative subsets: immature mTEC ($p = 0.00022$) and Aire-negative mTEC subpopulation ($p = 0.00016$) (Figure 7). The genes downregulated in Aire-deficient mTEC cells were likewise enriched in genes encoding APECED TR autoantigens ($p = 0.00022$). By contrast, the NTR group showed no such correlations. Furthermore, the NTR group was associated even more strongly with intracellular phosphoproteins, expressed in lymphoid tissues.

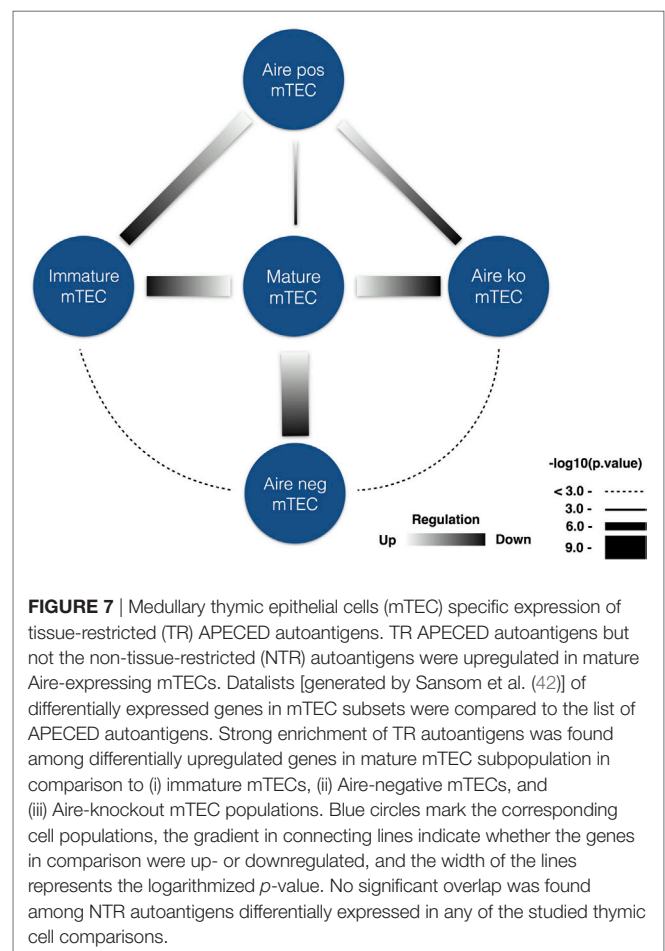


FIGURE 7 | Medullary thymic epithelial cells (mTEC) specific expression of tissue-restricted (TR) APECED autoantigens. TR APECED autoantigens but not the non-tissue-restricted (NTR) autoantigens were upregulated in mature Aire-expressing mTECs. Datalists [generated by Sansom et al. (42)] of differentially expressed genes in mTEC subsets were compared to the list of APECED autoantigens. Strong enrichment of TR autoantigens was found among differentially upregulated genes in mature mTEC subpopulation in comparison to (i) immature mTECs, (ii) Aire-negative mTECs, and (iii) Aire-knockout mTEC populations. Blue circles mark the corresponding cell populations, the gradient in connecting lines indicate whether the genes in comparison were up- or downregulated, and the width of the lines represents the logarithmized p -value. No significant overlap was found among NTR autoantigens differentially expressed in any of the studied thymic cell comparisons.

DISCUSSION

Our profiling of APECED autoantibody reactivities yielded a broad autoantibody repertoire and, except type I IFN and Th17 related cytokines, remarkable inter-individual variability. The number of candidate autoantigens ranged to almost thousand reactive proteins. Many of these proteins had lower signal intensities than type I IFN and Th17 cytokines and may partly represent a physiological (i.e., non-pathological) autoimmunity in the patients, similarly to natural autoantibodies in healthy individuals. However, in contrast to the genes activated by Aire in mTECs, only the minority was tissue-restricted proteins as we found many of the targets expressed in cell types with shared presence in lymphoid organs. Our study is in contrast to previous report (15), which identified only two novel targets (PDILT and MAGE-B2), also detected by our screening here, and with a key observation that autoimmunity in APECED preferentially targets molecules with restricted tissue expression profiles. The discrepancy may be related to conditions of serum samples, serum dilutions, differences in the versions of the Protoarray platforms, screening process and data analysis. While the previous study set highly stringent criteria considering only antigens that were common to the patient group we included the rare patient-specific reactivities, which to some extent may contain false positives.

Among tissue-restricted proteins, we found reactivity to many CT-As, implying a central role of the thymus in antitumor immunity. These included members of MAGE-A, MAGE-B, and GAGE families, and in addition sperm-specific proteins, recognized by several (including female) patient sera. By contrast, we did not detect reactivities to MAGE-D or MAGE-E, the non-CT-A members of MAGE protein family (43) that are expressed in all tissues. Importantly, the only cell type expressing CT-As outside of tumors and testis is mTEC (44), and in agreement with our findings of extensive anti-CT-A immunity in APECED, Aire-deficient mice confer strong rejection of melanoma by thymus-dependent T cell responses (45–47). Furthermore, Aire has a dual role in the maintenance of immune tolerance as it also drives the development of a subset of regulatory T cells; indeed, suppressive Aire-dependent regulatory T cells were recruited to tumor sites in a mouse model of prostate cancer (48). Thus, our data in human patients highlight the role of AIRE in modulating immune responses to CT-As with implications for cancer immunotherapy.

The repertoire and properties of target autoantigens, which represent the collection of proteins without any recognizable rule, have been enigmatic. Clearly, the property to become an autoantigen is not a single intrinsic feature but a variable combination of protein characteristics. These features may include antigen structure, susceptibility to proteolytic cleavage, localization in apoptotic blebs, and release into the extracellular space (49). Other studies have highlighted structural motifs (50), evolutionary conservation (41), posttranslational modifications (39), and a pro-inflammatory milieu of tissues (51). Post-translational modifications have been associated with various autoimmune diseases and include citrullination in rheumatoid arthritis (52), deamidation in celiac disease (53) and phosphorylation in systemic lupus erythematosus (54). We indeed found enrichment of evolutionarily conserved intracellular phosphoproteins, suggesting this posttranslational modification as one key factor in eliciting autoantibodies, and that specific protein properties contribute to B cell autoimmunity. In parallel to B cell epitopes, antigen phosphorylation is widespread and preserved among T cell epitopes on major histocompatibility complex (MHC) class I and II (55, 56), and deregulated phosphorylation creates tumor-specific neoantigens by affecting the antigenic identity or binding to MHC (57).

The high and neutralizing autoantibody titers to pro-inflammatory cytokines type I IFNs, IL-17A, IL-17F, and IL-22 implicate the inflammatory environment in the generation of the APECED autoantigen repertoire, although their scarcity in Aire-deficient mice (29) remains unexplained. Second, as high titer neutralizing anti-IFN α and anti-IFN ω autoantibodies are present in AIRE-deficient thymoma and in recently described RAG-hypomorphic patients who lack AIRE expression (58), this strongly suggests the impairment of AIRE-dependent thymic tolerance in the development of anti-cytokine antibodies in humans. However, type I IFNs and Th17 cytokines are not restricted in their expression to mTECs; likewise the expression of GAD1, steroidogenic enzymes CYP17A1 and CYP21A2, and thyroglobulin is present in other thymic cells and they have no correlation with AIRE expression (59–61), in contrast to insulin and the alpha-subunit of AChR (59).

In AIRE-deficient thymoma samples, some APECED autoantigens are expectedly under-expressed, but many are not, including several adrenocortical, gonadal and neuro-ectodermal targets (60, 62). Hence, other cell types in the thymus should contribute to the negative selection of autoreactive T cells. Thus, other mechanisms should be considered, in addition to the role of AIRE in shaping negative selection by upregulating the expression of TR antigens. Indeed, the very early onset of clinical symptoms in APECED patients have suggested that AIRE deficiency may create an actively immunizing tissue environment where tolerance of AIRE-independent antigens is broken (63).

Despite the fact that approximately 90% of the overall group of autoantigens were not tissue-restricted, the correlation of TR-specific subset with mature mTEC population and Aire dependency was strikingly strong. Thus, our results demonstrate two distinct subgroups of autoantigens; first, the smaller subgroup, which consists of approximately 10% of autoantigens, is expressed in specific tissues, and of which many are expressed in mTECs under Aire regulation. The breakdown of tolerance to these APECED autoantigens is likely driven by their lack of expression in the thymus, causing the defect in negative selection of autoreactive thymocytes. The characteristic members of this group are GIF, CYP2A7, LCN1, as well as GAD2, the expression of which followed AIRE's expression pattern in thymomas (62), and conceivably CT-As, for which AIRE-dependency in human thymus remains unknown. By contrast, the second subgroup of NTR autoantigens is associated with intracellular phosphoproteins, expressed in multiple tissues with enrichment in lymphoid tissues (lymph node, spleen, bone marrow, and tonsils), and as such represents the mTEC-independent breach of tolerance, albeit caused by AIRE mutations. Autoantibodies to these proteins emerge by actions of yet unknown mechanisms associated, for example, with apoptotic cell death or by dysfunctional B cell tolerance during differentiation in lymphoid tissues. Our findings are supported by RNA-seq analysis of autoantigen-encoding genes, which identified a subset of autoantigens, associated with autoimmune diseases, to be expressed ubiquitously but enriched in immune tissues (64). It should be noted that, in contrast to other immune tissues, the thymus was not available via Human Protein Atlas (20). Nevertheless, given the proposed hypothesis of active autoimmunization in AIRE-deficient thymus, this raises intriguing questions of whether the second set of lymphoid autoantigens might represent the antigens acquired from apoptotic thymocytes.

Finally, we identified so far unrevealed clinical associations with pernicious anemia, vitiligo, and autoimmune hepatitis. These correlations need further studies as well as the analysis of the expression of target proteins in corresponding diseased organs and tissues. Despite several outstanding correlations of clinical disease and specific autoantibodies in APECED, the majority of autoantibody reactivities seem not to have relevance to specific clinical entities. They can be just a bystander result of T cell responses, not necessarily reflecting full-blown autoimmune attack or their reactivity may depend on other factors, for example, the presence of posttranslational modifications or complexes with nucleic acids, which can operate as adjuvants. In contrast to single autoantigen responses, our results highlight

the overall spread of autoantibody repertoire as a driver for the expansion of clinical profiles in APECED. Alternatively, these autoantibodies may have unexpected protective roles as we recently showed a negative correlation of anti-IFNA antibodies with the incidence of T1D (9). The unexpectedly broad APECED autoimmunome forms a unique platform for further analysis of B cell autoimmunity toward self-antigens and their correlation with clinical manifestations.

ETHICS STATEMENT

The study was carried out in accordance with the recommendations of local ethics committees (Finland: HUS Medical ERB, 8/13/03/01/2009; Slovenia: National Medical Ethics Committee number 22/09/09 and 28/02/13; Italy: Ethics Committee Prot. PG/2015/20440; Norway: Research Ethics Committee of Western Norway, health registry number 047.96, bio-bank number 2013-1504, project number 2012/1850; Estonia: Research Ethics Committee of the University of Tartu, 235/M-23) with written informed consent from all subjects. All subjects gave written informed consent in accordance with the Declaration of Helsinki.

AUTHOR CONTRIBUTIONS

DF, KKisand, CH, and PP analyzed the Protoarray data. CH and MR assisted and supervised seroreactivity screenings of

Protoarrays. MP and ARemm performed LIPS analyses. PA, HP, and JV contributed and supervised bioinformatic analyses of Protoarray data. AP, AM, KP, TB, ØB, AW, EH, NK, KKrohn, and ARanki sampled APECED patient samples and contributed to clinical database. AH and PP supervised research. DF, KKisand, CH, AH, and PP wrote the paper with contributions from other authors.

ACKNOWLEDGMENTS

We are extremely grateful to APECED patients who provided sera and to the Finnish APECED patient association, attending physicians and care-takers of the patients. We are likewise grateful to ImmunoQure AG and Drs. Ed Stuart and Karsten Henco for their help and discussions of this research. We thank financial support from Wellcome Trust grant 106292/Z/14/Z, Cancer Research UK, Estonian Research Council grant IUT2-2 and IUT34-4. The research was also supported by the European Union through the European Regional Development Fund (Project No. 2014-2020.4.01.15-0012) and CoE of Estonian ICT research EXCITE.

SUPPLEMENTARY MATERIAL

The Supplementary Material for this article can be found online at <http://journal.frontiersin.org/article/10.3389/fimmu.2017.00976/full#supplementary-material>.

REFERENCES

- Goodnow CC, Vinuesa CG, Randall KL, Mackay F, Brink R. Control systems and decision making for antibody production. *Nat Immunol* (2010) 11(8):681–8. doi:10.1038/ni.1900
- Kisand K, Peterson P. Autoimmune polyendocrinopathy candidiasis ectodermal dystrophy. *J Clin Immunol* (2015) 35(5):463–78. doi:10.1007/s10875-015-0176-y
- Abramson J, Husebye ES. Autoimmune regulator and self-tolerance – molecular and clinical aspects. *Immunol Rev* (2016) 271(1):127–40. doi:10.1111/imr.12419
- Mathis D, Benoist C. Aire. *Annu Rev Immunol* (2009) 27:287–312. doi:10.1146/annurev.immunol.25.022106.141532
- Peterson P, Org T, Rebane A. Transcriptional regulation by AIRE: molecular mechanisms of central tolerance. *Nat Rev Immunol* (2008) 8(12):948–57. doi:10.1038/nri2450
- Meager A, Visvalingam K, Peterson P, Moll K, Murumagi A, Krohn K, et al. Anti-interferon autoantibodies in autoimmune polyendocrinopathy syndrome type 1. *PLoS Med* (2006) 3(7):e289. doi:10.1371/journal.pmed.0030289
- Wolff ASB, Sarkadi AK, Marodi L, Kaerner J, Orlova E, Oftedal BEV, et al. Anti-cytokine autoantibodies preceding onset of autoimmune polyendocrine syndrome type I features in early childhood. *J Clin Immunol* (2013) 33(8):1341–8. doi:10.1007/s10875-013-9938-6
- Kisand K, Link M, Wolff AS, Meager A, Tserel L, Org T, et al. Interferon autoantibodies associated with AIRE deficiency decrease the expression of IFN-stimulated genes. *Blood* (2008) 112(7):2657–66. doi:10.1182/blood-2008-03-144634
- Meyer S, Woodward M, Hertel C, Vlaicu P, Haque Y, Kärner J, et al. AIRE-deficient patients harbor unique high-affinity disease-ameliorating autoantibodies. *Cell* (2016) 166(3):582–95. doi:10.1016/j.cell.2016.06.024
- Kisand K, Boe Wolff AS, Podkrajsek KT, Tserel L, Link M, Kisand KV, et al. Chronic mucocutaneous candidiasis in APECED or thymoma patients correlates with autoimmunity to Th17-associated cytokines. *J Exp Med* (2010) 207(2):299–308. doi:10.1084/jem.20091669
- Puel A, Doffinger R, Natividad A, Chrabieh M, Barcenas-Morales G, Picard C, et al. Autoantibodies against IL-17A, IL-17F, and IL-22 in patients with chronic mucocutaneous candidiasis and autoimmune polyendocrine syndrome type I. *J Exp Med* (2010) 207(2):291–7. doi:10.1084/jem.20091983
- Meffre E, Wardemann H. B-cell tolerance checkpoints in health and autoimmunity. *Curr Opin Immunol* (2008) 20(6):632–8. doi:10.1016/j.coi.2008.09.001
- Herold KC, Vignali DA, Cooke A, Bluestone JA. Type 1 diabetes: translating mechanistic observations into effective clinical outcomes. *Nat Rev Immunol* (2013) 13(4):243–56. doi:10.1038/nri3422
- Bratland E, Husebye ES. Cellular immunity and immunopathology in autoimmune Addison's disease. *Mol Cell Endocrinol* (2011) 336(1–2):180–90. doi:10.1016/j.mce.2010.12.015
- Landegren N, Sharon D, Freyhult E, Hallgren Å, Eriksson D, Edqvist PH, et al. Proteome-wide survey of the autoimmune target repertoire in autoimmune polyendocrine syndrome type 1. *Sci Rep* (2016) 6:20104. doi:10.1038/srep20104
- Abel L, Kutschki S, Turewicz M, Eisenacher M, Stoutjesdijk J, Meyer HE, et al. Autoimmune profiling with protein microarrays in clinical applications. *Biochim Biophys Acta* (2014) 1844(5):977–87. doi:10.1016/j.bbapap.2014.02.023
- Sboner A, Karpikov A, Chen G, Smith M, Mattoon D, Dawn M, et al. Robust-linear-model normalization to reduce technical variability in functional protein microarrays. *J Proteome Res* (2009) 8(12):5451–64. doi:10.1021/pr900412k
- Turewicz M, May C, Ahrens M, Woitalla D, Gold R, Casjens S, et al. Improving the default data analysis workflow for large autoimmune biomarker discovery studies with ProtoArrays. *Proteomics* (2013) 13(14):2083–7. doi:10.1002/pmic.201200518
- Ritchie ME, Phipson B, Wu D, Hu Y, Law CW, Shi W, et al. limma powers differential expression analyses for RNA-sequencing and microarray studies. *Nucleic Acids Res* (2015) 43(7):e47. doi:10.1093/nar/gkv007
- Uhlén M, Fagerberg L, Hallström BM, Lindskog C, Oksvold P, Mardinoglu A, et al. Proteomics. Tissue-based map of the human proteome. *Science* (2015) 347(6220):1260419. doi:10.1126/science.1260419

21. Binder JX, Pletscher-Frankild S, Tsafou K, Stolte C, O'Donoghue SI, Schneider R, et al. COMPARTMENTS: unification and visualization of protein subcellular localization evidence. *Database (Oxford)* (2014) 2014:bau012. doi:10.1093/database/bau012
22. Lee TY, Huang HD, Hung JH, Huang HY, Yang YS, Wang TH. dbPTM: an information repository of protein post-translational modification. *Nucleic Acids Res* (2006) 34(Database issue):D622–7. doi:10.1093/nar/gkj083
23. Consortium U. UniProt: a hub for protein information. *Nucleic Acids Res* (2015) 43(Database issue):D204–12. doi:10.1093/nar/gku989
24. Yates A, Akanni W, Amode MR, Barrell D, Billis K, Carvalho-Silva D, et al. Ensembl 2016. *Nucleic Acids Res* (2016) 44(D1):D710–6. doi:10.1093/nar/gkv1157
25. Kriventseva EV, Tegenfeldt F, Petty TJ, Waterhouse RM, Simão FA, Pozdnyakov IA, et al. OrthoDB v8: update of the hierarchical catalog of orthologs and the underlying free software. *Nucleic Acids Res* (2015) 43(Database issue):D250–6. doi:10.1093/nar/gku1220
26. Gough J, Karplus K, Hughey R, Chothia C. Assignment of homology to genome sequences using a library of hidden Markov models that represent all proteins of known structure. *J Mol Biol* (2001) 313(4):903–19. doi:10.1006/jmbi.2001.5080
27. Reimand J, Arak T, Adler P, Kolberg L, Reisberg S, Peterson H, et al. g:Pro-filer—a web server for functional interpretation of gene lists (2016 update). *Nucleic Acids Res* (2016) 44(W1):W83–9. doi:10.1093/nar/gkw199
28. Burbelo PD, Browne SK, Sampaio EP, Giaccone G, Zaman R, Kristosturyan E, et al. Anti-cytokine autoantibodies are associated with opportunistic infection in patients with thymic neoplasia. *Blood* (2010) 116(23):4848–58. doi:10.1182/blood-2010-05-286161
29. Kärner J, Meager A, Laan M, Maslovskaja J, Pihlap M, Remm A, et al. Anti-cytokine autoantibodies suggest pathogenetic links with autoimmune regulator deficiency in humans and mice. *Clin Exp Immunol* (2013) 171(3):263–72. doi:10.1111/cei.12024
30. Navone R, Lunardi C, Gerli R, Tinazzi E, Peterlana D, Bason C, et al. Identification of tear lipocalin as a novel autoantigen target in Sjögren's syndrome. *J Autoimmun* (2005) 25(3):229–34. doi:10.1016/j.jaut.2005.09.021
31. Pisetsky DS. The complex role of DNA, histones and HMGB1 in the pathogenesis of SLE. *Autoimmunity* (2014) 47(8):487–93. doi:10.3109/08916934.2014.921811
32. Simpson AJ, Caballero OL, Jungbluth A, Chen YT, Old LJ. Cancer/testis antigens, gametogenesis and cancer. *Nat Rev Cancer* (2005) 5(8):615–25. doi:10.1038/nrc1669
33. Zhang XD, Miao SY, Wang LF, Li Y, Zong SD, Yan YC, et al. Human sperm membrane protein (hSMP-1): a developmental testis-specific component during germ cell differentiation. *Arch Androl* (2000) 45(3):239–46. doi:10.1080/01485010050194020
34. de Bock L, Somers K, Fraussen J, Hendriks JJ, van Horssen J, Rouwette M, et al. Sperm-associated antigen 16 is a novel target of the humoral autoimmune response in multiple sclerosis. *J Immunol* (2014) 193(5):2147–56. doi:10.4049/jimmunol.1401166
35. Toh BH. Pathophysiology and laboratory diagnosis of pernicious anemia. *Immunol Res* (2017) 65:326–30. doi:10.1007/s12026-016-8841-7
36. Gebre-Medhin G, Husebye ES, Gustafsson J, Winqvist O, Goksoyr A, Rorsman F, et al. Cytochrome P450IA2 and aromatic L-amino acid decarboxylase are hepatic autoantigens in autoimmune polyendocrine syndrome type I. *FEBS Lett* (1997) 412(3):439–45. doi:10.1016/S0014-5793(97)00797-7
37. Husebye ES, Gebre-Medhin G, Tuomi T, Perheentupa J, Landin-Olsson M, Gustafsson J, et al. Autoantibodies against aromatic L-amino acid decarboxylase in autoimmune polyendocrine syndrome type I. *J Clin Endocrinol Metab* (1997) 82(1):147–50. doi:10.1210/jcem.82.1.3647
38. Landegren N, Sharon D, Shum AK, Khan IS, Fasano KJ, Hallgren Å, et al. Transglutaminase 4 as a prostate autoantigen in male subfertility. *Sci Transl Med* (2015) 7(292):292ra101. doi:10.1126/scitranslmed.aaa9186
39. Doyle HA, Yang ML, Raycroft MT, Gee RJ, Mamula MJ. Autoantigens: novel forms and presentation to the immune system. *Autoimmunity* (2014) 47(4):220–33. doi:10.3109/08916934.2013.850495
40. Stadler MB, Arnold D, Frieden S, Luginbühl S, Stadler BM. Single nucleotide polymorphisms as a prerequisite for autoantigens. *Eur J Immunol* (2005) 35(2):371–8. doi:10.1002/eji.200425481
41. Backes C, Ludwig N, Leidinger P, Harz C, Hoffmann J, Keller A, et al. Immunogenicity of autoantigens. *BMC Genomics* (2011) 12:340. doi:10.1186/1471-2164-12-340
42. Sansom SN, Shikama-Dorn N, Zhanybekova S, Nussbaumer G, Macaulay IC, Deadman ME, et al. Population and single-cell genomics reveal the Aire dependency, relief from Polycomb silencing, and distribution of self-antigen expression in thymic epithelia. *Genome Res* (2014) 24(12):1918–31. doi:10.1101/gr.171645.113
43. Katsura Y, Satta Y. Evolutionary history of the cancer immunity antigen MAGE gene family. *PLoS One* (2011) 6(6):e20365. doi:10.1371/journal.pone.0020365
44. Gotter J, Brors B, Hergenbahn M, Kyewski B. Medullary epithelial cells of the human thymus express a highly diverse selection of tissue-specific genes colocalized in chromosomal clusters. *J Exp Med* (2004) 199(2):155–66. doi:10.1084/jem.20031677
45. Träger U, Sierro S, Djordjevic G, Bouzo B, Khandwala S, Meloni A, et al. The immune response to melanoma is limited by thymic selection of self-antigens. *PLoS One* (2012) 7(4):e35005. doi:10.1371/journal.pone.0035005
46. Zhu ML, Nagavalli A, Su MA. Aire deficiency promotes TRP-1-specific immune rejection of melanoma. *Cancer Res* (2013) 73(7):2104–16. doi:10.1158/0008-5472.CAN-12-3781
47. Khan IS, Mouchess ML, Zhu ML, Conley B, Fasano KJ, Hou Y, et al. Enhancement of an anti-tumor immune response by transient blockade of central T cell tolerance. *J Exp Med* (2014) 211(5):761–8. doi:10.1084/jem.20131889
48. Malchow S, Leventhal DS, Nishi S, Fischer BI, Shen L, Paner GP, et al. Aire-dependent thymic development of tumor-associated regulatory T cells. *Science* (2013) 339(6124):1219–24. doi:10.1126/science.1233913
49. Plotz PH. The autoantibody repertoire: searching for order. *Nat Rev Immunol* (2003) 3(1):73–8. doi:10.1038/nri976
50. Carl PL, Temple BR, Cohen PL. Most nuclear systemic autoantigens are extremely disordered proteins: implications for the etiology of systemic autoimmunity. *Arthritis Res Ther* (2005) 7(6):R1360–74. doi:10.1186/ar1832
51. Suurmond J, Diamond B. Autoantibodies in systemic autoimmune diseases: specificity and pathogenicity. *J Clin Invest* (2015) 125(6):2194–202. doi:10.1172/JCI78084
52. Clancy KW, Weerapana E, Thompson PR. Detection and identification of protein citrullination in complex biological systems. *Curr Opin Chem Biol* (2016) 30:1–6. doi:10.1016/j.cbpa.2015.10.014
53. Stamnaes J, Sollid LM. Celiac disease: autoimmunity in response to food antigen. *Semin Immunol* (2015) 27(5):343–52. doi:10.1016/j.smim.2015.11.001
54. Neugebauer KM, Merrill JT, Wener MH, Lahita RG, Roth MB. SR proteins are autoantigens in patients with systemic lupus erythematosus. Importance of phosphopeptides. *Arthritis Rheum* (2000) 43(8):1768–78. doi:10.1002/1529-0131(200008)43:8<1768::AID-ANR13>3.0.CO;2-9
55. Depontieu FR, Qian J, Zarling AL, McMiller TL, Salay TM, Norris A, et al. Identification of tumor-associated, MHC class II-restricted phosphopeptides as targets for immunotherapy. *Proc Natl Acad Sci U S A* (2009) 106(29):12073–8. doi:10.1073/pnas.0903852106
56. Zarling AL, Polefrone JM, Evans AM, Mikesch LM, Shabanowitz J, Lewis ST, et al. Identification of class I MHC-associated phosphopeptides as targets for cancer immunotherapy. *Proc Natl Acad Sci U S A* (2006) 103(40):14889–94. doi:10.1073/pnas.0604045103
57. Mohammed F, Cobbold M, Zarling AL, Salim M, Barrett-Wilt GA, Shabanowitz J, et al. Phosphorylation-dependent interaction between antigenic peptides and MHC class I: a molecular basis for the presentation of transformed self. *Nat Immunol* (2008) 9(11):1236–43. doi:10.1038/ni.1660
58. Walter JE, Rosen LB, Csomos K, Rosenberg JM, Mathew D, Keszei M, et al. Broad-spectrum antibodies against self-antigens and cytokines in RAG deficiency. *J Clin Invest* (2015) 125(11):4135–48. doi:10.1172/JCI80477
59. Taubert R, Schwendemann J, Kyewski B. Highly variable expression of tissue-restricted self-antigens in human thymus: implications for self-tolerance and autoimmunity. *Eur J Immunol* (2007) 37(3):838–48. doi:10.1002/eji.200636962
60. Ströbel P, Murumägi A, Klein R, Luster M, Lahti M, Krohn K, et al. Deficiency of the autoimmune regulator AIRE in thymomas is insufficient to elicit autoimmune polyendocrinopathy syndrome type 1 (APS-1). *J Pathol* (2007) 211(5):563–71. doi:10.1002/path.2141

61. Li B, Li J, Hsieh CS, Hale LP, Li YJ, Devlin BH, et al. Characterization of cultured thymus tissue used for transplantation with emphasis on promiscuous expression of thyroid tissue-specific genes. *Immunol Res* (2009) 44(1–3):71–83. doi:10.1007/s12026-008-8083-4
62. Wolff AS, Kärner J, Owe JF, Oftedal BE, Gilhus NE, Erichsen MM, et al. Clinical and serologic parallels to APS-I in patients with thymomas and autoantigen transcripts in their tumors. *J Immunol* (2014) 193(8):3880–90. doi:10.4049/jimmunol.1401068
63. Kisand K, Lilic D, Casanova JL, Peterson P, Meager A, Willcox N. Mucocutaneous candidiasis and autoimmunity against cytokines in APECED and thymoma patients: clinical and pathogenetic implications. *Eur J Immunol* (2011) 41(6):1517–27. doi:10.1002/eji.201041253
64. Burbelo PD, Iadarola MJ, Alevizos I, Sapio MR. Transcriptomic segregation of human autoantigens useful for the diagnosis of autoimmune diseases. *Mol Diagn Ther* (2016) 20(5):415–27. doi:10.1007/s40291-016-0211-6

Conflict of Interest Statement: The authors CH and MR were the employees of ImmunoQure AG when the study was conducted. PP, KKisand, KKrohn, AR, and AH are shareholders of ImmunoQure AG. The remaining authors declare no competing financial interests. The work is relevant US Patent Application US20170051055A1 (Human anti-IFN-alpha antibodies).

Copyright © 2017 Fishman, Kisand, Hertel, Rothe, Remm, Pihlap, Adler, Vilo, Peet, Meloni, Podkrajsek, Battelino, Bruserud, Wolff, Husebye, Kluger, Krohn, Ranki, Peterson, Hayday and Peterson. This is an open-access article distributed under the terms of the Creative Commons Attribution License (CC BY). The use, distribution or reproduction in other forums is permitted, provided the original author(s) or licensor are credited and that the original publication in this journal is cited, in accordance with accepted academic practice. No use, distribution or reproduction is permitted which does not comply with these terms.

D. Fishman, I. Kuzmin, P. Adler, J. Vilo, and H. Peterson

PAWER: Protein Array Web ExploreR

BMC Bioinformatics, 17, September 2020

The article is reprinted with permission of the copyright owner.

SOFTWARE

Open Access



PAWER: protein array web exploreR

Dmytro Fishman^{1,2}, Ivan Kuzmin¹, Priit Adler^{1,2}, Jaak Vilo^{1,2} and Hedi Peterson^{1,2*} 

*Correspondence:

hedi.peterson@ut.ee

¹Institute of Computer Science,
University of Tartu, Narva mnt 18,
51009 Tartu, Estonia

²Quretec Ltd, Ülikooli 6a, 51003
Tartu, Estonia

Abstract

Background: Protein microarray is a well-established approach for characterizing activity levels of thousands of proteins in a parallel manner. Analysis of protein microarray data is complex and time-consuming, while existing solutions are either outdated or challenging to use without programming skills. The typical data analysis pipeline consists of a data preprocessing step, followed by differential expression analysis, which is then put into context via functional enrichment. Normally, biologists would need to assemble their own workflow by combining a set of unrelated tools to analyze experimental data. Provided that most of these tools are developed independently by various bioinformatics groups, making them work together could be a real challenge.

Results: Here we present PAWER, the online web tool dedicated solely to protein microarray analysis. PAWER enables biologists to carry out all the necessary analysis steps in one go. PAWER provides access to state-of-the-art computational methods through the user-friendly interface, resulting in publication-ready illustrations. We also provide an R package for more advanced use cases, such as bespoke analysis workflows.

Conclusions: PAWER is freely available at <https://biit.cs.ut.ee/pawer>.

Keywords: Protein microarray, Data analysis, Web tool, Normalisation, Visualisation

Background

Protein microarray is the leading high-throughput method to study protein interactions [1], antibody specificity or autoimmunity [2]. In functional protein microarrays, full-length functional protein targets or protein domains are attached to the surface of the slide and then incubated with a biological sample that contains interacting molecules (e.g. autoantibodies) [3]. After molecules bind to their targets, labelling is done via secondary antibody with a fluorescent marker attached. Resulting fluorescent signal of high intensity indicates the reaction, which can be registered by the specialised scanner. The most popular microarray platforms (e.g. Human Proteome Microarray (HuProt), ProtoArray, NAPP arrays, Human Protein Fragment arrays and Immunome arrays) allow to measure autoantibody reaction to thousands of unique human protein abundances simultaneously [4, 5].



© The Author(s). 2020 **Open Access** This article is licensed under a Creative Commons Attribution 4.0 International License, which permits use, sharing, adaptation, distribution and reproduction in any medium or format, as long as you give appropriate credit to the original author(s) and the source, provide a link to the Creative Commons licence, and indicate if changes were made. The images or other third party material in this article are included in the article's Creative Commons licence, unless indicated otherwise in a credit line to the material. If material is not included in the article's Creative Commons licence and your intended use is not permitted by statutory regulation or exceeds the permitted use, you will need to obtain permission directly from the copyright holder. To view a copy of this licence, visit <http://creativecommons.org/licenses/by/4.0/>. The Creative Commons Public Domain Dedication waiver (<http://creativecommons.org/publicdomain/zero/1.0/>) applies to the data made available in this article, unless otherwise stated in a credit line to the data.

Hundreds of studies that use different types of protein microarrays are conducted every year [6]. All these studies largely depend on well executed data analysis. Usual analysis workflow starts with pre-processing of raw data obtained from GenePix Pro - one of *de facto* standard softwares used to read the microarrays [7]. The pre-processing step involves quality control and normalisation. It is followed by the differential protein analysis, in which protein reactivity levels that are significantly different between studied conditions are identified. These reactive protein levels are visualised, e.g. with boxplots. Finally, the results are interpreted using the body of prior knowledge via applying functional enrichment analysis tools. Setting up and executing these steps requires a lot of time and care from the researchers as each analysis step needs to be documented to ensure reproducibility.

Protein microarrays are similar to DNA microarrays as both technologies measure abundance of thousands of probes immobilised on the surface of the slide [8]. In the early days of protein microarrays research, this technological resemblance allowed practitioners to adapt methods and computational tools, originally developed for DNA microarrays [9]. However, a number of studies have shown that the same set of assumptions is not necessarily applicable to both types of microarrays, especially in terms of normalisation [5, 8, 9]. For example, in DNA microarrays the overall amount of signal is considered to be roughly the same between samples, while in protein microarrays only a small number of proteins are expected to show reactivity to probed serum. Applying quantile normalisation, that is usually utilised in DNA microarray analysis, may eliminate the relevant biological signal [8]. Thus, analytical pipelines tailored to protein microarrays are required in order to enable correct data analysis and consequently, biologically relevant results.

To date, four major tools for protein microarray analysis are Prospector, Protein Array Analyser (PAA) [10], Protein Microarray Analyser (PMA) [5] and online tool available as part of Protein Microarray Database (PMD) [11]. Prospector, provided by ThermoFisher Scientific, allows easy point and click analysis. However, it has not been updated since 2015, is a closed source software and runs only on the Windows 7 operating system [12]. PAA [10] builds on top of Prospector's core functionality, and provides workflow customisation and tools for biomarker discovery in R. Although PAA is flexible and robust, it requires substantial programming skills from the user. PMA is a multi-platform desktop application, built in Java and published in 2018. It can be used via simple graphical user interface as well as executed from the command line. Although, PMA implements state-of-the-art normalisation and pre-processing strategies, working with it can be challenging, as to this date no relevant documentation is available. The only web-based tool for analysing protein microarray experiments, developed prior to current work can be found on Protein Microarray Database website [11]. Unlike previously mentioned software packages, PMD tool offers an all-encompassing analysis according to the original publication. The PMD website openly prioritises depositing and archiving of protein microarray datasets, but its accompanying analysis tool lacks user-interaction and clear guidance.

Here, we present Protein Array Web Explorer (PAWER), the only interactive web tool solely dedicated to analysing protein microarray data. PAWER builds upon the strengths of previously-described tools, while eliminating their major limitations. PAWER is suitable for experimental biologists who want to analyse their own data without the need to

write code. PAWER has already been used for multiple projects, with the underlying R codebase central for analysis in two recent studies of APECED syndrome [2, 13].

Implementation

Key features

PAWER implements the following key features:

1. Public web service that can be used by anyone with protein microarray data in standard format
2. Interactive results table for convenient exploration of the results
3. Clear interactive visuals that can be downloaded in publication-ready formats
4. Parameterised algorithms at key steps (robust linear model (RLM), moderated T-test [14])
5. Downloadable intermediate results after each analysis step
6. Connection with g:Profiler [15] tool through its R package (gprofiler2) for fast enrichment analysis of differential protein features
7. An open source R package that the PAWER web service is built upon

Data upload and preprocessing

To start using PAWER, the user first needs to upload the fluorescent signal array readings - GenePix Results (GPR) files by either dragging and dropping files into the upload area or selecting them directly from the file system (via file upload window). Upon upload, PAWER automatically checks if submitted files come from the same platform and have the same extension. Detailed error message is shown in case any of these assumptions are not met. Once files have been successfully uploaded, the user is asked to select features that represent foreground and background intensities. In the case of ProtoArray and HuProt platforms, these values are chosen automatically, for other platforms user may have to manually search through the possible options from the drop-down menu. As soon as this is done, a global data matrix for the entire experiment is assembled from uploaded files using the limma R package [14]. Next, the background intensities are subtracted from the foreground values and signal from technical replicates is averaged. Resulting values are then log-transformed.

To reduce the technical noise in the data, we used a robust linear model trained on the set of protein features that are assumed to exhibit constant level of signal regardless of biological differences between samples. Such proteins are called positive controls and used in most of the platforms. Usually they are uniquely denoted in GPR files so that computer algorithms could identify them automatically. Hence, after files are uploaded, PAWER searches for such proteins and creates a list of potential positive controls. The list is then shown to the user for validation. User can alter it, by either removing or adding individual proteins. Robust linear model [8] is then used to predict the signal of control proteins based on their location (array and block) and type. In an ideal noise-free scenario, the resulting model will rely solely on protein type when predicting its signal, as any non-negative coefficient associated with array index or block id would indicate technical bias. In practice, unfortunately, noise is hard to avoid. Therefore, non-zero coefficients associated with individual protein arrays and blocks are subtracted from corresponding protein signals to remove technical bias. Data upload and normalisation steps normally take a few

minutes, for example it took about 2 minutes to preprocess a dataset of size 770 Mb, with 100 samples.

After the normalisation step is complete, user can download the normalised data as a separate file. The file can be used as an input to other tools for additional analysis. Namely, in order to enable more elaborate cluster analysis, PAWER is linked to ClustVis [16]. ClustVis is a stand-alone online tool for cluster analysis and visualisation. ClustVis implements heatmaps and principal component analysis.

The final step in the PAWER data analysis pipeline is differential expression analysis which aims to identify proteins, which signal levels significantly differ between the sample groups. To execute this step, metadata (e.g. information about patients and controls) for each sample is required. User can either upload a separate metadata file or manually annotate every GPR file using the set of radio-buttons. The metadata file should contain only two columns: the list of filenames and corresponding sample groups.

PAWER output

Differential protein features are identified using a moderated t-test, implemented using limma R package [14]. In order to perform a moderated t-test, the number of samples must be larger than the number of conditions (at least by one). Therefore, PAWER requires at least three samples (in total) to perform the differential analysis. To account for multiple testing, obtained p-values are adjusted by the Benjamini-Hochberg method. Proteins with adjusted p-values of less than 0.05 are considered significant and shown to the user in a table. User can filter the table by any value (e.g. protein name) and sort each field. By default it is sorted by the adjusted p-value. Results can be downloaded as a CSV text file for further analysis, as an Excel file to supplement a publication or as a PDF file to include into a presentation. To explore the underlying data distribution, individual protein expression values are visualised using interactive boxplots, which can be downloaded in a form of a publication-ready figure.

Additionally, enrichment of differential proteins is enabled by the gprofiler2 R package that provides interface for g:Profiler service [15]. g:Profiler gives functional enrichment results from a number of different categories, such as Gene Ontology [17], pathways and other structured data sources for instance KEGG [18], Reactome [19], Human Phenotype Ontology [20] and Human Protein Atlas [21]. The six most significant terms are visualised as a downloadable bar plot figure. The complete list of significantly enriched terms is accessible at the g:Profiler website.

Tool development

We developed the PAWER web service as a tool that covers all the necessary steps in protein microarray analysis. Its core has been implemented using R version 3.4.2, limma [22] (v. 3.34.4) for reading in the GPR format files and performing differential analysis, MASS [23] (v. 7.3.47), reshape2 [24] (v. 1.4.2) for normalisation and preprocessing of protoarray data and gprofiler2 [15] (v. 0.1.4) to enable protein identifier conversion and enrichment analysis. Web interface was implemented as a single page application using React.js and Redux architecture with node.js on the server side. Figures have been created and rendered with a help of D3.js [25] and DataTables libraries. Both the R package and the web server code are freely available under the GNU GPL v2. license.

Supported platforms

PAWER has been initially designed to support data produced mainly by ProtoArray and HuProt platforms. Later, support for the ArrayCam imaging system was added on request. Eventually, the decision was made to support as many platforms as possible by enabling customization at every step of the pipeline. Therefore, PAWER is in principle compatible with any protein microarray system or technology as long as the latter outputs text files with identical headers for each sample, and user knows several key properties of the system (background, foreground intensities and control proteins).

Comparison to existing tools

To the best of our knowledge there are five available tools, dedicated to protein microarray analysis — Prospector, PAA, PMA, PMD and PAWER. All the alternatives perform protein array specific normalisation and all but one (PMA) have capacity to identify potential biomarkers. The detailed comparison of the key features is highlighted in Table 1. Prospector was the first protein microarray analysis tool on the market, introduced by the Invitrogen company. It was originally developed for the Windows XP and later in 2015 updated to be compatible with Windows 7. Strict operating system dependency makes the number of potential Prospector users limited. In 2013 an R package, called PAA emerged [10]. Now users, independent from the platform, had an opportunity to design and apply custom analysis pipelines for their protein microarrays. At the same time, PAA requires users to be familiar with R programming language. Another tool, PMA - a Java desktop application, provided a graphical user interface and implemented cutting edge preprocessing techniques. However, it lacks documentation and does not allow for the integrated downstream analysis [5]. Finally, Protein Microarray Database website offers a possibility to analyse protein microarray experiments using their online tool. According to the original publication, PMD offers functionality for enrichment analysis, detection of differentially expressed proteins and generation of user reports based on the results [11]. However, upon closer examination, we were not able to execute the analysis using available GPR files and thus failed to confirm these claims. Neither documentation page nor original publication provide exhaustive details as to which specific methods were implemented in PMD. Also a pdf file with guidelines for interpreting the output of the tool linked from the help page was not accessible. In response to all the

Table 1 Comparison between currently available protein microarray analysis tools: Prospector, PAA, PMA, PMD and PAWER

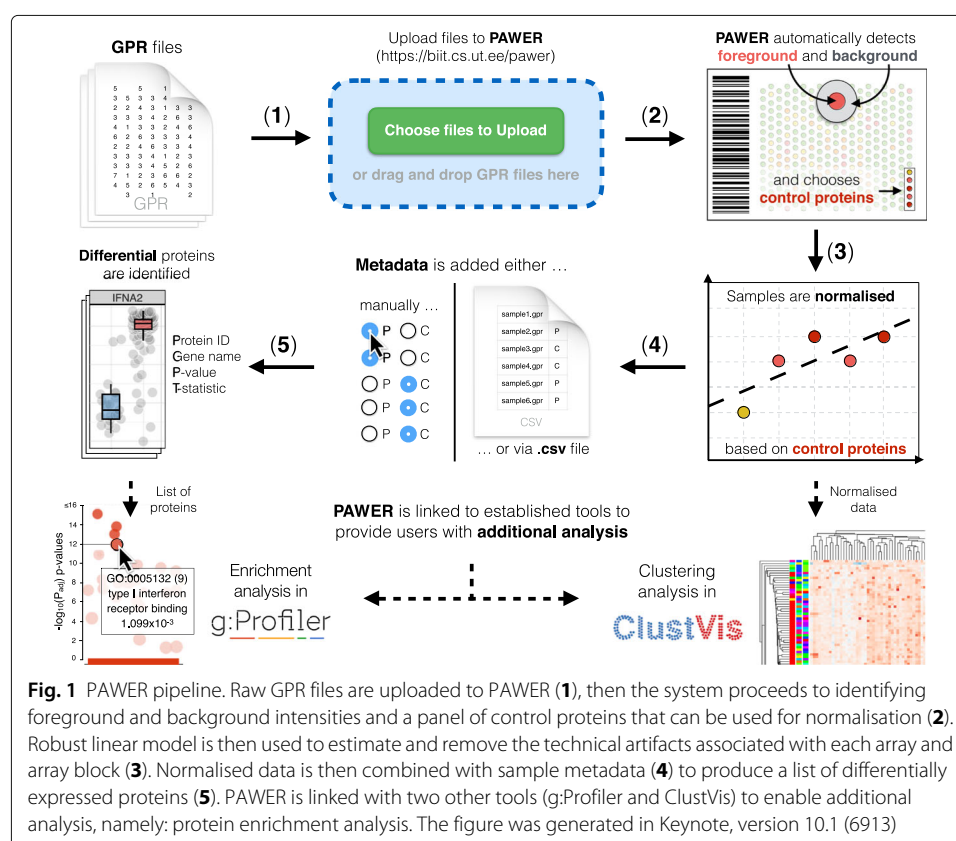
Tool name	License	Last updated	Platform	GUI	Normalisation	Biomarker identification	Functional annotation	Downloadable visuals
Prospector	No license specified	2015	Windows 7 desktop application	+	+	+		
PAA	BSD 3	2019	R package	+	+	+		+
PMA	No license specified	2018	Java desktop application	+	+			
PMD	No license specified	2020	Web server R code	+		+	+	+
PAWER	GNU GPL V2.	2020	Web server, R package	+	+	+	+	+

Presence or absence of relevant features (in columns) are shown as pluses highlighted in green (present features) or minuses in red (absent features). We were not able to obtain results using PMD tool, thus all the relevant entries are based on the claims made in the original publication [11] and highlighted in gray

challenges described above, we developed PAWER - a freely accessible web service as an alternative way to analyse protein microarrays. PAWER has a user-friendly interactive graphical interface that helps researchers to apply standard protein microarray analysis pipeline with ease (Fig. 1). Being comparable to PAA in its core strengths (protein specific normalisation and biomarker identification capabilities), PAWER also interprets the results of the analysis by providing detailed functional annotation of the identified differential proteins. Other key features are an interactive results table and accompanying attractive figures. Both figures and the table can be downloaded and used in the publications or scientific presentations. Notably, all the key steps of the analysis pipeline are well documented and presented on a separate help page.

Conclusions

PAWER is the state-of-the-art protein microarray analysis pipeline with clean and intuitive web interface. The result of the analysis is presented as a searchable and filterable table. Interactive figures related to the table allow to explore reactivities in a more detailed manner. Both the table and the figures can be downloaded in various file formats, including in publication-ready visuals. In order to encourage further development of protein microarray analysis methods, both the R and the web application code are made openly available. PAWER has already been used in multiple projects, with the underlying R codebase central for analysis in two recent studies of APECED syndrome [2, 13].



To enable a closer interaction with our users and facilitate continuous improvement of PAWER, we have made available the PAWER feature roadmap, which can be accessed from the help page. It allows users to post feature requests and provide feedback.

Availability and requirements

Project name: PAWER

Project home page: <https://biit.cs.ut.ee/pawer>

Operating system(s): Platform independent

Programming language: JavaScript for web interface and R for package

Other requirements: R 3.4.2

License: Both R package and the web server code are available under GNU GPL v2 license

Any restrictions to use by non-academics: Not applicable

Abbreviations

PAWER: Protein microarray web explorer; GPR: GenePix results; RLM: Robust linear model; PAA: Protein array analyser; PMA: Protein microarray analyser; PMD: Protein microarray database online tool

Acknowledgements

The authors would like to acknowledge Pärt Peterson and Kai Kisand for introducing us to protein microarrays and their expert insight into the autoimmunity field. Also, we would like to thank Leopold Parts, Kaur Alasoo and Liis Kolberg for critical reading and comments on the manuscript. Special thanks go to Ms Boson for providing ideas that laid down the basis for the name and logo of PAWER.

Authors' contributions

DF, PA analyzed protein microarray data and developed the R package. IK, PA, DF developed the web tool. DF and HP wrote the paper with a contribution from IK, JV and PA. HP supervised the project. All authors read, edited and approved the final manuscript.

Funding

This work was supported by the Estonian Research Council grants [PSG59, IUT34-4]; European Regional Development Fund for CoE of Estonian ICT research EXCITE projects; European Union through the Structural Fund [Project No 2014-2020.4.01.16-0271, ELIXIR].

Availability of data and materials

PAWER web server and accompanied R package are both freely available online at <https://biit.cs.ut.ee/pawer/>. R package repository at <https://gl.cs.ut.ee/biit/pawer>. Web interface repository can be accessed at https://gl.cs.ut.ee/biit/pawer_web_client.

Ethics approval and consent to participate

Not applicable

Consent for publication

Not applicable

Competing interests

The authors declare that they have no competing interests.

Received: 27 April 2020 Accepted: 25 August 2020

Published online: 17 September 2020

References

1. Fan Q, Huang LZ, Zhu XJ, Zhang KK, Ye HF, Luo Y, Sun XH, Zhou P, Lu Y. Identification of proteins that interact with alpha A-crystallin using a human proteome microarray. *Mol Vis*. 2014;20:117–24.
2. Meyer S, Woodward M, Hertel C, Vlaicu P, Haque Y, Karner J, Macagno A, Onuoha SC, Fishman D, Peterson H, Metskula K, Uibo R, Jantti K, Hokynar K, Wolff ASB, Krohn K, Ranki A, Peterson P, Kisand K, Hayday A, Meloni A, Kluger N, Husebye ES, Podkrajsek KT, Battelino T, Bratanić N, Peet A. AIRE-Deficient Patients Harbor Unique High-Affinity Disease-Ameliorating Autoantibodies. *Cell*. 2016;166(3):582–95. <https://doi.org/10.1016/j.cell.2016.06.024>.
3. Sharon D, Snyder M. Serum profiling using protein microarrays to identify disease related antigens. In: *Methods in Molecular Biology*, vol 1176. New York: Springer; 2014. p. 169–78.
4. Jeong JS, Jiang L, Albino E, Marrero J, Rho HS, Hu J, Hu S, Vera C, Bayron-Poueymiroy D, Rivera-Pacheco ZA, Ramos L, Torres-Castro C, Qian J, Bonaventura J, Boeke JD, Yap WY, Pino I, Eichinger DJ, Zhu H, Blackshaw S. Rapid identification of monospecific monoclonal antibodies using a human proteome microarray. *Mol Cell Proteomics*. 2012;11(6):111–016253. <https://doi.org/10.1074/mcp.O111.016253>.

5. Duarte JDG, Goosen RW, Lawry PJ, Blackburn JM. PMA: Protein microarray analyser, a user-friendly tool for data processing and normalization. *BMC Res Notes*. 2018;11(1):. <https://doi.org/10.1186/s13104-018-3266-0>.
6. Yu X, Petritis B, Duan H, Xu D, LaBaer J. Advances in cell-free protein array methods. *Expert Rev Proteomics*. 2017;15(1):1–11. <https://doi.org/10.1080/14789450.2018.1415146>.
7. Abel L, Kutschki S, Turewicz M, Eisenacher M, Stoutjesdijk J, Meyer HE, Woitalla D, May C. Autoimmune profiling with protein microarrays in clinical applications. *Biochim Biophys Acta (BBA) Protein Proteomics*. 2014;1844(5): 977–98. <https://doi.org/10.1016/j.bbapap.2014.02.023>.
8. Sboner A, Karpikov A, Chen G, Smith M, Mattoon D, Dawn M, Freeman-Cook L, Schweitzer B, Gerstein MB. Robust-linear-model normalization to reduce technical variability in functional protein microarrays. *J Proteome Res*. 2009;8(12):5451–64. <https://doi.org/10.1021/pr900412k>.
9. Duarte JG, Blackburn JM. Advances in the development of human protein microarrays. *Expert Rev Proteomics*. 2017;14(7):627–41. <https://doi.org/10.1080/14789450.2017.1347042>.
10. Turewicz M, Ahrens M, May C, Marcus K, Eisenacher M. PAA: an R/bioconductor package for biomarker discovery with protein microarrays. *Bioinformatics*. 2016;32(10):1577–9. <https://doi.org/10.1093/bioinformatics/btw037>.
11. Xu Z, Huang L, Zhang H, Li Y, Guo S, Wang N, Wang S-H, Chen Z, Wang J, Tao S-C. PMD: A resource for archiving and analyzing protein microarray data. *Sci Rep*. 2016;6(1):. <https://doi.org/10.1038/srep19956>.
12. Turewicz M, May C, Ahrens M, Woitalla D, Gold R, Casjens S, Pesch B, Brüning T, Meyer HE, Nordhoff E, Böckmann M, Stephan C, Eisenacher M. Improving the default data analysis workflow for large autoimmune biomarker discovery studies with protoarrays. *Proteomics*. 2013;13(14):2083–7. <https://doi.org/10.1002/pmic.201200518>.
13. Fishman D, Kisand K, Hertel C, Rothe M, Remm A, Pihlap M, Adler P, Vilo J, Peet A, Meloni A, Podkrajsek KT, Battelino T, Bruserud, Wolff ASB, Husebye ES, Kluger N, Krohn K, Ranki A, Peterson H, Hayday A, Peterson P. Autoantibody Repertoire in APECED Patients Targets Two Distinct Subgroups of Proteins. *Front Immunol*. 2017;8: 976. <https://doi.org/10.3389/fimmu.2017.00976>.
14. Smyth GK. Linear models and empirical bayes methods for assessing differential expression in microarray experiments. *Stat Appl Genet Mol Biol*. 2004;3:3. <https://doi.org/10.2202/1544-6115.1027>.
15. Raudvere U, Kolberg L, Kuzmin I, Arak T, Adler P, Peterson H, Vilo J. g:profiler: a web server for functional enrichment analysis and conversions of gene lists (2019 update). *Nucleic Acids Res*. 2019;47(W1):191–8. <https://doi.org/10.1093/nar/gkz369>.
16. Mersalu T, Vilo J. ClustVis: a web tool for visualizing clustering of multivariate data using principal component analysis and heatmap. *Nucleic Acids Res*. 2015;43(W1):566–70. <https://doi.org/10.1093/nar/gkv468>.
17. Ashburner M, Ball CA, Blake JA, Botstein D, Butler H, Cherry JM, Davis AP, Dolinski K, Dwight SS, Eppig JT, et al. Gene ontology: tool for the unification of biology. the gene ontology consortium. *Nat Genet*. 2000;25(1):25–9. <https://doi.org/10.1038/75556>.
18. Kanehisa M, Furumichi M, Tanabe M, Sato Y, Morishima K. KEGG: new perspectives on genomes, pathways, diseases and drugs. *Nucleic Acids Res*. 2016;45(D1):353–61. <https://doi.org/10.1093/nar/gkw1092>.
19. Fabregat A, Jupe S, Matthews L, Sidiropoulos K, Gillespie M, Garapati P, Haw R, Jassal B, Koeninger F, May B, Milacic M, Roca CD, Rothfels K, Sevilla C, Shamovsky V, Shorser S, Varusai T, Viteri G, Weiser J, Wu G, Stein L, Hermjakob H, D'Eustachio P. The reactome pathway knowledgebase. *Nucleic Acids Res*. 2018;46(D1):649–55. <https://doi.org/10.1093/nar/gkx1132>.
20. Köhler S, Carmody L, Vasilevsky N, Jacobsen JOB, Danis D, Gourdiene J-P, Gargano M, Harris NL, Matentzoglou N, McMurry JA, Osumi-Sutherland D, Cipriani V, Balhoff JP, Conlin T, Blau H, Baynam G, Palmer R, Gratian D, Dawkins H, Segal M, Jansen AC, Muaz A, Chang WH, Bergerson J, Laulederkind SJF, Yüksel Z, Beltran S, Freeman AF, Sergouniotis PI, Durkin D, Storm AL, Hanauer M, Brudno M, Bello SM, Sincan M, Rageth K, Wheeler MT, Oegema R, Loughri H, Rocca MGD, Thompson R, Castellanos F, Priest J, Cunningham-Rundles C, Hegde A, Lovering RC, Hajek C, Olry A, Notarangelo L, Similuk M, Zhang XA, Gómez-Andrés D, Lochmüller H, Dollfus H, Rosenzweig S, Marwaha S, Rath A, Sullivan K, Smith C, Milner JD, Leroux D, Boerkoel CF, Klion A, Carter MC, Groza T, Smedley D, Haendel MA, Mungall C, Robinson PN. Expansion of the human phenotype ontology (HPO) knowledge base and resources. *Nucleic Acids Res*. 2019;47(D1):1018–27. <https://doi.org/10.1093/nar/gky1105>.
21. Uhlen M, Fagerberg L, Hallström BM, Lindskog C, Oksvold P, Mardinoglu A, Sivertsson Å, Kampf C, Sjöstedt E, Asplund A, et al. Tissue-based map of the human proteome. *Science*. 2015;347(6220):1260419. <https://doi.org/10.1126/science.1260419>.
22. Ritchie ME, Phipson B, Wu D, Hu Y, Law CW, Shi W, Smyth GK. limma powers differential expression analyses for RNA-sequencing and microarray studies. *Nucleic Acids Res*. 2015;43(7):47. <https://doi.org/10.1093/nar/gkv007>.
23. Venables WN, Ripley BD. *Modern Applied Statistics with S-PLUS*. Berlin, Germany: Springer; 2013.
24. Wickham H, et al. Reshaping data with the reshape package. *J Stat Softw*. 2007;21(12):1–20. <https://doi.org/10.18637/jss.v021.i12>.
25. Bostock M, Ogievetsky V, Heer J. D³: Data-Driven Documents. *IEEE Trans Vis Comput Graph*. 2011;17(12):2301–9. <https://doi.org/10.1109/TVCG.2011.185>.

Publisher's Note

Springer Nature remains neutral with regard to jurisdictional claims in published maps and institutional affiliations.

T. Knific, **D. Fishman**, A. Vogler, M. Gstöttner, R. Wenzl, H. Peterson and T. Lanisnik Rizner

Multiplex analysis of 40 cytokines do not allow separation between endometriosis patients and controls

Scientific Reports, 13 November 2019

The article is reprinted with permission of the copyright owner.

OPEN

Multiplex analysis of 40 cytokines do not allow separation between endometriosis patients and controls

Tamara Knific^{1,6}, Dmytro Fishman^{2,3,6}, Andrej Vogler⁴, Manuela Gstöttner⁵, René Wenzl⁵, Hedi Peterson^{2,3} & Tea Lanišnik Rižner^{1*}

Endometriosis is a common gynaecological condition characterized by severe pelvic pain and/or infertility. The combination of nonspecific symptoms and invasive laparoscopic diagnostics have prompted researchers to evaluate potential biomarkers that would enable a non-invasive diagnosis of endometriosis. Endometriosis is an inflammatory disease thus different cytokines represent potential diagnostic biomarkers. As panels of biomarkers are expected to enable better separation between patients and controls we evaluated 40 different cytokines in plasma samples of 210 patients (116 patients with endometriosis; 94 controls) from two medical centres (Slovenian, Austrian). Results of the univariate statistical analysis showed no differences in concentrations of the measured cytokines between patients and controls, confirmed by principal component analysis showing no clear separation amongst these two groups. In order to validate the hypothesis of a more profound (non-linear) differentiating dependency between features, machine learning methods were used. We trained four common machine learning algorithms (decision tree, linear model, k-nearest neighbour, random forest) on data from plasma levels of proteins and patients' clinical data. The constructed models, however, did not separate patients with endometriosis from the controls with sufficient sensitivity and specificity. This study thus indicates that plasma levels of the selected cytokines have limited potential for diagnosis of endometriosis.

Endometriosis is a common benign gynaecological disease where endometrium like tissue is displaced and found outside the uterine cavity at ectopic locations. Endometriosis affects mainly women of reproductive age and is associated with pelvic pain and infertility^{1,2}. Based on location of endometriotic lesions three types of endometriosis can be defined: ovarian, peritoneal and deep infiltrating endometriosis^{3,4}. Laparoscopic visualization of the lesions followed by histological examination enables confirmation of endometriosis and according to the extent and location of lesions the disease is classified into four stages (minimal, mild, moderate and severe). The combination of non-specific symptoms and invasive laparoscopic procedure needed for the definitive diagnosis, results in up to 10 years of delay from the start of the symptoms to the definitive diagnosis of endometriosis^{1,5}. Although several theories have been proposed that attempt to explain reasons for the clinical manifestation of endometriosis (metaplasia, transplantation), Sampson's theory of retrograde menstruation still remains most widely accepted^{1,6–9}. This theory states that the blood containing endometrial cells flows through the fallopian tubes into the pelvic cavity during menstruation, leading to ectopic endometrial lesions. Endometriosis is also an oestrogen-dependent and chronic inflammatory disease. Thus, several additional factors, such as impaired immune system, genetic and epigenetic predispositions as well as environmental factors were shown to play a role in determining whether an individual will develop the condition¹⁰. Endometrial tissue, which is displaced at different parts of the peritoneal cavity, induces inflammation. Inflammation is a complex process which is regulated by cytokines, a vast and diverse group of proteins that have a key role in the proliferation, activation of

¹Institute of Biochemistry, Faculty of Medicine, University of Ljubljana, 1000, Ljubljana, Slovenia. ²Institute of Computer Science, University of Tartu, Liivi 2, 50409, Tartu, Estonia. ³Quretec Ltd., Ülikooli 6A, Tartu, 51003, Estonia. ⁴Department of Obstetrics and Gynaecology, University Medical Centre Ljubljana, 1000, Ljubljana, Slovenia. ⁵Department of Obstetrics and Gynecology, Medical University Vienna, 1090, Vienna, Austria. ⁶These authors contributed equally: Tamara Knific and Dmytro Fishman. *email: Tea.Lanisnik-Rizner@mf.uni-lj.si

B cells, adhesion and cell chemotaxis. Cytokines via inflammation can therefore influence the onset and progression of endometriosis¹¹. These proteins include growth factors, interferons, interleukins (IL) and chemokines^{12,13}. Chemokines are a small (8–10 kDa) group of pro-inflammatory polypeptides and signal proteins as they induce chemotaxis and are involved in the inflammatory response. Based on the distance between the first two cysteine residues chemokines can be divided into four groups; namely C (γ chemokines), CC (β chemokines), CXC (α chemokines), and CX3C (δ chemokines). The CXC group of chemokines can be further subdivided according to the presence/absence of ELR (glutamic acid-leucine-arginine) motif¹⁴. Since cytokines and chemokines can be released into the bloodstream their plasma/serum concentrations can easily be determined and thus represent potential biomarkers for the non-invasive diagnosis of endometriosis. There have been several thorough review papers published by May *et al.*, Rižner, Gupta *et al.* and Nisenblat *et al.* describing potential biomarkers for endometriosis, reported from 1984 to 2015^{15–18}. In addition, Borrelli *et al.* systematically reviewed published studies on chemokines as potential biomarkers of endometriosis where in total 27 different chemokines have been evaluated where the majority of the studies focused on the diagnostic potential of CXCL8, CCL2 and CCL5¹⁹. The authors of these systematic reviews emphasized the importance of employing high quality standardized procedures when evaluating biomarkers for the diagnosis of endometriosis. Starting from sample collection and storage to collecting more detailed clinical data. These reviews emphasized also a need for multicentre validation studies performed on an independent set of patients from different populations.

In our previous study we evaluated the concentrations of 16 cytokines and other secretory proteins in peritoneal fluid and serum samples from patients with ovarian endometriosis, benign ovarian cysts and healthy women²⁰. In peritoneal fluid the models with the highest diagnostic accuracies included: (i) IL-8 and the ratio of ficolin2 to glycodelin (ii) the ratio of biglycan to leptin and also the ratio of RANTES to IL-6; both in combination with age; the model with the highest diagnostic accuracy had an area under the curve (AUC) of 0.9. In serum the best characteristics were shown for models including: (i) the ratio between leptin and glycodelin and (ii) the ratio between ficolin2 and glycodelin; again both in combination with age; where the models with the highest diagnostic accuracies had a slightly lower AUC of 0.86 and 0.85, respectively²⁰. The present study was performed on a different set of patient samples that were collected from two medical centres (Slovenian, Austrian) and included evaluation of 40 different cytokines - mainly chemokines in plasma samples. We decided to evaluate a different set of proteins from aforementioned studies in order to broaden the set of potential biomarkers for further validation studies that could include previous, as well as potential novel biomarkers. To the best of our knowledge this is the first study that evaluated such a broad spectrum of inflammatory proteins in plasma samples from a large, well-defined group of patients with different types of endometriosis. Aims of the present study were therefore to evaluate whether a single cytokine or combination of cytokines in a large, well-defined patient population can differentiate patients with endometriosis from control patients. If we identified cytokines with diagnostic potential we planned to design a diagnostic model with sufficient sensitivity and specificity, based on the plasma concentrations of cytokines and gathered patients' clinical data, and with the use of appropriate statistical and bioinformatics analysis.

Materials and Methods

Study design and sample source. The prospective case-control study was approved by both (i.e. Slovenian and Austrian) National Medical Ethics Committees (0120-127/2016-2 and EMMA 545/2010, respectively) and all the participants signed their written informed consent before being included in the study. Inclusion criteria comprised endometriosis-like symptoms (i.e. infertility and/or pain) as well as benign gynaecological conditions (i.e. different types of cysts and/or myomas). Exclusion criteria included pregnancy, age below 18 or above 50 years, menopausal status, gynaecological malignancies, other types of cancer, cancelled operation, HIV infection and the presence of haemolysis in plasma samples. The aim was to collect approximately 200 samples, with approximately one-to-one ratio of patients and controls to achieve more than 80% statistical power (probability to reject null hypothesis if it is false) and less than 5% Type I error rate under assumption that mean concentrations of cytokines noticeably differ between conditions.

Patient enrolment took place from March 2013 to September 2016 at the Departments of Obstetrics and Gynaecology, University Medical Centre Ljubljana, Slovenia and the Medical University Vienna, Austria. At both Departments of Gynecology patients were recruited by senior gynecologists with the help of study nurses. Blood samples were analyzed in 2016. The time interval between recruitment/surgery and blood analysis (index test) was few weeks to 3 years. On the day of the surgery (Vienna) or one day to one week before surgery (Ljubljana) blood samples were collected according to a strict standard operating procedure. Blood samples of 4 ml were taken into BD Vacutainer tubes, (#368861, Becton Dickinson and Company, NJ, USA). Within one hour after collection the samples were centrifuged at 1400 g for 10 min at 4 °C. The plasma was aspirated and samples were aliquoted into 100 μ L volumes and stored at -80°C until analysis. Participants were interviewed regarding their ethnic origin, life style (i.e. diet, smoking status, sport and recreation, stress level), medical history especially with regards to different types of pain that are associated with endometriosis (pelvic pain, dysmenorrhea, dyschezia and dyspareunia) as well as medication intake a week prior to surgery, the use of oral contraceptives and hormonal therapy, current or in the three months prior to surgery. The intensity of dysmenorrhea and dyspareunia were evaluated using a validated visual analogue scale of 10 points. The reference test was laparoscopy (in exceptional cases laparotomy) with visualization of typical lesions and histological evaluation. Laparoscopy and laparotomy were performed by expert surgeons with at least ten years of experience. In total out of 233 patients 210 met inclusion criteria of whom 116 were laparoscopically (or by laparotomy) and histologically characterized by the presence of endometriosis and 94 by the absence of it (Table 1, Fig. 1).

Additional pathologies/conditions were identified after the surgical procedure. The phase of the menstrual cycle was estimated based on the date of the last menstruation and the thickness, as well as appearance, of the endometrium determined by ultrasound. The study was designed to meet the principles of the Declaration of

Characteristic	Subgroup	Controls n = 94		Patients with endometriosis n = 116		P-value [§]
		Frequency	[%]	Frequency	[%]	
Age (years)	<26	17	18.1	17	14.7	ns
	26–29.9	19	20.2	22	19.0	
	30–35.9	26	27.7	49	42.2	
	36–40.9	21	22.3	22	19.0	
	>41	11	11.7	6	5.2	
BMI (kg/m ²)	<18.5	3	3.2	11	9.5	<0.05
	18.6–24.9	59	62.8	78	67.2	
	25–29.9	25	26.6	16	13.8	
	>30	7	7.4	11	9.5	
Smoking status	Nonsmoker	45	47.9	68	58.6	ns
	Smoker	31	33.0	29	25.0	
	Occasional smoker	5	5.3	6	5.2	
	Former smoker	12	12.8	12	10.3	
	Missing data	1	1.1	1	0.9	
Menstrual phase	Proliferative	41	43.6	49	42.2	ns
	Secretory	41	43.6	59	50.9	
	Anovulatory	2	2.1	0	0	
	Oral contraceptives	4	4.3	6	5.2	
	Missing data	6	6.4	2	1.7	
Hormonal therapy three months prior to surgery	No	86	91.5	104	89.7	ns
	Yes	8	8.5	12	10.3	
	Missing data	0	0	0	0	
Oral contraceptives three months prior to surgery	No	83	88.3	101	87.1	ns
	Yes	11	11.7	15	12.9	
	Missing data	0	0	0	0	
Medication intake a week prior to surgery	No	55	58.5	62	53.4	ns
	Yes	39	41.5	54	46.6	
	Missing data	0	0	0	0	
Additional pathologies/conditions Cysts	No	63	67.0	102	87.9	<0.01
	Yes	31	33.0	14	12.1	
Fallopian tube related	No	79	84.0	113	97.4	<0.01
	Yes	15	16.0	3	2.6	
Uterus related	No	86	91.5	107	92.2	ns
	Yes	8	8.5	9	7.8	
Adenomyosis	No	92	97.9	113	97.4	ns
	Yes	2	2.1	3	2.6	
Adhesions	No	80	85.1	89	76.7	ns
	Yes	14	14.9	27	23.3	
Inflammation related conditions	No	83	88.3	113	97.4	<0.05
	Yes	11	11.7	3	2.6	
Borderline ovarian tumour	No	92	97.9	116	100	ns
	Yes	2	2.1	0	0	

Table 1. Clinical characteristics of the study participants ([§]Mann-Whitney test for continuous variables and Fisher's or Chi-square test for categorical variables; P values calculated by comparing controls to patients with endometriosis); ns, not significant.

Helsinki (Ethical Principles for Medical Research Involving Human Subjects), Oviedo Convention (Protecting Human Rights in the Biomedical Field) and the Code of Medical Ethics.

Biomarker measurements. All methods were performed in accordance with the relevant guidelines and regulations. The Luminex xMAP multiplexing and the Bio-Plex Pro™ Human Chemokine Assay platforms (#171ak99mr2, lots: #64025638, #64040537 Bio-Rad Laboratories, CA, USA) were used according to the manufacturer's protocol. Briefly, the method is based on 5.5 µm polystyrene beads that are labelled with two different fluorescent dyes in different ratios assigned for each individual antibody, thus enabling quantification of 40 different cytokines, mainly chemokines in each sample (Table 2). The intra assay and inter assay variability of the Human Chemokine Assay, as specified by the producer, was 2–6% CV and 2–8% CV, respectively. The samples

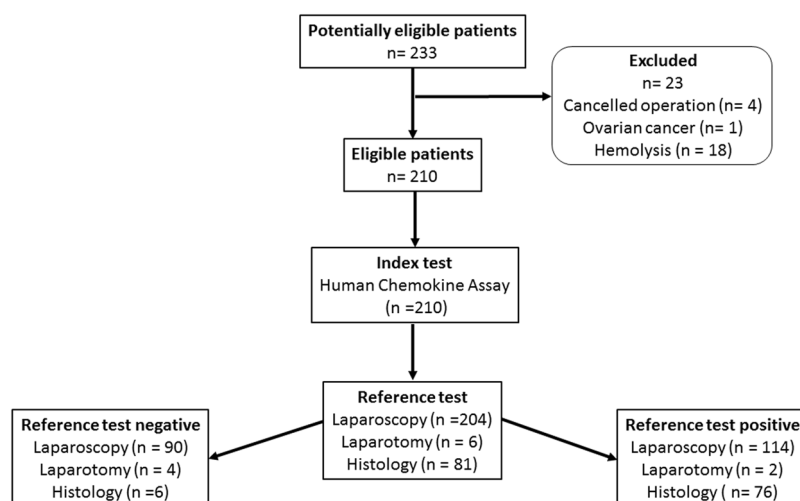


Figure 1. Flowchart of patient recruitment.

were anonymized and the person performing the assays was blind to identity of the samples and the result of the surgery. According to the producers' instruction manual plasma was diluted fourfold prior to analysis. Bio-PlexTM Manager Software with a 5-parameter logistic regression modelling was used to calculate final concentrations. Calibrations and verifications were performed prior to every analysis with the use of commercially available and recommended kits (MPX-PVER-K25, MPX-CAL-K25; Luminex, Austin, Texas, USA). Clinical data that were obtained from the patients (i.e. metadata) was included in the statistical modelling. The data were processed using Microsoft Excel 2003, and for statistical analysis we used GraphPad Prism Software version 5.00 for Windows (San Diego, CA, USA), R programming language²¹ version 3.4.3 (2017-11-30) – “Kite-Eating-Tree” and R Studio version 1.1.383 with packages such as *mice*, *caret* and *ggplot2*. Corrected P value of <0.05 was considered significant.

Statistics. For univariate statistical analysis two sided Wilcoxon rank-sum test (Mann-Whitney U test) was used to assess statistical significance of the difference in plasma concentrations of 40 different cytokines and chemokines between endometriosis patients (i.e. also according to the different types of endometriosis) and control group of women. Results of the univariate analysis were then also corrected according to Bonferroni's correction for multiple testing. To assess the normality of the distributions Shapiro-Wilk test was used. Fisher's exact and Chi-square tests were used for comparison of categorical variables. Results of the descriptive analysis (i.e. patient's clinical data) were presented as mean \pm standard deviation (SD) while the concentrations of the measured proteins were presented as median and also as mean \pm SD (Tables 1 and 2, respectively). Before further analysis we excluded proteins with reported out of range concentrations (i.e. GM-CSF, CXCL5). Apart from the remaining single proteins additional variables were constructed which represented ratios of the protein's concentrations. Batch effect between samples collected in different centres was identified with principle component analysis (PCA) and removed using mean-centring and normalisation of standard deviations of all protein features across samples from each batch.

Machine learning. Machine learning algorithms such as decision tree²², generalised linear model²³, weighted k-nearest neighbour²⁴ and random forest²⁵ were applied to identify proteins or panels of proteins that would discriminate patients with endometriosis from the controls. R packages *rpart*, *GLMNET*, *KKNN* and *RandomForest* were used to implement aforementioned models. Selected machine learning methods represent very popular, however, intrinsically different classes of classification algorithms. Each employed method is sufficiently simple to produce interpretable results, but at the same time powerful enough to model complex and often non-linear interactions between input features. In order to ensure robustness of the reported results, 4-fold repeated cross-validation (4-fold repeated CV) technique has been used. For each classifier average accuracy across all the folds and repetitions were reported. Reported accuracy has been compared to the accuracy of the hypothetical random classifier trained on the same data to assess the diagnostic potential of the trained models. At times when number of samples was not equal in modelled groups, balanced accuracy which takes into account imbalanced representation of samples was applied instead of regular accuracy. We have included additional clinical data into our analysis such as the use of hormonal therapy and/or oral contraception three months prior to surgery, medication intake a week prior to surgery as potential important confounders or effect modifiers. The obtained metadata are included in the Table 1 and in the Supplementary Table S1.

Results

Characteristics of the patient's cohorts. Our case group comprised 116 patients with different types of endometriosis (Tables 1 and S1). Staging of endometriosis was done according to the revised American Society for Reproductive Medicine classification³. Minimal to mild endometriosis was present in 72 patients (62%) and moderate to severe in 40 patients (35%) and for four (3%) patients the information regarding the extent of

	Controls; n = 94			Patients with endometriosis; n = 116			Controls; n = 94			Patients with endometriosis; n = 116			
	Median	Mean \pm SD	Range	Median	Mean \pm SD	Range	Median	Mean \pm SD	Range	Median	Mean \pm SD	Range	
CCL21	4812.6	5198.8 \pm 1769.4	2491.1–11051.8	4966.4	5695.7 \pm 2031.5	1870.2–14517.3	IL-16	339.3	347.6 \pm 111.7	97.9–609.3	341.7	351.4 \pm 128.7	82.4–967.4
CXCL13	17.4	26.1 \pm 30.8	8.1–205.4	17.9	21.6 \pm 18.4	3.6–157.5	CXCL10	26.6	32.7 \pm 24.7	13.3–226.2	26.5	31.3 \pm 20.7	7.8–170.7
CCL27	584.0	607.3 \pm 239.3	82.8–1255.1	637.9	658.9 \pm 265.2	172.7–1675.3	CXCL11	109.7	138.0 \pm 122.5	12.1–1068.74	122.9	141.1 \pm 79.8	44.2–657.8
CXCL5	165.1	168.4 \pm 112.8	11.1–494.2	141.7	159.2 \pm 108.8	6.83–440.6	CCL22	586.5	626.9 \pm 258.6	203.3–2024.0	578.6	598.9 \pm 205.6	149.5–1236.6
CCL11	76.0	78.2 \pm 13.8	50.1–116.1	73.4	74.6 \pm 13.0	46.5–104.6	MIF	955.4	1398.0 \pm 1550.4	167.9–10307.6	830.0	1338.4 \pm 1425.3	192.9–8217.7
CCL24	98.4	122.2 \pm 99.8	3.4–595.3	89.9	117.7 \pm 95.8	8.3–447.8	CCL2	19.0	19.8 \pm 7.4	3.9–47.0	17.5	18.6 \pm 6.9	8.7–65.2
CCL26	10.5	9.1 \pm 5.2	0.1–20.9	8.9	8.3 \pm 4.6	0.4–18.2	CCL8	15.4	16.6 \pm 8.2	3.9–72.4	15.7	15.9 \pm 6.1	2.8–37.9
CX3CL1	102.2	120.2 \pm 83.2	56.7–695.2	99.6	108.1 \pm 47.1	50.9–519.3	CCL7	41.3	43.8 \pm 11.6	29.2–103.5	39.2	41.1 \pm 7.9	29.2–74.0
CXCL6	20.0	21.3 \pm 8.4	10.1–47.9	21.0	22.5 \pm 9.3	8.5–59.3	CCL13	17.7	23.4 \pm 15.5	5.0–103.6	18.3	21.6 \pm 11.9	6.9–66.0
GMCSF	5.7	5.9 \pm 3.7	1.0–14.5	4.3	4.9 \pm 3.6	1.0–10.6	TNF- α	14.2	15.1 \pm 5.4	9.2–50.6	13.4	13.9 \pm 2.8	6.4–23.6
CXCL1	149.6	155.4 \pm 33.0	92.5–322.7	145.2	148.5 \pm 30.6	92.5–276.6	CCL17	19.4	28.3 \pm 26.5	6.4–168.6	22.5	27.9 \pm 19.9	3.8–115.2
CXCL2	56.3	86.0 \pm 74.1	23.5–367.9	65.4	102.1 \pm 90.8	16.9–426.9	CCL25	259.0	256.2 \pm 87.0	112.9–648.2	241.5	240.6 \pm 69.7	112.9–545.1
CCL1	44.2	44.7 \pm 12.0	26.8–83.0	42.7	42.6 \pm 10.4	24.6–71.0	CXCL9	119.7	185.3 \pm 422.9	50.6–4189.5	121.3	170.5 \pm 359.2	68.9–3925.5
IFN- γ	1.8	1.9 \pm 0.6	1.1–5.9	1.8	1.8 \pm 0.4	1.1–3.6	CCL3	5.2	5.6 \pm 2.6	3.8–29.2	4.9	5.1 \pm 0.8	3.6–7.6
IL-1 β	10.3	13.4 \pm 17.5	2.5–129.0	11.6	12.9 \pm 13.2	1.5–143.4	CCL15	4540.9	5893.6 \pm 4562.9	1259.4–26163.1	4113.2	5262.9 \pm 3497.7	893.2–21597.0
IL-2	3.5	4.1 \pm 5.0	1.3–50.1	3.5	3.4 \pm 1.0	1.3–5.8	CCL20	7.6	16.4 \pm 56.0	3.6–512.1	7.4	8.9 \pm 5.6	4.0–54.1
IL-4	9.0	9.4 \pm 3.2	2.7–19.4	10.0	9.7 \pm 3.3	0.9–16.5	CCL19	51.7	59.3 \pm 37.3	24.9–284.8	48.3	54.6 \pm 24.1	20.0–167.3
IL-6	8.1	10.1 \pm 8.4	3.4–76.8	8.1	8.2 \pm 2.4	3.9–15.5	CCL23	316.9	324.8 \pm 155.1	19.2–681.2	339.0	332.3 \pm 150.4	9.8–827.4
IL-8	8.9	10.3 \pm 7.6	4.1–76.8	8.9	9.0 \pm 2.5	3.9–19.3	CXCL16	372.4	384.8 \pm 122.3	111.6–715.4	361.4	380.2 \pm 130.7	130.1–799.8
IL-10	18.9	20.7 \pm 10.4	10.1–82.0	19.9	20.4 \pm 8.6	7.0–73.3	CXCL12	1164.7	1130.0 \pm 305.8	423.8–2075.7	1189.1	1174.4 \pm 308.5	552.3–2882.1

Table 2. Plasma concentrations of the measured cytokines in pg/mL (with no significant differences between patients with endometriosis and controls).

endometriosis was not known. Patients with endometriosis were 32 ± 6 years of age (range between 19 and 50 years) and with a body mass index (BMI) of 23 ± 5 kg/m² (range between 16 and 50 kg/m²). According to the menstrual phase 59 patients (51%) were in their secretory and 49 (42%) in their proliferative phase (Table 1), six (5%) patients were on oral contraceptives at the time of the hospitalization, and for two (2%) patients this information was missing.

Patients with benign gynaecological conditions (i.e. different types of cysts and/or myoma), unexplained infertility and/or severe pain where laparoscopy excluded the presence of endometriosis totalled 94 controls. Controls were 32 ± 8 years of age (range between 18 and 50 years) and with a BMI of 24 ± 4 kg/m² (range between 18 and 42 kg/m²). In total 41 (44%) controls were in secretory and the same number of controls were in proliferative phase of their menstrual cycle (Table 1) while four (4%) controls were taking oral contraceptives at the time of the surgery and for eight (8%) controls the information was missing or the phase of the menstrual cycle could not be determined.

Three months prior to surgery the vast majority of our study participants was not on hormonal therapy, only 8.5% controls and 10.3% of endometriosis patients used hormonal therapy (mainly progesterone and progestins), and additional 11.7% controls and 12.9% patients with endometriosis was on oral contraception (Table 1). A week before surgery 54 patients with endometriosis (47%) and 39 controls (42%) were taking medications, mostly analgesics, anti-inflammatory and anti-rheumatic products and psychoanaleptics. More than half of the patients with endometriosis (59%) and less than a half of controls (48%) were non-smokers (Table 1). Sport or recreation two days before surgery was reported for 39 patients with endometriosis (34%) and 19 (20%) controls.

The two study groups did not differ in age, menstrual phase, use of hormonal therapy and oral contraceptives three months prior to surgery, use of other medications a week before surgery, and smoking status. However, they differed in BMI distribution ($P < 0.05$), frequency of dysmenorrhea ($P < 0.01$), intensity of dysmenorrhea ($P < 0.05$) and in presence of additional pathologies/conditions such as fallopian tube related pathologies ($P < 0.01$), cysts ($P < 0.01$) and inflammation related conditions ($P < 0.05$). Most of the study participants (59%) were of Slovene or Austrian origin and all of the participants were of European descent. This clinical information is summarized in Tables 1 and S1.

Levels of cytokines in patients with endometriosis and in control. In all 210 plasma samples concentrations of all 40 different chemokines were measured (Table 2). Univariate statistical analysis revealed that there are no statistically significant differences in cytokine levels between all patients and controls. We also compared plasma concentrations of cytokines from patients with different types of endometriosis with controls where we identified eleven potential biomarkers for a specific type of endometriosis. In total we have identified seven potential biomarkers for peritoneal endometriosis (i.e. CCL21, CCL11, CCL26, CX3CL1, CCL1, IL-6, and CCL3), two for the presence of peritoneal and ovarian endometriosis (i.e. CXCL11, CXCL12), one for peritoneal and deep infiltrating endometriosis (i.e. IFN- γ) and two for all three types of endometriosis (i.e. CCL15, CXCL12). The

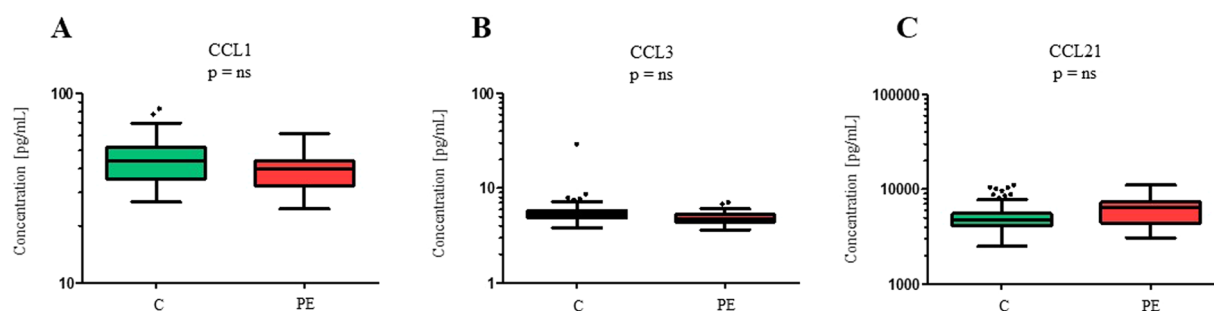


Figure 2. Box plots comparing plasma levels of the three cytokines that differ between the control group of patients and patients with peritoneal endometriosis in the univariate analysis. Plasma levels of cytokines are presented as Tukey box-and-whiskers plots with median, the box from the 25th to 75th percentiles, and whiskers correspond to the 25th percentile minus 1.5 times IQR (interquartile range) and to the 75th percentile plus 1.5 IQR. After correction for multiple testing no statistical difference (ns) was observed. Plasma concentrations of the cytokines are represented on a logarithmic scale. C, controls; PE, peritoneal endometriosis.

most differential proteins for peritoneal endometriosis CCL1, CCL3 and CCL21 (Fig. 2) but after correction for multiple testing a boundary of the statistical significance was set at $P < 0.001$ and the differences in the concentrations of these proteins were not statistically significant.

Analysis of cytokines by different machine learning approaches did not allow separation between cases and controls.

As more biomarkers potentially increase the reliability of a diagnostic test we decided to use machine learning to evaluate whether a panel of proteins with or without incorporation of metadata can differentiate among our two phenotypes. Results of the PCA showed there was no meaningful separation between patients with endometriosis and the controls based on the measured plasma levels of cytokines (Fig. 3). The highest average classification performance was achieved by the random forest algorithm (balanced accuracy = 59%, see Fig. 4a) with signal of six most influential features (i.e. proteins) illustrated as boxplots in Fig. 4. Obtained accuracy was not sufficiently different from random chance. Next, we trained the random forest model on different numbers of protein features to test a hypothesis that model trained on fewer proteins would generate better diagnostic characteristics (i.e. higher sensitivity, specificity and AUC) rather than using the whole panel of proteins and protein ratios at once. Results showed that a combination of three proteins would generate the highest combination of the selected diagnostic characteristics with a sensitivity of 40%, specificity of 65% and an AUC of 0.61 (Fig. 5), which, however is still far from being acceptable for diagnostics.

We then added metadata features (included in Tables 1 and S1) along with protein levels to the training data, but it did not improve the overall fit of the models and we could still not see a clear separation between patients with endometriosis and controls (Fig. 6). Performing separate analysis on individual types of endometriosis with the inclusion of metadata revealed no significant differences (Fig. 7). Comparing all four stages (minimal, mild, moderate and severe) of endometriosis as well as comparing minimal/mild with moderate/severe endometriosis with controls did not end up in significantly different features. Except for $\text{TNF}\alpha/\text{CCL27}$ protein ratio that has been consistently reported by the random forest algorithm as the most valuable feature for separating patients with minimal/mild endometriosis from controls. However, despite high importance of $\text{TNF}\alpha/\text{CCL27}$, the accuracy achieved by the algorithm remained modest (57.4%). We also did not observe any significant differences between patients and controls when divided with respect to the medication intake (use of any kind of medication or the use of nonsteroidal anti-inflammatory drugs or the use of any type of hormonal medication). Other personal and clinical data also showed no differences in the plasma profiles of the patients and controls.

Discussion

Endometriosis is a common benign gynaecological condition that is characterized by the presence of endometrial lesions in the peritoneal cavity and is thus also described as a chronic inflammatory disease where diagnostic biomarkers that would be applicable for clinical use have not yet been identified¹⁶. Cytokines have already been investigated as potential biomarkers of endometriosis in the blood and/or peritoneal fluid. In addition to individual inflammatory proteins, also panels of cytokines in conjunction with other proteins have been studied, although the results of these studies varied^{16,19,26}. The majority of these studies investigated IL-6 and $\text{INF-}\gamma$ which are included in the activation and differentiation of inflammatory cells and are also involved in the pathogenesis of endometriosis^{27–30}.

In the current study there were no statistically significant differences in cytokine plasma levels between patient with different types of endometriosis and controls. Although we found potential importance of the ratio $\text{TNF}\alpha/\text{CCL27}$ for separating patients with minimal/mild endometriosis from the control group of patients, the accuracy achieved by the algorithm was insufficient. Univariate analysis revealed the lowest P values when we compared concentrations of cytokines/chemokines CCL1, CCL3, CCL21 in patients with peritoneal endometriosis and controls. We found no published studies evaluating blood levels of these cytokines/chemokines in patients with endometriosis Borrelli *et al.*, evaluated the levels of CCL21 in the peritoneal fluid of 36 patients with endometriosis and 27 controls and reported no significant differences³¹. Other studies focused on the expression of the corresponding genes. Unchanged or changed expression (i.e. increased/decreased) in the endometrium from

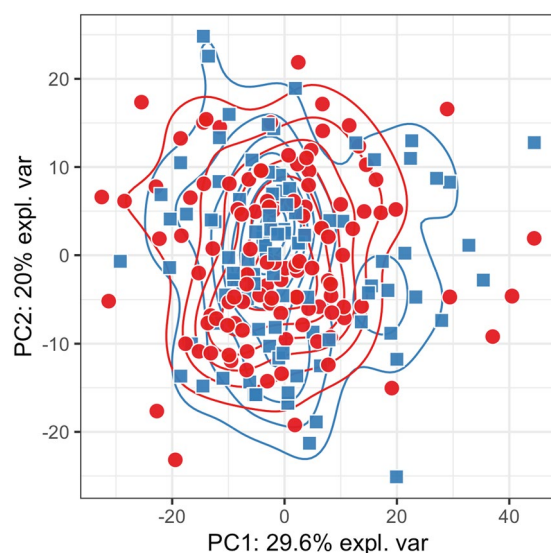


Figure 3. Principal component analysis plot. Data from the protein concentrations were scaled and normalized. The PCA plot is based on the whole protein set and coloured according to the disease status (red circles - patients with endometriosis; blue squares - controls). Transformed data show no meaningful grouping between patients with endometriosis and controls.

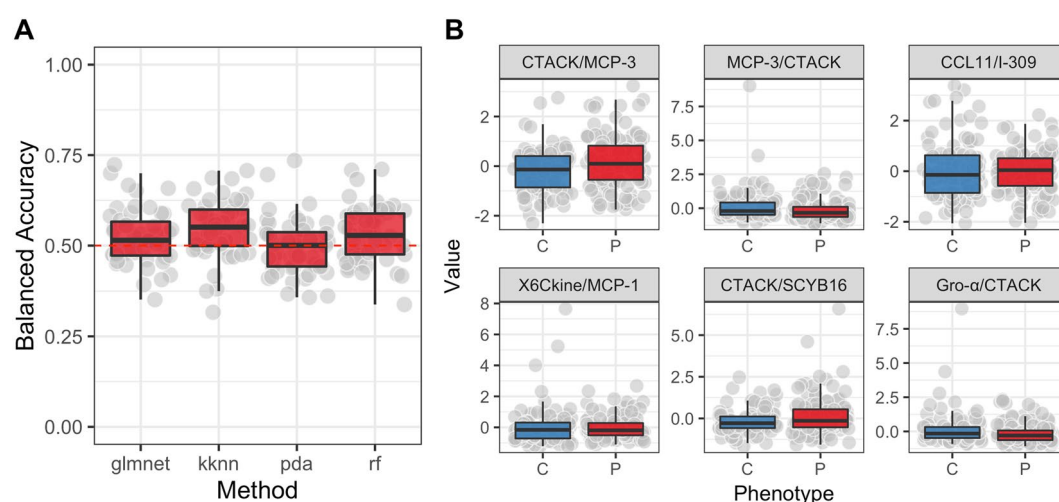


Figure 4. Averaged classification performance of four classifiers and box plots for the selected features that were used for training a random forest model. (A) Four different classifiers were used based on the data from the training set with the highest average classification performance (i.e. accuracy) achieved with random forest (balanced accuracy of ~59%). (B) Box plots of the six most important features that were used for training a RandomForest model based on the training set and were the most differential between patients with endometriosis and controls. Red color designate patients with endometriosis and blue color controls. Machine Learning models used: glmnet, elastic-net regularized generalized models; kkn, Weighted k-Nearest Neighbors; rpart, Recursive Partitioning and Regression Trees; rf, RandomForest. Dashed red line indicates expected balanced accuracy of a random chance.

patients with endometriosis was reported for *CCL21* with no explanation on how these changes might contribute to the aetiology or pathogenesis of endometriosis^{32–34}. Expression and/or role of *CCL1* and its receptor (i.e. *CCR8*) in endometrial tissue was studied by Shi *et al.*^{35,36} and revealed higher expression and their potential role in the pathogenesis of endometriosis. Although these three cytokines/chemokines identified in our study have so far not been sufficiently investigated in endometriosis our experimental data link changes in concentrations of these proteins to peritoneal endometriosis, which implies that *CCL1*, *CCL3* and *CCL21* might have a role in the aetiology and pathogenesis of this type of endometriosis.

The studies that evaluated blood concentrations of cytokines and chemokines as potential biomarkers of endometriosis are scarce, as the most studies so far evaluated the diagnostic potential of inflammatory proteins in peritoneal fluid and/or tissue samples (i.e. eutopic/ectopic endometrium) of patients with endometriosis. Kalu

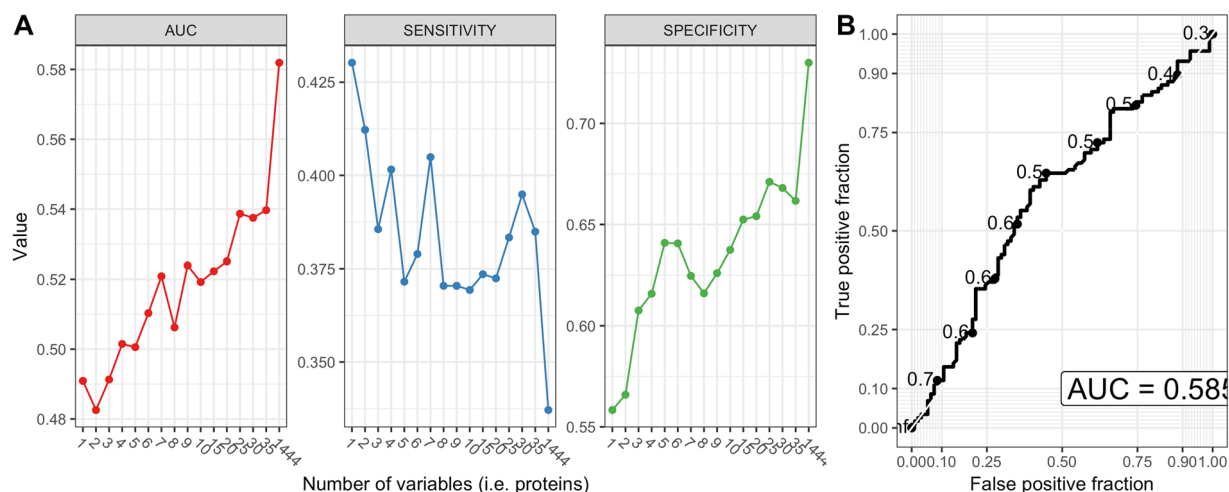


Figure 5. Modelling results from the recursive feature elimination method. **(A)** Each dot that forms curves was chosen automatically by the random forest algorithm trained on the number of protein features specified by x-axis. The best performance was achieved by random forest that was trained on all 1444 protein concentrations or ratios of protein concentrations remaining after pre-processing which achieved AUC of 0.585 for all samples with a sensitivity of 34% and specificity of over 70%. **(B)** ROC curve based on the highest values of sensitivity, specificity and AUC. ROC, receiver operating characteristic; AUC, area under the curve.

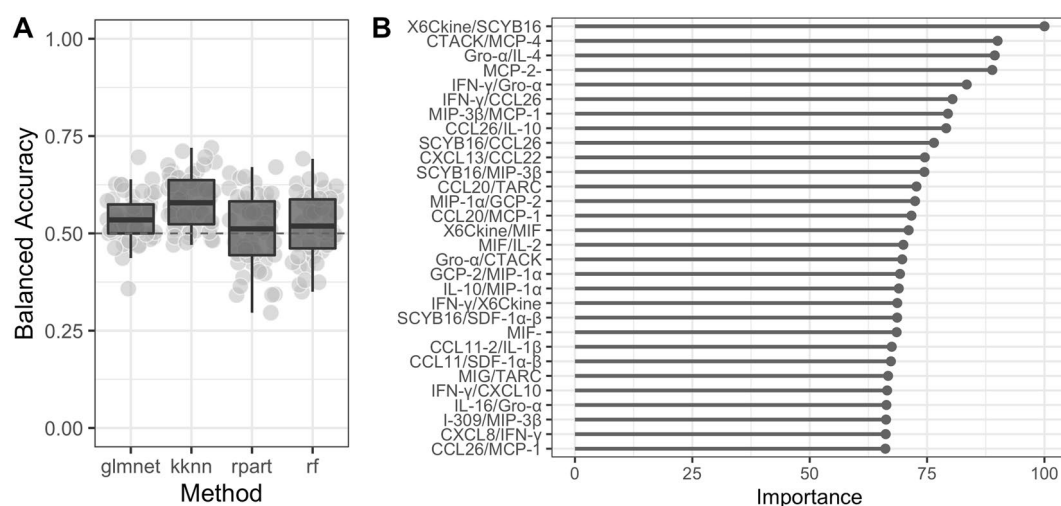


Figure 6. Modelling results after inclusion of metadata. **(A)** Random forest achieved the highest balanced accuracy on average (~0.55). **(B)** Both protein and metadata features ranked by their relative importance for RandomForest predictive performance. The last step was to evaluate if there is any clear separation between patients within individual types of endometriosis and controls with the inclusion of metadata. Results also showed that there is no improvement of discriminating performance of the classifiers if we look into individual type of endometriosis.

et al., evaluated a panel of 10 cytokines in peritoneal fluid and serum of women undergoing laparoscopy for unexplained infertility. Their study group comprised of women with minimal or mild endometriosis that were compared to the control group of women with unexplained infertility and absence of endometriosis. Elevated levels of CCL2, IL-8 and IL-6 were found in peritoneal fluid while the equivalent increase in serum samples was not found³⁷. Similar study was later on conducted by Hassa *et al.* that evaluated the diagnostic potential of four cytokines (IL-2, IL-4, IL-10, IFN-γ) and immune cells in serum and peritoneal fluid of patients with endometriosis comparing to healthy group of patients³⁸. No significant differences were observed when comparing control group with early and late stage endometriosis patients. Recently, Fan *et al.* evaluated seven cytokines including IL-10, IL-6, IL-4 and IL-2 in serum and peritoneal fluid from endometriosis patients and control patients and found significantly higher levels of IL-10 and lower levels of IL-2 in serum, but significantly higher levels of IL-2 in peritoneal fluid³⁹. Amongstudies evaluating cytokines as blood biomarkers Rocha *et al.*⁴⁰ followed a criteria for case-control studies where case and control groups originate from the same cohort⁴¹. In their study all of the patients presented with at least one endometriosis-like symptom (i.e. chronic pelvic pain and/or infertility and/

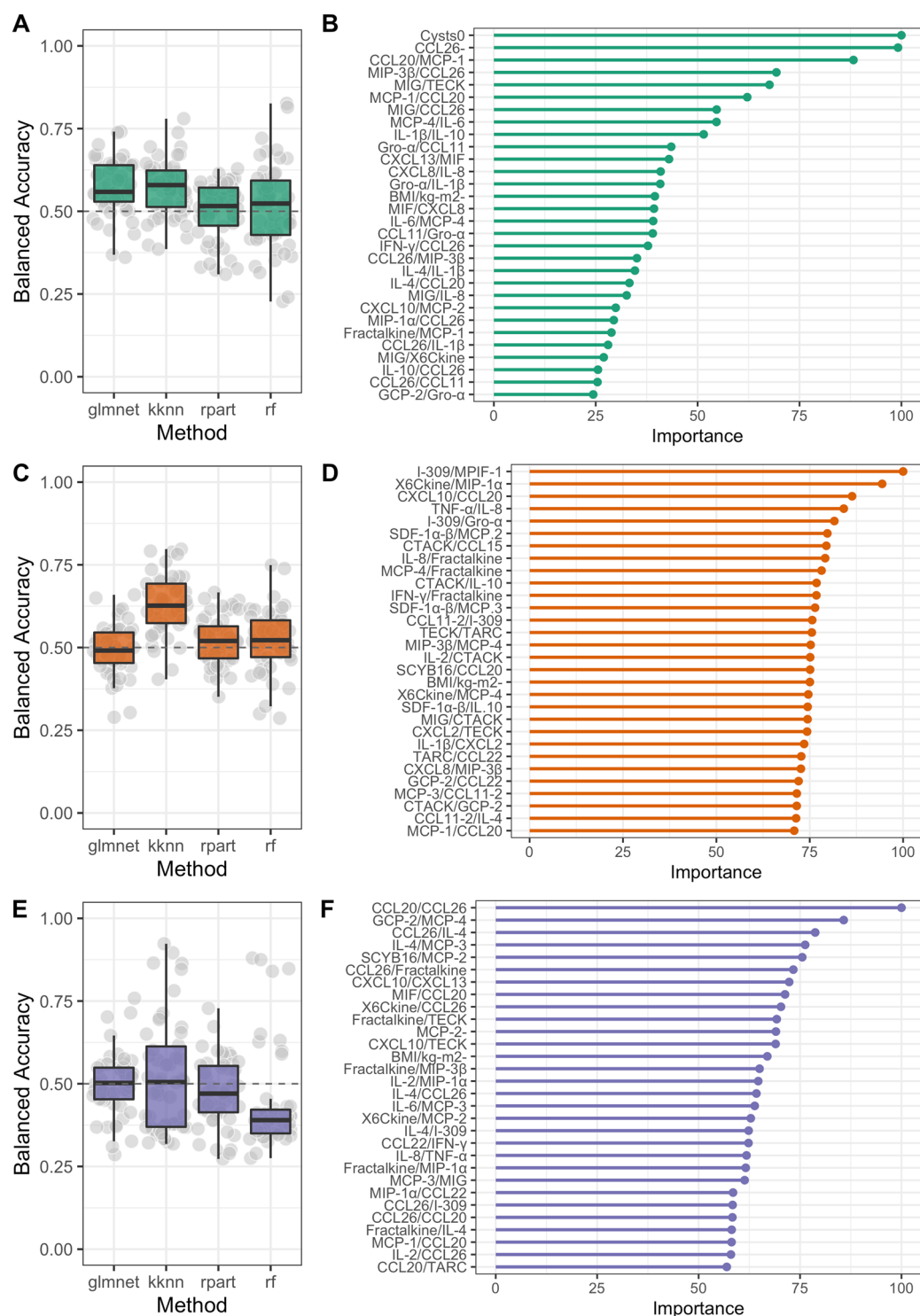


Figure 7. Modelling results after inclusion of metadata for individual types of endometriosis and controls. Nested Cross-validation results for three machine learning methods on patients with ovarian (A,B) peritoneal (C,D) and deep infiltrating endometriosis (E,F) and control samples. 5-fold CV was repeated 10 times without any parameter learning or sharing allowed between the folds to ensure generalisation and robustness of the obtained models. Results suggest that machine learning models cannot differentiate between different types of endometriosis and controls with an accuracy that exceeds the one of random chance.

or potential presence of endometrioma based on the ultrasound). After the laparoscopic operation and histological evaluation patients were divided into two groups; patients with endometriosis ($n = 44$) and control group of patients ($n = 31$). Concentrations of seven different cytokines (i.e. IL-2, IL-4, IL-6, IL-10, CCL2, CXCL10, and CCL11) were simultaneously determined using cytometric bead array and results showed that based on the

panel of these cytokines and clinical data it was not possible to predict the presence of endometriosis in a group of symptomatic patients⁴⁰.

Recently, Aalamat *et al.* published a systematic review on the use of multiplex technology for identification of potential novel biomarkers of endometriosis among inflammation associated proteins⁴². They reported that the majority of studies that adapted multiplex technology evaluated potential novel biomarkers of endometriosis in peritoneal fluid^{20,31,43–47}. Although peritoneal fluid is collected by a semi-invasive method it is the most representative sample that closely reflects inflammatory changes that are associated with the pathogenesis of endometriosis⁴⁸. Based on the literature and our published studies²⁰, we conclude that cytokines and chemokines in peritoneal fluid have a far greater diagnostic potential for endometriosis than their plasma or serum concentrations. Results of our study are also in concordance with the study conducted by Lee *et al.* that evaluated the diagnostic potential of pro-inflammatory oxylipins and cytokines in serum samples of 103 women undergoing laparoscopy. Results of their study showed limited diagnostic potential of the measured circulating biomarkers for the diagnosis of endometriosis, warranting additional studies to evaluate the exact role of systemic inflammation in endometriosis⁴⁹.

Although we evaluated a broad spectrum of inflammatory proteins in plasma samples of patients with different types of endometriosis and controls with several different multifactorial benign gynaecological conditions, both within a well-defined cohort, included detailed protocols, obtained a large set of clinical data, included different nationalities, combined with high throughput methodology and advanced statistical approaches, our results were consistent with several previous studies indicating limited diagnostic potential of circulating cytokines for the diagnosis of endometriosis. Having said this, presented results need to be considered carefully as they might be subject to various sources of bias and noise. Self-reporting of metadata by patients, undetected technical batch effects, unpredictable statistical fluctuations are all potential sources of bias and thus, limiting factors of the current study.

Conclusions

In this study we evaluated the diagnostic potential of 40 different cytokines in plasma samples from 210 patients with different types of endometriosis and control group of patients from two medical centres. Although several studies have associated inflammation with the development and progression of endometriosis, and inflammatory cytokines in endometrial tissue, peritoneal fluid and blood have been evaluated as potential biomarkers for endometriosis, the published results are inconsistent and identified no clinically useful biomarker to date. Based on the evaluated plasma concentrations of these 40 different cytokines, clinical data and appropriate statistical analysis we were unable to develop a diagnostic algorithm that would separate patients with endometriosis from the control group of patients with sufficient sensitivity and specificity. For development of a model with potential clinical applicability, which would enable diagnosis of patients with endometriosis with sufficient accuracy, further approaches of targeted and non-targeted “omics” technologies will be needed in conjunction with appropriate statistical/bioinformatics methods. These have to be followed by independent validation studies to confirm the results obtained in a research setting.

Data availability

All data are fully available without restriction.

Received: 24 July 2019; Accepted: 24 October 2019;

Published online: 13 November 2019

References

- Giudice, L. C. & Kao, L. C. Endometriosis. *Lancet* **364**, 1789–1799, [https://doi.org/10.1016/S0140-6736\(04\)17403-5](https://doi.org/10.1016/S0140-6736(04)17403-5) (2004).
- Burney, R. O. Biomarker development in endometriosis. *Scand. J. Clin. Lab. Invest. Suppl.* **244**, 75–81; discussion 80, <https://doi.org/10.3109/00365513.2014.936692> (2014).
- Revised American Society for Reproductive Medicine classification of endometriosis: 1996. *Fertil. Steril.* **67**, 817–821 (1997).
- Nisolle, M. & Donnez, J. Peritoneal endometriosis, ovarian endometriosis, and adenomyotic nodules of the rectovaginal septum are three different entities. *Fertil. Steril.* **68**, 585–596 (1997).
- Ahn, S. H., Singh, V. & Tayade, C. Biomarkers in endometriosis: challenges and opportunities. *Fertil. Steril.* **107**, 523–532, <https://doi.org/10.1016/j.fertnstert.2017.01.009> (2017).
- Sampson, J. A. The development of the implantation theory for the origin of peritoneal endometriosis. *Am. J. Obstet. Gynecol.* **40**, 549–557 (1940).
- Berkkanoglu, M. & Arici, A. Immunology and endometriosis. *Am. J. Reprod. Immunol.* **50**, 48–59 (2003).
- Nap, A. W., Groothuis, P. G., Demir, A. Y., Evers, J. L. & Dunselman, G. A. Pathogenesis of endometriosis. *Best Pract. Res. Clin. Obstet. Gynaecol.* **18**, 233–244, <https://doi.org/10.1016/j.bpobgyn.2004.01.005> (2004).
- Olive, D. L. & Schwartz, L. B. Endometriosis. *N. Engl. J. Med.* **328**, 1759–1769, <https://doi.org/10.1056/NEJM199306173282407> (1993).
- Bulun, S. E. Endometriosis. *N. Engl. J. Med.* **360**, 268–279, <https://doi.org/10.1056/NEJMra0804690> (2009).
- Hornung, D., Bentzien, F., Wallwiener, D., Kiesel, L. & Taylor, R. N. Chemokine bioactivity of RANTES in endometriotic and normal endometrial stromal cells and peritoneal fluid. *Mol. Hum. Reprod.* **7**, 163–168 (2001).
- Riccio, L. *et al.* Immunology of endometriosis. *Best Pract Res Clin Obstet Gynaecol.* <https://doi.org/10.1016/j.bpobgyn.2018.01.010> (2018).
- Khan, M. M. Role of cytokines. In: *Immunopharmacology*. 33–59 (Springer, 2016).
- Luster, A. D. Chemokines—chemotactic cytokines that mediate inflammation. *N. Engl. J. Med.* **338**, 436–445, <https://doi.org/10.1056/NEJM199802123380706> (1998).
- May, K. E. *et al.* Peripheral biomarkers of endometriosis: a systematic review. *Hum. Reprod. Update* **16**, 651–674, <https://doi.org/10.1093/humupd/dmq009> (2010).
- Rizner, T. L. Noninvasive biomarkers of endometriosis: myth or reality? *Expert Rev. Mol. Diagn.* **14**, 365–385, <https://doi.org/10.1586/14737159.2014.899905> (2014).
- Nisenblat, V. *et al.* Blood biomarkers for the non-invasive diagnosis of endometriosis. *Cochrane Database Syst Rev*, CD012179, <https://doi.org/10.1002/14651858.CD012179> (2016).

18. Gupta, D. *et al.* Endometrial biomarkers for the non-invasive diagnosis of endometriosis. *Cochrane Database Syst Rev* **4**, CD012165, <https://doi.org/10.1002/14651858.CD012165> (2016).
19. Borrelli, G. M., Abrao, M. S. & Mechsner, S. Can chemokines be used as biomarkers for endometriosis? A systematic review. *Hum. Reprod.* **29**, 253–266, <https://doi.org/10.1093/humrep/det401> (2014).
20. Kocbek, V., Vouk, K., Bersinger, N. A., Mueller, M. D. & Rižner, T. L. Panels of cytokines and other secretory proteins as potential biomarkers of ovarian endometriosis. *J. Mol. Diagn.* **17**, 325–334, <https://doi.org/10.1016/j.jmoldx.2015.01.006> (2015).
21. Team, R. C. R: A language and environment for statistical computing. R Foundation for Statistical Computing, Vienna, Austria (2014).
22. Therneau, T., Atkinson B., Ripley, B. rpart: Recursive Partitioning and Regression Trees. R package version 4.1–11, <https://CRAN.R-project.org/package=rpart> (2017).
23. Friedman, J., Hastie, T. & Tibshirani, R. Regularization Paths for Generalized Linear Models via Coordinate Descent. *J Stat Softw* **33**, 1–22 (2010).
24. Schliep, K. & Hechenbichler, K. kkn: Weighted k-Nearest Neighbors. R package version 1.3.1. <https://CRAN.R-project.org/package=kkn> (2016).
25. Liaw, A., Wiener, M. Classification and regression by randomForest. *R news* **2.3**, 18–22 (2002).
26. May, K. E., Villar, J., Kirtley, S., Kennedy, S. H. & Becker, C. M. Endometrial alterations in endometriosis: a systematic review of putative biomarkers. *Hum. Reprod. Update* **17**, 637–653, <https://doi.org/10.1093/humupd/dmr013> (2011).
27. Li, S. *et al.* Role of Interleukin-6 and Its Receptor in Endometriosis. *Med Sci Monit* **23**, 3801–3807 (2017).
28. Tanaka, T., Narazaki, M. & Kishimoto, T. IL-6 in inflammation, immunity, and disease. *Cold Spring Harb Perspect Biol* **6**, a016295, <https://doi.org/10.1101/cshperspect.a016295> (2014).
29. Kitawaki, J. *et al.* Interferon-gamma gene dinucleotide (CA) repeat and interleukin-4 promoter region (-590C/T) polymorphisms in Japanese patients with endometriosis. *Hum. Reprod.* **19**, 1765–1769, <https://doi.org/10.1093/humrep/deh337> (2004).
30. Chiang, C. M. & Hill, J. A. Localization of T cells, interferon-gamma and HLA-DR in eutopic and ectopic human endometrium. *Gynecol. Obstet. Invest.* **43**, 245–250, <https://doi.org/10.1159/000291866> (1997).
31. Borrelli, G. M., Kaufmann, A. M., Abrao, M. S. & Mechsner, S. Addition of MCP-1 and MIP-3beta to the IL-8 appraisal in peritoneal fluid enhances the probability of identifying women with endometriosis. *J. Reprod. Immunol.* **109**, 66–73, <https://doi.org/10.1016/j.jri.2015.01.003> (2015).
32. Kopelman, A. *et al.* Analysis of Gene Expression in the Endocervical Epithelium of Women With Deep Endometriosis. *Reprod. Sci.* **23**, 1269–1274, <https://doi.org/10.1177/1933719116638179> (2016).
33. Bellelis, P. *et al.* Transcriptional changes in the expression of chemokines related to natural killer and T-regulatory cells in patients with deep infiltrative endometriosis. *Fertil. Steril.* **99**, 1987–1993, <https://doi.org/10.1016/j.fertnstert.2013.02.038> (2013).
34. Chand, A. L. *et al.* Laser capture microdissection and cDNA array analysis of endometrium identify CCL16 and CCL21 as epithelial-derived inflammatory mediators associated with endometriosis. *Reprod. Biol. Endocrinol.* **5**, 18, <https://doi.org/10.1186/1477-7827-5-18> (2007).
35. Shi, Y. L., Luo, X. Z., Zhu, X. Y. & Li, D. J. Combination of 17beta-estradiol with the environmental pollutant TCDD is involved in pathogenesis of endometriosis via up-regulating the chemokine I-309-CCR8. *Fertil. Steril.* **88**, 317–325, <https://doi.org/10.1016/j.fertnstert.2006.11.129> (2007).
36. Shi, Y. L. *et al.* Effects of combined 17beta-estradiol with TCDD on secretion of chemokine IL-8 and expression of its receptor CXCR1 in endometriotic focus-associated cells in co-culture. *Hum. Reprod.* **21**, 870–879, <https://doi.org/10.1093/humrep/dei414> (2006).
37. Kalu, E. *et al.* Cytokine profiles in serum and peritoneal fluid from infertile women with and without endometriosis. *J. Obstet. Gynaecol. Res.* **33**, 490–495, <https://doi.org/10.1111/j.1447-0756.2007.00569.x> (2007).
38. Hassa, H., Tanir, H. M., Tekin, B., Kirilmaz, S. D. & Sahin Mutlu, F. Cytokine and immune cell levels in peritoneal fluid and peripheral blood of women with early- and late-staged endometriosis. *Arch. Gynecol. Obstet.* **279**, 891–895, <https://doi.org/10.1007/s00404-008-0844-8> (2009).
39. Fan, Y. Y. *et al.* Expression of inflammatory cytokines in serum and peritoneal fluid from patients with different stages of endometriosis. *Gynecol Endocrinol* **34**, 507–512, <https://doi.org/10.1080/09513590.2017.1409717> (2018).
40. Rocha, A. L., Vieira, E. L., Maia, L. M., Teixeira, A. L. & Reis, F. M. Prospective Evaluation of a Panel of Plasma Cytokines and Chemokines as Potential Markers of Pelvic Endometriosis in Symptomatic Women. *Gynecol. Obstet. Invest.* **81**, 512–517, <https://doi.org/10.1159/000443956> (2016).
41. Zondervan, K. T., Cardon, L. R. & Kennedy, S. H. What makes a good case-control study? Design issues for complex traits such as endometriosis. *Hum. Reprod.* **17**, 1415–1423 (2002).
42. O, D. F. *et al.* Multiplex immunoassays in endometriosis: An array of possibilities. *Front Biosci (Landmark Ed)* **22**, 479–492 (2017).
43. Wickiewicz, D. *et al.* Diagnostic accuracy of interleukin-6 levels in peritoneal fluid for detection of endometriosis. *Arch. Gynecol. Obstet.* **288**, 805–814, <https://doi.org/10.1007/s00404-013-2828-6> (2013).
44. Bersinger, N. A., Dechaud, H., McKinnon, B. & Mueller, M. D. Analysis of cytokines in the peritoneal fluid of endometriosis patients as a function of the menstrual cycle stage using the Bio-Plex(R) platform. *Arch. Physiol. Biochem.* **118**, 210–218, <https://doi.org/10.3109/13813455.2012.687003> (2012).
45. Mier-Cabrera, J., Jimenez-Zamudio, L., Garcia-Latorre, E., Cruz-Orozco, O. & Hernandez-Guerrero, C. Quantitative and qualitative peritoneal immune profiles, T-cell apoptosis and oxidative stress-associated characteristics in women with minimal and mild endometriosis. *BJOG* **118**, 6–16, <https://doi.org/10.1111/j.1471-0528.2010.02777.x> (2011).
46. Podgaec, S. *et al.* Endometriosis: an inflammatory disease with a Th2 immune response component. *Hum. Reprod.* **22**, 1373–1379, <https://doi.org/10.1093/humrep/del516> (2007).
47. Jorgensen, H. *et al.* Peritoneal fluid cytokines related to endometriosis in patients evaluated for infertility. *Fertil. Steril.* **107**, 1191–1199 e1192, <https://doi.org/10.1016/j.fertnstert.2017.03.013> (2017).
48. Rižner, T. L. Diagnostic potential of peritoneal fluid biomarkers of endometriosis. *Expert Rev. Mol. Diagn.* **15**, 557–580, <https://doi.org/10.1586/14737159.2015.1015994> (2015).
49. Lee, Y. H. *et al.* Limited value of pro-inflammatory oxylipins and cytokines as circulating biomarkers in endometriosis - a targeted 'omics study. *Sci. Rep.* **6**, 26117, <https://doi.org/10.1038/srep26117> (2016).

Acknowledgements

The authors thank their study participants, who kindly donated their samples and time. The authors thank the personnel of the Department of Obstetrics and Gynaecology, University Medical Centre Ljubljana, Ljubljana, Slovenia, and especially Tanja Lončar and Klara Primc, for their support in the enrolling of the study participants. The authors also thank Mrs. Vera Troha Poljančič and Prof. Dr. Joško Osredkar at the University Medical Centre Ljubljana, Clinical Institute of Clinical Chemistry and Biochemistry for processing the samples. The authors acknowledge Prof. Jaak Vilo at the University of Tartu for his guidance and support. D.F. and H.P. were supported by Estonian Research Council grants [PSG59, IUT34-4] and European Regional Development Fund through EXCITE Center of Excellence. The preparation of this manuscript was supported by grant J3-1755 from the Slovenian Research Agency to T.L.R.

Author contributions

T.K. carried out the experiments, helped with the clinical data and wrote the manuscript. A.V., M.G., R.W. enrolled patients into the study and gathered clinical data. D.F. carried out the statistical evaluation/analysis, prepared the figures and contributed to the manuscript. H.P. supervised statistical analysis and reviewed the manuscript. T.L.R. designed the study and contributed to writing the manuscript. All authors reviewed the final manuscript.

Competing interests

The authors declare no competing interests.

Additional information

Supplementary information is available for this paper at <https://doi.org/10.1038/s41598-019-52899-8>.

Correspondence and requests for materials should be addressed to T.L.R.

Reprints and permissions information is available at www.nature.com/reprints.

Publisher's note Springer Nature remains neutral with regard to jurisdictional claims in published maps and institutional affiliations.



Open Access This article is licensed under a Creative Commons Attribution 4.0 International License, which permits use, sharing, adaptation, distribution and reproduction in any medium or format, as long as you give appropriate credit to the original author(s) and the source, provide a link to the Creative Commons license, and indicate if changes were made. The images or other third party material in this article are included in the article's Creative Commons license, unless indicated otherwise in a credit line to the material. If material is not included in the article's Creative Commons license and your intended use is not permitted by statutory regulation or exceeds the permitted use, you will need to obtain permission directly from the copyright holder. To view a copy of this license, visit <http://creativecommons.org/licenses/by/4.0/>.

© The Author(s) 2019

CURRICULUM VITAE

Personal data

Name: Dmytro Fishman
Date of birth: 06.02.1991
Citizenship: Ukraine
Contact: dmytro.fishman@ut.ee
Current position: Junior Lecturer in Artificial Intelligence

Education

2013–2021 Ph.D. Candidate, University of Tartu
2011–2013 MSc. Software Engineering, University of Tartu and Tallinn Technical University
2007–2011 BSc. Computer Science (*cum laude*), National Technical University of Ukraine "Igor Sikorsky Kyiv Polytechnic Institute"

Employment

2020–... Junior Lecturer of Artificial Intelligence, Institute of Computer Science, University of Tartu
2018–2020 Assistant of Data Science, Institute of Computer Science, University of Tartu
2015–2018 Junior Researcher Fellow in Bioinformatics, Institute of Computer Science, University of Tartu
2014–2015 Research Project Specialist, Institute of Computer Science, University of Tartu
2013–2014 Assistant of Informatics, Institute of Computer Science, University of Tartu

Honours & awards

- Ustus Agur personal scholarship for the significant contribution to the development of Estonian information society, fall 2018;
- Raefond personal scholarship to outstanding international MSc students studying in the University of Tartu, fall 2012;

Teaching

- Lecturer for Machine Learning course at University of Tartu in fall 2020;
- Lecturer for Machine Learning course at Ukrainian Catholic University (Lviv, Ukraine) in spring 2020 and 2021;

- Lecturer for Advanced Machine Learning and Time Series Modelling course at Kyiv School of Economics (Kyiv, Ukraine) in spring 2020;
- Teaching assistant for Advanced Algorithms course at University of Tartu in 2013, 2014, 2016, 2017, 2018 and 2019;
- Teaching assistant for Data Mining course at University of Tartu in 2014, 2015 and 2017;
- Teaching assistant for Text Algorithms course at University of Tartu in fall 2013;
- Leading the seminars on Bioinformatics (in 2015 and 2016) as well as Special course in Machine Learning (in 2019).

Supervised theses

- Kaspar Hollo (MSc): Anomaly segmentation in microscopy images using deep learning.
- Navid Bamdad Roshan (MSc): Change detection in HD-maps using camera images for autonomous driving.
- Dmytro Zabolotnii (MSc): High-definition map generation for autonomous driving.
- Iaroslav Plutenko (MSc): Metadata for semantic segmentation by employing channel attention mechanism.
- Mihkel Ilisson (MSc): Application of statistical analysis and machine learning methods for analysing blood metabolites.
- Richard Annilo (BSc): Using deep learning for medical sound analysis.
- Vladyslav Fediukov (MSc): Detection of Changes in Maps Using LiDAR Point Clouds.
- Oleh Misko (MSc): Ensembling and transfer learning for multi-domain microscopy image segmentation.
- Mikhail Papkov (MSc): Deep neural networks application for cell phenotyping in mixed cultures. Co-supervised with Leopold Parts.
- Oleksandr Pryhoda (BSc): Tissue segmentation in histological whole-slide images with deep learning.
- Yurii Toma (MSc): Predicting the Impact of Non-Coding Genetic Variants on Transcription Factor Binding with Machine Learning. Co-supervised with Kaur Alasoo.
- Sten-Oliver Salumaa (MSc): Convolutional Neural Networks for Cellular Segmentation. Co-supervised with Leopold Parts.
- Vitalii Peretiatko (MSc): Using Robust Rank Aggregation for prioritising autoimmune targets on protein microarrays. Co-supervised with Elena Sügis.

Scientific work

Main fields of interest:

- Bioinformatics
- Machine Learning and Deep Learning
- Computer Vision

Served as a reviewer:

- International Conference on Machine Learning (2020, 2021)
- International Conference on Learning Representations (2020)
- Nature Machine Intelligence, BMC Bioinformatics, Nature Scientific Reports, and Bioinformatics.

ELULOOKIRJELDUS

Isikuandmed

Nimi: Dmytro Fishman
Sünniaeg: 06.02.1991
Kodakondsus: Ukraina
E-mail: dmytro.fishman@ut.ee

Haridus

2013–2021 Tartu Ülikool, loodus- ja täppisteaduste valdkond, informaatika, doktoriõpe
2011–2013 Tartu Ülikool, loodus- ja täppisteaduste valdkond, tarkvara-
ratehnika, magistriõpe
2007–2011 Ukraina Rahvuslik Tehnoloogiaülikool, Igor Sikorski nimeline Kiievi Polütehniline Instituut, bakalaureuseõpe (*cum laude*)

Teenistuskäik

2020–... Tartu Ülikool, loodus- ja täppisteaduste valdkond, arvutiteaduse instituut, andmeteaduse nooremlektor
2018–2020 Tartu Ülikool, loodus- ja täppisteaduste valdkond, arvutiteaduse instituut, andmeteaduse assistent
2015–2018 Tartu Ülikool, loodus- ja täppisteaduste valdkond, arvutiteaduse instituut, bioinformaatika nooremteadur
2014–2015 Tartu Ülikool, loodus- ja täppisteaduste valdkond, arvutiteaduse instituut, teadusprojekti spetsialist
2013–2014 Tartu Ülikool, loodus- ja täppisteaduste valdkond, arvutiteaduse instituut, informaatika assistent

Teaduspreemiad ja tunnustused

- Ustus Aguri nimeline stipendium silmapaistva panuse eest Eesti infoühiskonna teerajajana, väljaandja Eesti Infotehnoloogia ja Telekommunikatsiooni Liit, sügis 2018;
- Raefondi stipendium Tartu Ülikooli silmapaistvatele rahvusvahelistele tudengitele, sügis 2012;

Õppetöö

- Tartu Ülikool, loodus- ja täppisteaduste valdkond, arvutiteaduse instituut, lektor aines masinõpe, sügis 2020;

- Ukraina Katoliku Ülikool (Lviv, Ukraina), lektor aines masinõpe, kevad 2020 ja kevad 2021;
- Kiievi Majanduskool (Kiiev, Ukraina), lektor aines masinõpe edasijõudnutele ja aegridade modelleerimine, kevad 2020;
- Tartu Ülikool, loodus- ja täppisteaduste valdkond, arvutiteaduse instituut, õppeassistent aines algoritmid edasijõudnutele, aastatel 2013, 2014, 2016, 2017, 2018, 2019;
- Tartu Ülikool, loodus- ja täppisteaduste valdkond, arvutiteaduse instituut, õppeassistent aines andmekaeve 2014, 2015, 2017;
- Tartu Ülikool, loodus- ja täppisteaduste valdkond, arvutiteaduse instituut, õppeassistent aines tekstialgoritmid, sügis 2013;
- Seminaride juhendaja ainetes bioinformaatika aastatel 2015, 2016 ja erikursus masinõppes, 2019.

Juhendatud väitekirjad

- Kaspar Hollo (MSc): Anomaly segmentation in microscopy images using deep learning.
- Navid Bamdad Roshan (MSc): Change detection in HD-maps using camera images for autonomous driving.
- Dmytro Zabolotnii (MSc): High-definition map generation for autonomous driving.
- Iaroslav Plutenko (MSc): Metadata for semantic segmentation by employing channel attention mechanism.
- Mihkel Ilisson (MSc): Application of statistical analysis and machine learning methods for analysing blood metabolites.
- Richard Annilo (BSc): Using deep learning for medical sound analysis.
- Vladyslav Fediukov (MSc): Detection of Changes in Maps Using LiDAR Point Clouds.
- Oleh Misko (MSc): Ensembling and transfer learning for multi-domain microscopy image segmentation.
- Mikhail Papkov (MSc): Deep neural networks application for cell phenotyping in mixed cultures. Kaasjuhendaja Leopold Parts.
- Oleksandr Pryhoda (BSc): Tissue segmentation in histological whole-slide images with deep learning.
- Yurii Toma (MSc): Predicting the Impact of Non-Coding Genetic Variants on Transcription Factor Binding with Machine Learning. Kaasjuhendaja Kaur Alasoo.
- Sten-Oliver Salumaa (MSc): Convolutional Neural Networks for Cellular Segmentation. Kaasjuhendaja Leopold Parts.

- Vitalii Peretiatko (MSc): Using Robust Rank Aggregation for prioritising autoimmune targets on protein microarrays. Kaasjuhendaja Elena Sügis.

Teadustöö

Peamised uurimisvaldkonnad:

- Bioinformaatika
- Masinõpe ja süvaõpe
- Arvutinägemine

Tegevus retsensendina:

- International Conference on Machine Learning (2020, 2021)
- International Conference on Learning Representations (2020)
- Nature Machine Intelligence, BMC Bioinformatics, Nature Scientific Reports, and Bioinformatics.